



HAL
open science

Design of exotic architected materials in linear elasticity

Guangjin Mou

► **To cite this version:**

Guangjin Mou. Design of exotic architected materials in linear elasticity. Solid mechanics [physics.class-ph]. Sorbonne Université, 2023. English. NNT : 2023SORUS519 . tel-04554235

HAL Id: tel-04554235

<https://theses.hal.science/tel-04554235v1>

Submitted on 22 Apr 2024

HAL is a multi-disciplinary open access archive for the deposit and dissemination of scientific research documents, whether they are published or not. The documents may come from teaching and research institutions in France or abroad, or from public or private research centers.

L'archive ouverte pluridisciplinaire **HAL**, est destinée au dépôt et à la diffusion de documents scientifiques de niveau recherche, publiés ou non, émanant des établissements d'enseignement et de recherche français ou étrangers, des laboratoires publics ou privés.



SORBONNE UNIVERSITÉ

ÉCOLE DOCTORALE

Sciences Mécaniques, Acoustique, Électronique et Robotique de Paris
SMAER (ED 391)

THESIS

to obtain the degree of
DOCTOR OF SORBONNE UNIVERSITÉ

Discipline: Mechanics

Presented and defended by:

Guangjin MOU

on 19 october 2023

Design of exotic architected materials in linear elasticity

Under the supervision of:

M. Boris DESMORAT	Maitre de conférences, Sorbonne Université	Director
M. Nicolas AUFRAY	Professeur des universités, Sorbonne Université	Co-director

Committee members:

M. Justin DIRRENBARGER	Maitre de conférences, CNAM	Reviewer
M. François-Xavier IRISARRI	Ingénieur de recherche, ONERA	Reviewer
M. Qi-Chang HE	Professeur des universités, Université Gustave Eiffel	Examiner
M. Jean-Camille CHASSAING	Professeur des universités, Sorbonne Université	Examiner
M. Michel CORET (Committee president)	Professeur des universités, Ecole Centrale Nantes	Examiner
Mme. Federica DAGHIA	Maitresse de conférences, ENS Paris-Saclay	Examiner

Acknowledgement

I would like to express firstly my gratitude to Dr. Boris Desmorat and Dr. Nicolas Auffray, my thesis supervisors, for welcoming me into this field of research, for their valuable advice, and for their availability despite their teaching responsibilities. My appreciation also goes to Dr. Marc Olive, who stood by me during my first year of thesis work and provided me with substantial help, supporting me in mathematics and sharing his ideas.

I am grateful to the rapporteurs, François-Xavier IRISARRI and Justin Dirrenberger, for their willingness to read this document in its entirety. I am thankful for the keen interest they took in understanding every chapter in detail. Their numerous comments have enhanced this work.

I would also like to express my gratitude to Mrs. Federica Daghia, as well as to Messrs. Qi-Chang He, Jean Camille Chassaing, and Michel Coret. It is likely that their feedback during the presentation will serve as a reference for future research.

Finally, I extend my greetings to all my colleagues at the d'Alembert laboratory whom I have interacted with and who have contributed to creating a friendly atmosphere. I particularly appreciate the collaborative work with Nassim Kesmia and Saad El Ouafa, my colleagues from our MAX-OASIS and MOMAP projects, with whom I have had numerous highly enriching scientific discussions on numerical aspects.

Nomenclature

Tensors	
$\underset{\sim}{\sigma}$	Stress tensor
$\underset{\sim}{\varepsilon}$	Infinitesimal strain tensor
\mathbb{T}	n -th order tensor
$\underset{\sim}{\mathbb{C}}, \underset{\sim}{\mathbb{S}}$	Elasticity tensor
$\underset{\sim}{\mathbb{I}}$	Identity tensor of $S^2(\mathbb{R}^2)$
$\underset{\sim}{1}$	Identity tensor of \mathbb{R}^2
\mathcal{K}	Kelvin convention of a tensor representation
$\mathfrak{R}^{(n)}$	An orthonormal basis of \mathbb{K}^n
$\underset{\sim}{\mathbb{P}}$	Piezoelectricity tensor
$D_T(\cdot)$	The topological derivative of a tensor
Tensor operations	
\otimes	Tensor product
$\overline{\otimes}$	Twisted tensor product
S^2	Symmetrized tensor product
Λ^2	Anti-symmetrized tensor product
$:$, $::$, n	Contraction of order 2, 4 and n between two tensors
$(\cdot)^s$	Complete symmetric part of a tensor
$(\cdot)^d$	Deviatoric part of a tensor
$*$	Harmonic product between two harmonic tensors
\odot	Symmetric tensor product between two tensors
\times	The skew-symmetric contraction between two totally symmetric tensors
tr	Trace of a tensor
\boxtimes	The special tensor product
Spaces	
d	Dimension of the physical space
\mathbb{E}^d	Euclidean affine space of dimension d ($d = 2, 3$)
\mathbb{V}^d	Vector spaces of dimension d
\mathbb{R}^d	Real space of dimension d
\mathbb{T}^n	Space of n -th order tensors
$\mathbb{E}la(d)$	Elasticity tensors space of dimension d

$\mathbb{E}la^+$	Positive defined elasticity tensors space
$\mathbb{E}la$	Elasticity tensors space without zero determinant elements
\mathbb{K}^n	n -th order harmonic tensors space in \mathbb{R}^2
\mathbb{H}^n	n -th order harmonic tensors space in \mathbb{R}^3
Orb	Orbit of elasticity tensors
$\Sigma_{[H]}$	The open strata of $[H]$
$\bar{\Sigma}_{[H]}$	The closed strata of $[H]$
Fix	Fixed point set
Piez	Space of the piezoelectric law
Cos	The space of the Cosserat elasticity law
$\tilde{\mathcal{U}}_\mu$	The minimally constrained space of kinematically displacements
$\mathcal{U}_\mu \subset \tilde{\mathcal{U}}_\mu$	The subspace of kinematically admissible displacement
Basis	
\mathcal{B}	Orthonormal basis
\mathcal{IB}	Integrity basis
Groups	
G	A compact group
$O(d)$	Orthogonal groups
$SO(d)$	Special orthogonal groups
$\mathbf{r}(\theta)$	Transformation of rotation by angle θ in \mathbb{R}^2
$\mathbf{r}(\underline{n}, \theta)$	Transformation of rotation by angle θ around the unit vector $\underline{n} \in \mathbb{R}^3$
$\mathbf{m}_{\underline{n}}$	The reflection across the line normal to \underline{n}
Z_k	cyclic group with k elements generated by the rotation $\mathbf{r}(\frac{2\pi}{k})$
D_k	Dihedral group with $2k$ elements generated by $\mathbf{r}(\frac{2\pi}{k})$ and $\mathbf{m}_{\underline{e}_2}$
\mathcal{O}	The octahedral group
-1	Transformation of inversion
$GL(d)$	The group of invertible linear transformation of \mathbb{R}^d
Domains	
Ω	Closed domain used to represent a material
Ω_μ	Domain of the Representative Volume Element (RVE)
$\partial\Omega_\mu$	Boundary of the domain of the RVE
\mathcal{H}_ρ	Domain of the circular hole with radius ρ
\mathcal{I}_ρ	Domain of the circular inclusion with radius ρ
Functions	
S	Application of totally symmetrisation
\mathcal{L}	Linear application of a space onto itself(not sure)
$p(\cdot)$	Polynomial functions
$Cov_n(\cdot)$	Polynomial covariant algebra of order n
Others	
σ	Index permutation function of n -th order tensors

$(\cdot)^T$	Transpose of a tensor
\star	Group action
J	Cost function
λ_v	Penalisation constraint on the volume ratio
\mathfrak{J}	A set of conjugacy classes (symmetry classes)
\simeq	O(2) or SO(3)-equivariant isomorphism
HB(\cdot)	Harmonic bouquet
\odot	Clips operation
$\#\mathcal{E}$	Number of exotic sets
$\#\mathcal{C}$	Number of symmetry classes

List of Figures

1.1	Different structure types of architected materials	10
1.2	Recent development on architected materials	11
1.3	Four architected materials in the literature that harness mechanical instability for specific behaviours.	12
1.4	Approaches listed in the literature to identify the 3D tensorial symmetries	14
1.5	Two different optimisation modellings (a) Mono-scale modelling [1] and (b) Multi-scale modelling [2]	15
1.6	Comparison of shape optimisation and topology optimisation [3]	16
2.1	Representation of the domain Ω in a given reference frame($d = 2$)	19
2.2	Active transformation on the left figure: a new vector is obtained; Passive transformation on the right figure, in which only the basis is changed.	25
2.3	G-Orbit of \mathbb{C} : equivalent tensors related by orthogonal transformations	25
2.4	Geometric description of linear elastic material space	31
3.1	The action of $\mathbf{r}(\theta)$ on $\tilde{\mathbf{h}}$ and $\tilde{\mathbf{H}}$	40
3.2	Harmonic normal form of a generic elasticity tensor.	49
3.3	Harmonic normal form of non-generic elasticity tensors.	49
3.4	Semi-algebraic variety of elastic materials with respect to (I_2, J_2, I_3)	51
4.1	Harmonic normal form of generic and exotic orthotropic elasticity tensors.	56
5.1	Macro-continua solid with a local microstructure	63
5.2	Topological perturbation at microscale	64
5.3	Illustration of vectors $\underline{\mathbf{g}}$ and $\underline{\psi}$	70
5.4	Illustration of the initial level set function	73
5.5	Initial microstructure (a) Initial finite element mesh adopted and (b) Initial topology	73
5.6	Horizontal rigidity maximization: (a)Optimised RVE topology, and (b) Corresponding periodic mesostructure.	75
5.7	Horizontal rigidity maximization. Convergence history: (a) Cost function, and (b) Angle θ	75
5.8	Initialisation: (a)Initial unit cell used for computation and (b) Initial lattice assembled of unit cells	78
5.9	Optimised design	79
5.10	Initial unit cell of different symmetry types	80
5.11	Design for Cauchy elasticity materials with tetragonal initialisation	81
5.12	Design for Cauchy elasticity materials with orthotropic initialisation	82
6.1	A complete structure of different symmetry classes of $\mathbb{E}la$	98

6.2	Illustration of the partition of tensor space with respect to their symmetry classes	100
7.1	Illustration of clips operations	108
7.2	Illustration of complete clips operations structure	109
7.3	Clips operation results for $\mathbb{E}la$	110
7.4	Result of a numerical test on a coupled triclinic material under hydrostatic loading (compression)	122
7.5	Result of a numerical test on a decoupled triclinic material under hydrostatic loading (compression)	123
7.6	Testing device for architected materials	128
7.7	In compression, the hexagonal honeycomb generates different patterns depending on its boundary conditions [4] (from right to left: initial geometry, under uniaxial compression, under biaxial compression, and under equibiaxial compression)	129
B.1	Flowchart of the level set based topological derivative algorithm	135

List of Tables

3.1	Classification of $O(2)$ subsets according to their invariance properties	36
3.2	Polynomial conditions for membership of an open stratum	50
4.1	Number of exotic sets for tensor spaces in linear cosserat elasticity	61
5.1	Comparison between optimised topology for shear modulus maximization	76
5.2	Comparison between optimised topology for minimization of a modified Poisson's ratio	77
6.1	The Platonic solids	88
6.2	Clips operations for $SO(3)$	97
6.3	Polynomial conditions for membership of an open stratum	104
7.1	An example of complete clips operation structure.	108
7.2	Intermediate clips operation results for $\mathbb{E}la$ and determination of exotic sets	111
7.3	clips operation results for $\mathbb{E}la$ and determination of exotic sets	112
7.4	3D R_0 -orthotropy	119
7.5	Transversely isotropic materials with its deviatoric elasticity isotropic	120
7.6	Triclinic exotic elastic materials	121
7.7	Orthotropic materials with isotropic Young's modulus	124
7.8	Transversely isotropic materials with isotropic Young's modulus	125

Introduction

Anisotropy characterises the way a physical property varies with respect to material directions. Linear properties, such as elasticity or conductivity, are encoded using constitutive tensors. Depending on their order, these tensors can model different types of anisotropies ranging from complete anisotropy to isotropy. These different possibilities are called *symmetry classes*, and have attracted much interest in recent years [5, 6, 7].

The geometrical tools developed to determine the symmetry classes of a tensor space have also revealed the richness of these spaces, as well as the existence of a whole range of intermediate possibilities beyond the symmetry classes. Indeed, these tools allow to describe the linear material space in a very fine way and to detect materials with non-standard anisotropic properties. These intermediate possibilities are referred to here as *exotic*.

This possibility was identified very early on by authors working in this field [8, 9, 10]. For example, in the case of 2D linear elasticity, P. Vannucci has identified a particular situation which he calls R_0 -orthotropy. He says about it:

"The existence of a particular type of planar orthotropic material, [...] but, [...], not linked to a particular type of elastic symmetry condition. For this reason, the existence of this type of material cannot be revealed only by the use of certain symmetry conditions on the Cartesian components of \mathbb{C}^1 ." [9]

At the same moment, J. Rychlewski made some related observations and noticed that

"The thing is that materials of substantially different anisotropy can behave, in certain situations and in certain aspects, quite alike or just identically. In particular, some essentially anisotropic materials can retain certain important features of isotropic materials." [8]

But these early works seem to be curiosities and have not aroused much interest. This is owing to two major lacks that limited the applicability of these discoveries to the community:

1. lack of an *operative* mathematical definition of what an exotic elasticity is. In the contributions cited, only particular cases of exotic elastic materials have been studied, and no systematic classification has been undertaken. This is certainly due to the lack of a good definition for such a study;
2. to the best of our knowledge, mesostructures generating these exotic properties were not determined at this time². It is understandable because the topology optimisation was not as mature a technique as it is now [11, 12] and additive manufacturing was also less democratised than now. In fact, there was also something missing with regard to practical applications.

Today, these practical locks have been broken. Very efficient multi-scale topology optimisation codes have been developed by the applied mathematics and mechanics communities [2, 13, 14]. And further,

¹ \mathbb{C} being the elasticity tensor.

²It should be noted, however, that P. Vannucci has determined a stacking sequence of elementary orthotropic layers producing a global elastic behaviour R_0 -orthotropic for a laminated plate [9].

3D printers have almost become standard laboratory tools. These tools have already been applied to the design of architected materials. However, all these studies are concerned with the optimisation of specific coefficients of the stiffness (or compliance) tensor in a given base. While this intuition-based method is effective in some cases, it is still rather home-made and does not exploit the progress that has been made in describing the geometry of the elastic material space.

It is hence important to revisit this topic because the understanding of exotic linear behaviours opens up multiple possibilities for the smart optimal design of architected materials that can accommodate seemingly incompatible design constraints. This is particularly true in 3D, and concerns both static and dynamic applications [15, 16, 17].

To go further in the design of custom elastic materials and to exploit exotic symmetry sets, it is necessary to understand the geometry of the elastic tensor space. In particular, how to characterise the strata of this space, i.e. the subsets of tensors of the same anisotropy type. It is from this description that we will be able to bring out the mathematical concept of exotic anisotropy.

The questions we ask ourselves and which my Ph.D. work proposes to answer are the following:

1. What is the definition of exotic materials?
2. What are the properties of these materials?
3. Can we, *a priori*, list the different possibilities of exotic situations ?

In order to provide a mathematical definition while keeping a reasonable level of complexity, we will start in a 2D framework, and then generalise it to 3D.

Following the observations made by Vanucci [9] and Rychlewski [8], we propose to adopt the following *mechanical* definition of what an *exotic* linear material is:

1. **Specific design:** they satisfy constraints independent of those imposed by symmetry arguments;
2. **Hypersymmetric:** they produce more symmetrical behaviour than that imposed by material symmetries.

It should be noted that some specifically designed materials may have interesting non-standard properties while not meeting the hypersymmetry requirement. These materials will be referred to as *semi-exotic*. As will be seen, this mechanical definition will lead to a mathematical one and is operative since allowing to enumerate the exotic sets of a constitutive tensor space. As we shall see, in this context, general results can be obtained.

This Ph.D. thesis is divided into seven chapters. The first two chapters aim to present the state-of-the-art of this study:

Chapter 1 will present the recent developments in architected materials, including their different types, additive manufacturing technologies, and some popular numerical algorithms to design them. Besides, the non-standard mechanical behaviors emerging from the architected materials will be emphasized in this chapter.

Chapter 2 come up with some geometric tools including group theory, harmonic decomposition, and polynomial invariant theory. These notions will be used in the following chapters to explore the anisotropic linear properties of materials.

The aforementioned mathematical framework will be employed to explore the space of 2D linear elasticity tensor space:

Chapter 3 focuses on the partition of 2D linear elasticity tensor space into 4 different strata according to their corresponding symmetry classes. The membership to a symmetry class is determined by polynomial invariant conditions.

Chapter 4 deals with the materials with non-standard anisotropic properties associated with intermediate possibilities beyond symmetry classes. These materials are called *exotic materials*. And the only exotic material for 2D linear elasticity will be introduced in this chapter.

Chapter 5 realises the numerical design of an exotic material and a semi-exotic material by using a level set-based topological derivative algorithm.

We then extended our study into 3D linear elasticity, the structure of the following chapters is the same as that for the 2D case :

Chapter 6 presents the partition of 3D linear elasticity tensor space into 8 different strata according to their corresponding symmetry classes. The membership to a symmetry class is determined by polynomial covariant conditions.

Chapter 7 deals with the identification of exotic materials for 3D linear elasticity. There are 1052 possibilities of exotic materials in total and 3 of them will be discussed as examples.

The design of 3D exotic materials is ongoing, they will be published in the forthcoming paper. And thus, Chapters 4, 5, and 7 regroup the specific contributions of my Ph.D. Some conclusions and perspectives for future developments are drawn in the last conclusion chapter and some technical points are detailed in the appendices.

Contents

I	State of the art	7
1	Architected materials	8
1.1	Architected Materials (A.M.) in brief	9
1.2	Anisotropic linear elasticity of A.M.	13
1.3	Topology optimisation of multi-scale structure	15
2	Geometry of tensor spaces	18
2.1	Linear elastic constitutive law	19
2.2	$SO(d)$ and $O(d)$ linear representation on $\mathbb{E}la(d)$	20
2.3	Harmonic decomposition	23
2.4	Definition of elastic materials	24
2.5	Invariants and integrity basis	26
2.6	From symmetry group to symmetry class	27
2.6.1	Symmetry group	28
2.6.2	Symmetry class	29
2.6.3	Clips operation	29
2.7	Symmetry stratum	30
II	Anisotropic 2D linear elasticity	33
3	Geometry of 2D linear elasticity tensors space	34
3.1	Group $O(2)$ and its subgroups	35
3.1.1	Group $O(2)$	35
3.1.2	Subgroups of $O(2)$	36
3.2	2D harmonic tensors space: \mathbb{K}^n	37
3.3	Harmonic decomposition of $\mathbb{E}la$	38
3.4	Parametrisation of elasticity tensors	42
3.4.1	Harmonic parametrisation	42
3.4.2	Polar parametrisation	43
3.4.3	Parametrisation of the inverse of a tensor	44
3.5	Invariants and integrity basis	45
3.6	Symmetry classes of $\mathbb{E}la$	47
3.7	Conditions of belonging to a symmetry class	48
3.7.1	Covariant-based conditions	48
3.7.2	Polynomial invariant conditions	50
3.7.3	Inverse stability of the symmetry class	51

4	2D exotic and semi-exotic sets	53
4.1	Mechanical definition of exotic materials	54
4.2	Exotic elastic materials: R_0 -orthotropy	55
4.3	Semi-exotic elastic materials: Cauchy elasticity	57
4.4	Generalisation to other constitutive laws	58
4.4.1	A general theorem	59
4.4.2	Application to coupled constitutive laws	60
5	Mesostructure design of 2D exotic materials	62
5.1	Multi-scale based homogenization	63
5.2	Topological sensitivity of the homogenized elasticity tensor	67
5.3	Topological derivative-based algorithm	68
5.4	Finite element implementation	72
5.4.1	Initialization	72
5.4.2	Numerical examples	74
5.5	Numerical result for exotic material: R_0 -Orthotropy	78
5.6	Numerical results for semi-exotic material: Cauchy elasticity	79
5.7	Synthesis	82
III	Extension to 3D linear elasticity	83
6	Geometry of 3D linear elasticity tensors space	84
6.1	From $O(3)$ to $SO(3)$ subgroups	85
6.1.1	$O(3)$ and its subgroups	85
6.1.2	Symmetry group of an even order tensor	86
6.1.3	$SO(3)$ and its subgroups	87
6.2	Harmonic decompositions of $\mathbb{E}la$	89
6.2.1	3D harmonic tensor space: \mathbb{H}^n	89
6.2.2	Harmonic structure	91
6.2.3	Explicit harmonic decompositions	93
6.3	Symmetry classes of $\mathbb{E}la$	96
6.4	Condition of belonging to a symmetry class	98
6.4.1	Polynomial invariants and their limitation	99
6.4.2	Covariants: a geometric path	101
6.4.3	Covariant-based membership relations	102
7	3D exotic sets	105
7.1	Exotic sets of $\mathbb{E}la(3)$	106
7.1.1	Clips operation for $\mathbb{E}la(3)$	107
7.1.2	Determination of exotic sets	109
7.2	Covariants conditions for exotic sets	112
7.3	Exotic elastic materials	117
7.3.1	R_0 -orthotropy in \mathbb{R}^3	117
7.3.2	Triclinic exotic elastic material	121
7.3.3	Anisotropic materials with isotropic Young's modulus	123

IV	Conclusions and perspectives	126
A	Mathematical notations	130
B	Level set based topological derivative algorithm	133
B.1	Flowchart of the algorithm	133
B.2	Defining subdomains for different materials	133
B.3	Line search	134
B.4	Stopping criterion	134
C	Covariant criteria for tensor's symmetry	136
D	Generic and exotic sets of $\mathbb{E}la(3)$	140
D.1	Preliminary results of exotic sets for $\mathbb{E}la(3)$	141
D.2	Complete list of exotic sets for $\mathbb{E}la(3)$	144

Part I

State of the art

Chapter 1

Architected materials

1.1	Architected Materials (A.M.) in brief	9
1.2	Anisotropic linear elasticity of A.M.	13
1.3	Topology optimisation of multi-scale structure	15

This chapter remains a general review of related topics that are involved in my Ph.D. work. Firstly, a brief introduction to architected materials is given in [section 1.1](#), and the recent development in this field shows the importance of their corresponding anisotropic mechanical behavior. Several approaches that exist in literature are listed in [section 1.2](#) to analyze the anisotropic linear elasticity of a material. At the end, we present [section 1.3](#) several numerical methods for the design of architected materials.

1.1 Architected Materials (A.M.) in brief

Different types of architected materials

In response to the demand for lightweight, high-strength, impact- and shock-absorbing components in the industrial fields, the development of lightweight new materials or *architected materials* with better mechanical properties has become an important research direction [18, 19]. The development of new materials has a long lead time and high cost, which leads to limited applications. Therefore, the design of architected materials with specific mechanical properties has become a common approach. With the agreement of French mechanics at the conference of *Mécamat 2021+1* in Aussois, a definition of architected materials is provided:

1.1.1 Definition (Architected materials)

A material will be said to be architected if:

1. It presents, between its macrostructure and its microstructure, one or more other scales of organization of matter;
2. If the intermediate organization scales are commensurable with those of the microstructure and/or the macrostructure.

According to their spatial organisation modes, the variety of architected materials can be distinguished into three categories: periodic, quasi-periodic, and aperiodic. The applications for the last two modes can be found in [20, 21, 22, 23]. In my Ph.D., the *exotic material* will be designed with periodic mode, thanks to its simple computation limited to a unit cell. And in this case, the second condition of Definition 1.1.1 will nevertheless not be considered, since the non-standard behaviors of exotic materials are scale-independent.

A structure is periodic if the space is filled from specific translations of a single unit cell. And thanks to this particular organization, the physical properties are the same in the whole specimen, considering perfect geometries. The unit cell can be designed by different geometry types, including lattices (Figure 1.1a [24]), plate lattices (Figure 1.1b [25]), Triply Periodic Minimal Surfaces (TPMS in Figure 1.1c [26]).

- Lattice materials are spatial structures formed by combining multiple connecting rods in a lattice or lattice-like arrangement, including the common Face-Centred Cubic (BCC) and Diamond lattice materials [24, 27];
- Plate lattice materials have a specific arrangement of lattice grids that replace lattice nodes with plate vertices. By specific combinations, the plate lattice can generate multiple cavities, thereby achieving specific mechanical functions [28];
- TPMS architected materials are special spatially structured materials with continuous smooth surfaces in three independent directions [29].

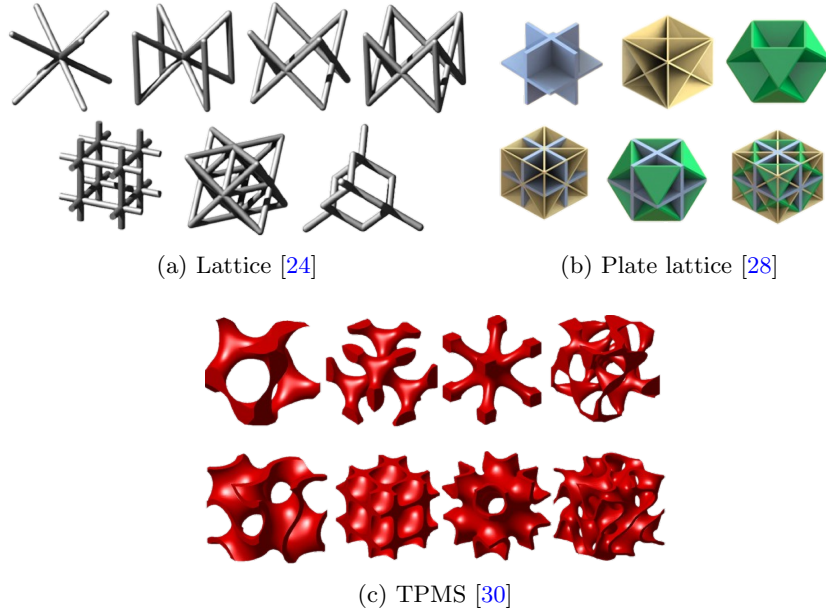


Figure 1.1: Different structure types of architected materials

The choice of a geometry type depends on the application field, since different geometry types possess different mechanical properties. Lattice materials exhibit excellent fatigue resistance and optimized bending deformability, making them suitable for the fabrication of bio-metamaterial components [27]. Plate lattice metamaterials have a uniform stress distribution and show minimal stress concentration when subjected to external loads. They can be used in the lightweight structural design of aerospace, automotive, and maritime applications [31]. The configuration of TPMS is similar to that of human bone tissue, exhibiting two distinct regions in space, free from any sharp bumps or depressions, which avoid stress concentration, and therefore can be used for the production of bone implants [30].

Additive manufacturing

Despite the significant advancements in the design of architected materials, the conventional subtractive manufacturing methods have proven inadequate in efficiently producing complex geometries. As a consequence, research on the concept of architected materials, especially for ultrafine complex structures, has been relatively limited since it was introduced [18, 19].

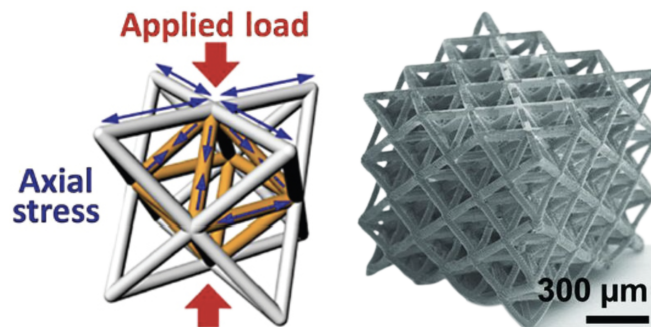
To meet the growing demand for producing A.M., the development of more efficient *additive manufacturing* technologies continues. They are technologies based on the discrete-stacking principle (instead of subtractive processes) for manufacturing metallic or non-metallic components. To be more specific, this technology discretises a 3D computer-aided design (CAD) model into 2D slices, scans these 2D slices layer by layer according to their shape, and produces the components according to a specific scan path and process parameters. Based on the above forming characteristics, additive manufacturing technology can produce A.M. with complex shapes and sizes ranging from meter to nanometer level. Since introduced in the late 1980s, additive manufacturing technology has come up with different processing methods [32]. They include, among others, StereoLithography Apparatus (SLA) [33], Fused Deposition Modeling (FDM) [34], Selective Laser Sintering (SLS) [35], Selective Laser Melting (SLM) [36], Laminated Objective Manufacturing (LOM) [37], Three Dimensional Printing (3DP) [38], and Laser Metal Deposition (LDM) [39]. It should be noted that different additive manufacturing technologies have different characteristics due to their distinct forming methods and thus there are significant differences in the formed materials, including size, resolution, and surface quality. It is necessary to choose an appropriate

technology based on the requirement of the desired material.

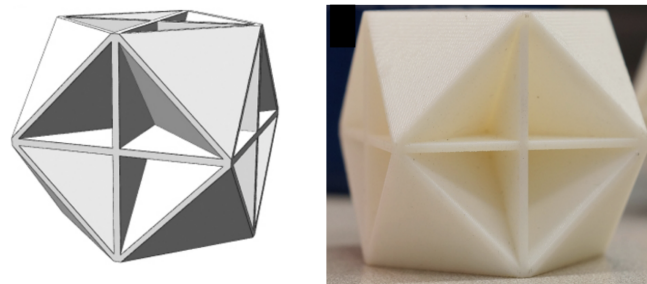
Recent progress in architected materials

In the past years, remarkable advancements in additive manufacturing [40] have catalyzed an accelerated growth of architected materials. These materials possess special physical properties not found in natural materials [41]. Since 2014, there have been exciting new studies in the field that significantly expanded available mechanical property spaces as well as introduced new properties not available before. They will be introduced as follows.

Figure 1.2 shows some of the examples of the recent developments: Zheng *et al.* [42] reported an ultralight and ultra-stiff (a substantial load bearing capability has been observed) materials with the minimum density of $0.87\text{kg}/\text{m}^3$, it is realized based on the rational design of architecture followed by high-resolution 3D printing (Figure 1.2a). In the same year, Meza *et al.* [43] reported 3D ceramic lattices with the same architecture. It performs high stiffness and, moreover, despite the fragility of ceramic, which tends to undergo plastic deformation or fracture under large deformation, the reported material could recover its original architecture shape after large deformation. The recent study by Berger *et al.* [31] achieved a geometry design (Figure 1.2b) that can realize a theoretical upper bound of isotropic elastic stiffness and the theoretical limit of Hashin-Shtrikman upper bounds. And it doesn't end there, there are many studies in the literature that expanded available material property spaces [44, 45].



(a) Octet-truss unit cells packed into a cubic microlattice [42]



(b) A 3D printed model of the foam's cellular structure with isotropic elastic stiffness and theoretical limit

Figure 1.2: Recent development on architected materials

Beyond expanding available property spaces, there have also been works tending to generate new properties or behaviours. In particular, there have been active studies that harness mechanical instability for specific behaviours. This topic is addressed in the Ph.D. thesis of Rachel Azulay [46] under the supervisor of Justin Dirrenberger. They proposed a method based on group theory to predict the possible

patterns of a stack of architected materials following a bifurcation. Besides, Shan *et al.* [47] and Frenzel *et al.* [48] reported architected materials (Figure 1.3a) with reusable energy absorption by harnessing mechanical instability. Beyond quasi-static loading conditions, there were also studies reporting architected materials for dynamic loading such as elastic wave propagation. Shan *et al.* [49] reported an architected material (Figure 1.3b) with tunable vibration propagation and absorption by triggering different mechanical instability-induced pattern formation; Matlack *et al.* [50] reported an architected material (Figure 1.3c) with low-frequency broadband vibration absorption. Raney *et al.* [51] reported stable propagation of mechanical signals in soft media (Figure 1.3d) by storing elastic strain energy using mechanical instability.

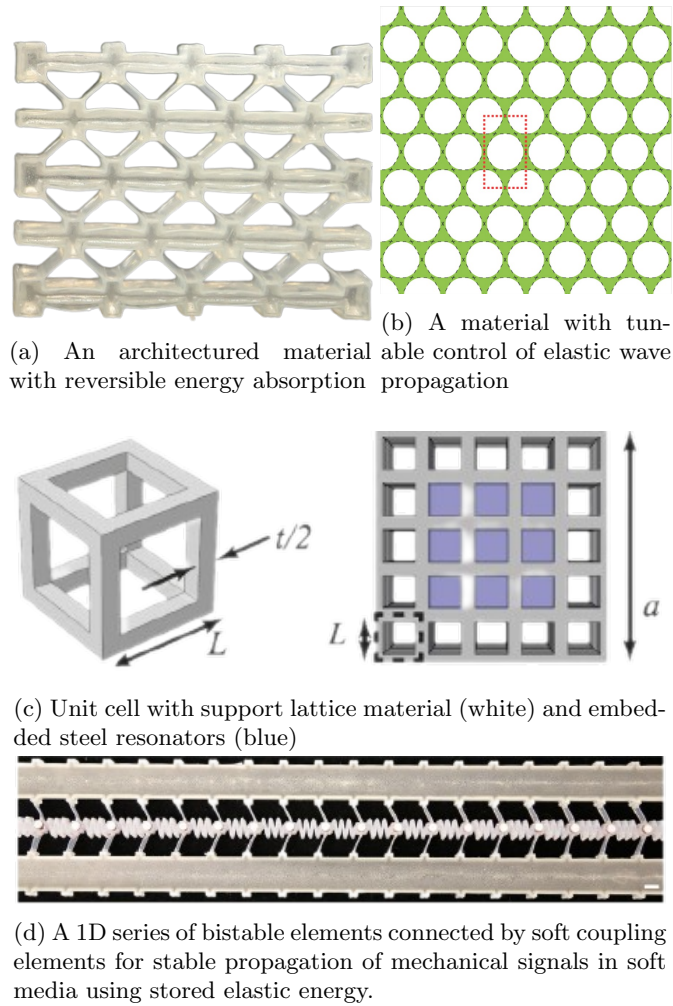


Figure 1.3: Four architected materials in the literature that harness mechanical instability for specific behaviours.

Moreover, there have been also studies that reported architected materials with unusual or exotic properties such as negative Poisson’s ratio materials [52], negative bulk modulus materials [53], pentamode materials [54]. These examples demonstrate the cases where architected materials exhibit properties that are different from their constituents, which gives us intriguing new opportunities for the design of materials and structure. However, the previously listed exotic properties concern mainly the isotropic part. Indeed, what makes architected materials truly intriguing is that their unusual mechanical properties stem not from the properties of their individual components, but rather from the intricate geometry of their unit cell. Since the internal geometry is added as a new variable, it is natural to think about the

resulting anisotropy properties. Some non-standard anisotropic linear elasticities have also been observed by researchers. We introduce as follows two of them.

In 2D, the early paper of Vannucci [9] has shown the existence of a particular type of planar orthotropic material, the number of independent elastic constants for this kind of material is three (as for the case of tetragonal symmetry) instead of four for a general orthotropic layer, meaning that it cannot be revealed only by using symmetry conditions. Indeed, this kind of material has been obtained by using the polar formalism, introduced in 1982 by Verchery [55], in which an extra condition is added compared to a standard orthotropic material. This kind of material is named for the sake of brevity as *R₀-orthotropy*. The reasons that make *R₀-orthotropic* laminate rather interesting for application are well-discussed in [9], and it comes up with a method to obtain *R₀-orthotropic* composite laminate. Besides, for the 3D case, Rychlewsky [8] and He [10] have shown that anisotropic (orthotropic or transversely isotropic) materials could have their Young or shear or area modulus isotropic. However, the related architected material designs for these cases have never been proposed. Moreover, similar studies on the non-standard anisotropic properties have not received much attention.

With the current advancement in A.M. technology, we now have the opportunity to revisit this topic and conduct further research focusing on the following two aspects:

- to explore the whole range of elastic materials and identify the non-standard anisotropic elastic materials;
- to propose a complete design methodology adapted to architected materials.

This research is part of the MAX-OASIS (Matériaux Architecturée eXotique, Ondes, AniSotropie, InStabilités) project funded by ANR (AAP2019). The reason for us to be interested in the aforementioned aspects is to provide a unified perspective on architected materials with respect to their anisotropic mechanical properties and, above all, the cases scattered here and there in the literature can be shown to be the special ones of what is obtained through the application of these theoretical investigations.

1.2 Anisotropic linear elasticity of A.M.

Anisotropy characterizes the way a physical property varies with respect to material directions. Linear properties, such as elasticity or conductivity, are encoded using constitutive tensors. Depending on their order, these tensors can model different types of anisotropies ranging from complete anisotropy to isotropy. These different possibilities are called *symmetry classes*. Different definitions of symmetry classes can be found in the literature [5, 56, 57], and for my thesis, I will adopt the definition proposed by Forte and Vianello [5], which will be detailed in [chapter 2](#). For linear elasticity, a definite classification was obtained in the same reference as well as in [57] that the space of 3D elasticity tensors is partitioned into 8 symmetry classes. These results are deduced by using *group theory*. Based on it, Olive et al. [58, 59] have developed a tool, called *clips operation*, to determine the symmetry classes of the direct sum of two spaces. Combined with the harmonic decomposition, clips operations allow the computation of the symmetry classes of the elasticity tensor space.

Another question now is how to identify the symmetry class of a given constitutive tensor. For the case of linear elasticity, in addition to experimental and numerical approaches, the literature is abundant in theoretical investigations that focus on developing coordinates-free criteria for characterizing the symmetry class of a given elasticity tensor. The most elementary approach is based on the matrix of tensor's

components with respect to a given basis of \mathbb{R}^6 . Some authors have used the *Kelvin representation* of the elasticity tensor to achieve this goal [60, 61, 62], which consists in formulating necessary and sufficient conditions involving multiplicity of the 6 eigenvalues of the Kelvin representation and of the eigenvalues of its eigentensors (second-order tensors).

Besides, there are alternative treatments in the literature relying on geometrical approaches to provide a *visual* intuition on this algebraic problem. For 2D case, the polar method is introduced by Verchery [55] as early as 1982 to treat anisotropic plan problems, it is a frame-independent approach, for which one can explicit the symmetry conditions by polar invariant [63]. It is rewritten by Desmorat [64] in a tensorial form by tensorial polar decomposition: a 2D elasticity tensor can be expressed thanks to two scalars and to two symmetric second-order deviatoric tensors, through which symmetry classes can be explicitly appeared. However, as mentioned before, this method is limited to \mathbb{R}^2 . As for \mathbb{R}^3 , François [65] has proposed a pole figure-based approach, the method of which consists in considering a function over a unit sphere, constructed from the tensor representation, the zeros of which indicate the normal vectors to physical symmetry planes. Huang et al. [66] extended this method into a 6-th order tensor based on the fact that to every symmetry class, a set of symmetry planes can be associated. This association is nevertheless not one-to-one. Remarkable efforts have gone into *harmonic decomposition* of the elasticity tensor followed by the initial work of Backus [67]. This approach allows to extract partial information about the symmetry class of an elasticity tensor from its harmonic components. To this end, Maxwell [68] has proposed a graphical approach, which is to treat a harmonic tensor of order n as a n -tuple vector, the Maxwell multipoles. Backus [67] has used these multipoles to detect different symmetry classes of elasticity tensors. This approach is also used in [69, 70, 71].

More recently, based on the harmonic decomposition, the question of classification of elasticity tensor is reconsidered in the general framework of *Real Algebraic Geometry* [72, 73]. For the 2D case, the computation is quite simple and already done by Vianello [74] (see also [75]) for the full 2D elasticity tensor. As for 3D, in [76], the authors have used a generating set of the invariant algebra of fourth-order harmonic tensors proposed in [77] to characterize the symmetry classes of this tensor. However, this approach becomes increasingly complicated with respect to full 3D elasticity tensor, and to the best of the author’s knowledge, the determination of its symmetry classes using this approach has not been documented in the literature. Under this context, the recent work of Olive et al. [78] has proposed an alternative approach to solve this classification problem via polynomial covariants instead of invariants, and in this way, the symmetry classes of an elasticity tensor are characterized by polynomial equations involving its covariants. Moreover, in [79], authors proposed an effective geometrical approach to recover the normal form of a given elasticity tensor by using its covariants, and based on it, determining its symmetry class. The aforementioned approaches are summarised in Figure 1.4.

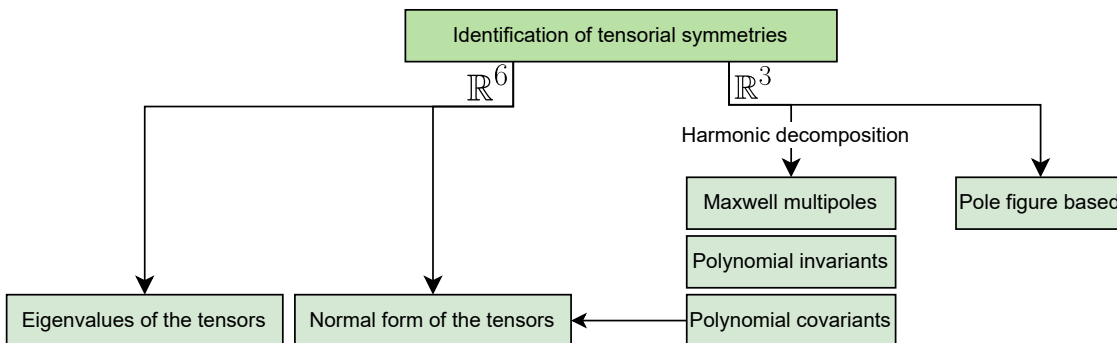


Figure 1.4: Approaches listed in the literature to identify the 3D tensorial symmetries

Despite the well-developed approaches in the literature to identify the symmetry classes of elasticity tensor, the intermediate possibilities (non-standard anisotropic properties such as R_0 -orthotropy) beyond the symmetry classes have never been clearly identified. Indeed, the clips operation allows to describe the linear material space in a very fine way and to detect materials with non-standard anisotropic properties. The objective of my Ph.D. is to first establish the whole range of symmetry possibilities both in \mathbb{R}^2 and \mathbb{R}^3 , and then to identify them by polynomial equations involving invariants or covariants of the elasticity tensor.

The mesostructure of materials with non-standard anisotropic linear elasticity is obtained using an optimization problem and the proposed polynomial conditions can be efficiently integrated into this problem as the cost function. The cost function is expressed in terms of the effective elasticity tensor computed using the homogenization approach [80, 81]. Moreover, the formulation of such optimization problem is not limited to classical elasticity, it can be extended to other constitutive laws.

1.3 Topology optimisation of multi-scale structure

Topology optimization involves optimizing the material distribution within a discretized design domain to generate a specific structural layout that maximizes performance while meeting relevant design specifications. This notion was originally introduced by Bendsøe and Kikuchi [82]. However, due to the manufacturing difficulties of multi-scale materials, it is generally used in mono-scale structure optimisation [83, 84, 85] (Figure 1.5a). Over the past few years, along with advances in AM technology, there has been a renewed enthusiasm in the optimal design of multi-scale structures (Figure 1.5b). The mono-scale modeling used to mono-scale structure optimisation can also be used to design multi-scale structures by using finer meshes of the design domain. And it is referred to as full-scale approaches¹. However, it requires an enormous augmentation in computational cost. The proposed multi-scale modeling is beneficial for computational efficiency by using a homogenisation approach [82]. Here, the theory of homogenisation is proposed to bridge the scale between the microscopic geometries and their effective properties on the macro-scale. The multi-scale modeling based on homogenisation approach will be used in this thesis for the design of periodic architected materials.

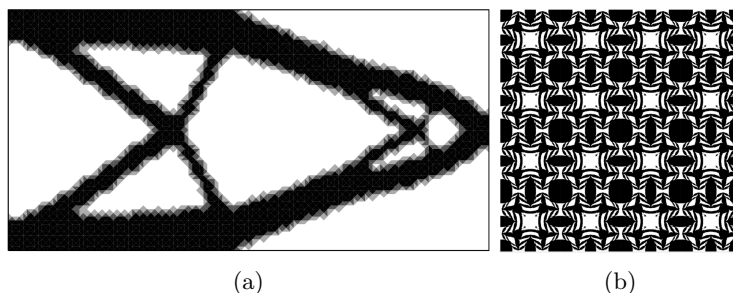


Figure 1.5: Two different optimisation modellings (a) Mono-scale modelling [1] and (b) Multi-scale modelling [2]

Given the rapid development of topology optimisation of multi-scale structures over the last three decades, a variety of optimisation methods have been proposed, among which the density-based method [84, 85], the level set method [86, 87] and the topological derivative [88] are the most representatives.

¹Topology optimisation approaches are classified into mono-scale (or full-scale) and multi-scale approaches, according to whether or not the separation of length scales is assumed in the modeling.

Density-based method

The density-based method performs a continuous optimisation strategy instead of the original 0-1 discrete optimisation problem. For this method, the previously proposed homogenisation approach will not be used since it is difficult to implement for mathematical complications. Subsequently, an alternative method named solid isotropic material with penalisation (SIMP) was proposed [89]. This approach represents the material distribution within a design domain using a scalar field, where each element in the discretized domain is assigned a relative density value ($\rho = 1$ means solid and $\rho = 0$ means empty). Each element is considered as isotropic and homogeneous. Material property (i.e. Young's modulus) is obtained by a power law, in which a penalisation parameter p (exponent of the power law) is involved:

$$E(\rho_i) = \rho_i^p E_0$$

The choice of the penalisation parameter depends strongly on the physical problem being solved [90]. It should be noted that this factor effect only works in the presence of a volume constraint. The SIMP approach is easy to implement and has been embedded in commercial software [91, 92].

Level set method

The level set method defines the boundary of the design by the zero level smooth contour of the level set function, the distribution of the material in the design domain depends on the level set value: $\rho = 1$ if the level set function takes the positive value and $\rho = 0$ if inversely [87, 93].

Most often the level set function is updated during the optimisation process via the use of the Hamilton-Jacobi equation, which is composed of two parts:

- the design evolution (shape sensitivity) in the optimisation process.
- the speed function, scaled by the spatial gradient of the level set function, used to control the design evolution speed [94]. The speed function is developed by introducing new models or methods, following the work in [95, 96].

Nevertheless, it is important to acknowledge that this level-set method has certain limitations. One notable drawback is their constraint on geometry evolution, as they can only modify existing boundaries and are unable to generate new voids within a solid material, this method primarily facilitates shape evolution rather than significant changes in topology. Figure 1.6 illustrate the difference between shape optimisation and topology optimisation.

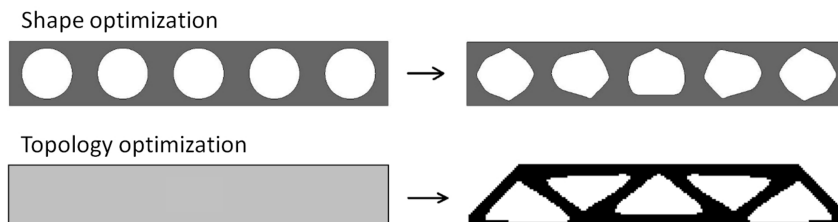


Figure 1.6: Comparison of shape optimisation and topology optimisation [3]

To nucleate new holes, the original form of the Hamilton-Jacobi equation has been augmented by adding new terms [96, 97]. Although updating the level set function through the solution of the Hamilton-Jacobi equation has demonstrated significant potential, the numerous formulations of the Hamilton-Jacobi

equations and the intricacies involved in constructing the speed function introduce additional complexity to the process. To solve this, another level set method (independent of the Hamilton-Jacobi equation) that allows for the nucleation of new holes will be discussed later.

Topological derivative method

The use of topological derivatives in topology optimisation was initiated by Eschenauer et al. [98]. The main idea is to predict the influence of introducing an infinitesimal hole at any point in the design domain. This influence is measured by topological gradient [88, 99]. One interesting branching of this method is that it connects the sensitivity of the macroscopic effective properties (obtained in the context of homogenisation) response with changes in the underlying microstructure. And in this way, gives an optimisation direction to get an optimal design. The main drawback of this procedure is its inability to add matter in some places where it has been removed 'by mistake' at the previous iteration [1].

Lately, hybrid approaches have appeared, such as the topological derivative combined with a level-set domain representation [2]. Unlike the conventional level-set methods relying on the use of the Hamilton-Jacobi equation, which is highly dependent on the initial guess, the proposed topological derivative allows all kinds of topology changes. It is already applied to the synthesis of elastic micro-structures [2, 100], with macroscopic properties estimated by the multi-scale framework and periodic homogenisation.

To be more specific, the topological sensitivity relies on an exact formula, it has been proposed in [101], considering concepts of topological asymptotic analysis and topological derivative. Therefore, the key advantage of this method is that the sensitivities are obtained in an exact form, enabling the utilization of simpler optimization algorithms. This eliminates the need for artificial algorithmic parameters, leading to a more straightforward and robust optimization process. This method will be used in my thesis to realise the design of multi-scale architected materials, more details can be found in [chapter 5](#).

Chapter 2

Geometry of tensor spaces

2.1	Linear elastic constitutive law	19
2.2	$SO(d)$ and $O(d)$ linear representation on $\mathbb{E}la(d)$	20
2.3	Harmonic decomposition	23
2.4	Definition of elastic materials	24
2.5	Invariants and integrity basis	26
2.6	From symmetry group to symmetry class	27
2.6.1	Symmetry group	28
2.6.2	Symmetry class	29
2.6.3	Clips operation	29
2.7	Symmetry stratum	30

This chapter is essentially based on publications [75, 102, 103, 104]. These are works starting from the 1980s, G. Verchery [55], M. Vianello [74], and others built fundamental knowledge on the study of linear elastic tensors space. During the thesis of N. Auffray [105], these notions have been recapped to explore the anisotropic linear properties of cellular materials. It is extended later during his collaboration with mathematicians B. Kolev [76, 106] and M. Olive [58, 59]. This chapter will present their results and provide some valuable mathematical tools for exploring the geometry of linear elastic tensors space.

2.1 Linear elastic constitutive law

To begin this chapter, we will consider the Euclidean affine space of dimension d ($d = 2, 3$) as a model of the physical space \mathbb{E}^d . In this model, the *body* is considered as a closed domain Ω embedded in \mathbb{E}^d (Figure 2.1) and having attached to each of its points $P \in \Omega$ a microstructure. This microstructure can be a crystalline network, the organization of polymer chains, the weaving of textiles, etc., depending on the nature of the material being studied [107].

Let O be a fixed origin, and each point P is associated by a unique vector $\underline{x}^P = \underline{OP}$ in vector space \mathbb{V}^d . Consider $\mathcal{B} = \{\underline{e}_1, \underline{e}_2, \dots, \underline{e}_d\}$ be an orthonormal basis of \mathbb{V}^d and $\mathcal{R} = (O, \mathcal{B})$ the associated coordinate system, we have:

$$\underline{x}^P = x_1 \underline{e}_1 + x_2 \underline{e}_2 + \dots + x_d \underline{e}_d.$$

with $(x_1, x_2, \dots, x_d)_{\mathcal{B}}$ the corresponding coordinates.

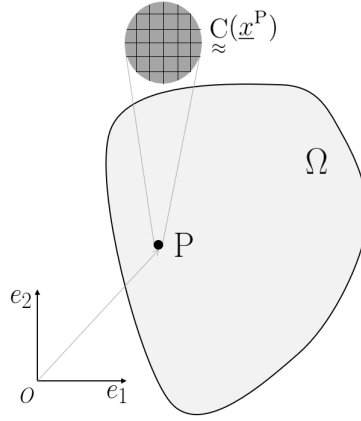


Figure 2.1: Representation of the domain Ω in a given reference frame ($d = 2$)

In the present work, we will assume the hypothesis of infinitesimal strain theory. The stress tensor $\underline{\sigma} \in S^2(\mathbb{R}^d)$, represents the stress state at each point P , with $S^2(\mathbb{R}^d)$ the vector space of real symmetric tensors of order 2 in dimension d . The infinitesimal strain tensor has the following definition:

$$\underline{\varepsilon} = \frac{1}{2}(\underline{u} \otimes \underline{\nabla} + \underline{\nabla} \otimes \underline{u}),$$

in which \underline{u} is the displacement vector at a point of Ω . In components with respect to \mathcal{B} , it has the following expression:

$$\varepsilon_{ij} = \frac{1}{2}(u_{i,j} + u_{j,i}),$$

in which $u_{i,j}$ denote the partial derivation with respect to x_i .

It remains now to describe the relationship between the stress $\underline{\sigma}$ and the strain $\underline{\varepsilon}$ at any point of the solid. Such a relationship is given by a constitutive law. For linear elasticity, the elasticity tensor $\underline{\underline{C}}$ is introduced to construct a linear relation between $\underline{\sigma}$ and $\underline{\varepsilon}$ [108]:

$$\underline{\sigma} = \underline{\underline{C}} : \underline{\varepsilon}, \quad \sigma_{ij} = C_{ijkl} \varepsilon_{kl}, \quad (2.1)$$

in which $\underline{\underline{C}}$ provides the elastic coefficients of the material located at P .

The elasticity tensor $\underline{\underline{C}}$ is a linear application of the space $S^2(\mathbb{R}^d)$ to itself, i.e. $\underline{\underline{C}} \in \mathcal{L}(S^2(\mathbb{R}^d))$.

Consequently, $\underset{\approx}{\mathbb{C}}$ is a fourth-order tensor with minor index symmetries:

$$C_{ijkl} = C_{jikl} = C_{ijlk},$$

which will be denoted as $C_{(ij)(kl)}$. We also have the major symmetry when we consider the potential energy associated with the elastic behaviour:

$$C_{ijkl} = C_{klij},$$

which is denoted as $C_{\underline{ij}\underline{kl}}$. The index symmetries of $\underset{\approx}{\mathbb{C}}$ are thus summarised by $C_{\underline{(ij)}\underline{(kl)}}$. The space of tensors with such index symmetries will be denoted by $\mathbb{E}la(d)$:

$$\mathbb{E}la(d) := \{\underset{\approx}{\mathbb{C}} \in \otimes^4 \mathbb{R}^d \mid C_{\underline{(ij)}\underline{(kl)}}\},$$

where d is the dimension of the physical space. To make reading easier, $\mathbb{E}la(d)$ and \mathbb{V}^d will be abbreviated respectively to $\mathbb{E}la$ and \mathbb{V} in this chapter, as there is no ambiguity concerning the dimension.

To be physically admissible, all elasticity tensors should have their inversions. We will denote by $\mathbb{E}la^*$ to represent the space consisting of elasticity tensors possessing their inversions. Compared to $\mathbb{E}la$, the elasticity tensors with zero determinant are eliminated in $\mathbb{E}la^*$. Besides, an elasticity tensor, considered as a quadratic form on $S^2(\mathbb{R}^d)$, should be positive definite, meaning that its eigenvalues λ_i should verify

$$\exists M \in \mathbb{R}^{*+}, \quad 0 < \lambda_i \leq M.$$

Let us denote by $\mathbb{E}la^+$ the set of elasticity tensors that satisfy this requirement. We have the following property

$$\forall \underset{\approx}{\mathbb{C}} \in \mathbb{E}la^+, \exists! \underset{\approx}{\mathbb{S}} \in \mathbb{E}la^+, \underset{\approx}{\mathbb{S}} : \underset{\approx}{\mathbb{C}} = \underset{\approx}{\mathbb{C}} : \underset{\approx}{\mathbb{S}} = \underset{\approx}{\mathbb{I}},$$

with $\underset{\approx}{\mathbb{I}} = \underset{\approx}{1} \otimes \otimes \otimes \underset{\approx}{1}$ the identity of $S^2(\mathbb{R}^2)$, and $\underset{\approx}{1}$ the identity of \mathbb{R}^2 . Such an element is known as the compliance tensor and allows inverting the constitutive law

$$\underset{\approx}{\sigma} = \underset{\approx}{\mathbb{C}} : \underset{\approx}{\varepsilon} \Leftrightarrow \underset{\approx}{\varepsilon} = \underset{\approx}{\mathbb{S}} : \underset{\approx}{\sigma}.$$

In the following the notation $\underset{\approx}{\mathbb{S}} = \underset{\approx}{\mathbb{C}}^{-1}$ and $\underset{\approx}{\mathbb{C}} = \underset{\approx}{\mathbb{S}}^{-1}$ will be used.

We may consider the application, $\varphi : \Omega \mapsto \mathbb{E}la$, which associates to any point $P \in \Omega$ an elasticity tensor $\underset{\approx}{\mathbb{C}}(\underline{x}^P)$ (Figure 2.1). Thus, we have:

$$\underline{x}^P \xrightarrow{\varphi} \varphi(\underline{x}^P) = \underset{\approx}{\mathbb{C}}(\underline{x}^P).$$

In the case of homogeneous materials or structures, the dependence on solid point disappears and for $\forall P \in \Omega, \varphi(\underline{x}^P) = \underset{\approx}{\mathbb{C}}$. When it comes to mesostructure optimisation, its anisotropy properties will be a crucial issue. The following sections aim to describe how elasticity tensors are transformed when subjected to an orthogonal transformation (i.e. linear isometry). Based on it, we can identify the anisotropic class to which the given elasticity tensor belongs.

2.2 $SO(d)$ and $O(d)$ linear representation on $\mathbb{E}la(d)$

The linear elastic anisotropy of a material is related to the invariance properties of its elasticity tensor with respect to linear isometries (under the transformations of rotation, reflection, and their combination).

Group

Before studying how tensors transform, we will investigate, in a first step, the notion of transformations. Transformations of a material verify a few properties: firstly, carrying out two transformations one after the other is always equivalent to carrying out a single third transformation. Additionally, each transformation has an inverse that reverses it thanks to an identity transformation. These kinds of transformation sets are referred to as *group*.

2.2.1 Definition (Group)

A *group* is a set G together with a multiplication on G which satisfies four axioms [109]:

1. (Closed) Multiplication of any ordered pair \mathbf{g}, \mathbf{h} of elements from the set G imply a unique "product" $\mathbf{g} \cdot \mathbf{h}$ which also lies in the set G .
2. (Associative) $\mathbf{g} \cdot (\mathbf{h} \cdot \mathbf{k}) = (\mathbf{g} \cdot \mathbf{h}) \cdot \mathbf{k}$ for any three (not necessarily distinct) elements from G .
3. (Existence of an identity element) there is an element $\mathbf{e} \in G$, called an identity element, such that $\mathbf{g} \cdot \mathbf{e} = \mathbf{e} \cdot \mathbf{g} = \mathbf{g}$ for $\forall \mathbf{g} \in G$.
4. (Existence of an inverse) each element $\mathbf{g} \in G$ has a (so called) inverse \mathbf{g}^{-1} which belongs to the set G and satisfies $\mathbf{g}^{-1} \cdot \mathbf{g} = \mathbf{e} = \mathbf{g} \cdot \mathbf{g}^{-1}$.

When we talk about linear isometries, apart from the previous four axioms, they also exhibit another property: conservation of the scalar product. To exploit the mathematical interpretation of this conservation, we take vectors in the space \mathbb{R}^d as an example, in which case, the conservation is shown as follows.

Example 1

Let $\underline{\mathbf{u}}, \underline{\mathbf{v}}$ be two vectors in space \mathbb{V}^d , let $\langle \underline{\mathbf{u}}, \underline{\mathbf{v}} \rangle$ their scalar product, and G the group of linear isometries, for $\forall \mathbf{g} \in G$, the conservation of scalar product gives us:

$$\langle \underline{\mathbf{u}}^*, \underline{\mathbf{v}}^* \rangle = \langle \mathbf{g} \cdot \underline{\mathbf{u}}, \mathbf{g} \cdot \underline{\mathbf{v}} \rangle = \langle \underline{\mathbf{u}}, (\mathbf{g}^T \cdot \mathbf{g}) \underline{\mathbf{v}} \rangle = \langle \underline{\mathbf{u}}, \underline{\mathbf{v}} \rangle$$

Since $\mathbf{g}^T \cdot \mathbf{g} = \mathbf{I}_n$ with \mathbf{I}_n the identity tensor of order n , we have :

$$\mathbf{g}^T = \mathbf{g}^{-1} \tag{2.2}$$

The transformation which satisfies the Equation 2.2 is called an orthogonal transformation. Although the example is given for vectors, it is also valid for n -th order tensors in \mathbb{R}^d .

The set of orthogonal transformations is the *orthogonal group*, denoted by $O(d)$. It is the group of all linear isometries of \mathbb{R}^d , defined by :

$$O(d) := \{ \mathbf{g} \in \text{GL}(d) \mid \mathbf{g}^T = \mathbf{g}^{-1} \}. \tag{2.3}$$

with $\text{GL}(d)$ the group of invertible linear transformations of \mathbb{R}^d , i.e. $\mathbf{g} \in \text{GL}(d)$ iff $\det(\mathbf{g}) \neq 0$.

Remark. Let $\mathbf{g} \in O(d)$, the determinant

$$\det(\mathbf{g} \cdot \mathbf{g}^T) = \det(\mathbf{g}) \times \det(\mathbf{g}^T) = (\det(\mathbf{g}))^2 = 1.$$

We can conclude that the elements of the group $O(d)$ can be classified into 2 categories according to the value of the determinants of \mathbf{g} :

- $\det(\mathbf{g}) = 1$: they are rotations or products of an even number of reflections. We notice that if $\det(\mathbf{g}_1) = 1$ and $\det(\mathbf{g}_2) = 1$ then $\det(\mathbf{g}_1\mathbf{g}_2) = 1$, so the rotations form a subgroup of $O(d)$, it is denoted by $SO(d)$,
- $\det(\mathbf{g}) = -1$: these are transformations with an odd number of reflections among them. Note that these elements do not form a subgroup of $O(d)$ because either $\det(\mathbf{g}_1) = -1$ or $\det(\mathbf{g}_2) = -1$, but $\det(\mathbf{g}_1\mathbf{g}_2) = 1$.

Group representation

We have defined the groups $O(d)$ and $SO(d)$ and now we are ready to look how a linear group acts on an elasticity tensor. Such an action is described by the mathematical theory of *group representation*, which is essentially a way to represent the action of the elements of a group on a vector space.

2.2.2 Definition (Group representation)

Let G be any group and \mathbb{V} a vector space. A representation of G on \mathbb{V} is a morphism from G into $GL(\mathbb{V})$:

$$\rho : G \rightarrow GL(\mathbb{V})$$

For each element $\mathbf{g}_1, \mathbf{g}_2 \in G$, we have $\rho(\mathbf{g}_1\mathbf{g}_2) = \rho(\mathbf{g}_1)\rho(\mathbf{g}_2)$ and for the identity element $\mathbf{e} \in G$, we have $\rho(\mathbf{e}) = I_{\mathbb{V}}$, with $I_{\mathbb{V}}$ the identity tensor on \mathbb{V} . The group representation is denoted by (ρ, \mathbb{V}, G) , when there is no ambiguity about G , we simply note (ρ, \mathbb{V}) .

Two representations (ρ_1, \mathbb{V}_1) and (ρ_2, \mathbb{V}_2) of G are said to be *equivalent* if there exists an isomorphism φ such that:

$$\forall \underline{v}_1 \in \mathbb{V}_1, \forall \mathbf{g} \in G \quad \varphi(\mathbf{g} \cdot \underline{v}_1) = \mathbf{g} \cdot \varphi(\underline{v}_1)$$

meaning that the following diagram is commutative:

$$\begin{array}{ccc} \mathbb{V}_1 & \xrightarrow{\varphi} & \mathbb{V}_2 \\ \rho_1(\mathbf{g}) \downarrow & & \downarrow \rho_2(\mathbf{g}) \\ \mathbb{V}_1 & \xrightarrow{\varphi} & \mathbb{V}_2 \end{array}$$

Consider now the case $\mathbb{V} = \mathbb{T}^n(\mathbb{R}(d))$, with $\mathbb{T}^n(\mathbb{R}(d))$ a n -th order tensorial vector space in $\mathbb{R}(d)$, it will be abbreviated to \mathbb{T}^n in later contents. The image of $T \in \mathbb{T}^n$ by $\mathbf{g} \in G$ is given by $\rho(\mathbf{g})(T)$. Its expression in components reads:

$$(\rho(\mathbf{g})(T))_{i_1 i_2 \dots i_n} = g_{i_1 j_1} g_{i_2 j_2} \dots g_{i_n j_n} T_{j_1 j_2 \dots j_n},$$

To simplify the reading, \star is used to represent the group action \mathbf{g} on the space \mathbb{T}^n and is expressed in an orthonormal basis by:

$$(\mathbf{g} \star T)_{i_1 i_2 \dots i_n} = g_{i_1 j_1} g_{i_2 j_2} \dots g_{i_n j_n} T_{j_1 j_2 \dots j_n}.$$

For the case of $\mathbb{T}^n = \mathbb{E}la$ and $G = O(d)$, the notion of representation is used to describe the transfor-

mation of an elasticity tensor. For any $\mathbf{g} \in O(d)$ and $\mathbb{C} \in \mathbb{E}la$, we have:

$$\bar{\mathbb{C}}_{\approx} = \mathbf{g} \star \mathbb{C}. \quad (2.4)$$

In components, with respect to \mathcal{B} , this action is as follows:

$$\bar{C}_{ijkl} = g_{im}g_{jn}g_{kp}g_{lq}C_{mnpq}. \quad (2.5)$$

2.3 Harmonic decomposition

As isometric transformations of elasticity tensors are described by $O(d)$ representation on $\mathbb{E}la$, in order to know the anisotropic elastic properties of a given material, it remains now to determine the anisotropic class of a given elasticity tensor. However, since it is a fourth-order tensor, the order of associated transform reaches to 8 (as illustrated in Equation 2.5, $g_{im}g_{jn}g_{kp}g_{lq}$ is of order 8), and their different parts transform differently: some components are left fixed while others transform at different speeds. To understand these different mechanisms of transformation, we will have to decompose the corresponding space into a direct sum of irreducible elementary spaces under the action of the group $O(d)$.

Stability and irreducibility

We first introduce some essential notions for the decomposition of \mathbb{V} into irreducible spaces \mathbb{V}_i .

2.3.1 Definition (Stability and irreducibility)

A space \mathbb{V} is said to be G -stable if:

$$\forall \mathbf{v} \in \mathbb{V}, \forall \mathbf{g} \in G, \mathbf{g} \star \mathbf{v} \in \mathbb{V}$$

The linear representation (ρ, \mathbb{V}) is irreducible if $\{0\}$ and \mathbb{V} are the only stable subspaces of \mathbb{V} .

Due to Peter-Weyl's theorem [110], it is known that any finite-dimensional representation \mathbb{V} of a group G can be decomposed as a direct sum of irreducible finite-dimensional representations:

$$\mathbb{V} \simeq \mathbb{V}_{k_1} \oplus \mathbb{V}_{k_2} \oplus \cdots \oplus \mathbb{V}_{k_n}$$

Such a decomposition is said to be G -irreducible. For each k_i , $(\rho_{k_i}, \mathbb{V}_{k_i})$ is an irreducible representation of G , and \simeq denotes an G -equivariant isomorphism.

We also consider the isotypic decomposition in which equivalent factors are grouped :

$$\mathbb{V} \simeq \alpha_1 \mathbb{V}_{k_1} \oplus \alpha_2 \mathbb{V}_{k_2} \oplus \cdots \oplus \alpha_n \mathbb{V}_{k_n}, \quad \alpha_i \mathbb{V}_{k_i} := \bigoplus_{l=1}^{\alpha_i} \mathbb{V}_{k_i}$$

The integer α_i indicates the multiplicity of \mathbb{V}_{k_i} into the decomposition. The advantage of such irreducible decomposition is that it allows us to study a complicated object as a collection of simple ones.

Harmonic structure

When applied to orthogonal group $O(d)$ ($d \in \{2, 3\}$), the isotypic decomposition is often referred to as the *harmonic decomposition* [67]. We denote $\mathbb{H}^n(\mathbb{R}^d)$, the space of harmonic tensors. The notion of harmonic tensors was introduced by G. Backus in [67].

2.3.2 Definition (Harmonic tensors)

A tensor $H \in \mathbb{H}^n(\mathbb{R}^d)$ is called a harmonic tensor if it satisfies the following properties:

- Tensor of order n ;
- Total symmetry with respect to index permutation;
- $\text{tr}H = 0$ in which $\text{tr}H$ represents the contraction of any two indices i, j .

Any tensor space \mathbb{T}^n can be decomposed into a finite number of harmonic spaces under the group $O(d)$ [106], we have:

$$\mathbb{T}^n \simeq \bigoplus_{i=1}^q \mathbb{H}^{k_i}(\mathbb{R}^d)$$

with $k_i < +\infty$ and \simeq represents a $O(d)$ -equivariant isomorphism. As mentioned for irreducible decompositions, we can group together harmonic spaces of the same order :

$$\mathbb{T}^n \simeq \bigoplus_{i=1}^m \alpha_i \mathbb{H}^{k_i}(\mathbb{R}^d), \quad \alpha_i \mathbb{H}^{k_i}(\mathbb{R}^d) = \bigoplus_{l=1}^{\alpha_i} \mathbb{H}^{k_i}(\mathbb{R}^d) \quad (2.6)$$

the integer α_i indicates the multiplicity of $\mathbb{H}^{k_i}(\mathbb{R}^d)$, such isotypic decomposition is called the *harmonic structure*. It is uniquely determined by index symmetries of \mathbb{T}^n . As for its explicit decomposition, it is unique only if for $\forall i, \alpha_i = \{0, 1\}$, otherwise there are infinitely many isomorphisms.

It should be noted that the partition of a tensor space with respect to its anisotropic properties does not require the computation of an explicit harmonic decomposition, only the knowledge of the harmonic structure is required. The determination of the harmonic structure in the cases $\mathbb{E}la(2)$ and $\mathbb{E}la(3)$ will be discussed in [chapter 3](#) and [chapter 6](#).

2.4 Definition of elastic materials

When subjected to an isometry, the nature of an elastic material does not change. That is to say that the transformations of a material in space, through actions $\mathbf{g} \in O(d)$ on an elasticity tensor, will lead to a set of tensors that describe the same elastic material. The constitutive law of an elastic material is thus not characterized by a single elasticity tensor but by the collection of all the elasticity tensors related by orthogonal transformations. It results that, generically, multiple elasticity tensors are associated to the same elastic material.

An important point to avoid any misunderstanding is the following. In most parts of this document, we are considering the *active interpretation* of a transformation. This means that, with respect to a fixed reference, the transformation of an object gives rise to a new object which is usually different from the original object. This interpretation has to be distinguished from the *passive interpretation* in which the object is unchanged but the basis used for its description is transformed. The difference is illustrated [Figure 2.2](#)

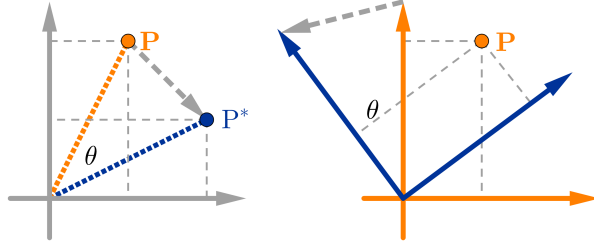


Figure 2.2: **Active transformation** on the left figure: a new vector is obtained; **Passive transformation** on the right figure, in which only the basis is changed.

To speak intrinsically of an elastic material, it is necessary to remove information attached to a particular elasticity tensor. What follows will define the set of all elasticity tensors describing the same elastic material.

Two stiffness tensors $\underset{\approx}{\mathbb{C}}, \bar{\underset{\approx}{\mathbb{C}}} \in \mathbb{E}la$ are said to be equivalent, and denoted $\underset{\approx}{\mathbb{C}} \sim \bar{\underset{\approx}{\mathbb{C}}}$, when they are related by an orthogonal transformation, namely

$$\underset{\approx}{\mathbb{C}} \sim \bar{\underset{\approx}{\mathbb{C}}} \Leftrightarrow \exists \mathbf{g} \in O(d) \mid \underset{\approx}{\mathbb{C}} = \mathbf{g} \star \bar{\underset{\approx}{\mathbb{C}}}.$$

In such case, $\underset{\approx}{\mathbb{C}}$ and $\bar{\underset{\approx}{\mathbb{C}}}$ describe the same elastic material. The collection of all elasticity tensors describing the same elastic material is a geometric object called the orbit of $\underset{\approx}{\mathbb{C}}$ and is defined as follows:

2.4.1 Definition (G-orbit of $\underset{\approx}{\mathbb{C}}$)

Let, $\underset{\approx}{\mathbb{C}} \in \mathbb{E}la$, the G-orbit of $\underset{\approx}{\mathbb{C}}$ is the set

$$\text{Orb}(\underset{\approx}{\mathbb{C}}, G) = \left\{ \bar{\underset{\approx}{\mathbb{C}}} \in \mathbb{E}la \mid \bar{\underset{\approx}{\mathbb{C}}} = \mathbf{g} \star \underset{\approx}{\mathbb{C}}, \mathbf{g} \in G \right\}$$

From a mathematical point of view, an elastic material is defined as the G-orbit¹ of $\underset{\approx}{\mathbb{C}}$ as showed in Figure 2.3.

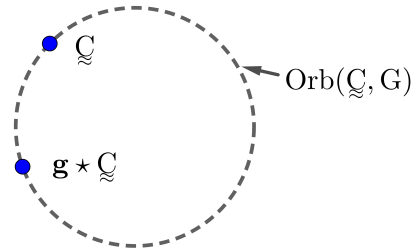


Figure 2.3: G-Orbit of $\underset{\approx}{\mathbb{C}}$: equivalent tensors related by orthogonal transformations

The set of $\text{Orb}(\underset{\approx}{\mathbb{C}}, G)$ in $\mathbb{E}la$ forms an orbit space denoted by $\mathbb{E}la/O(d)$. More mathematical interpretations of orbit space can be found in [76]. In geometric terms, each point in this space represents an elastic material. As observed by M. Olive in [103], an orbit space has a complicated structure, since, according to the symmetry class of the elasticity tensor, the orbits can be of various types.

¹ $G = O(2)$ for bidimensional physical space and $G = SO(3)$ for 3D space

A natural question is therefore how to distinguish points in $\mathbb{E}la/O(d)$ with respect to their anisotropy types and to realize the partition of $\mathbb{E}la$. We will introduce in later chapters the different anisotropy types for $\mathbb{E}la(2)$ and $\mathbb{E}la(3)$.

2.5 Invariants and integrity basis

The previous questions can be formulated in a more understandable way as asked by Boehler et al. in [77]: consider the measurements of the same anisotropic elastic materials in two different labs, and suppose that there is no way to choose, a priori, a specific orientation of the material. These two measurements will result in two different elasticity tensors. How can one decide whether the two tensors describe, or not, the same material? To answer this question, we need to define $O(d)$ -invariant functions on $\mathbb{E}la$ which are independent of a specific elasticity tensor.

2.5.1 Definition (Invariant function [77])

A function F is G -invariant on \mathbb{V} if:

$$F(\mathbf{g} \star \mathbf{v}) = F(\mathbf{v}), \forall \mathbf{g} \in G, \forall \mathbf{v} \in \mathbb{V}$$

Since $O(d)$ -invariant functions are constant on each orbit and take different values on different orbits, they allow to *separate* the orbits of $\mathbb{E}la$.

2.5.2 Definition (Separating set [111])

A finite set $\mathcal{S} := \{\kappa_1, \dots, \kappa_r\}$ of G -invariant functions is a *separating set* of $\mathbb{E}la/O(d)$ if for any $\mathbb{C}, \overline{\mathbb{C}}$ in $\mathbb{E}la$

$$\text{Orb}(\mathbb{C}) = \text{Orb}(\overline{\mathbb{C}}) \iff \kappa_i(\mathbb{C}) = \kappa_i(\overline{\mathbb{C}}), \quad i = 1, \dots, r.$$

A separating set \mathcal{S} is said to be *minimal* if any strict subset \mathcal{S}' of \mathcal{S} is no longer a separating set.

Such a set of invariant functions is described in the literature under the generic name of *functional basis* [103]. However, there is no known algorithm to obtain them. This is the reason why we have chosen to focus on *polynomial invariants* and the *integrity basis*, for which computations are possible.

Let consider the representation $(\rho, \mathbb{E}la, O(d))$, the action is denoted by Equation 2.4, this action extends to the algebra $\mathbb{R}[\mathbb{E}la]$ of *polynomial functions* defined on $\mathbb{E}la$ with $p \in \mathbb{R}[\mathbb{E}la]$ by:

$$\begin{aligned} p : \mathbb{E}la &\rightarrow \mathbb{R} \\ \mathbb{C} &\mapsto p(\mathbb{C}). \end{aligned}$$

2.5.3 Definition (Polynomial function [77])

Let \mathbb{V} be a vector space and \mathcal{B} a basis, a polynomial function p on \mathbb{V} is a function that depends polynomially on the coordinates of $\mathbf{v} \in \mathbb{V}$ in \mathcal{B}

A polynomial function in \mathbb{C} is a polynomial in the components of \mathbb{C} expressed with respect to a given basis. We then introduce the polynomial invariants:

2.5.4 Definition (Polynomial invariant [77])

Let (ρ, \mathbb{V}) be a finite-dimensional representation of G , a polynomial function p on \mathbb{V} is a polynomial G -invariant if

$$p(\mathbf{g} \star \mathbf{v}) = p(\mathbf{v}), \forall \mathbf{g} \in G, \forall \mathbf{v} \in \mathbb{V}$$

We can further consider the algebra $\mathbb{R}[\mathbb{Ela}]^{O(d)}$ of $O(d)$ -invariant polynomials:

$$\mathbb{R}[\mathbb{Ela}]^{O(d)} := \left\{ p \in \mathbb{R}[\mathbb{Ela}], \quad p(\mathbf{g} \star \underset{\approx}{\mathbb{C}}) = p(\underset{\approx}{\mathbb{C}}), \quad \forall \mathbf{g} \in O(d), \quad \forall \underset{\approx}{\mathbb{C}} \in \mathbb{Ela} \right\}.$$

A route to compute polynomial invariants of a vector space \mathbb{V} is to first decompose this space into G -irreducible ones [104]. This step is performed based on the harmonic decomposition introduced in section 2.3.

As a consequence of Hilbert's finiteness theorem [112], such polynomial invariants are finitely generated. The generating property means that any $O(d)$ -invariant polynomial $J \in \mathbb{R}[\mathbb{Ela}]^{O(d)}$ is a polynomial function in I_1, \dots, I_N :

$$J(\underset{\approx}{\mathbb{C}}) = p(I_1(\underset{\approx}{\mathbb{C}}), \dots, I_N(\underset{\approx}{\mathbb{C}})), \quad \underset{\approx}{\mathbb{C}} \in \mathbb{Ela},$$

where p is a polynomial in N variables. Any finite generating set $\{I_1, \dots, I_N\}$ of $\mathbb{R}[\mathbb{Ela}]^{O(d)}$ is called an *integrity basis* [74] and denoted by $\mathcal{IB}(\mathbb{Ela}, O(d))$.

2.5.5 Definition (Integrity basis)

A finite set $\{I_1, \dots, I_N\}$ of invariant polynomials on \mathbb{V} is called an integrity basis if every invariant polynomial on \mathbb{V} can be written as a polynomial in I_1, \dots, I_N .

An integrity basis is *minimal* if no proper subset of it is an integrity basis. Knowing an integrity basis is interesting for applications since their elements:

- **Generate the algebra of $O(d)$ -invariant polynomials:** any $O(d)$ -polynomial function can be written as a polynomial in the elements of the integrity basis, which is finitely generated, i.e. $\#\mathcal{IB}(\mathbb{Ela}, O(d)) < +\infty$;
- **Separate the orbits:** the invariants of the integrity basis take the same value if evaluated on two sets of constitutive tensors that just differ up to an isometry, and take different values if not:

$$\mathcal{IB}(\mathbb{Ela}, O(2))(\underset{\approx}{\mathbb{C}}_1) = \mathcal{IB}(\mathbb{Ela}, O(2))(\underset{\approx}{\mathbb{C}}_2) \Leftrightarrow \underset{\approx}{\mathbb{C}}_1 \in \text{Orb}(\underset{\approx}{\mathbb{C}}_2)$$

The ability to express $O(d)$ -invariant polynomials is twofold in practice, apart from the orbit separation, it allows the classification of linear anisotropic elastic materials in the orbit space.

2.6 From symmetry group to symmetry class

The purpose of this section is to introduce the right language to speak about the symmetry properties of the elasticity tensors. In the literature, there are at least five approaches for classifying the symmetry of a n -th order tensor in \mathbb{R}^d :

1. **Spectral approach:** It is an approach based on the eigenstructure of the matrix representation of a given tensor [61], which will reveal its invariance properties. Since it involves the computation of eigenvalues of tensors, this approach is also highly sensitive to the inherent noise of the data.

2. **Symmetry plane approach:** It is a graphical approach extended from the pole figures approach proposed by François [65], the method of which consists in considering a function over a unit sphere, constructed from the tensor representation, the zeros of which indicate the normal vectors to physical symmetry planes.
3. **Maxwell's multipoles approach:** Another graphical approach originally proposed by Maxwell [68] which is to construct a geometrical picture of a harmonic tensor: to decompose a harmonic tensor of order n as a n -tuple vectors, and in this way to detect its different symmetry classes. In three dimensions there is a very simple geometrical picture of elasticity tensors given in [69].
4. **Covariant based approach:** More recently, in [76, 78], the authors have used a generating set of covariants to characterise the symmetry classes of a tensor.

2.6.1 Symmetry group

The tensors can remain invariant with respect to certain orthogonal transformations $\mathbf{g} \in O(d)$, and the set of these symmetry transformations forms a point group, the symmetry group:

2.6.1 Definition (Symmetry group [4])

The symmetry group of $\mathbf{v} \in \mathbb{V}$ is defined as the collection of all transformations $\mathbf{g} \in G$ such that $\mathbf{g} \star \mathbf{v} = \mathbf{v}$:

$$G_{\mathbf{v}} := \{\mathbf{g} \in G, | \mathbf{v} = \mathbf{g} \star \mathbf{v}\}$$

Let consider the image $\overline{\mathbb{C}}$ of \mathbb{C} by an isometric transformation:

$$\overline{\mathbb{C}} = \mathbf{g} \star \mathbb{C}, \mathbf{g} \in O(d).$$

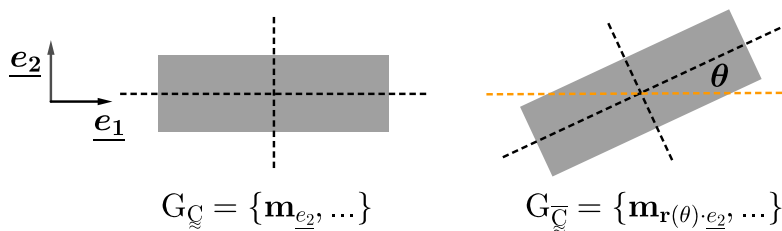
For some transformations, the resulting tensor may be identical to the original one. The set of such transformations constitutes the symmetry group of \mathbb{C} :

$$G_{\mathbb{C}} := \{\mathbf{g} \in O(d) | \mathbb{C} = \mathbf{g} \star \mathbb{C}\}.$$

In brief, the symmetry group of an elasticity tensor represents the set of transformations that keep the tensor unchanged. However, when it comes to an orbit, the notion of symmetry group can not be used to intrinsically define the anisotropy property of this orbit since the associated symmetry groups of its elements are different.

Example 2

To be more specific, we will consider an example in 2D. The obtained symmetry group of an elasticity tensor \mathbb{C} depends on the orientation of the corresponding material in space:



with $\mathbf{m}_{\underline{e}_2}$ the reflection across the line normal to \underline{e}_2 and $\mathbf{r}(\theta)$ the rotation by an angle θ . It can be seen

that these two groups are generated by different elements.

Even though these symmetry groups are different, they can be related by conjugacy.

2.6.2 Definition (Conjugacy)

Two subgroups H_1 and H_2 of G are conjugate if $\forall h_1 \in H_1, \exists h_2 \in H_2$ and $\exists \mathbf{g} \in G$ such as $h_2 = \mathbf{g}h_1\mathbf{g}^{-1}$.

Tensors on the same orbit have conjugate symmetry groups. It is possible to define a weaker equivalence relationship than being on the same orbit, which consists only of having a conjugate symmetry group. This weaker equivalence relation among elements of $\mathbb{E}a$ is defined as follows:

$$\underline{\mathbb{C}} \sim \overline{\mathbb{C}} \Leftrightarrow \{\exists \mathbf{g} \in O(d) \mid G_{\underline{\mathbb{C}}} = \mathbf{g}G_{\overline{\mathbb{C}}}\mathbf{g}^{-1}\}. \quad (2.7)$$

This relation indicates that two tensors are *equivalent* if their symmetry groups are conjugate.

2.6.2 Symmetry class

We define the conjugacy class as the set $[\mathbf{H}]$ of all subgroups of G conjugate to \mathbf{H} :

2.6.3 Definition (Conjugacy class)

Let \mathbf{H} be any subgroup of G , the set of subgroups conjugate to \mathbf{H} constitute a conjugacy class $[\mathbf{H}]$:

$$[\mathbf{H}] := \{\mathbf{g}\mathbf{H}\mathbf{g}^{-1}, \mid \mathbf{g} \in G\}$$

The conjugacy class of a symmetry subgroup $G_{\underline{\mathbb{C}}}$ of a tensor $\underline{\mathbb{C}}$ is the *symmetry class* of the tensor $\underline{\mathbb{C}}$, denoted $[G_{\underline{\mathbb{C}}}]$. In other words, two tensors are equivalent if and only if their symmetry groups belong to the same symmetry class.

Thus, the G -orbit space can be partitioned into different sets with respect to the symmetry classes of their elements. From the knowledge of harmonic structures [section 2.3](#), the set of symmetry classes of a given tensor space can be obtained [\[58, 59, 106\]](#). To do this, the results from the literature concerning symmetry classes of irreducible spaces are combined via the clips operation defined by M. Olive during his Ph.D. The use of this tool allows us to obtain very general results on the symmetry classes of a given constitutive tensor.

2.6.3 Clips operation

As discussed in [section 2.3](#), the whole vector space \mathbb{V} can be decomposed into a direct sum of irreducible \mathbb{V}_i ($i = 1, \dots, N$). To obtain the symmetry classes of \mathbb{V} , we must therefore compute the symmetry classes of a direct sum $\mathbb{V}_1 \oplus \dots \oplus \mathbb{V}_N$, knowing independently the symmetry classes of each space \mathbb{V}_i . To do so, we introduce in this section a general theory of *clips* [\[102\]](#).

Lemma 2.1. *Let \mathbb{V} be a vector space that decomposes into the direct sum of two G -equivariant subspaces:*

$$\mathbb{V} = \mathbb{V}_1 \oplus \mathbb{V}_2, \text{ where } \mathbf{g} \star \mathbb{V}_1 \subset \mathbb{V}_1 \text{ and } \mathbf{g} \star \mathbb{V}_2 \subset \mathbb{V}_2, \forall \mathbf{g} \in G$$

If \mathcal{J} is the set of conjugacy classes of \mathbb{V} , \mathcal{J}_i those of \mathbb{V}_i , then $[\mathbf{H}] \in \mathcal{J}$ if and only if there exist $[\mathbf{H}_1] \in \mathcal{J}_1$ and $[\mathbf{H}_2] \in \mathcal{J}_2$ such that $\mathbf{H} = \mathbf{H}_1 \cap \mathbf{H}_2$

Lemma 2.1 shows us that the conjugacy classes of a direct sum are related to intersections of classes of its subspaces. However, as the intersection of classes is meaningless, the result cannot be directly extended. The *clips operation* solves this problem.

2.6.4 Definition (clips operation)

For each conjugacy class $[H_1]$ and $[H_2]$, we define the clip operator of $[H_1]$ and $[H_2]$, denoted by $[H_1] \odot [H_2]$:

$$[H_1] \odot [H_2] := \{ [H_1 \cap \mathbf{g}H_2\mathbf{g}^{-1}], \forall \mathbf{g} \in G \}$$

This definition immediately extends to two families (finite or infinite) \mathcal{F}_1 and \mathcal{F}_2 of conjugacy classes:

$$\mathcal{F}_1 \odot \mathcal{F}_2 := \bigcup_{[H_1] \in \mathcal{F}_1, [H_2] \in \mathcal{F}_2} [H_1] \odot [H_2]$$

This clips operation defines thus an operation on the set of conjugacy classes \mathfrak{J} which is associative and commutative. We have moreover

$$[1] \odot [H] = [1] \text{ and } [G] \odot [H] = [H]$$

for every conjugacy class $[H]$, where $1 := \{\mathbf{e}\}$ and \mathbf{e} is the identity element of G .

The conjugacy classes of a direct sum of subspaces are obtained by the clips of their respective conjugacy classes.

Lemma 2.2. [102] *Let (ρ, \mathbb{V}_1) and (ρ, \mathbb{V}_2) be two linear representations of G . Then*

$$\mathfrak{J}(\mathbb{V}_1 \oplus \mathbb{V}_2) = \mathfrak{J}(\mathbb{V}_1) \odot \mathfrak{J}(\mathbb{V}_2)$$

Using this lemma 2.2, we deduce a general algorithm to obtain the conjugacy classes $\mathfrak{J}(\mathbb{V})$ of a finite dimensional representation (ρ, \mathbb{V}, G) :

1. a decomposition of space \mathbb{V} into irreducible subspaces;
2. the conjugacy classes \mathfrak{J} for each irreducible subspace;
3. clips operation $[H_1] \odot [H_2]$ between conjugacy classes of closed subgroups of G .

We will apply clips operation to the linear representation of $O(2)$ and $SO(3)$ in the following chapters. Besides, this tool will be of crucial importance for the determination of exotic sets for elastic materials in [chapter 4](#) and [chapter 7](#).

2.7 Symmetry stratum

In this section, we partition the space of $\mathbb{E}la$ based on the idea that two tensors are in the same subset if they have the same symmetry class [75].

As shown in [Equation 2.7](#) the relation \sim is an equivalence relation on $\mathbb{E}la$. An equivalence class for this equivalence relation is called a *stratum* [113]. More specifically, in what follows $\Sigma_{[H]}$ will denote the equivalent class of elasticity tensors having their symmetry group conjugate to H , with $[H]$ the corresponding symmetry class [76, 106]. In brief, $\mathbb{E}la$ can be partitioned into different strata (results for $\mathbb{E}la(2)$ and $\mathbb{E}la(3)$ is given respectively in [chapter 3](#) and [chapter 6](#)).

2.7.1 Definition (stratum)

The G -stratum $\Sigma_{[H]}$ denotes the set of tensors whose symmetry groups are conjugate to H

$$\Sigma_{[H]} := \{T \in \mathbb{T}^n, \mid \exists \mathbf{g} \in G, G_T = \mathbf{g}H\mathbf{g}^{-1}\}$$

We distinguish two types of strata:

- $\Sigma_{[H]}$: the open strata which is the strata of tensors whose symmetry class is exactly $[H]$;
- $\bar{\Sigma}_{[H]}$: the closed strata which is the strata of tensors whose symmetry class is at least $[H]$.

Remark. *It can be noted that generally, an open stratum is not a vector space: for instance, the null tensor which is isotropic does not belong to a stratum other than $\Sigma_{[O(d)]}$. Hence, it prevents $\Sigma_{[H]}$ from being a vector space, with H the subgroup of $O(d)$. However, the situation for the closed strata is more delicate.*

An immediate and intuitive picture of the partition of $\mathbb{E}la$ is illustrated in Figure 2.4 with access to all associated notions: tensors, orbits, and partition of the tensor space. As shown in this figure, an orbit composed of equivalent elasticity tensors is modeled by a circle, and in this case, we obtain another illustration of the space of $\mathbb{E}la$ in figure Figure 2.4(2).

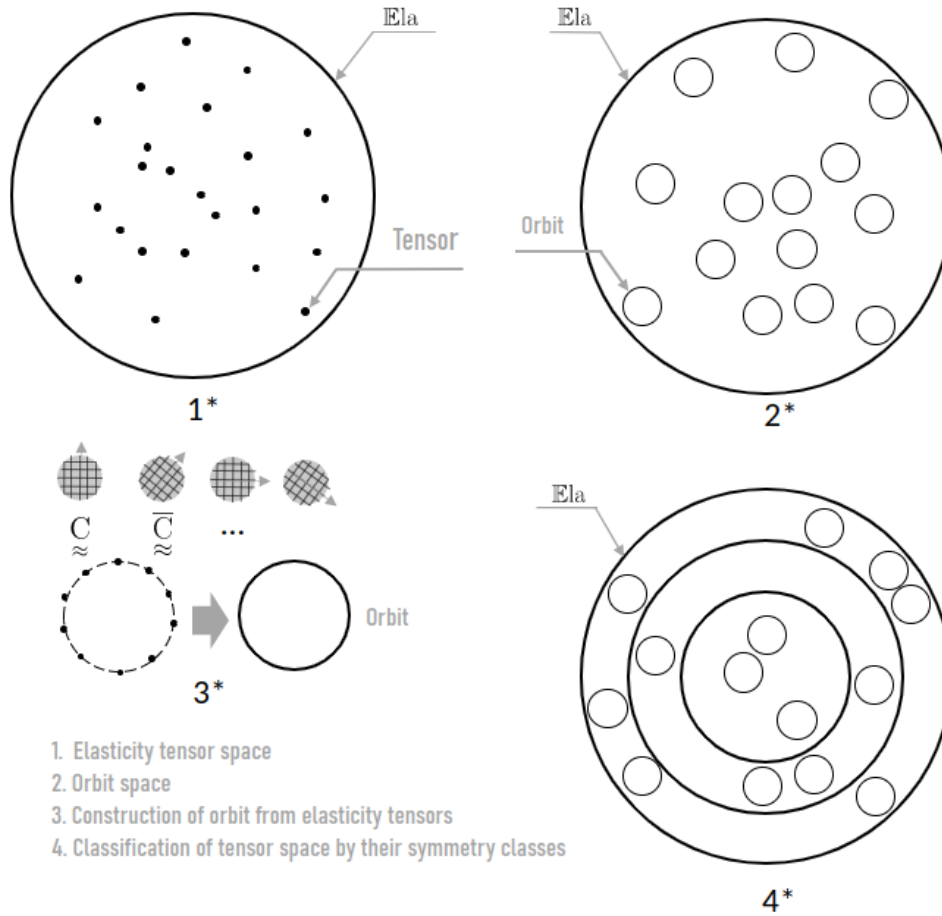


Figure 2.4: Geometric description of linear elastic material space

We present an abstract on the geometric description of linear elastic material space: The *orbit* of $\mathbb{C} \approx$ allows us to describe linear elastic materials independently of elasticity tensors. Given that two tensors

lying on the same orbit belong to the same stratum (as showed in [Figure 2.4](#) that there would not be orbit occupying two sets at the same time), the partition of $\mathbb{E}la$ into different strata naturally partition the orbit space $\mathbb{E}la/O(d)$ into different sets according to their symmetry classes.

Normal form

Among all the elements $\underset{\approx}{C} \in \mathbb{E}la/H$, we define the normal form of $\mathbb{E}la/H$ as the tensor $\underset{\approx}{C}_0$, for which the corresponding symmetry group is exactly H . Before giving an explicit definition of normal form, we first define the notion of a fixed point set, denoted $\mathbb{F}ix$.

2.7.2 Definition (Fix)

Let H be a subgroup of $O(d)$ in $\mathbb{E}la$, the $\mathbb{F}ix$ of H is defined by [\[114\]](#):

$$\mathbb{F}ix(H) := \{\underset{\approx}{C} \in \mathbb{E}la, | \forall \mathbf{h} \in H, \mathbf{h} \star \underset{\approx}{C} = \underset{\approx}{C}\}$$

Previously, we used the notion of *strata* to represent all elasticity tensors possessing the same symmetry class. The proposed notion $\mathbb{F}ix(H)$ is to define a collection of elasticity tensors possessing the same symmetry group. Since independent of the conjugacy relation, it is used to define the normal form.

2.7.3 Definition (Normal form)

Let H be a subgroup of $O(d)$, a normal form of a tensor $\underset{\approx}{C} \in \Sigma_{[H]}$ is a tensor $\underset{\approx}{C}_0$ such that for certain $\mathbf{g} \in O(d)$ (not necessarily unique):

$$\underset{\approx}{C}_0 = \mathbf{g} \star \underset{\approx}{C} \in \mathbb{F}ix(H)$$

Part II

Anisotropic 2D linear elasticity

Chapter 3

Geometry of 2D linear elasticity tensors space

3.1	Group $O(2)$ and its subgroups	35
3.1.1	Group $O(2)$	35
3.1.2	Subgroups of $O(2)$	36
3.2	2D harmonic tensors space: \mathbb{K}^n	37
3.3	Harmonic decomposition of $\mathbb{E}la$	38
3.4	Parametrisation of elasticity tensors	42
3.4.1	Harmonic parametrisation	42
3.4.2	Polar parametrisation	43
3.4.3	Parametrisation of the inverse of a tensor	44
3.5	Invariants and integrity basis	45
3.6	Symmetry classes of $\mathbb{E}la$	47
3.7	Conditions of belonging to a symmetry class	48
3.7.1	Covariant-based conditions	48
3.7.2	Polynomial invariant conditions	50
3.7.3	Inverse stability of the symmetry class	51

The geometric tools introduced in the previous chapter will be used in the particular case of $\mathbb{E}la(2)$. To simplify the notation, $\mathbb{E}la(2)$ will be abbreviated by $\mathbb{E}la$ in this part. The outline of this chapter is as follows. After the introduction of the closed-subgroups of $O(2)$ in [section 3.1](#), the harmonic structure of $\mathbb{E}la$ will be determined in [section 3.2](#) and [section 3.3](#). Having this knowledge at hand, the $O(2)$ -invariant polynomials are obtained in [section 3.5](#), which allows specifying sets of materials in the orbit space. The [section 3.6](#) introduces the symmetry classes of $\mathbb{E}la$ and its partition into disjoint isotropy strata. The transition between these strata is discussed in [section 3.7](#).

3.1 Group $O(2)$ and its subgroups

The symmetry group of a material's physical property encoded by a tensor \mathbf{T} is defined as the set of operations that leave this tensor invariant. In \mathbb{R}^2 , these operations are represented by actions of the orthogonal group $\mathbf{g} \in O(2)$. The symmetry group $G_{\mathbf{T}}$ of $\mathbf{T} \in \mathbb{T}^n$ is defined as:

$$G_{\mathbf{T}} := \{\mathbf{g} \in O(2), | \mathbf{T} = \mathbf{g} \star \mathbf{T}\}$$

meaning that the physical symmetry group of \mathbf{T} corresponds to a closed *subgroup* of $O(2)$ [115].

3.1.1 Definition (Subgroup)

A subset $H \subset G$ is a subgroup of (G, \cdot) if (H, \cdot) is itself a group.

To be more specific, let us now detail the nature of the subgroups of $O(2)$. Such a collection is infinite but can be reduced, up to conjugacy, to a finite set. The conjugacy class of a subgroup H of $O(2)$ is defined as

$$[H] := \{\mathbf{g}H\mathbf{g}^T \subset O(2), | \mathbf{g} \in O(2)\}$$

Furthermore, it is known that for a finite-dimensional vector space and for $O(2)$, there is only a finite set of symmetry classes. These symmetry classes are all conjugate to a closed subgroup of $O(2)$.

3.1.1 Group $O(2)$

As we are working in \mathbb{R}^2 , we will consider the group of linear isometries of \mathbb{R}^2 . Let $O(2)$ the set of invertible transformations \mathbf{g} of \mathbb{R}^2 satisfying $\mathbf{g}^{-1} = \mathbf{g}^T$, i.e.

$$O(2) := \{\mathbf{g} \in GL(2), \mathbf{g}^T = \mathbf{g}^{-1}\}$$

It is the set of vectorial isometries and is called the orthogonal group (Equation 2.3). This group is generated by

- $\mathbf{r}(\theta)$: the rotation by an angle θ ;
- $\mathbf{m}_{\underline{n}}$: the reflection across the line normal to \underline{n} ,

$$\mathbf{m}_{\underline{n}} := \underset{\sim}{1} - 2\underline{n} \otimes \underline{n}, \quad \|\underline{n}\| = 1,$$

with $\underset{\sim}{1}$ the second order identity tensor.

It can be seen that this group is non-commutative, but the generators satisfy the relation

$$\mathbf{m}_{\underline{n}}\mathbf{r}(\theta) = \mathbf{r}(-\theta)\mathbf{m}_{\underline{n}}$$

In terms of matrix under the orthonormal basis $\mathcal{B} = \{\underline{e}_1, \underline{e}_2\}$, we have,

$$[\mathbf{r}(\theta)] := \begin{pmatrix} \cos \theta & -\sin \theta \\ \sin \theta & \cos \theta \end{pmatrix}_{\mathcal{B}} \quad \text{with } 0 \leq \theta < 2\pi \quad \text{and} \quad [\mathbf{m}_{\underline{e}_2}] := \begin{pmatrix} 1 & 0 \\ 0 & -1 \end{pmatrix}_{\mathcal{B}},$$

As a special transformation we mention the inversion $-\mathbf{1}$, which matrix representation is simply

$$[-\mathbf{1}] := \begin{pmatrix} -1 & 0 \\ 0 & -1 \end{pmatrix}_{\mathcal{B}}$$

in \mathbb{R}^2 , $-1 = \mathbf{r}(\pi)$.

3.1.2 Subgroups of $O(2)$

The purpose of this section is to introduce, up to conjugacy, the different subgroups of $O(2)$. A detailed proof of subgroups of $O(2)$ was given in a book by Armstrong (see [[109], page 20] and [[116], page 81]), we conclude here that they belong to the following collection [114] :

$$\{1, Z_2^{\mathbf{m}_{e_2}}, Z_k, D_k, SO(2), O(2)\}_{k \geq 2}$$

in which:

- 1 stands for the trivial subgroup;
- $Z_2^{\mathbf{m}_{e_2}}$ is the group generated by \mathbf{m}_{e_2} , which is the reflection across the axis normal to e_2 ;
- Z_k is the cyclic group with k elements generated by the rotation $\mathbf{r}(\frac{2\pi}{k})$, with the convention that $Z_1 = 1$
- D_k is the dihedral group with $2k$ elements generated by $\mathbf{r}(\frac{2\pi}{k})$ and \mathbf{m}_{e_2} , with the convention that $D_1 = Z_2^{\mathbf{m}_{e_2}}$
- $SO(2)$ is the continuous rotation group, it can be viewed as Z_∞ ;
- $O(2)$ is the full orthogonal group, it can be viewed as D_∞ .

It should be noted that the determination of the symmetry classes of a vector tensor space is not a straightforward result. Such a determination implies the use of mathematical tools such as the harmonic structure. The detailed process for symmetry class determination of $\mathbb{E}la$ will be introduced later.

Centrosymmetry and chirality

The classification of subgroups based on generators as introduced earlier can be refined. For this purpose, we will introduce the notions of chiral groups and centro-symmetric groups. This classification will be useful to analyse the properties of the constitutive tensors.

3.1.2 Definition (Centrosymmetry and chirality)

A subgroup of $O(2)$ would be said to be:

- *centrosymmetric* (denoted by \mathbf{i}) if it contains the inversion $\mathbf{r}(\pi)$, and *non-centrosymmetric* (denoted by $\bar{\mathbf{i}}$) otherwise;
- *chiral* (denoted by \mathbf{c}) if it does not contain reflection $\mathbf{m}_{\underline{n}}$, and *achiral* (denoted by $\bar{\mathbf{c}}$) otherwise.

It should be emphasised that centrosymmetry and chirality are two distinct invariance properties. Based on this classification, the set of closed subgroups of $O(2)$ can be divided into four subsets:

	\mathbf{i} (centrosymmetry)	$\bar{\mathbf{i}}$ (non-centrosymmetry)
$\bar{\mathbf{c}}$ (achiral)	D_{2k}	D_{2k+1}
\mathbf{c} (chiral)	Z_{2k}	Z_{2k+1}

Table 3.1: Classification of $O(2)$ subsets according to their invariance properties

3.2 2D harmonic tensors space: \mathbb{K}^n

The space of n -th order harmonic tensors in \mathbb{R}^2 will be denoted by \mathbb{K}^n . As mentioned in [section 2.3](#), it is a natural $O(2)$ -irreducible space, and any tensor $T \in \mathbb{K}^n$ satisfies the following two properties:

- Totally symmetric with respect to index permutation, meaning that

$$T_{i_1 i_2 \dots i_n} = T_{i_{\sigma(1)} i_{\sigma(2)} \dots i_{\sigma(n)}}$$

with σ the permutation of the symbols $\{1, 2, \dots, n\}$;

- Traceless with respect to any two indices i, j , denoted by $\text{tr}T = 0$.

In \mathbb{R}^2 , these properties result in the following lemma:

Lemma 3.1 (Dimension of \mathbb{K}^n). *In \mathbb{R}^2 , the dimension of a n -th order harmonic space \mathbb{K}^n is determined by:*

$$\dim \mathbb{K}^n = \begin{cases} 2, & n \geq 1 \\ 1, & n = 0 \text{ or } -1 \end{cases}$$

The harmonic spaces with different order can be interpreted as follows [\[106\]](#):

- \mathbb{K}^{-1} is the space of pseudo-scalars, or hemitropic coefficients;
- \mathbb{K}^0 is the space of scalars, that is isotropic coefficients;
- \mathbb{K}^1 is the space of vectors;
- \mathbb{K}^2 is the space of deviators;
- $\mathbb{K}^n (n \geq 2)$ is the space of n -th order deviators.

Harmonic parametrisation

The elements of space \mathbb{K}^0 or \mathbb{K}^{-1} can be parameterized by scalars. For higher order space ($n \geq 1$), we present two simple examples of tensor $\underset{\sim}{h} \in \mathbb{K}^2$ and tensor $\underset{\sim}{H} \in \mathbb{K}^4$, to provide intuitive evidence on such two-dimensional construction. Since satisfying the restriction of traceless and totally symmetric, these two matrices are constructed as follows:

$$[\underset{\sim}{h}] := \begin{pmatrix} h_1 & h_2 \\ h_2 & -h_1 \end{pmatrix}_{\mathcal{B}} \quad [\underset{\sim}{H}] := \begin{pmatrix} H_1 & -H_1 & \sqrt{2}H_2 \\ -H_1 & H_1 & -\sqrt{2}H_2 \\ \sqrt{2}H_2 & -\sqrt{2}H_2 & -2H_1 \end{pmatrix}_{\mathcal{K}}$$

with $\underset{\sim}{H}$ expressed under the Kelvin convention¹. It can be seen that each matrix is formed by two independent components.

What follows will show us how $\mathbf{g} \in O(2)$ acts on $T \in \mathbb{K}^n$.

¹Kelvin convention will be presented in [subsection 3.4.1](#)

O(2)-representation on \mathbb{K}^n

For the case $n = 0, -1$, the O(2)-representation ρ_n remains on the one dimensional space \mathbb{R} . Specifically, ρ_0 is the trivial representation of the identity O(2)-action and ρ_{-1} is the multiplication by the determinant of O(2)-action. For $\mathbf{g} \in \text{O}(2)$, we have:

$$\rho_0(\mathbf{g}) := 1, \quad \rho_{-1}(\mathbf{g}) := \det(\mathbf{g})$$

When it comes to the space $\mathbb{K}^n (n \geq 1)$, since they are two-dimensional, let us introduce $\mathfrak{K}^{(n)} = (\mathbf{k}_1^{(n)}, \mathbf{k}_2^{(n)})$ an orthonormal basis of $\mathbb{K}^n (n \geq 1)$ constructed from the canonical basis \mathcal{B} of \mathbb{R}^2 (the constructions for $\mathfrak{K}^{(2)}$ and $\mathfrak{K}^{(4)}$ are detailed in [subsection 3.4.1](#) [117]. Based on Lemma 6.1 (see also a detailed information in [118]), for $\mathbf{T} \in \mathbb{K}^n (n \geq 1)$, we have²:

$$\mathbf{T} = T_1 \mathbf{k}_1^{(n)} + T_2 \mathbf{k}_2^{(n)}$$

As a consequence, we define for two-dimensional tensor \mathbf{T} a vector:

$$\{\mathbf{T}\}_{\mathfrak{K}^{(n)}} := (T_1, T_2)_{\mathfrak{K}^{(n)}}^T \quad (3.1)$$

For each integer $n \geq 1$, the representation ρ_n of O(2)-action is given by:

$$[\rho_n(\mathbf{r}(\theta))] := \begin{pmatrix} \cos n\theta & -\sin n\theta \\ \sin n\theta & \cos n\theta \end{pmatrix}_{\mathfrak{K}^{(n)}}, \quad [\rho_n(\mathbf{m}_{\underline{e}_2})] := \begin{pmatrix} 1 & 0 \\ 0 & -1 \end{pmatrix}_{\mathfrak{K}^{(n)}}, \quad (3.2)$$

which means that a transformation of rotation by angle θ on a n -th order tensor acts as a rotation of $n\theta$ on its associated vector ([Equation 3.1](#)), further details can be found in [74, 119] and a graphical representation of rotations for elements in \mathbb{K}^2 and \mathbb{K}^4 are given in [Figure 3.1](#).

3.3 Harmonic decomposition of $\mathbb{E}a$

Harmonic structure

A classical result is that any tensor space of \mathbb{R}^2 can be decomposed into a finite number of harmonic spaces (mentioned in [section 2.3](#)). The harmonic structure of $\mathbb{E}a$ can easily be determined using the *Clebsh-Gordan formula*:

Lemma 3.2 (Clebsh-Gordan formula). *The tensor product of two O(2)-irreducible spaces is reducible and decomposes according to:*

\otimes	\mathbb{K}^n	\mathbb{K}^0	\mathbb{K}^{-1}
\mathbb{K}^m	$\begin{cases} \mathbb{K}^{m+n} \oplus \mathbb{K}^{ m-n }, & m \neq n \\ \mathbb{K}^{2n} \oplus \mathbb{K}^0 \oplus \mathbb{K}^{-1}, & m = n \end{cases}$	\mathbb{K}^m	\mathbb{K}^m
\mathbb{K}^0	\mathbb{K}^n	\mathbb{K}^0	\mathbb{K}^{-1}
\mathbb{K}^{-1}	\mathbb{K}^n	\mathbb{K}^{-1}	\mathbb{K}^0

In the case where the spaces are identical, the tensor product can be decomposed into S^2 and Λ^2 , represent respectively, a symmetrized product and an anti-symmetrized product³:

²Any component $T_{i_1 i_2 \dots i_n}$ of tensor \mathbf{T} can be expressed as the linear combination of $\{T_1, T_2\}$

³let \mathbb{V} a vector space of dimension d , and \underline{v}_i the basis of \mathbb{V} , thus the basis of $\mathbb{V} \otimes \mathbb{V}$ is defined by: $\mathcal{B}(\mathbb{V} \otimes \mathbb{V}) = \underline{v}_i \otimes \underline{v}_j$, we

$$\forall n \geq 1, \mathbb{K}^n \otimes \mathbb{K}^n = S^2(\mathbb{K}^n) \oplus \Lambda^2(\mathbb{K}^n)$$

Therefore, Lemma 3.2 is completed by the following lemma:

Lemma 3.3 (Clebsch-Gordan formula). *For all $n \geq 1$, we have the following isotropic decompositions, in which meaningless products are indicated by \times :*

S^2	\mathbb{K}^n	\mathbb{K}^0	\mathbb{K}^{-1}
\mathbb{K}^n	$\mathbb{K}^{m+n} \oplus \mathbb{K}^0$	\times	\times
\mathbb{K}^0	\times	\mathbb{K}^0	\times
\mathbb{K}^{-1}	\times	\times	\mathbb{K}^0

Λ^2	\mathbb{K}^n	\mathbb{K}^0	\mathbb{K}^{-1}
\mathbb{K}^n	\mathbb{K}^{-1}	\times	\times
\mathbb{K}^0	\times	0	\times
\mathbb{K}^{-1}	\times	\times	0

Proposition 3.1. *The space $\mathbb{E}la$ possess the following harmonic structure [106]:*

$$\mathbb{E}la \simeq 2\mathbb{K}^0 \oplus \mathbb{K}^2 \oplus \mathbb{K}^4 \tag{3.3}$$

in which \simeq indicates an $O(2)$ -equivariant isomorphism.

Proof. $\mathbb{E}la$ can be seen as $S^2(S^2(\mathbb{R}^2))$:

$$\begin{aligned} \mathbb{E}la &\simeq S^2(S^2(\mathbb{R}^2)) \simeq S^2(S^2(\mathbb{K}^1)) \simeq S^2(\mathbb{K}^0 \oplus \mathbb{K}^2) \\ &\simeq S^2(\mathbb{K}^0) \oplus S^2(\mathbb{K}^2) \oplus (\mathbb{K}^0 \otimes \mathbb{K}^2) \\ &\simeq 2\mathbb{K}^0 \oplus \mathbb{K}^2 \oplus \mathbb{K}^4 \end{aligned}$$

□

Let us denote by f an explicit harmonic decomposition, each elasticity tensor $\underset{\approx}{\mathbb{C}} \in \mathbb{E}la$ can be written as:

$$\underset{\approx}{\mathbb{C}} = f(\alpha, \beta, \underset{\approx}{\mathfrak{h}}, \underset{\approx}{\mathfrak{H}}),$$

The $O(2)$ -equivariance property verifies:

$$\forall \mathfrak{g} \in O(2), \quad \mathfrak{g} \star \underset{\approx}{\mathbb{C}} = f(\alpha, \beta, \mathfrak{g} \star \underset{\approx}{\mathfrak{h}}, \mathfrak{g} \star \underset{\approx}{\mathfrak{H}}).$$

The harmonic decomposition splits any elasticity tensor $\underset{\approx}{\mathbb{C}}$ into an

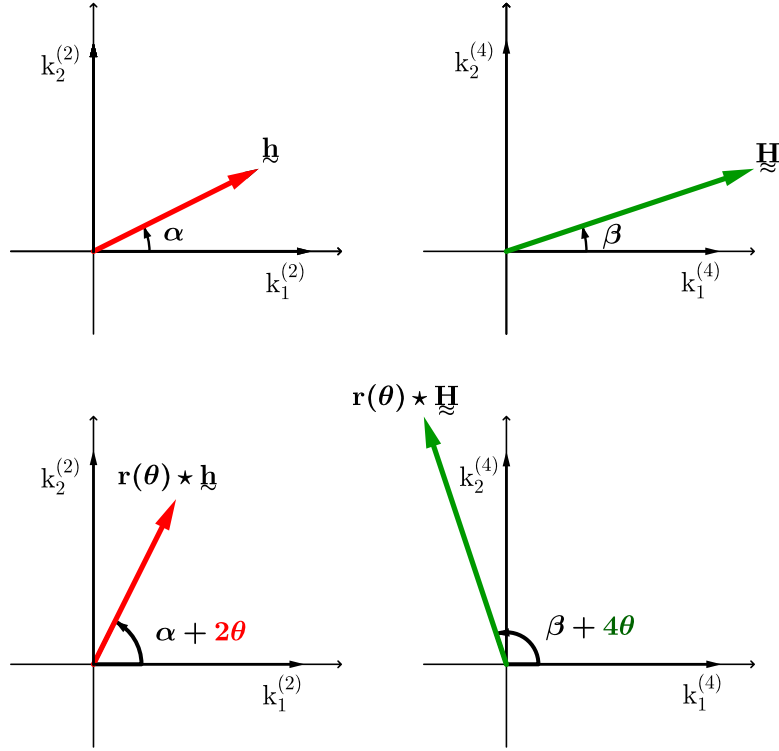
- isotropic part defined by two scalars α and β ;
- anisotropic part comprising $\underset{\approx}{\mathfrak{h}} \in \mathbb{K}^2$ and $\underset{\approx}{\mathfrak{H}} \in \mathbb{K}^4$.

Harmonic bouquet

In order to facilitate further discussion, the set of $\{\underset{\approx}{\mathfrak{h}}, \underset{\approx}{\mathfrak{H}}\}$ will be referred to as the *harmonic bouquet* of $\underset{\approx}{\mathbb{C}}$, and denoted by $\text{HB}(\underset{\approx}{\mathbb{C}})$ [111]. Following Figure 3.1 and Equation 3.2, we illustrate how the *harmonic bouquet* transforms under a θ -angle rotation:

have:

$$\begin{aligned} \mathcal{B}(S^2(\mathbb{V})) &= \frac{1}{2}(\underline{\mathbf{v}}_i \otimes \underline{\mathbf{v}}_j + \underline{\mathbf{v}}_j \otimes \underline{\mathbf{v}}_i) \\ \mathcal{B}(\Lambda^2(\mathbb{V})) &= \frac{1}{2}(\underline{\mathbf{v}}_i \otimes \underline{\mathbf{v}}_j - \underline{\mathbf{v}}_j \otimes \underline{\mathbf{v}}_i) \end{aligned}$$


 Figure 3.1: The action of $r(\theta)$ on $\underset{\sim}{h}$ and $\underset{\approx}{H}$

Explicit harmonic decomposition

Note that any linear combination of $\alpha, \beta \in \mathbb{K}^0$ leads to another explicit decomposition of the elasticity tensor, hence there is no uniqueness of the explicit harmonic decomposition. For instance, α, β can be regarded as the *Lamé numbers* λ and μ , but can also be regarded as the *shear modulus* G and the *bulk modulus* K , which are related to the former by a linear relation (in 2D):

$$G = \mu, \quad K = \lambda + \mu$$

In 2D, the different decompositions are almost identical and their differences only concern the isotropic part⁴. Among the different possibilities, the following one (known as the Clebsch-Gordan harmonic decomposition [120]) will be considered:

Proposition 3.2. *The tensor $\underset{\approx}{C} \in \mathbb{E}la$ admits the uniquely defined Clebsch-Gordan harmonic decomposition associated with the family of projectors $\{\underset{\approx}{J}, \underset{\approx}{K}\}$ ⁵:*

$$\underset{\approx}{C} = \alpha \underset{\approx}{J} + \beta \underset{\approx}{K} + \frac{1}{2} (\underset{\sim}{1} \otimes \underset{\sim}{h} + \underset{\sim}{h} \otimes \underset{\sim}{1}) + \underset{\approx}{H}, \quad (3.4)$$

in which $(\alpha, \beta, \underset{\sim}{h}, \underset{\approx}{H}) \in \mathbb{K}^0 \times \mathbb{K}^0 \times \mathbb{K}^2 \times \mathbb{K}^4$. Conversely, the different elements of the decomposition can be computed as a function of $\underset{\approx}{C}$:

⁴In 3D, as will be seen in chapter 6, the choice of a decomposition also involves the anisotropic components and is therefore more important.

\mathbb{K}^0	\mathbb{K}^2	\mathbb{K}^4
$\beta = \underset{\approx}{\mathbb{K}} :: \underset{\approx}{\mathbb{C}}$	$\underset{\sim}{\mathfrak{h}} = \underset{\approx}{\mathbb{J}} : \underset{\approx}{\mathbb{C}} : \underset{\sim}{\mathbb{1}}$	
$\alpha = \frac{1}{2} \underset{\approx}{\mathbb{D}} :: \underset{\approx}{\mathbb{J}}$		$\underset{\approx}{\mathbb{H}} = \underset{\approx}{\mathbb{D}} - \alpha \underset{\approx}{\mathbb{J}}$

in which $\underset{\approx}{\mathbb{D}} = \underset{\approx}{\mathbb{J}} : \underset{\approx}{\mathbb{C}} : \underset{\approx}{\mathbb{J}}$ is used to characterise the deviatoric linear elasticity.

Proof of this proposition is provided here:

Proof. The stress tensor $\underset{\sim}{\sigma} \in S^2(\mathbb{R}^2)$ (or strain tensor $\underset{\sim}{\varepsilon}$) admits the following decomposition:

$$\underset{\sim}{\sigma} = \underset{\sim}{\sigma}^d + \underset{\sim}{\sigma}^s$$

where $\underset{\sim}{\sigma}^d$ and $\underset{\sim}{\sigma}^s$ are, respectively, the deviatoric and spheric part of $\underset{\sim}{\sigma}$. We have :

$$\underset{\sim}{\sigma}^s = \frac{1}{2} \underset{\sim}{\mathbb{1}} : \underset{\sim}{\sigma} : \underset{\sim}{\mathbb{1}} \quad \underset{\sim}{\sigma}^d = \underset{\sim}{\sigma} - \frac{1}{2} \underset{\sim}{\mathbb{1}} : \underset{\sim}{\sigma} : \underset{\sim}{\mathbb{1}}$$

with $\underset{\sim}{\mathbb{1}}$ the identity tensor of $S^2(\mathbb{R}^2)$. Two projectors $\underset{\approx}{\mathbb{K}}$ and $\underset{\approx}{\mathbb{J}}$ are introduced here such that:

$$\underset{\sim}{\sigma}^s = \underset{\approx}{\mathbb{K}} : \underset{\sim}{\sigma}, \quad \underset{\sim}{\sigma}^d = \underset{\approx}{\mathbb{J}} : \underset{\sim}{\sigma}.$$

with

$$\underset{\approx}{\mathbb{K}} = \frac{1}{2} \underset{\sim}{\mathbb{1}} \otimes \underset{\sim}{\mathbb{1}}, \quad \underset{\approx}{\mathbb{J}} = \underset{\sim}{\mathbb{I}} - \frac{1}{2} \underset{\sim}{\mathbb{1}} \otimes \underset{\sim}{\mathbb{1}}.$$

$\underset{\sim}{\mathbb{I}}$ is the fourth-order identity tensor of $S^2(S^2(\mathbb{R}^2))$, by definition: $\underset{\sim}{\mathbb{I}}_{ijkl} = \frac{1}{2}(\delta_{ik}\delta_{jl} + \delta_{il}\delta_{kj})$. The projector $\underset{\approx}{\mathbb{J}}$ and $\underset{\approx}{\mathbb{K}}$ satisfies the following relations :

$$\underset{\approx}{\mathbb{J}} : \underset{\sim}{\sigma}^d = \underset{\sim}{\sigma}^d \quad \underset{\approx}{\mathbb{K}} : \underset{\sim}{\sigma}^s = \underset{\sim}{\sigma}^s \quad \underset{\approx}{\mathbb{J}} : \underset{\approx}{\mathbb{J}} = \underset{\approx}{\mathbb{J}} \quad \underset{\approx}{\mathbb{J}} : \underset{\approx}{\mathbb{K}} = \underset{\approx}{\mathbb{K}} : \underset{\approx}{\mathbb{J}} = \underset{\sim}{\mathbb{0}} \quad \underset{\approx}{\mathbb{K}} : \underset{\approx}{\mathbb{K}} = \underset{\approx}{\mathbb{K}}$$

Since $\underset{\approx}{\mathbb{C}}$ is a linear application on $S^2(\mathbb{R}^2)$, let us now extend the previous procedure to fourth-order tensor $\underset{\approx}{\mathbb{C}}$:

$$\begin{aligned} \underset{\sim}{\sigma} = \underset{\sim}{\sigma}^s + \underset{\sim}{\sigma}^d &= \underset{\approx}{\mathbb{K}} : \underset{\sim}{\sigma} + \underset{\approx}{\mathbb{J}} : \underset{\sim}{\sigma} \\ &= \underset{\approx}{\mathbb{K}} : \underset{\approx}{\mathbb{C}} : \underset{\sim}{\varepsilon} + \underset{\approx}{\mathbb{J}} : \underset{\approx}{\mathbb{C}} : \underset{\sim}{\varepsilon} \\ &= \underset{\approx}{\mathbb{K}} : \underset{\approx}{\mathbb{C}} : (\underset{\approx}{\mathbb{J}} : \underset{\sim}{\varepsilon} + \underset{\approx}{\mathbb{K}} : \underset{\sim}{\varepsilon}) + \underset{\approx}{\mathbb{J}} : \underset{\approx}{\mathbb{C}} : (\underset{\approx}{\mathbb{J}} : \underset{\sim}{\varepsilon} + \underset{\approx}{\mathbb{K}} : \underset{\sim}{\varepsilon}) \\ &= (\underset{\approx}{\mathbb{K}} : \underset{\approx}{\mathbb{C}} : \underset{\approx}{\mathbb{J}} + \underset{\approx}{\mathbb{K}} : \underset{\approx}{\mathbb{C}} : \underset{\approx}{\mathbb{K}} + \underset{\approx}{\mathbb{J}} : \underset{\approx}{\mathbb{C}} : \underset{\approx}{\mathbb{J}} + \underset{\approx}{\mathbb{J}} : \underset{\approx}{\mathbb{C}} : \underset{\approx}{\mathbb{K}}) : \underset{\sim}{\varepsilon} \end{aligned}$$

Thus, $\underset{\approx}{\mathbb{C}}$ is decomposed into 4 parts, with the definition of two harmonic components:

$$\beta = \frac{1}{2} (\underset{\sim}{\mathbb{1}} : \underset{\approx}{\mathbb{C}} : \underset{\sim}{\mathbb{1}}) \quad \underset{\sim}{\mathfrak{h}} = \underset{\approx}{\mathbb{J}} : \underset{\approx}{\mathbb{C}} : \underset{\sim}{\mathbb{1}} = \underset{\sim}{\mathbb{1}} : \underset{\approx}{\mathbb{C}} : \underset{\approx}{\mathbb{J}}$$

we have:

$$\underset{\approx}{\mathbb{K}} : \underset{\approx}{\mathbb{C}} : \underset{\approx}{\mathbb{K}} = \beta \underset{\approx}{\mathbb{K}} \quad \underset{\approx}{\mathbb{J}} : \underset{\approx}{\mathbb{C}} : \underset{\approx}{\mathbb{K}} + \underset{\approx}{\mathbb{K}} : \underset{\approx}{\mathbb{C}} : \underset{\approx}{\mathbb{J}} = \frac{1}{2} (\underset{\sim}{\mathbb{1}} \otimes \underset{\sim}{\mathfrak{h}} + \underset{\sim}{\mathfrak{h}} \otimes \underset{\sim}{\mathbb{1}})$$

⁵The deviatoric projector $\underset{\approx}{\mathbb{J}}$ and spheric projector $\underset{\approx}{\mathbb{K}}$ are defined in the proof of proposition 3.2.

$\underset{\approx}{\mathbb{J}} : \underset{\approx}{\mathbb{C}} : \underset{\approx}{\mathbb{J}}$ result in a deviatoric tensor, which consists in writing the elasticity tensor as a symmetric linear application on $\mathbb{K}^4 \oplus \mathbb{K}^0$. In this case, we write:

$$\underset{\approx}{\mathbb{J}} : \underset{\approx}{\mathbb{C}} : \underset{\approx}{\mathbb{J}} = \underset{\approx}{\mathbb{H}} + \alpha \underset{\approx}{\mathbb{J}}$$

with $\underset{\approx}{\mathbb{H}}$ the fourth order harmonic tensor and α an associated scalar, if we apply a scalar product for each side by $\underset{\approx}{\mathbb{J}}$, we get:

$$\alpha = \frac{1}{2} (\underset{\approx}{\mathbb{J}} : \underset{\approx}{\mathbb{C}} : \underset{\approx}{\mathbb{J}}) :: \underset{\approx}{\mathbb{J}}$$

In consequence, the decomposition of $\underset{\approx}{\mathbb{C}}$ is expressed in respect of α , β , $\underset{\approx}{\mathbb{h}}$ and $\underset{\approx}{\mathbb{H}}$:

$$\underset{\approx}{\mathbb{C}} = \alpha \underset{\approx}{\mathbb{J}} + \beta \underset{\approx}{\mathbb{K}} + \frac{1}{2} (1 \otimes \underset{\approx}{\mathbb{h}} + \underset{\approx}{\mathbb{h}} \otimes 1) + \underset{\approx}{\mathbb{H}}$$

□

This particular form of harmonic decomposition amounts to considering the constitutive law of linear elasticity in [Equation 2.1](#) as a coupled behaviour in which the deviatoric part and the spherical part are considered independent.

$$\begin{cases} \underset{\approx}{\sigma}^d = \underset{\approx}{\mathbb{C}}^{dd} : \underset{\approx}{\varepsilon}^d + \underset{\approx}{\mathbb{C}}^{ds} : \underset{\approx}{\varepsilon}^s \\ \underset{\approx}{\sigma}^s = \underset{\approx}{\mathbb{C}}^{sd} : \underset{\approx}{\varepsilon}^d + \underset{\approx}{\mathbb{C}}^{ss} : \underset{\approx}{\varepsilon}^s \end{cases} \quad (3.5)$$

The elasticity tensor appears to be structured by blocks:

$$\underset{\approx}{\mathbb{C}} = \begin{pmatrix} \underset{\approx}{\mathbb{C}}^{dd} & \underset{\approx}{\mathbb{C}}^{ds} \\ \underset{\approx}{\mathbb{C}}^{ds} & \underset{\approx}{\mathbb{C}}^{ss} \end{pmatrix}, \quad (3.6)$$

in which

$$\underset{\approx}{\mathbb{C}}^{dd} = \underset{\approx}{\mathbb{H}} + \alpha \underset{\approx}{\mathbb{J}}, \quad \underset{\approx}{\mathbb{C}}^{ds} = \frac{1}{2} \underset{\approx}{\mathbb{h}} \otimes 1, \quad \underset{\approx}{\mathbb{C}}^{sd} = \frac{1}{2} 1 \otimes \underset{\approx}{\mathbb{h}}, \quad \underset{\approx}{\mathbb{C}}^{ss} = \beta \underset{\approx}{\mathbb{K}}$$

3.4 Parametrisation of elasticity tensors

3.4.1 Harmonic parametrisation

The generalized Hooke's law reads

$$\sigma_{ij} = C_{ijkl} \varepsilon_{kl}$$

in which $\underset{\approx}{\mathbb{C}}$ is a fourth-order tensor. High-order tensors are not easy objects to handle and it is often convenient to rewrite them as matrices. There are two well-known conventions to do that, the *Voigt's convention* and the *Kelvin's one*.

The Kelvin convention consists of introducing a tensor-based basis for the space $S^2(\mathbb{R}^2)$, denoted \mathcal{K} , and to write $\underset{\approx}{\sigma}$ and $\underset{\approx}{\varepsilon}$ as a vector with respect to it. As a consequence, $\underset{\approx}{\mathbb{C}}$ can be rewritten as a matrix with regard to \mathcal{K} .

In \mathbb{R}^2 the Kelvin basis is as follows:

$$\mathcal{K} = \{\mathbf{e}_1 \otimes \mathbf{e}_1, \mathbf{e}_2 \otimes \mathbf{e}_2, \frac{\sqrt{2}}{2} (\mathbf{e}_1 \otimes \mathbf{e}_2 + \mathbf{e}_2 \otimes \mathbf{e}_1)\}$$

Differ from the *Voigt notation* (another common practice representation), the advantage of Kelvin notation is that it performs the same for stress- and strain-type quantities based on the same orthonormal

basis, For 2D linear elasticity, the transformation is performed as follows:

$$\begin{aligned}\sigma_{ij} &\rightarrow \{\tilde{\sigma}\}_{\mathcal{K}} = (\sigma_{11}, \sigma_{22}, \sqrt{2}\sigma_{12})_{\mathcal{K}}^T \\ \varepsilon_{ij} &\rightarrow \{\tilde{\varepsilon}\}_{\mathcal{K}} = (\varepsilon_{11}, \varepsilon_{22}, \sqrt{2}\varepsilon_{12})_{\mathcal{K}}^T\end{aligned}$$

As a consequence, stress-strain relations [Equation 2.1](#) for a linear elastic material can be written as follows :

$$\begin{pmatrix} \sigma_{11} \\ \sigma_{22} \\ \sqrt{2}\sigma_{12} \end{pmatrix}_{\mathcal{K}} = \begin{pmatrix} C_{1111} & C_{1122} & \sqrt{2}C_{1112} \\ & C_{2222} & \sqrt{2}C_{2212} \\ & & 2C_{1212} \end{pmatrix}_{\mathcal{K}} \begin{pmatrix} \varepsilon_{11} \\ \varepsilon_{22} \\ \sqrt{2}\varepsilon_{12} \end{pmatrix}_{\mathcal{K}}$$

As is shown, such Kelvin convention acts as a simple replacement of fourth-order tensors having the necessary symmetries by 3×3 matrices and symmetric second-order tensors by vectors in \mathbb{R}^3 .

[Equation 3.4](#) shows that an elasticity tensor \mathbb{C} can be expressed by harmonic components. To this end, followed by [Equation 3.1](#), the components of \mathbb{h} and \mathbb{H} in the two-dimensional spaces \mathbb{K}^2 and \mathbb{K}^4 , defined through:

$$\mathbb{h} = h_1 \mathbf{k}_1^{(2)} + h_2 \mathbf{k}_2^{(2)} \quad \mathbb{H} = H_1 \mathbf{k}_1^{(4)} + H_2 \mathbf{k}_2^{(4)}$$

with [\[119\]](#),

$$\begin{aligned}\mathbf{k}_1^{(2)} &= \frac{\sqrt{2}}{2}(\mathbf{e}_1 \otimes \mathbf{e}_1 - \mathbf{e}_2 \otimes \mathbf{e}_2) & \mathbf{k}_2^{(2)} &= \frac{\sqrt{2}}{2}(\mathbf{e}_1 \otimes \mathbf{e}_2 + \mathbf{e}_2 \otimes \mathbf{e}_1) \\ \mathbf{k}_1^{(4)} &= \frac{\sqrt{2}}{2}(\mathbf{k}_1^{(2)} \otimes \mathbf{k}_1^{(2)} - \mathbf{k}_2^{(2)} \otimes \mathbf{k}_2^{(2)}) & \mathbf{k}_2^{(4)} &= \frac{\sqrt{2}}{2}(\mathbf{k}_1^{(2)} \otimes \mathbf{k}_2^{(2)} + \mathbf{k}_2^{(2)} \otimes \mathbf{k}_1^{(2)})\end{aligned}$$

thus, the Kelvin representation of \mathbb{C} in terms of harmonic components is:

$$\begin{pmatrix} \frac{\alpha}{2} + \frac{\beta}{2} + \frac{h_1}{\sqrt{2}} + \frac{H_1}{2\sqrt{2}} & -\frac{\alpha}{2} + \frac{\beta}{2} - \frac{H_1}{2\sqrt{2}} & \frac{h_2}{2} + \frac{H_2}{2} \\ -\frac{\alpha}{2} + \frac{\beta}{2} - \frac{H_1}{2\sqrt{2}} & \frac{\alpha}{2} + \frac{\beta}{2} - \frac{h_1}{\sqrt{2}} + \frac{H_1}{2\sqrt{2}} & \frac{h_2}{2} - \frac{H_2}{2} \\ \frac{h_2}{2} + \frac{H_2}{2} & \frac{h_2}{2} - \frac{H_2}{2} & \alpha - \frac{H_1}{\sqrt{2}} \end{pmatrix}_{\mathcal{K}} \quad (3.7)$$

3.4.2 Polar parametrisation

The mechanical property of a material is represented by a tensor using Cartesian components. It is widely used because of its simplicity in seeing the phenomena in classical mechanics and performing tensor operations. But anisotropy is the dependence of a mechanical property on the direction. In this case, the Cartesian representation meets its limitation since it is not an intrinsic representation, saying that it is strongly dependent on the chosen reference.

Thus, we make desirable a different tensor representation, based on tensor invariants, i.e. describing the mechanical behaviour of a material by intrinsic quantities. Apart from the empirical algebraic approach that obtaining invariants from the harmonic decomposition ([section 3.3](#), [section 3.5](#)), we describe here the polar method based on complex variables proposed by Verchery[\[55\]](#). The objectives of polar parametrisation in this section are twofold:

1. To establish a precise connection between polar components and harmonic components;
2. Since the polar components of the inverse tensor \mathbb{C}^{-1} can be easily obtained as functions of those of \mathbb{C} [\[9\]](#), it can be used to deduce the inverse components for harmonic parametrisation.

The construction of polar parametrisation is outlined in great detail in [9, 63], and for the reader's convenience, we present here the final results for $\mathbb{C} \in \text{Ela}$. The polar components expressed in terms of the Cartesian ones obtained as follows:

$$\begin{aligned}
 8T_0 &= C_{1111} - 2C_{1122} + 4C_{1212} + C_{2222}, \\
 8T_1 &= C_{1111} + 2C_{1122} + C_{2222}, \\
 8R_0 e^{4i\Phi_0} &= C_{1111} - 2C_{1122} - 4C_{1212} + C_{2222} + 4i(C_{1112} - C_{1222}), \\
 8R_1 e^{2i\Phi_1} &= C_{1111} - C_{2222} + 2i(C_{1112} + C_{1222}).
 \end{aligned} \tag{3.8}$$

with $\{T_0, T_1, R_0, R_1, \Phi_0, \Phi_1\}$ the polar components of \mathbb{C} , and inversely we obtain the polar parametrisation of \mathbb{C} , compared to that of harmonic parametrisation, we have :

	Harmonic parametrisation				Polar parametrisation			
C_{1111}	$\alpha/2$	$+\beta/2$	$+h_1/\sqrt{2}$	$+H_1/2\sqrt{2}$	T_0	$+2T_1$	$+4R_1 \cos 2\Phi_1$	$+R_0 \cos 4\Phi_0$
C_{1112}			$h_2/2\sqrt{2}$	$+H_2/2\sqrt{2}$			$2R_1 \sin 2\Phi_1$	$+R_0 \sin 4\Phi_0$
C_{1122}	$-\alpha/2$	$+\beta/2$		$-H_1/2\sqrt{2}$	$-T_0$	$+2T_1$		$-R_0 \cos 4\Phi_0$
C_{1212}	$\alpha/2$			$-H_1/2\sqrt{2}$	T_0			$-R_0 \cos 4\Phi_0$
C_{1222}			$h_2/2\sqrt{2}$	$-H_2/2\sqrt{2}$			$2R_1 \sin 2\Phi_1$	$-R_0 \sin 4\Phi_0$
C_{2222}	$\alpha/2$	$+\beta/2$	$-h_1/\sqrt{2}$	$+H_1/2\sqrt{2}$	T_0	$+2T_1$	$-4R_1 \cos 2\Phi_1$	$+R_0 \cos 4\Phi_0$

which indicates the following relations:

$$\alpha = 2T_0 \quad \beta = 4T_1 \quad \underset{\sim}{h} \rightarrow 4R_1 e^{2i\Phi_1} \quad \underset{\sim}{H} \rightarrow R_0 e^{4i\Phi_0} \tag{3.9}$$

where " \rightarrow " means to represent a given tensor in the polar coordinate. The following harmonic quantities in terms of polar components will be used in the upcoming inverse computation (subsection 3.4.3):

- Scalars

$$\underset{\sim}{h} : \underset{\sim}{h} = 32R_1^2 \quad \underset{\sim}{H} :: \underset{\sim}{H} = 8R_0^2; \quad \underset{\sim}{h} : \underset{\sim}{H} : \underset{\sim}{h} = 64R_0R_1^2 \cos 4(\Phi_0 - \Phi_1)$$

- 2nd order harmonic tensor

$$\underset{\sim}{H} : \underset{\sim}{h} \rightarrow 8R_0R_1 e^{(4\Phi_0 - 2\Phi_1)i}$$

- 4th order harmonic tensor

$$\underset{\sim}{h} * \underset{\sim}{h} \rightarrow 8R_1^2 e^{4i\Phi_1}$$

with $*$ the harmonic product between two harmonic tensors:

$$\underset{\sim}{h} * \underset{\sim}{h} := (\underset{\sim}{h} \otimes \underset{\sim}{h})^s - \frac{1}{2}(\underset{\sim}{1} \otimes (\underset{\sim}{h} \cdot \underset{\sim}{h}))^s$$

$(\cdot)^s$ represent the complete symmetrisation of a tensor, for $T_1, T_2 \in \mathbb{T}^n$:

$$(T_1 \otimes T_2)^s = \frac{1}{2}(T_1 \otimes T_2 + T_2 \otimes T_1)$$

3.4.3 Parametrisation of the inverse of a tensor

The polar components of the inverse tensor \mathbb{C}^{-1} can be easily found since Equation 3.8 are also valid for \mathbb{C}^{-1} , and if the Cartesian components of \mathbb{C}^{-1} are expressed in terms of those of \mathbb{C} and the latter by their polar components, the polar components of \mathbb{C}^{-1} , in the following designated by lower case letters $\{t_0, t_1, r_0, r_1, \varphi_0, \varphi_1\}$, are obtained in terms of $\{T_0, T_1, R_0, R_1, \Phi_0, \Phi_1\}$:

$$t_0 = 4 \frac{T_0 T_1 - R_1^2}{\Delta}, \quad t_1 = \frac{T_0^2 - R_0^2}{\Delta}, \quad (3.10)$$

$$r_0 e^{4i\varphi_0} = 4 \frac{(R_1 e^{2i\Phi_1})^2 - T_1 R_0 e^{4i\Phi_0}}{\Delta}, \quad r_1 e^{2i\varphi_1} = -2R_1 e^{2i\Phi_1} \frac{T_0 - R_0 e^{4i(\Phi_0 - \Phi_1)}}{\Delta}. \quad (3.11)$$

with

$$\Delta = 16T_1 (T_0^2 - R_0^2) - 32R_1^2 [T_0 - R_0 \cos 4(\Phi_0 - \Phi_1)]$$

The explicit decomposition of $\mathbb{S} = \mathbb{C}^{-1}$ has the same structure as that of \mathbb{C}

$$\mathbb{C}^{-1} = \mathbb{S} = f(\alpha^-, \beta^-, \mathfrak{h}^-, \mathfrak{H}^-),$$

in which $\{\alpha^-, \beta^-, \mathfrak{h}^-, \mathfrak{H}^-\}$ denotes the harmonic components of \mathbb{C}^{-1} . The relations between polar components and harmonic components of \mathbb{C} established in [subsection 3.4.2](#) is also valid for that of \mathbb{C}^{-1} . Therefore, the harmonic components $\{\alpha^-, \beta^-, \mathfrak{h}^-, \mathfrak{H}^-\}$ can be expressed in terms of those of \mathbb{C} :

$$\alpha^- = \frac{1}{4\Delta} (4\alpha\beta - \mathfrak{h} : \mathfrak{h}), \quad \beta^- = \frac{1}{2\Delta} (2\alpha^2 - \mathfrak{H} :: \mathfrak{H}), \quad (3.12)$$

$$\mathfrak{h}^- = \frac{1}{\Delta} (\mathfrak{H} : \mathfrak{h} - \alpha\mathfrak{h}), \quad \mathfrak{H}^- = \frac{1}{2\Delta} (\mathfrak{h} * \mathfrak{h} - 2\beta\mathfrak{H}), \quad (3.13)$$

with Δ defined as:

$$\Delta = \alpha^2\beta - \frac{1}{2}\beta\mathfrak{H} :: \mathfrak{H} - \frac{1}{2}\alpha\mathfrak{h} : \mathfrak{h} + \frac{1}{2}\mathfrak{h} : \mathfrak{H} : \mathfrak{h},$$

3.5 Invariants and integrity basis

Since the space $\mathbb{E}la$ has been explicitly decomposed into a collection of $O(2)$ -irreducible spaces in [proposition 3.1](#), the question is now to determine an associated integrity basis (introduced in [section 2.5](#)). It has to be noted that this result has been known since the second half of the 90' [[74](#), [121](#), [122](#)] (see also the recent paper [[117](#)]). Such an integrity basis has the following structure:

$$\{I_1, J_1, I_2, J_2, I_3\}$$

in which I_k indicates a homogeneous polynomial of degree k in \mathbb{C} . From the explicit harmonic decomposition ([Equation 3.4](#)), we have the following result:

Theorem 3.1: Integrity basis of $\mathbb{E}la$

A minimal integrity basis for $O(2)$ -action on $\mathbb{E}la$ is given by

$$\mathcal{IB} = \{I_1, J_1, I_2, J_2, I_3\}.$$

in which

$$I_1 = \alpha, \quad J_1 = \beta, \quad I_2 = \mathfrak{h} : \mathfrak{h}, \quad J_2 = \mathfrak{H} :: \mathfrak{H}, \quad I_3 = \mathfrak{h} : \mathfrak{H} : \mathfrak{h}.$$

These elements are independent, meaning that they are not related by any polynomial relation. They satisfy, however, the following inequalities [[75](#)]:

$$I_2 \geq 0, \quad J_2 \geq 0, \quad I_2^2 J_2 - 2I_3^2 \geq 0. \quad (3.14)$$

As such, they define a closed domain of \mathbb{R}^5 , denoted by \mathcal{V} . The last inequality implies that $I_3 = 0$ as soon as I_2 or J_2 is zero.

These invariants can be expressed in terms of the harmonic components with respect to the basis $\mathfrak{R}^{(n)}$, and tensor components C_{ijkl} with respect to the canonical tensor basis \mathcal{B} :

- Linear invariants

$$\begin{aligned} I_1 &= \alpha = \frac{1}{4}(C_{1111} - 2C_{1122} + 4C_{1212} + C_{2222}) \\ J_1 &= \beta = \frac{1}{2}(C_{1111} + 2C_{1122} + C_{2222}) \end{aligned}$$

- Quadratic invariants

$$\begin{aligned} I_2 &= \underset{\sim}{\mathfrak{h}} : \underset{\sim}{\mathfrak{h}} = 2(h_1^2 + h_2^2) \\ &= 2(C_{1112} + C_{1222})^2 + \frac{1}{2}(C_{1111} - C_{2222})^2 \\ J_2 &= \underset{\approx}{\mathfrak{H}} :: \underset{\approx}{\mathfrak{H}} = 8(H_1^2 + H_2^2) \\ &= 2(C_{1112} - C_{1222})^2 + \frac{1}{8}(C_{1111} - 2C_{1122} - 4C_{1212} + C_{2222})^2 \end{aligned}$$

In terms of the graphical interpretation introduced in [Figure 3.1](#), these quantities are nothing but the square norms of the vectors in the harmonic bouquet $\text{HB}(\underset{\approx}{\mathbb{C}})$.

- Cubic invariants

$$\begin{aligned} I_3 &= 4 \left| \underset{\sim}{\mathfrak{h}} \right|^2 \left| \underset{\approx}{\mathfrak{H}} \right| \cos(\beta - 2\alpha) = \underset{\sim}{\mathfrak{h}} : \underset{\approx}{\mathfrak{H}} : \underset{\sim}{\mathfrak{h}} \\ &= 4h_1^2 H_1 - 4h_2^2 H_1 + 8h_1 h_2 H_2 \\ &= \frac{1}{8}(C_{1111}^3 - (2C_{1122} + 4C_{1212} + C_{2222})C_{1111}^2 + (4(C_{1112} + C_{1222}))(3C_{1112} - 5C_{1222}) \\ &\quad + (4C_{1122} + 8C_{1212} - C_{2222})C_{2222}C_{1111} + C_{2222}^3 + 8(C_{1122} + 2C_{1212})(C_{1112} + C_{1222})^2 \\ &\quad - 2(C_{1122} + 2C_{1212})C_{2222}^2 - 4(5C_{1112} - 3C_{1222})(C_{1112} + C_{1222})C_{2222}) \end{aligned}$$

This last invariant can be seen as a tensor product in \mathbb{K}^4 between $\underset{\approx}{\mathfrak{H}}$ and $\underset{\sim}{\mathfrak{h}} * \underset{\sim}{\mathfrak{h}}$.

Remark. We define the following application from $\mathbb{E}a$ to orbit space $\mathbb{E}a/\text{O}(2)$ which associates to a tensor its (uniquely defined) elastic material:

$$\mathcal{IB}(\underset{\approx}{\mathbb{C}}) := \left(I_1(\underset{\approx}{\mathbb{C}}), J_1(\underset{\approx}{\mathbb{C}}), I_2(\underset{\approx}{\mathbb{C}}), J_2(\underset{\approx}{\mathbb{C}}), I_3(\underset{\approx}{\mathbb{C}}) \right).$$

This application introduces coordinates on the orbit space.

Let us now parameterise the invariants of $\underset{\approx}{\mathbb{S}} = \underset{\approx}{\mathbb{C}}^{-1}$ in terms of those of $\underset{\approx}{\mathbb{C}}$. The invariants of $\underset{\approx}{\mathbb{S}}$ are denoted $(I_1^-, J_1^-, I_2^-, J_2^-, I_3^-)$ and are rational functions of those of $\underset{\approx}{\mathbb{C}}$:

$$\begin{aligned} I_1^- &= \frac{1}{4\Delta} (4I_1 J_1 - I_2), & J_1^- &= \frac{1}{2\Delta} (2I_1^2 - J_2), \\ I_2^- &= \frac{1}{\Delta^2} \left(\frac{1}{2} J_2 I_2 - 2I_1 I_3 + I_1^2 I_2 \right), & J_2^- &= \frac{1}{4\Delta^2} \left(\frac{1}{2} I_2^2 - 4J_1 I_3 + 4J_1^2 J_2 \right), \end{aligned}$$

and

$$I_3^- = \frac{1}{2\Delta^3} \left(I_3^2 - \frac{1}{4} I_2^2 J_2 - J_1 J_2 I_3 - I_1 I_2 I_3 + 2I_1 J_1 I_2 J_2 + \frac{1}{2} I_1^2 I_2^2 - 2I_1^2 J_1 I_3 \right),$$

in which Δ is the determinant of \mathbb{C} :

$$\Delta = \frac{1}{2}(I_3 - I_1 I_2 - J_1 J_2 + 2I_1^2 J_1).$$

It is obvious that for \mathbb{C} to be invertible $\Delta \neq 0$. These relations can be obtained using the results of [subsection 3.4.3](#).

3.6 Symmetry classes of $\mathbb{E}a$

So far, the question of the symmetry classes of $\mathbb{E}a$ has been postponed. As indicated in [2.6.2](#), their determination can be achieved from the harmonic structure of $\mathbb{E}a$.

To do this, and as the procedure in [subsection 2.6.3](#) indicates, this determination supposes to know the symmetry classes of the \mathbb{K}^n spaces. This is the object of the following theorem [[106](#)]:

Theorem 3.2: Symmetry classes of \mathbb{K}^n

The symmetry classes for the $O(2)$ -irreducible space \mathbb{K}^n are:

$$\mathfrak{J}(\mathbb{K}^n) = \begin{cases} \{[\text{SO}(2)], [\text{O}(2)]\}; & n = -1 \\ \{[\text{O}(2)]\}; & n = 0 \\ \{[\text{D}_n], [\text{O}(2)]\}; & n \geq 1 \end{cases}$$

with the convention $\text{D}_1 = \text{Z}_2^{\mathbf{m}_{e_2}}$

The symmetry classes of $\mathbb{E}a$ can now be computed using iterated clips operations and the following table:

Theorem 3.3: Clips operations between $O(2)$ -closed subgroups

\odot	[Id]	$[\text{Z}_2^{\sigma_x}]$	$[\text{Z}_n]$	$[\text{D}_n]$	$[\text{SO}(2)]$	$[\text{O}(2)]$
[Id]	[Id]					
$[\text{Z}_2^{\sigma_x}]$	[Id]	[Id], $[\text{Z}_2^{\sigma_x}]$				
$[\text{Z}_m]$	[Id]	[Id]	$[\text{Z}_{d(n,m)}]$			
$[\text{D}_m]$	[Id]	[Id], $[\text{Z}_2^{\sigma_x}]$	$[\text{Z}_{d(n,m)}]$	$[\text{Z}_{d(n,m)}], [\text{D}_{d(n,m)}]$		
$[\text{SO}(2)]$	[Id]	[Id]	$[\text{Z}_n]$	$[\text{Z}_n]$	$[\text{SO}(2)]$	
$[\text{O}(2)]$	[Id]	$[\text{Z}_2^{\sigma_x}]$	$[\text{Z}_n]$	$[\text{D}_n]$	$[\text{SO}(2)]$	$[\text{O}(2)]$

where $\text{Z}_1 := 1$, $\text{D}_1 := \text{Z}_2^{\mathbf{m}_{e_2}}$ and $d(n, m) := \text{gcd}(n, m)$. Due to the commutativity of the clips operator, this table is symmetric and only a half part has been filled.

The space of $\mathbb{E}a$ can be partitioned into strata based on the fact that two tensors are in the same stratum if they have the same symmetry class.

Theorem 3.4: Strata of $\mathbb{E}la$

$\mathbb{E}la$ is partitioned into 4 strata [74]:

$$\mathbb{E}la = \Sigma_{[Z_2]} \cup \Sigma_{[D_2]} \cup \Sigma_{[D_4]} \cup \Sigma_{[O(2)]} \quad (3.15)$$

Proof. The symmetry classes of $\mathbb{E}la$ can be obtained using clips products. This determination starts with the harmonic structure of $\mathbb{E}la$:

$$\mathbb{E}la \simeq 2\mathbb{K}^0 \oplus \mathbb{K}^2 \oplus \mathbb{K}^4.$$

Since $\mathfrak{J}(\mathbb{K}^0) = [O(2)]$ the symmetry classes of $\mathbb{E}la$ are given by

$$\mathfrak{J}(\mathbb{E}la) = \mathfrak{J}(\mathbb{K}^2) \odot \mathfrak{J}(\mathbb{K}^4).$$

The symmetry classes of the harmonic components are

$$\mathfrak{J}(\mathbb{K}^2) = \{[D_2], [O(2)]\}, \quad \mathfrak{J}(\mathbb{K}^4) = \{[D_4], [O(2)]\}.$$

it results that

$$\begin{aligned} \mathfrak{J}(\mathbb{E}la) &= \{[D_2], [O(2)]\} \odot \{[D_4], [O(2)]\} \\ &= \{[D_2] \odot [D_4]\} \cup \{[D_2] \odot [O(2)]\} \cup \{[O(2)] \odot [D_4]\} \cup \{[O(2)]\} \\ &= \{[Z_2], [D_2], [D_4], [O(2)]\} \end{aligned}$$

□

Remark. In mechanical terms, $\Sigma_{[Z_2]}$ corresponds to the set of biclinic tensors, $\Sigma_{[D_2]}$ to the set of orthotropic tensors, $\Sigma_{[D_4]}$ to the set of tetragonal tensors and $\Sigma_{[O(2)]}$ to the isotropic tensors.

3.7 Conditions of belonging to a symmetry class

3.7.1 Covariant-based conditions

Let us start by defining a totally generic elasticity tensor with the lowest level of spatial invariance.

Genericity

The inequality $I_2^2 J_2 - 2I_3^2 > 0$ defines a totally generic elasticity tensor with the lowest level of spatial invariance. Almost all elasticity tensors are generic, meaning the probability is 1 of randomly picking elasticity tensors satisfying these relations.

From a geometric point of view, the anisotropic harmonic bouquet $HB = \{\underset{\sim}{\mathfrak{h}}, \underset{\sim}{\mathfrak{H}}\}$ is non-degenerated, i.e.

- neither $\underset{\sim}{\mathfrak{h}}$ nor $\underset{\sim}{\mathfrak{H}}$ is nil;
- they are not *aligned*, meaning that $(\underset{\sim}{\mathfrak{h}} * \underset{\sim}{\mathfrak{h}}) \times \underset{\sim}{\mathfrak{H}} \neq 0$;

in which $*$ and \times stand, respectively, for the *harmonic* and *generalised cross product* as defined in [Appendix A](#). This last condition motivates the introduction of the concept of *Homogeneous Harmonic Bouquet* $H HB = \{\underset{\sim}{\mathfrak{h}} * \underset{\sim}{\mathfrak{h}}, \underset{\sim}{\mathfrak{H}}\}$, in which all elements belong to the same harmonic space and therefore transform in the same way. This notion will allow us to introduce the *harmonic normal form* of an elasticity

tensor. To this end, recall the orthonormal basis $\mathfrak{K}^{(n)} = (k_1^n, k_2^n)$ of \mathbb{K}^n mentioned in [section 3.2](#). Since elasticity tensors sharing the same orbit have conjugate HHB, the following result is natural

$$\forall \underline{\underline{C}} \in \text{Ela}, \exists \mathbf{g} \in O(2) \text{ s.t. } (\mathbf{g} \star \underline{\underline{H}})_1 > 0, (\mathbf{g} \star \underline{\underline{H}})_2 = 0$$

with $(\underline{\underline{H}})_i = \underline{\underline{H}} :: k_i^{(4)}$. A generic tensor $\underline{\underline{C}}$ is in its harmonic normal form, if $(\underline{\underline{H}})_1 > 0$, and $(\underline{\underline{H}})_2 = 0$. Geometrically, this corresponds to the configuration depicted on [Figure 3.2](#).

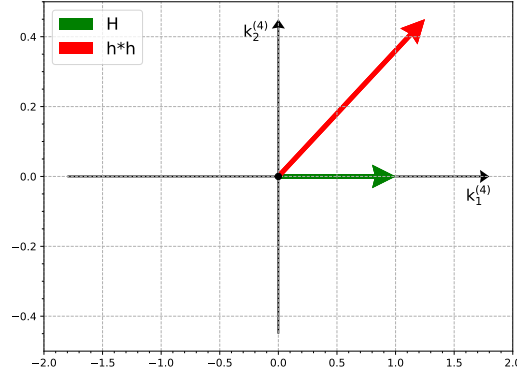


Figure 3.2: Harmonic normal form of a generic elasticity tensor.

Harmonic bouquets not satisfying the genericity conditions are said *degenerated*. Tensors that are invariant w.r.t. some spatial transformations usually possess degenerated bouquet⁶. But, as will be seen, this mechanism is not surjective, meaning that some degenerated systems may not imply a specific spatial invariance. This is particularly true for tensors with a large harmonic bouquet.

The four strata in [Theorem 3.4](#) are organized as follows⁷:

$$\Sigma_{[Z_2]} \xrightarrow{(\underline{\underline{h}} \star \underline{\underline{h}}) \times \underline{\underline{H}} = 0} \Sigma_{[D_2]} \xrightarrow{\underline{\underline{h}} : \underline{\underline{h}} = 0} \Sigma_{[D_4]} \xrightarrow{\underline{\underline{H}} :: \underline{\underline{H}} = 0} \Sigma_{[O(2)]}. \quad (3.16)$$

Geometrically, the harmonic normal forms of elasticity tensors in the three remaining classes are⁸:

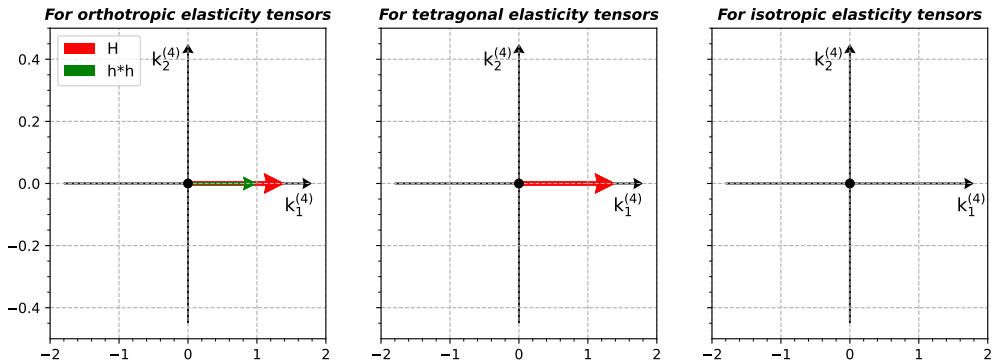


Figure 3.3: Harmonic normal form of non-generic elasticity tensors.

⁶The case of even-order tensors is a bit special, since generic even-order tensors are Z_2 -invariant.

⁷It should be noted that such an in-line structure is exceptional and is very specific to 2D linear elasticity.

⁸A tetragonal tensor $\underline{\underline{C}}$ is in its harmonic normal form if $(\underline{\underline{h}} \star \underline{\underline{h}})_1 = 0$, and $(\underline{\underline{h}} \star \underline{\underline{h}})_2 > 0$.

The symmetry class of the elements belonging to the *open* stratum $\Sigma_{[H]}$ is *exactly* $[H]$. The closed strata $\bar{\Sigma}_{[H]}$ on its side contains elements whose symmetry classes are at least $[H]$. Since the lattice of symmetry classes is linear (3.16):

$$\begin{aligned}\bar{\Sigma}_{[Z_2]} &= \Sigma_{[Z_2]} \cup \Sigma_{[D_2]} \cup \Sigma_{[D_4]} \cup \Sigma_{[O(2)]} (= \mathbb{E}1a), \\ \bar{\Sigma}_{[D_2]} &= \Sigma_{[D_2]} \cup \Sigma_{[D_4]} \cup \Sigma_{[O(2)]}, \\ \bar{\Sigma}_{[D_4]} &= \Sigma_{[D_4]} \cup \Sigma_{[O(2)]}, \\ \bar{\Sigma}_{[O(2)]} &= \Sigma_{[O(2)]}.\end{aligned}$$

At the exception of $\Sigma_{[O(2)]}$, open strata are not vector spaces. The simplest reason for this is that the identity element does not belong to strata other than the isotropic one. For the closed strata, the situation is different. Since elements within a stratum have conjugate symmetry groups, the stability with regard to linear combination is not automatic. It can be proved that for 2D linear elasticity, all closed strata, except the orthotropy one, are vector spaces [74, 123].

3.7.2 Polynomial invariant conditions

For the least symmetric class, that is for biclinic elastic materials, the polynomial invariants of \mathcal{IB} are algebraically independent. A biclinic material is described by five independent quantities, that is by a point in $\mathcal{V} \subset \mathbb{R}^5$. The location of this point is not any, since constrained by the relations (3.14).

For elastic materials with higher symmetries, polynomial relations (also called syzygies) between elements of \mathcal{IB} appear. For example, for (at least) orthotropic materials the following polynomial relation is satisfied:

$$I_2^2 J_2 - 2I_3^2 = 0,$$

hence orthotropic materials belong to $\partial\mathcal{V}$ which is a 4D surface in \mathbb{R}^5 . These relations for all strata are provided in the following table.

Table 3.2: Polynomial conditions for membership of an open stratum

stratum	Tensor representations	Polynomial conditions
$\Sigma_{[Z_2]}$	$(\alpha, \beta, \underline{h}, \underline{H})$	$I_2^2 J_2 - 2I_3^2 > 0$
$\Sigma_{[D_2]}$	$(\alpha, \beta, \underline{\tilde{h}}, \underline{\tilde{H}})$	$I_2^2 J_2 - 2I_3^2 = 0$ and $I_2 \neq 0$
$\Sigma_{[D_4]}$	$(\alpha, \beta, 0, \underline{\tilde{H}})$	$I_2 = 0$ and $J_2 \neq 0$
$\Sigma_{[O(2)]}$	$(\alpha, \beta, 0, 0)$	$I_2 + J_2 = 0$

Polynomial transitions are summed up on the following lattice:

$$\Sigma_{[Z_2]} \xrightarrow{I_2^2 J_2 - 2I_3^2 = 0} \Sigma_{[D_2]} \xrightarrow{I_2 = 0} \Sigma_{[D_4]} \xrightarrow{J_2 = 0} \Sigma_{[O(2)]}.$$

In the case of 2D elasticity, the geometry of the elastic material space can be visualized⁹.

⁹Without taking the positive definiteness condition into account.

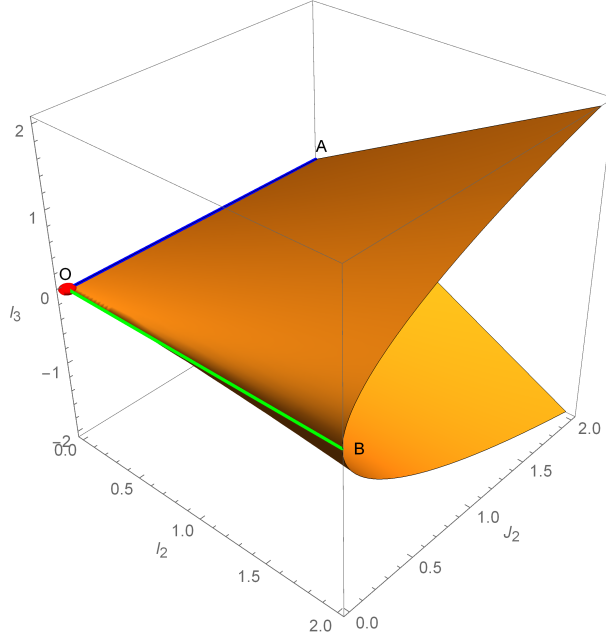


Figure 3.4: Semi-algebraic variety of elastic materials with respect to (I_2, J_2, I_3) .

Figure 3.4 depicts the elastic material space with respect to (I_2, J_2, I_3) . The surface, which corresponds to the polynomial equation: $I_2^2 J_2 - 2I_3^2 = 0$ contains all the *at-least-orthotropic* materials (stratum $\bar{\Sigma}_{[D_2]} = \Sigma_{[D_2]} \cup \Sigma_{[D_4]} \cup \Sigma_{[O(2)]}$). The condition $I_2^2 J_2 - 2I_3^2 > 0$ indicates on which side of the orthotropic surface are the biclinic materials located (stratum $\Sigma_{[Z_2]}$). Finally, we get that, independently of the values of the isotropic invariants I_1 and J_1 :

- point O corresponds to isotropic materials (stratum $\Sigma_{[O(2)]}$);
- open ray $]OA)$ corresponds to tetragonal materials (stratum $\Sigma_{[D_4]}$);
- surface without $\{O\} \cup]OA) \cup]OB)$ corresponds to ordinary orthotropic materials (stratum $\Sigma_{[D_2]}$);
- biclinic materials (stratum $\Sigma_{[Z_2]}$) are strictly inside the volume defined by the surface.

3.7.3 Inverse stability of the symmetry class

From a physical point of view, and for a given material, the stiffness tensor and the compliance tensor are two equivalent ways of describing the macroscopic behaviour resulting from an identical microstructure. It therefore seems natural that their symmetry groups, and thus their symmetry classes, coincide. This seems so natural that, up to the author's best knowledge, no mathematical proof of this point has been given. A simple proof of that point is provided here.

Theorem 3.5: Inverse stability of symmetry group

If \mathbb{C} and \mathbb{S} are two elasticity tensors satisfying $\mathbb{S} : \mathbb{C} = \mathbb{C} : \mathbb{S} = \mathbb{I}$ then $G_{\mathbb{C}} = G_{\mathbb{S}}$.

Proof. Let consider \mathbb{C} as a symmetric second-order tensor on $S^2(\mathbb{R}^3)$, and denote by $[\mathbb{C}]$ its matrix representation with respect to a basis of \mathbb{R}^3 . Let $p_{\mathbb{C}}(X)$ be the characteristic polynomial of $[\mathbb{C}]$,

$$p(X) = X^3 - \sigma_1 X^2 + \sigma_2 X - \sigma_3$$

in which σ_k are elementary symmetric polynomials:

$$\begin{cases} \sigma_1 = \lambda_1 + \lambda_2 + \lambda_3 = \text{tr}(\underline{\mathbb{C}}), \\ \sigma_2 = \lambda_1\lambda_2 + \lambda_2\lambda_3 + \lambda_1\lambda_3, \\ \sigma_3 = \lambda_1\lambda_2\lambda_3 = \det(\underline{\mathbb{C}}), \end{cases}$$

It should be noted that symmetric polynomials are $O(3)$ -invariant polynomials of $\underline{\mathbb{C}}$, i.e.

$$\forall \mathbf{g} \in O(3), \sigma_k(\mathbf{g} \star \underline{\mathbb{C}}) = \sigma_k(\underline{\mathbb{C}})$$

Hence since σ_k are $O(3)$ -invariant, they are also $O(2)$ -invariant for any $O(2)$ subgroups of $O(3)$.

From the Cayley-Hamilton theorem, it is known that $p(\underline{\mathbb{C}}) = 0$, i.e.

$$p(\underline{\mathbb{C}}) = \underline{\mathbb{C}}^3 - \sigma_1 \underline{\mathbb{C}}^2 + \sigma_2 \underline{\mathbb{C}} - \sigma_3 \underline{\mathbb{I}} = \mathbf{0}$$

Multiplying this relation on the left by $\underline{\mathbb{S}}$, and since $\sigma_3 \neq 0$, we obtain that

$$\underline{\mathbb{S}} = \frac{1}{\sigma_3} \left(\sigma_2 \underline{\mathbb{I}} - \sigma_1 \underline{\mathbb{C}} + \underline{\mathbb{C}}^2 \right)$$

Hence $\underline{\mathbb{S}}$ is polynomial in $\underline{\mathbb{C}}$, $\underline{\mathbb{S}} = P(\underline{\mathbb{C}})$. Let $\mathbf{g} \in G(\underline{\mathbb{C}})$,

$$\mathbf{g} \star \underline{\mathbb{S}} = \mathbf{g} \star P(\underline{\mathbb{C}}) = P(\mathbf{g} \star \underline{\mathbb{C}}) = P(\underline{\mathbb{C}}) = \underline{\mathbb{S}}$$

hence, $G(\underline{\mathbb{C}}) \subset G(\underline{\mathbb{S}})$. Since $\underline{\mathbb{C}}$ can be expressed in the same way as a polynomial function in $\underline{\mathbb{S}}$, the same reasoning leads to the reverse inclusion and to the final conclusion that

$$G(\underline{\mathbb{C}}) = G(\underline{\mathbb{S}})$$

□

Chapter 4

2D exotic and semi-exotic sets

4.1	Mechanical definition of exotic materials	54
4.2	Exotic elastic materials: R_0 -orthotropy	55
4.3	Semi-exotic elastic materials: Cauchy elasticity	57
4.4	Generalisation to other constitutive laws	58
4.4.1	A general theorem	59
4.4.2	Application to coupled constitutive laws	60

The geometric methods developed in the previous chapter are used to characterise spaces of linear materials in a very fine way. It can be observed that these spaces are very rich and a whole range of intermediate possibilities exist beyond symmetry classes. Materials with non-standard anisotropic properties associated with these intermediate possibilities are called *exotic materials*. This topic will be studied in this chapter [section 4.1](#) gives a mechanical definition of what is an exotic set of materials, this definition allowed us to verify in [section 4.2](#) that the space of 2D elasticity tensors has only one exotic set. And we also introduce an example of semi-exotic sets in [section 4.3](#). This definition also allows us to obtain in [section 4.4](#) a general result concerning any 2D constitutive tensor space.

4.1 Mechanical definition of exotic materials

The mechanical metamaterials are widely investigated in earlier work due to their superior mechanical performances, as in the important contribution by Vannucci [9] on R_0 -orthotropic materials. The number of independent elastic constants for this type of material is three, but they have only two orthogonal axes of symmetry, such property makes R_0 -orthotropic materials rather attractive for certain applications, especially when linked to laminate manufacturing. Apart from the anisotropic materials, a special isotropic material with negative Poisson's ratio is raised long ago by Lakes [124], which is then followed by subsequently related articles [125][126][127].

The goal of our research is to give a unified perspective towards these mechanical metamaterials and, above all, to show that these cases scattered here and there in the literature can be shown to be the special ones of what is obtained through the application of geometric tools presented in [chapter 3](#).

To avoid being too abstract, we come back to 2D materials, and it can be observed in [Table 6.3](#) that for isotropic and tetragonal materials, the spatial symmetries imply the vanishing of invariant polynomials. But this mechanism does not exhaust all possibilities since, for instance, no spatial symmetry results from the conditions $J_2 = 0$ or $I_3 = 0$. It follows that if one wants to design a mesostructure such that the effective elasticity tensor verifies these relationships, this cannot be done by imposing symmetry restrictions alone. These relations must be imposed by a specific design of the mesostructure. This aspect satisfies the first point of the properties defining *exotic* materials.

It may be tempting to define as *exotic* any material defined by the vanishing of polynomial quantities not associated to a symmetry invariance. However, it is not sufficient because it does not produce a paradoxical behaviour that is more symmetrical in appearance than expected.

As previously said, the mechanical definition of *exotic* materials is given out here:

4.1.1 Definition (Exotic materials)

An elasticity material will be said to be *exotic*, provided

1. it satisfies constraints independent of those that may be imposed by symmetry arguments;
2. its behaviour appears to be more symmetrical than that imposed by the material symmetries.

It should be noted that the second point excludes isotropic materials from the family of exotic materials. Indeed, since the material is already fully isotropic, a specific design, even if possible and potentially interesting, cannot produce a paradoxical increase in symmetry. Therefore, our definition here is adapted to anisotropic exotic behaviours.

Elastic materials that do not fulfill this second requirement will be referred to as *semi-exotic*. Even though such materials don't have a symmetry-related paradoxical behaviour, some of them do have other interesting physical performances. For 2D materials, a semi-exotic material will be introduced in [section 4.3](#).

In order to select from the many possibilities that really define exotic materials, we will recall the geometrical considerations in [section 3.6](#) and [section 3.7](#). At the core of this approach is the clip product, a tool for deducing the symmetry classes of a tensor space from its harmonic decomposition. It also

allows us to distinguish the exotic sets from the symmetry classes.

It is important to note that this approach extends almost directly to 3D situations [102]. This is the great strength of this approach.

4.2 Exotic elastic materials: R_0 -orthotropy

The symmetry classes of the harmonic bouquet $\{\underset{\sim}{\mathfrak{h}}, \underset{\approx}{\mathfrak{H}}\}$ in $\mathbb{K}^2 \oplus \mathbb{K}^4$ are obtained by the different possible clips of these elementary symmetry classes (obtained in section 3.6). Specifically, we have:

$\mathfrak{J}(\mathbb{K}^2) \odot \mathfrak{J}(\mathbb{K}^4)$	$[\mathbb{D}_4]$	$[\mathbb{O}(2)]$
$[\mathbb{D}_2]$	$[\mathbb{Z}_2], [\mathbb{D}_2]$	$[\mathbb{D}_2]$
$[\mathbb{O}(2)]$	$[\mathbb{D}_4]$	$[\mathbb{O}(2)]$

Several things can be observed from this Ela partition:

1. non-nil covariants $\underset{\sim}{\mathfrak{h}}$ and $\underset{\approx}{\mathfrak{H}}$ generates classes:

- $[\mathbb{Z}_2]$, which corresponds to a generic orientation of the pair $(\underset{\sim}{\mathfrak{h}}, \underset{\approx}{\mathfrak{H}})$, i.e.

$$(\underset{\sim}{\mathfrak{h}} * \underset{\sim}{\mathfrak{h}}) \times \underset{\approx}{\mathfrak{H}} \neq 0,$$

- $[\mathbb{D}_2]$, which corresponds to the *alignment* of the pair, i.e.

$$(\underset{\sim}{\mathfrak{h}} * \underset{\sim}{\mathfrak{h}}) \times \underset{\approx}{\mathfrak{H}} = 0.$$

2. the symmetry class $[\mathbb{D}_2]$ is obtained in two different manners¹

$$[\mathbb{D}_2]_{(\underset{\sim}{\mathfrak{h}}, \underset{\approx}{\mathfrak{H}})} = \{[\mathbb{D}_2]_{\underset{\sim}{\mathfrak{h}}} \odot [\mathbb{D}_4]_{\underset{\approx}{\mathfrak{H}}}, [\mathbb{D}_2]_{\underset{\sim}{\mathfrak{h}}} \odot [\mathbb{O}(2)]_{\underset{\approx}{\mathfrak{H}}}\},$$

It results that the stratum $\Sigma_{[\mathbb{D}_2]}$ can be divided into two subsets:

$$\Sigma_{[\mathbb{D}_2]} = \Sigma_{[\mathbb{D}_2]}^g \cup \Sigma_{[\mathbb{D}_2]}^e.$$

with the harmonic bouquet being of type $([\mathbb{D}_2]_{\underset{\sim}{\mathfrak{h}}}, [\mathbb{D}_4]_{\underset{\approx}{\mathfrak{H}}})$ for $\Sigma_{[\mathbb{D}_2]}^g$ while being $([\mathbb{D}_2]_{\underset{\sim}{\mathfrak{h}}}, [\mathbb{O}(2)]_{\underset{\approx}{\mathfrak{H}}})$ for $\Sigma_{[\mathbb{D}_2]}^e$. The first subset will be said *generic*², while the second will be called *exotic*, their graphic representations are given in Figure 4.1.

Elements in $\Sigma_{[\mathbb{D}_2]}^e$, which corresponds to the polynomial condition $J_2 = 0$, satisfy the following points:

1. this restriction does not only come from a symmetry requirement but also should satisfy an extra constraint;
2. the cancellation of $\underset{\approx}{\mathfrak{H}}$ results in an orthotropic material for which the deviatoric elasticity is isotropic, and thus more symmetrical than it should be. This will be clearer in the forthcoming Equation 4.2.

¹The notation $[H]_X$ indicates the symmetry class of X

²It should be noted that $\Sigma_{[\mathbb{D}_2]}^g$ is divided into two separate connected components, the membership of an elastic material to one or the other component is indicated by the sign of I_3 .

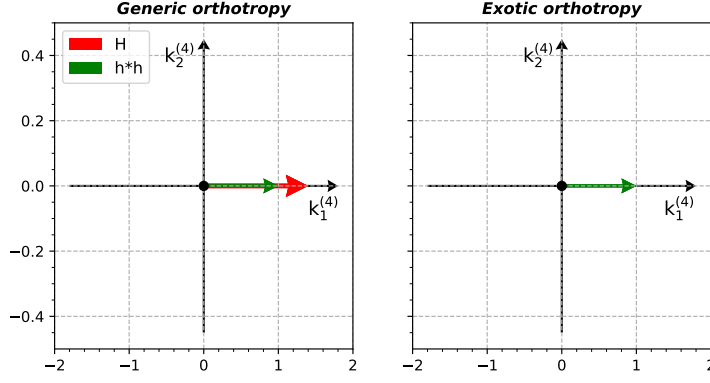


Figure 4.1: Harmonic normal form of generic and exotic orthotropic elasticity tensors.

Thus, following the Definition 4.1.1, these materials are called *exotic*, and can be represented by the harmonic components:

$$\underset{\approx}{\mathbb{C}} = f(\alpha, \beta, \underset{\approx}{h}, 0). \quad (4.1)$$

The set of such elastic materials is located on the open ray $]OB)$ in Figure 3.4. It corresponds to a subset of the stratum $\Sigma_{[D_2]}$. An important remark is that this property is not stable with respect to inversion. The harmonic components for $\underset{\approx}{\mathbb{S}} = \underset{\approx}{\mathbb{C}}^{-1}$ are denoted by $\{\alpha^-, \beta^-, \underset{\approx}{h}^-, \underset{\approx}{\mathbb{H}}^-\}$, and their expressions can be found in Equation 3.12. It can be observed that, in the case of $\underset{\approx}{\mathbb{H}} = 0$, the expression of $\underset{\approx}{\mathbb{H}}^-$ reduces to,

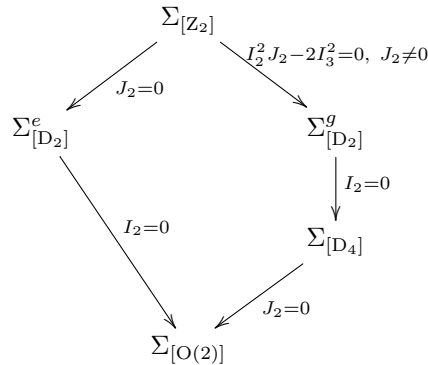
$$\underset{\approx}{\mathbb{H}}^- = \frac{2}{\Delta} (2\underset{\approx}{h} * \underset{\approx}{h}) \neq 0,$$

with $\Delta \neq 0$. Hence,

$$\underset{\approx}{\mathbb{C}} \in \Sigma_{[D_2]}^e \Rightarrow \underset{\approx}{\mathbb{S}} \notin \Sigma_{[D_2]}^e.$$

and conversely. A symmetry class is intrinsic to an elastic material, it is a property that does not depend on the choice of its description in terms of stiffness or compliance. Specifically, exotic sets of elastic materials can not be considered as symmetry classes. It results that exotic orthotropic materials can either be defined with respect to stiffness or with respect to compliance. But these materials are distinct since their respective inverse are not exotic [9].

In the end, this gives the following complete structure of transition between the different strata:



which can be detailed as a coupled elastic law (Equation 3.6) as follows

$$\begin{array}{ccc}
 & \begin{pmatrix} \mathbb{H} + \alpha \mathbb{J} & \frac{1}{2} \mathbb{h} \otimes \mathbb{1} \\ \frac{1}{2} \mathbb{1} \otimes \mathbb{h} & \beta \mathbb{K} \end{pmatrix} & \\
 & \swarrow_{J_2=0} & \searrow_{I_2^2 J_2 - 2I_3^2 = 0, J_2 \neq 0} \\
 \begin{pmatrix} \alpha \mathbb{J} & \frac{1}{2} \mathbb{h} \otimes \mathbb{1} \\ \frac{1}{2} \mathbb{1} \otimes \mathbb{h} & \beta \mathbb{K} \end{pmatrix} & & \begin{pmatrix} \mathbb{H} + \alpha \mathbb{J} & \frac{1}{2} \mathbb{h} \otimes \mathbb{1} \\ \frac{1}{2} \mathbb{1} \otimes \mathbb{h} & \beta \mathbb{K} \end{pmatrix} \\
 & \searrow_{I_2=0} & \downarrow_{I_2=0} \\
 & & \begin{pmatrix} \mathbb{H} + \alpha \mathbb{J} & 0 \\ 0 & \beta \mathbb{K} \end{pmatrix} \\
 & & \swarrow_{J_2=0} \\
 & & \begin{pmatrix} \alpha \mathbb{J} & 0 \\ 0 & \beta \mathbb{K} \end{pmatrix}
 \end{array}$$

This gives the following anisotropic elasticity law for a R_0 -orthotropic material

$$\begin{cases} \sigma_{\sim}^d = \alpha \varepsilon_{\sim}^d + \frac{1}{2} \text{tr}(\varepsilon_{\sim}^s) \mathbb{h}_{\sim} \\ \sigma_{\sim}^s = \frac{1}{2} (\mathbb{h}_{\sim} : \varepsilon_{\sim}^d) \mathbb{1}_{\sim} + \beta \varepsilon_{\sim}^s \end{cases} . \quad (4.2)$$

Finally, it can be shown that the set $\bar{\Sigma}_{[D_2]}^e$ is stable by linear combinations, i.e. it is a linear vector space. However, this property is not generically fulfilled by orthotropic tensors.

It should be noted that this is the only situation satisfying our definition that emerges through the clips product analysis. This exotic situation has been identified in the literature and is sometimes known as the R_0 -orthotropy³, while those in compliance are referred to as r_0 -orthotropic. We just demonstrate that it is the only exotic possibility for $\mathbb{E}la$. For example, the apparently interesting case corresponding to $I_3 = 0$, does not produce a paradoxical symmetric situation and therefore cannot be considered as an exotic elastic material. This situation is called *semi-exotic*. The following section will introduce an example of semi-exotic materials.

4.3 Semi-exotic elastic materials: Cauchy elasticity

It is a well-known fact that by imposing an extra constraint, the index symmetry of the elasticity tensor can be increased. As a result, it becomes completely symmetric with respect to index permutation. The constraint to be imposed is usually known as the *Cauchy relation* [128, 129]. Does Cauchy relation define an exotic set of materials? The answer is given in 2D by the following results:

Lemma 4.1. *A 2D elasticity tensor \mathbb{C}_{\sim} with an explicit expression*

$$\mathbb{C}_{\sim} = \alpha \mathbb{J}_{\sim} + \beta \mathbb{K}_{\sim} + \frac{1}{2} (\mathbb{1}_{\sim} \otimes \mathbb{h}_{\sim} + \mathbb{h}_{\sim} \otimes \mathbb{1}_{\sim}) + \mathbb{H}_{\sim},$$

³This name comes from the polar parameterization of bi-dimensional elasticity tensors [9]

is totally index symmetric if and only if

$$2\alpha = \beta. \quad (4.3)$$

Proof. Following the definition of harmonic tensors, the anisotropic part of an elasticity tensor denoted by $\underset{\approx}{\mathbb{C}} = f(0, 0, \underset{\approx}{\mathbf{h}}, \underset{\approx}{\mathbf{H}})$ is totally symmetric⁴. As a result, we focus here on the isotropic part. The isotropic elasticity tensor reads:

$$\underset{\approx}{\mathbb{C}} = \alpha \underset{\approx}{\mathbb{J}} + \beta \underset{\approx}{\mathbb{K}}.$$

In the case of 2D, some properties are satisfied:

$$\underset{\approx}{\mathbb{J}} = \frac{1}{2}(\underset{\approx}{\mathbb{I}}_2 + \underset{\approx}{\mathbb{I}}_3 - \underset{\approx}{\mathbb{I}}_1), \quad \underset{\approx}{\mathbb{K}} = \frac{1}{2}\underset{\approx}{\mathbb{I}}_1,$$

and a totally symmetric tensor $\underset{\approx}{\mathbb{C}}^{sym}$ is defined by:

$$\underset{\approx}{\mathbb{C}}^{sym} = \lambda(\underset{\approx}{\mathbb{I}}_1 + \underset{\approx}{\mathbb{I}}_2 + \underset{\approx}{\mathbb{I}}_3)$$

with λ any real number, $(\underset{\approx}{\mathbb{I}}_1)_{ijkl} = \delta_{ij}\delta_{kl}$, $(\underset{\approx}{\mathbb{I}}_2)_{ijkl} = \delta_{il}\delta_{jk}$ and $(\underset{\approx}{\mathbb{I}}_3)_{ijkl} = \delta_{ik}\delta_{jl}$.

We get

$$\underset{\approx}{\mathbb{C}} = \frac{\beta}{2}\underset{\approx}{\mathbb{I}}_1 + \frac{\alpha}{2}(\underset{\approx}{\mathbb{I}}_2 + \underset{\approx}{\mathbb{I}}_3 - \underset{\approx}{\mathbb{I}}_1).$$

$2\alpha = \beta$ implies that $\underset{\approx}{\mathbb{C}}$ is totally symmetric because the coefficients for $\underset{\approx}{\mathbb{I}}_1$, $\underset{\approx}{\mathbb{I}}_2$ and $\underset{\approx}{\mathbb{I}}_3$ are identical, and vice versa. \square

This result can also be obtained using the polar formalism $T_0 = T_1$, which can be deduced from [Equation 3.9](#), and is firstly given in [\[130\]](#).

Obviously, this constraint can not be only enforced by imposing symmetry requirements and hence resorting on a specific design. Since relying on a constraint upon isotropic components, the resulting behaviour does not produce a paradoxical increase of symmetry. Hence, in 2D, and according to a strict application of our definition, the set of Cauchy anisotropic materials is not an exotic set but a semi-exotic one⁵. The advantage of such materials is, that since the two isotropic components are related, their material modulus, e.g. Young's modulus and bulk modulus are isotropic.

Since the [Equation 3.12](#) provides expressions for the covariants of $\underset{\approx}{\mathbb{S}}$ in terms of those of $\underset{\approx}{\mathbb{C}}$, we have:

$$\begin{cases} \alpha^- = \frac{1}{4\Delta}(4\alpha^2 - \underset{\approx}{\mathbf{h}} : \underset{\approx}{\mathbf{h}}) \\ \beta^- = \frac{1}{2\Delta}(2\alpha^2 - \underset{\approx}{\mathbf{H}} :: \underset{\approx}{\mathbf{H}}) \end{cases} \Rightarrow 2\alpha^- \neq \beta^-$$

which shows that the Cauchy relations cannot be satisfied at the same time by $\underset{\approx}{\mathbb{C}}$ and $\underset{\approx}{\mathbb{S}}$, meaning that this property is not stable by inversion.

4.4 Generalisation to other constitutive laws

The aim of this section is twofold. First, it will be a question of deriving a general result concerning linear constitutive laws in \mathbb{R}^2 . We will then illustrate this result in two non-trivial situations ([subsection 4.4.2](#)).

⁴It is a very specific case of \mathbb{R}^2 that the tensor $(\underset{\approx}{\mathbf{1}} \otimes \underset{\approx}{\mathbf{h}} + \underset{\approx}{\mathbf{h}} \otimes \underset{\approx}{\mathbf{1}})$ belongs to $S^4(\mathbb{R}^2)$

⁵The 3D response is different anyway and leads to a truly exotic set of materials.

4.4.1 A general theorem

The approach used for elasticity in [section 3.3](#) and [4.2](#) can be generalised to any linear constitutive law in \mathbb{R}^2 based on the fact that in \mathbb{R}^2 , harmonic spaces are bi-dimensional. To obtain the number of exotic sets, one must enumerate all the particular geometric configurations that can occur between the components of the harmonic decomposition of a given tensor. In practice, one must enumerate:

- the number of possible cancellations of harmonic components;
- for a given configuration, the number of possible alignments between the non-zero harmonic components.

and subtract from this the number of symmetry classes. The number of exotic sets is given by the following result:

Theorem 4.1: The number of exotic anisotropic sets of \mathbb{T}

Consider \mathbb{T} a space of bidimensional constitutive tensors. Let N and M be, respectively, the number of harmonic spaces of order > 0 and -1 in the harmonic structure of \mathbb{T} . The number of exotic anisotropic sets of \mathbb{T} is

$$\#\mathcal{E} = \left(\sum_{p=0}^N \binom{N}{p} (2^p - p) \right) 2^M - \#\mathcal{C}.$$

with $\#\mathcal{C}$ the number of $O(2)$ symmetry classes of \mathbb{T} .

Proof. As indicated by [Theorem 3.2](#), the symmetry classes of \mathbb{K}^n are:

$$\mathfrak{J}(\mathbb{K}^n) = \begin{cases} n \geq 1, & \{[D_n], [O(2)]\} \\ n = -1, & \{[SO(2)], [O(2)]\} \\ n = 0, & \{[O(2)]\} \end{cases}.$$

Thus, the \mathbb{K}^0 play no role in the counting of classes, the \mathbb{K}^{-1} are on or off but independent of orientation, while the non-zero $\mathbb{K}^{n \geq 1}$ have an orientation. It results that, for $p, q \geq 1$,

$$\mathfrak{J}(\mathbb{K}^p \odot \mathbb{K}^q) = \{[Z_{d(p,q)}], [D_{d(p,q)}], [D_p], [D_q], [O(2)]\}.$$

with $d(p, q) := \gcd(p, q)$. Since no relative orientation is involved, the situation is simpler when $p = q = -1$ and

$$\mathfrak{J}(\mathbb{K}^{-1} \odot \mathbb{K}^{-1}) = \{[SO(2)], [O(2)]\}.$$

Therefore, the presence of M harmonic spaces of type \mathbb{K}^{-1} in the harmonic decomposition of \mathbb{T} generate 2^M different combinations.

Let N , the number of harmonic spaces $\mathbb{K}^{n \geq 1}$ in the harmonic decomposition of \mathbb{T} . Let us first assume that none of the associated harmonic components is zero. We then have a collection of N non-zero vectors. Among them, some can be aligned with others. We need to count the different alignments that can occur. There is a configuration with no alignment, $\binom{N}{2}$ configurations with a pair of aligned vectors, $\binom{N}{3}$ with 3 vectors, and so on... In the end, we can count $2^N - N$ configurations going from the generic configuration to the complete alignment. Suppose now that among those N harmonic components p of them are null. There are $\binom{N}{p}$ different manner to cancel p components among N , and each of them generated $2^p - p$ alignment configurations. Hence, by combining the vanishing and the alignments of

harmonic components we obtain

$$\left(\sum_{p=0}^N \binom{N}{p} (2^p - p) \right),$$

different configurations generated by harmonic tensors of order greater than 0. The total number of configurations is then obtained by taking into account the configurations of hemitropic components \mathbb{K}^{-1} , hence

$$\#\mathcal{S} = \left(\sum_{p=0}^N \binom{N}{p} (2^p - p) \right) 2^M.$$

To obtain the number of exotic situations, we need to remove those that generate genuine symmetry classes. Thus, the final formula used to obtain the number of exotic sets shown in Theorem 4.1 is obtained. \square

4.4.2 Application to coupled constitutive laws

This result is applied here to two classical coupled constitutive laws in the literature: piezoelectricity [131] and Cosserat elasticity [132].

Piezoelectricity

This constitutive law couples the mechanical state with the electric one. The *electrical* state is described by two vector fields: the electric displacement \tilde{d} and the electric field \tilde{e} . As in the mechanical situation, these fields are connected by a constitutive law that describes the behaviour of each different material. For linear conductivity, this relation can be written

$$\tilde{d} = \tilde{S} \cdot \tilde{e}$$

in which \tilde{S} is a second-order tensor, known as the *permittivity tensor* [133]. For non-centro symmetric materials, these two phenomena are not independent but coupled [133]. In this situation, the constitutive law reads

$$\begin{cases} \tilde{\sigma} = \tilde{C} : \tilde{\varepsilon} - \tilde{P} \cdot \tilde{e} \\ \tilde{d} = \tilde{P} : \tilde{\varepsilon} + \tilde{S} \cdot \tilde{e} \end{cases} \quad (4.4)$$

in which a third-order tensor \tilde{P} , known as the *piezoelectricity tensor*, responsible for the coupling appears⁶. The different constitutive tensors are summed up in the following table.

Tensor	Symmetries	T	Physical meaning
\tilde{C}	$\mathbb{T}_{(ij)(kl)}$	Ela	Fourth-order elasticity tensor
\tilde{P}	$\mathbb{T}_{i(jk)}$	Piez	Piezoelectric tensor
\tilde{S}	$\mathbb{T}_{(ij)}$	Con	Dielectric susceptibility tensor

The determination of the number of exotic sets requires the knowledge of the harmonic structure of the constitutive tensors. These structures together with the number of exotic sets are provided in the table below:

⁶Depending on the considered set of primary variables, four different conventions can be used to express the law of piezoelectricity [134]. The one chosen here is regarded as the most general according to the *IEEE Standard on Piezoelectricity* [134]. In any case, the results are independent of the chosen convention

T	\mathcal{H}	N	M	$\#\mathcal{S}$	$\#\mathcal{C}$	$\#\mathcal{E}$
Ela	$2\mathbb{K}^0 \oplus \mathbb{K}^2 \oplus \mathbb{K}^4$	2	0	5	4	1
Piez	$2\mathbb{K}^1 \oplus \mathbb{K}^3$	3	0	15	4	11
Con	$\mathbb{K}^0 \oplus \mathbb{K}^2$	1	0	2	2	0

We denote the space of the piezoelectric law by $\mathcal{P}iez$, its harmonic structure is obtained from those of the constitutive tensors that compose it

$$\mathcal{P}iez = 3\mathbb{K}^0 \oplus 2\mathbb{K}^1 \oplus 2\mathbb{K}^2 \oplus \mathbb{K}^3 \oplus \mathbb{K}^4.$$

Knowing that this law has 7 symmetry classes, the number of exotic sets is then determined

$$N = 6; \quad M = 0; \quad \#\mathcal{C} = 7 \quad \Rightarrow \quad \#\mathcal{E} = 530.$$

We observe that the number of exotic sets of the coupled law is not the sum of the exotic set of its constituents.

Cosserat elasticity

We consider here the classical formulation of Cosserat elasticity in small-strain as introduced for instance in [135, 136], using the linear stretch strain tensor $\underline{\underline{e}}$ and the linear wryness tensor $\underline{\underline{\kappa}}$. By duality, we define the stress tensors: $\underline{\underline{s}}$ the asymmetric stress tensor, and $\underline{\underline{m}}$ the couple-stress tensor. It should be emphasised that in contrast to the standard elasticity, the strain and stress tensors $\underline{\underline{e}}$ and $\underline{\underline{s}}$ are not symmetric. Consequently, the constitutive law of linear Cosserat elasticity is expressed as:

$$\begin{cases} \underline{\underline{s}} = \underline{\underline{A}} : \underline{\underline{e}} - \underline{\underline{B}} \cdot \underline{\underline{\kappa}} \\ \underline{\underline{m}} = \underline{\underline{B}}^T : \underline{\underline{e}} + \underline{\underline{d}} \cdot \underline{\underline{\kappa}} \end{cases}$$

The harmonic structure of this coupled elastic law has been derived in [132], and associated results are provided in the following table:

Tensor	Symmetries	T	\mathcal{H}	N	M	$\#\mathcal{S}$	$\#\mathcal{C}$	$\#\mathcal{E}$
$\underline{\underline{A}}$	$\mathbb{T}_{ij \quad kl}$	Cos	$\mathbb{K}^{-1} \oplus 3\mathbb{K}^0 \oplus 2\mathbb{K}^2 \oplus \mathbb{K}^4$	3	1	30	6	24
$\underline{\underline{B}}$	\mathbb{T}_{ijk}	Cou	$3\mathbb{K}^1 \oplus \mathbb{K}^3$	4	0	49	4	45
$\underline{\underline{d}}$	$\mathbb{T}_{(ij)}$	Rot	$\mathbb{K}^0 \oplus \mathbb{K}^2$	1	0	2	2	0

Table 4.1: Number of exotic sets for tensor spaces in linear cosserat elasticity

We denote by $\mathcal{C}os$ the space of the Cosserat elasticity law, its harmonic structure is obtained from those of the constitutive tensors that compose it

$$\mathcal{C}os \simeq \mathbb{K}^{-1} \oplus 4\mathbb{K}^0 \oplus 3\mathbb{K}^1 \oplus 3\mathbb{K}^2 \oplus \mathbb{K}^3 \oplus \mathbb{K}^4.$$

Knowing that this law has 10 symmetry classes [132], the number of exotic sets is then determined:

$$N = 1; \quad M = 1; \quad \#\mathcal{C} = 10 \quad \Rightarrow \quad \#\mathcal{E} = 11064.$$

Following these two examples, we can observe that the number of exotic sets for a given constitutive tensor space is significantly greater than the sum of the numbers of exotic sets for its constituent subspaces.

Chapter 5

Mesostructure design of 2D exotic materials

5.1	Multi-scale based homogenization	63
5.2	Topological sensitivity of the homogenized elasticity tensor	67
5.3	Topological derivative-based algorithm	68
5.4	Finite element implementation	72
5.4.1	Initialization	72
5.4.2	Numerical examples	74
5.5	Numerical result for exotic material: R_0 -Orthotropy	78
5.6	Numerical results for semi-exotic material: Cauchy elasticity	79
5.7	Synthesis	82

The proposed exotic and semi-exotic materials will be designed by mesostructure in this chapter. We will use the level set-based topological derivative algorithm introduced by S. Amstutz et al. in [2].

This chapter is organized as follows. First, in [section 5.1](#), a comprehensive review of the multi-scale based homogenization technique is presented, aiming to derive the macroscopic elasticity tensor. In [section 5.2](#), we introduce the concept of topological sensitivity derived from the asymptotic expansion, which serves as the fundamental component of the topological derivative algorithm. Following that, the level set-based topological derivative algorithm in [2] is introduced in [section 5.3](#). Subsequently, we present the implementation of this algorithm in [section 5.4](#), along with several numerical examples in [section 5.5](#) and [section 5.6](#), these are materials already discussed in the literature, but their mesostructure design has never been realized.

5.1 Multi-scale based homogenization

Beyond the external geometry control in the structural optimisation of a material, the recent progress in additive manufacturing enables microstructure control within the printed geometry, which leads to the increased popularity in the design of *architected materials*. This issue has been well discussed in the vast related literature [137, 138], which proposes a systematic shape optimisation based on the classic method of shape sensitivity. However, the main drawback is that it cannot vary the topology of the initial configuration. We introduce in this chapter a topology optimisation algorithm based on the so-called *multi-scale* constitutive theories [139, 140, 2].

Let D be a bounded and open subset of \mathbb{R}^n ($n = 2, 3$). A macro-continua solid is therefore modelised by a closed domain $\Omega \subset D$, and any point X (the corresponding coordinate is \underline{x}) of the macro-continua solid (Figure 5.1) is associated to a local Representative Volume Element (RVE) with its domain denoted by Ω_μ and the boundary $\partial\Omega_\mu$. Its characteristic length L_μ is much smaller than the characteristic length L of the macro-continua domain Ω . And the coordinate of any point Y is denoted by $\underline{y} \in \Omega_\mu$. Such theories enable the connection between micro-geometric inputs and macroscopic mechanical behaviour response, as a result of the use of homogenization techniques (detailed in later content of this section).

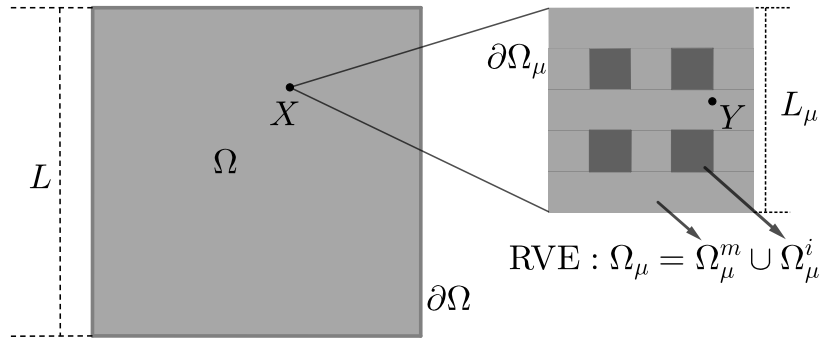


Figure 5.1: Macro-continua solid with a local microstructure

The optimisation problems encountered in this work are modeled as follows:

$$\min_{\Omega_\mu \in \mathcal{E}} J(\Omega_\mu, \underline{u}(\underline{x}, \underline{y})) \quad (5.1)$$

which is to minimize the cost function $J(\Omega_\mu, \underline{u}(\underline{x}, \underline{y}))$ with $\underline{u}(\underline{x}, \underline{y})$ the solution of a certain PDE posed in Ω_μ , we note later $J(\Omega_\mu, \underline{u}(\underline{x}, \underline{y})) = J(\Omega_\mu)$.

Some methods are proposed in the literature for addressing this issue (Equation 5.1) in topology optimization problems:

- the SIMP (Solid Isotropic Material with Penalization) method [3, 141];
- the level-set based shape optimization [14, 96];
- the topological derivative method [1].

In this work, we will concentrate on the last method combined with a level-set domain representation [2]. Unlike the conventional level-set methods relying on the use of the Hamilton-Jacobi equation (firstly proposed by S.Osher [93]), which is highly dependent on the initial guess, the proposed topological

derivative allows the nucleation of a new hole in the domain.

Based on the original RVE domain Ω_μ , to apply the concept of topological asymptotic expansion and topological derivative in the framework of multi-scale model, we define the perturbation domain $\Omega_{\mu\rho}$ by first introducing a circular hole \mathcal{H}_ρ of radius ρ centered at an arbitrary point $Y \in \Omega_\mu$ and then fill this hole by a circular inclusion \mathcal{I}_ρ of a different material. The perturbed domain is defined as $\Omega_{\mu\rho} = (\Omega_\mu \setminus \overline{\mathcal{H}_\mu}) \cup \mathcal{I}_\rho$ (Figure 5.2).

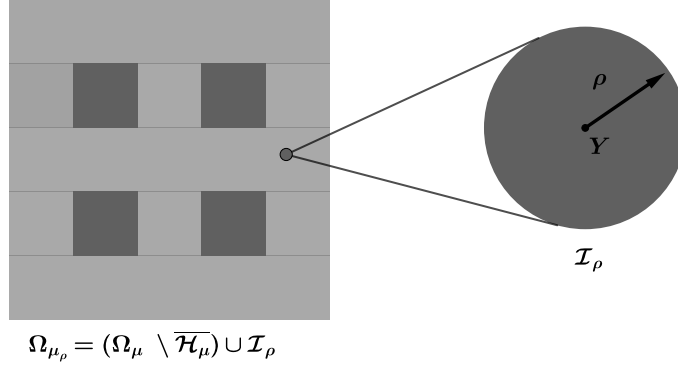


Figure 5.2: Topological perturbation at microscale

We follow here the method as introduced by Armstutz in [11, 2], for which four ingredients are considered:

- the strain/stress averaging relation: the macroscopic strain/stress tensor of a point in the macroscopic continuum is described as the volume average of its microscopic counterpart;
- the choice of the space of kinematically admissible displacement fluctuations;
- the mechanical equilibrium of the RVE;
- the Hill-Mandel principle of macro-homogeneity which connects the relation between micro- and macro-scales.

The strain and stress averaging relation

We begin with the assumption that the macroscopic strain tensor at a point X of the macro-continua solid, denoted by $\bar{\varepsilon}$, is defined as the volume average¹ of its microscopic strain field $\underline{\varepsilon}(\underline{y}) := \nabla^s \underline{u}(\underline{y})$ over the RVE:

$$\bar{\varepsilon} = \frac{1}{V_\mu} \int_{\Omega_\mu} \nabla^s \underline{u}(\underline{y}) \, dV \quad (5.2)$$

with V_μ the volume of Ω_μ and ∇^s the symmetric gradient operator. The strain tensor at $\underline{y} \in \Omega_\mu$ consists of two parts: an average contribution $\bar{\varepsilon}$ and a fluctuation part $\tilde{\varepsilon}(\underline{y})$:

$$\underline{\varepsilon}(\underline{y}) = \bar{\varepsilon} + \tilde{\varepsilon}(\underline{y}) \quad (5.3)$$

In the same manner, the microscopic stress field is defined as:

$$\underline{\sigma}(\underline{y}) = \bar{\sigma} + \tilde{\sigma}(\underline{y})$$

¹To simplify the notation, any macroscopic quantity $a(\underline{x})$ on point $X \in \Omega$ defined as the volume average over Ω_μ will be abbreviated to \bar{a} .

with the macroscopic stress tensor $\bar{\sigma}$ obtained by the volume average of this microscopic stress field, meaning $\bar{\sigma} = \int_{\Omega_\mu} \tilde{\sigma}(\underline{y}) \, dV$.

Space of kinematically admissible displacements

Generally, the displacement is decomposed into three parts:

$$\underline{u}(\underline{x}, \underline{y}) = \underline{u}(\underline{x}) + \bar{\varepsilon} \cdot \underline{y} + \tilde{\underline{u}}(\underline{y}) \quad (5.4)$$

$\underline{u}(\underline{x})$ represents the rigid displacement of the point \underline{x} , $\bar{\varepsilon} \cdot \underline{y}$ is the linear displacement component based on the idea of average strain and $\tilde{\underline{u}}(\underline{y})$ is the displacement fluctuation field. However, the rigid displacement $\underline{u}(\underline{x})$ will not be taken into account in the following, which allows an additional constraint of zero average of the fluctuation field such that $\int_{\Omega_\mu} \tilde{\underline{u}}(\underline{y}) \, dV = 0$.

Thus, the Equation 5.4 can be reduced to:

$$\underline{u}(\underline{y}) = \bar{\varepsilon} \cdot \underline{y} + \tilde{\underline{u}}(\underline{y})$$

Based on this, we define the minimally constrained space $\tilde{\mathcal{U}}_\mu$ of kinematically displacements so that any fluctuation displacement $\tilde{\underline{u}}(\underline{y})$ is encompassed by this space:

$$\tilde{\mathcal{U}}_\mu := \{ \underline{v} \in [H^1(\Omega_\mu)]^2 : \int_{\Omega_\mu} \underline{v} \, dV = 0, \int_{\partial\Omega_\mu} \underline{v} \otimes_s \underline{n} \, dS = 0 \}$$

with $H^1(\Omega_\mu)$ the Sobolev space.

However, this constraint on kinematically admissible displacements is not sufficient, the complete characterization of the multi-scale model is obtained by defining a subspace of kinematically admissible displacement fluctuations $\mathcal{U}_\mu \subset \tilde{\mathcal{U}}_\mu$. Three different cases of \mathcal{U}_μ are discussed in [2]. In this work, since the mesostructure is generated by periodic repetition. The displacement fluctuations must satisfy periodic conditions on the boundary of the RVE. We have:

$$\mathcal{U}_\mu := \{ \tilde{\underline{u}} \in \tilde{\mathcal{U}}_\mu : \tilde{\underline{u}}(\underline{y}^+) = \tilde{\underline{u}}(\underline{y}^-), \forall (\underline{y}^+, \underline{y}^-) \in P \} \quad (5.5)$$

with P the set of corresponding one-to-one periodicity points on opposite sides of the RVE boundary.

Mechanical equilibrium of RVE

We assume here that the external surface loads and body force field of the RVE vanish. The *principle of virtual work* establishes that the RVE is in equilibria if and only if the variational equation holds:

$$\int_{\Omega_\mu} \tilde{\sigma}(\underline{y}) : \nabla^s \underline{\eta} \, dV = 0 \quad \forall \underline{\eta} \in \mathcal{U}_\mu \quad (5.6)$$

with $\tilde{\sigma}(\underline{y})$ denotes its microscopic stress field. This variational equation of equilibria over the RVE can be equivalently written in the strong form, which can be found in [1]. This information will not be presented here as it is not relevant to the subsequent content.

The microscopic stress tensor field $\tilde{\sigma}(\underline{y})$ satisfies:

$$\tilde{\sigma}(\underline{y}) = \tilde{\mathbb{C}}(\underline{y}) : \nabla^s \underline{u}(\underline{y})$$

$\underline{\underline{\mathbb{C}}}(\underline{\mathbf{y}})$ is a pointwise fourth-order isotropic elasticity tensor field. Our work now is to find the displacement field $\underline{\mathbf{u}}(\underline{\mathbf{y}})$ in Ω_μ which satisfies this linear elasticity system.

Hill-Mandel principle of macro-homogeneity

The *Hill-Mandel principle* of macroscopic homogeneity [142, 143], which connects the mechanical energies of the micro- and macro-scales, plays a fundamental role in the formulation of multi-scale constitutive models:

Lemma 5.1. *Let $\underline{\underline{\varepsilon}}(\underline{\mathbf{y}})$ be a kinematically admissible strain field and $\underline{\underline{\sigma}}(\underline{\mathbf{y}})$ be a statically admissible stress field, then [144]:*

$$\frac{1}{V_\mu} \int_{\Omega_\mu} \underline{\underline{\sigma}}(\underline{\mathbf{y}}) : \underline{\underline{\varepsilon}}(\underline{\mathbf{y}}) \, dV - \underline{\underline{\bar{\sigma}}} : \underline{\underline{\bar{\varepsilon}}} = \frac{1}{V_\mu} \int_{\partial\Omega_\mu} \underline{\underline{\mathbf{u}}}(\underline{\mathbf{y}}) \cdot \underline{\underline{\tilde{\sigma}}}(\underline{\mathbf{y}}) \cdot \underline{\mathbf{n}} \, dV \quad (5.7)$$

The periodic boundary of fluctuation displacement results in $\underline{\underline{\mathbf{u}}}(\underline{\mathbf{y}})$ periodic and $\underline{\underline{\tilde{\sigma}}}(\underline{\mathbf{y}})$ anti-periodic. (5.7) can be simplified by:

$$\frac{1}{V_\mu} \int_{\Omega_\mu} \underline{\underline{\sigma}}(\underline{\mathbf{y}}) : \underline{\underline{\varepsilon}}(\underline{\mathbf{y}}) \, dV - \underline{\underline{\bar{\sigma}}} : \underline{\underline{\bar{\varepsilon}}} = 0 \quad (5.8)$$

Variational formulation

Lemma 5.2. *It exists $\underline{\underline{\mathbf{u}}}(\underline{\mathbf{y}}) \in \mathcal{U}_\mu$ so that:*

$$\int_{\Omega_\mu} (\underline{\underline{\bar{\varepsilon}}} + \nabla^s \underline{\underline{\mathbf{u}}}(\underline{\mathbf{y}})) : \underline{\underline{\mathbb{C}}}(\underline{\mathbf{y}}) : \nabla^s \eta \, dV = 0 \quad \forall \eta \in \mathcal{U}_\mu \quad (5.9)$$

Proof. (5.3)+(5.4)+(5.8):

$$\begin{aligned} & \frac{1}{V_\mu} \int_{\Omega_\mu} \underline{\underline{\sigma}}(\underline{\mathbf{y}}) : (\underline{\underline{\bar{\varepsilon}}} + \underline{\underline{\tilde{\varepsilon}}}(\underline{\mathbf{y}})) \, dV - \underline{\underline{\bar{\sigma}}} : \underline{\underline{\bar{\varepsilon}}} \\ = & \frac{1}{V_\mu} \int_{\Omega_\mu} \underline{\underline{\sigma}}(\underline{\mathbf{y}}) : \underline{\underline{\bar{\varepsilon}}} \, dV + \frac{1}{V_\mu} \int_{\Omega_\mu} \underline{\underline{\sigma}}(\underline{\mathbf{y}}) : \underline{\underline{\tilde{\varepsilon}}}(\underline{\mathbf{y}}) \, dV - \underline{\underline{\bar{\sigma}}} : \underline{\underline{\bar{\varepsilon}}} \\ = & \frac{1}{V_\mu} \int_{\Omega_\mu} \underline{\underline{\sigma}}(\underline{\mathbf{y}}) \, dV : \underline{\underline{\bar{\varepsilon}}} + \frac{1}{V_\mu} \int_{\Omega_\mu} \underline{\underline{\sigma}}(\underline{\mathbf{y}}) : \underline{\underline{\tilde{\varepsilon}}}(\underline{\mathbf{y}}) \, dV - \underline{\underline{\bar{\sigma}}} : \underline{\underline{\bar{\varepsilon}}} \\ = & \underline{\underline{\bar{\sigma}}} : \underline{\underline{\bar{\varepsilon}}} + \frac{1}{V_\mu} \int_{\Omega_\mu} \underline{\underline{\sigma}}(\underline{\mathbf{y}}) : \underline{\underline{\tilde{\varepsilon}}}(\underline{\mathbf{y}}) \, dV - \underline{\underline{\bar{\sigma}}} : \underline{\underline{\bar{\varepsilon}}} \\ = & \frac{1}{V_\mu} \int_{\Omega_\mu} \underline{\underline{\sigma}}(\underline{\mathbf{y}}) : \underline{\underline{\tilde{\varepsilon}}}(\underline{\mathbf{y}}) \, dV \\ = & 0 \end{aligned}$$

Since $\underline{\underline{\sigma}}(\underline{\mathbf{y}}) = (\underline{\underline{\bar{\varepsilon}}} + \underline{\underline{\tilde{\varepsilon}}}(\underline{\mathbf{y}})) : \underline{\underline{\mathbb{C}}}(\underline{\mathbf{y}})$ and $\underline{\underline{\tilde{\varepsilon}}}(\underline{\mathbf{y}}) = \nabla^s \underline{\underline{\tilde{u}}}(\underline{\mathbf{y}})$, Equation 5.9 is proved. \square

The above variational formulation (5.9) is not well-posed because of the existence of rigid body motions. This is done by considering an additional vectorial penalisation parameter λ and considering the following variational problem:

Find $(\underline{\underline{\tilde{u}}}(\underline{\mathbf{y}}), \lambda) \in \mathcal{U}_\mu \times \mathbb{R}^2$ such that:

$$\int_{\Omega_\mu} (\underline{\underline{\bar{\varepsilon}}} + \nabla^s \underline{\underline{\tilde{u}}}(\underline{\mathbf{y}})) : \underline{\underline{\mathbb{C}}}(\underline{\mathbf{y}}) : \nabla^s \eta \, dV + \int_{\Omega_\mu} (\lambda \eta + \widehat{\lambda} \underline{\underline{\tilde{u}}}(\underline{\mathbf{y}})) \, dV = 0 \quad \forall (\eta, \widehat{\lambda}) \in \mathcal{U}_\mu \times \mathbb{R}^2 \quad (5.10)$$

The homogenized elasticity tensor

The scalar-valued cost functions $J(\Omega)$ for the optimization of architected materials in this work are defined in terms of homogenized elasticity tensors. As noted by S.Amstutz in [2], this can be obtained by the method proposed in [145]. More specifically, it is realized by rewriting Equation 5.10 as a superposition of linear problems associated with the individual Cartesian components of the macroscopic strain tensor. The components of the homogenized elasticity tensor $\underline{\underline{C}}$, in the orthonormal basis \mathcal{B} , can be written as:

$$C_{ijkl} = \frac{1}{V_\mu} \int_{\Omega_\mu} (\underline{\underline{\sigma}}(\underline{\underline{u}}^{(kl)}(\underline{\underline{y}})))_{ij} dV \quad (5.11)$$

with respect to the Equation 5.4, the canonical microscopic displacement field $\underline{\underline{u}}^{(kl)}(\underline{\underline{y}})$ associated with the strain tensor $\underline{\underline{\varepsilon}}^{(kl)} = \underline{\underline{e}}_k \otimes \underline{\underline{e}}_l$ is the sum of:

$$\underline{\underline{u}}^{(kl)}(\underline{\underline{y}}) = (\underline{\underline{e}}_k \otimes \underline{\underline{e}}_l) \cdot \underline{\underline{y}} + \tilde{\underline{\underline{u}}}^{(kl)}(\underline{\underline{y}})$$

So that the homogenized tensor component in Equation 5.11 can be obtained by the variational formulation 5.10 by substituting $\tilde{\underline{\underline{u}}}(\underline{\underline{y}})$ with $\tilde{\underline{\underline{u}}}^{(kl)}(\underline{\underline{y}})$:

$$\int_{\Omega_\mu} (\underline{\underline{\varepsilon}} + \nabla^s \tilde{\underline{\underline{u}}}^{(kl)}(\underline{\underline{y}})) : \underline{\underline{C}}(\underline{\underline{y}}) : \nabla^s \eta dV + \int_{\Omega_\mu} (\lambda \eta + \hat{\lambda} \tilde{\underline{\underline{u}}}^{(kl)}(\underline{\underline{y}})) dV = 0 \quad \forall (\eta, \hat{\lambda}) \in \mathcal{U}_\mu \times \mathbb{R}^2 \quad (5.12)$$

5.2 Topological sensitivity of the homogenized elasticity tensor

To simplify the analysis, only two phases will be considered for the unit cell: the matrix phase denoted by Ω_μ^m and the inclusion phase denoted by Ω_μ^i . The perturbation \mathcal{I}_ρ is of the same material property and the inclusion phase, we have $\mathcal{I}_\rho \subset \Omega_\mu^i$. The pointwise elasticity tensor $\underline{\underline{C}}(\underline{\underline{y}})$ in Equation 5.11 is defined as:

$$\underline{\underline{C}}(\underline{\underline{y}}) := \frac{E(\underline{\underline{y}})}{1 - \nu^2(\underline{\underline{y}})} [(1 - \nu(\underline{\underline{y}})) \underline{\underline{I}} + \nu(\underline{\underline{y}}) (\underline{\underline{1}} \otimes \underline{\underline{1}})]$$

with $E(\underline{\underline{y}})$ and $\nu(\underline{\underline{y}})$ Young's modulus and Poisson's ratio field of the RVE:

$$E(\underline{\underline{y}}) := \begin{cases} E^m & \underline{\underline{y}} \in \Omega_\mu^m \\ E^i & \underline{\underline{y}} \in \Omega_\mu^i \end{cases} \quad \text{and} \quad \nu(\underline{\underline{y}}) := \begin{cases} \nu^m & \underline{\underline{y}} \in \Omega_\mu^m \\ \nu^i & \underline{\underline{y}} \in \Omega_\mu^i \end{cases} \quad (5.13)$$

It will be assumed that $E^i = \gamma E^m$, and $\nu^i = \nu^m = \nu$, with γ defining the contrast between Young's modulus of the matrix phase and the inclusion phase. The domain Ω_μ^i will be considered as void when $\gamma \rightarrow 0$.

The homogenized elasticity tensor for the unperturbed RVE domain Ω_μ is denoted by $\underline{\underline{C}}$. Within the above context, the topological asymptotic expansion of $\underline{\underline{C}}$ reads [2]:

Theorem 5.1: Topological asymptotic expansion of $\underline{\underline{C}}$

The topological asymptotic expansion of the macroscopic homogenised elasticity tensor $\underline{\underline{C}}$ in the present context is given by

$$\underline{\underline{C}}^\rho(\underline{\underline{y}}) = \underline{\underline{C}} + f(\rho) D_T \underline{\underline{C}}(\underline{\underline{y}}) + o(\rho^2)$$

in which

- $\underline{\underline{C}}^\rho(\underline{\underline{y}})$: the microscopic elasticity tensor of perturbed domain Ω_μ^ρ , the corresponding macroscopic

homogenised elasticity tensor reads $\underset{\approx}{\mathbb{C}}^\rho$;

- $f(\rho)$: the volume fraction of the inserted inclusion, defined by:

$$f(\rho) = \frac{\pi\rho^2}{V_\mu}$$

$f(\rho) \rightarrow 0$ when $\rho \rightarrow 0$ and $o(\rho^2)$ contains all terms of higher order of $f(\rho)$.

- $D_T \underset{\approx}{\mathbb{C}}(\underline{\mathbf{y}})$: the *topological derivative* of $\underset{\approx}{\mathbb{C}}$ for the unperturbed domain Ω_μ . It is a fourth-order tensor field with its Cartesian components read:

$$(D_T \underset{\approx}{\mathbb{C}})_{ijkl}(\underline{\mathbf{y}}) = \underset{\approx}{\sigma}(u^{(ij)}(\underline{\mathbf{y}})) : \underset{\approx}{\mathbb{H}}(\underline{\mathbf{y}}) : \underset{\approx}{\sigma}(u^{(kl)}(\underline{\mathbf{y}})) \quad (5.14)$$

it provides a rigorous first-order approximation to the change of $\underset{\approx}{\mathbb{C}}$ resulting from the insertion of a circular inclusion of radius ρ at $\underline{\mathbf{y}} \in \Omega_\mu^m$. The field $\underline{\mathbf{u}}^{(ij)}(\underline{\mathbf{y}})$ and $\underline{\mathbf{u}}^{(kl)}(\underline{\mathbf{y}})$ can be obtained by the solution of Equation 5.12 and the fourth order tensor $\underset{\approx}{\mathbb{H}}(\underline{\mathbf{y}})$ is defined as

$$\underset{\approx}{\mathbb{H}}(\underline{\mathbf{y}}) := -\frac{1}{E} \left(\frac{1-\gamma^*}{1+\alpha\gamma^*} \right) \left[4\underset{\approx}{\mathbb{I}} - \frac{1-\gamma^*(\alpha-2\beta)}{1+\beta\gamma^*} (\underset{\approx}{\mathbf{1}} \otimes \underset{\approx}{\mathbf{1}}) \right] \quad (5.15)$$

with $\gamma^* = \gamma$ if $\underline{\mathbf{y}} \in \Omega_\mu^m$ and $\gamma^* = 1/\gamma$ if $\underline{\mathbf{y}} \in \Omega_\mu^i$. And

$$\alpha = \frac{1+\nu}{1-\nu} \quad \beta = \frac{3-\nu}{1+\nu}$$

For the case of $\gamma \rightarrow 0$, the tensor $\underset{\approx}{\mathbb{H}}(\underline{\mathbf{y}})$ in Equation 5.15 will be simplified by:

$$\underset{\approx}{\mathbb{H}}(\underline{\mathbf{y}}) := \begin{cases} -\frac{1}{E} (4\underset{\approx}{\mathbb{I}} - \underset{\approx}{\mathbf{1}} \otimes \underset{\approx}{\mathbf{1}}) & \underline{\mathbf{y}} \in \Omega_\mu^m \\ \frac{1}{\alpha E} (4\underset{\approx}{\mathbb{I}} + \frac{\alpha-2\beta}{\beta} (\underset{\approx}{\mathbf{1}} \otimes \underset{\approx}{\mathbf{1}})) & \underline{\mathbf{y}} \in \Omega_\mu^i \end{cases} \quad (5.16)$$

The detailed derivation of the topological derivative of $\underset{\approx}{\mathbb{C}}$ can refer to [2].

5.3 Topological derivative-based algorithm

The previous analytical formula of topological derivative (Equation 5.14) provides an efficient strategy for topology optimization problems. We will use it as a descent direction in the level-set domain representation [1, 11]. A brief summary of this algorithm is provided below.

We begin by adapting the optimisation problem in Equation 5.1 into the present context as follows:

$$\min_{\Omega_\mu^m \subset \Omega_\mu} J(\Omega_\mu^m) = h(\underset{\approx}{\mathbb{C}}) + \lambda_v \frac{|\Omega_\mu^m|}{V_\mu} \quad (5.17)$$

in which λ_v is a fixed² penalisation parameter imposing a constraint on the volume ratio of Ω_μ^m , i.e. $f_v = \frac{|\Omega_\mu^m|}{V_\mu}$ and h is a generic function of the homogenized elasticity tensor $\underset{\approx}{\mathbb{C}}$. In the following sections, $\underset{\approx}{\mathbb{C}}$ is used to characterize optimised effective properties in the corresponding microstructure synthesis. For instance, the properties of interest such as the homogenised Young's, shear and bulk moduli. To this end, it is convenient to define the following types of functions $h(\underset{\approx}{\mathbb{C}})$:

²the value will not be changed throughout the iterations of optimisation. We have proposed to update it during the optimisation process with *RL-Dual Gradient Descent* method. However, we have decided against applying it here due to its requirement for an outer loop and its associated high computational cost.

- the first type

$$h(\underline{\underline{C}}) = \underline{\underline{C}}^{-1} :: \underline{\underline{\varphi}}^{mn} \otimes \underline{\underline{\varphi}}^{pq}$$

of which $\underline{\underline{\varphi}}^{mn}$ and $\underline{\underline{\varphi}}^{pq}$ are second-order tensors with $\underline{\underline{\varphi}}^{mn} = \underline{e}_m \otimes \underline{e}_n$, it is yet to be defined for each specific case.

- the second type

$$h(\underline{\underline{C}}) = \frac{\underline{\underline{C}}^{-1} :: \underline{\underline{\varphi}}^{mn} \otimes \underline{\underline{\varphi}}^{pq}}{\underline{\underline{C}}^{-1} :: \underline{\underline{\varphi}}^{kl} \otimes \underline{\underline{\varphi}}^{rs}}$$

- the third type

$$h(\underline{\underline{C}}) = \underline{\underline{C}} :: \underline{\underline{\varphi}}^{mn} \otimes \underline{\underline{\varphi}}^{pq}$$

- the fourth type

$$h(\underline{\underline{C}}) = (\underline{\underline{C}} :: \underline{\underline{\varphi}}^{mn} \otimes \underline{\underline{\varphi}}^{pq})(\underline{\underline{C}} :: \underline{\underline{\varphi}}^{kl} \otimes \underline{\underline{\varphi}}^{rs})$$

The topology sensitivity of $\underline{\underline{C}}$ in Equation 5.14 as well as the construction of $h(\underline{\underline{C}})$ allows the exact derivative of the cost function $J(\Omega_\mu^m)$ by the application of the conventional rules of differential calculus:

$$D_T J(\Omega_\mu^m)(\underline{y}) = \langle Dh(\underline{\underline{C}}), D_T \underline{\underline{C}}(\underline{y}) \rangle + \lambda_v \quad (5.18)$$

in which $\langle \cdot \rangle$ denotes the appropriate product between $Dh(\underline{\underline{C}})$ the derivative of h and $D_T \underline{\underline{C}}(\underline{y})$ the topological derivative of $\underline{\underline{C}}$. More specifically, the topological derivative of the cost function J with respect to the above four types of the function h is completed:

- the first type

$$D_T J(\Omega_\mu^m)(\underline{y}) = -(\underline{\underline{C}}^{-1} : D_T \underline{\underline{C}}(\underline{y}) : \underline{\underline{C}}^{-1}) :: \underline{\underline{\varphi}}^{mn} \otimes \underline{\underline{\varphi}}^{pq} + \lambda_v$$

- the second type

$$D_T J(\Omega_\mu^m)(\underline{y}) = \frac{-(\underline{\underline{M}} :: \underline{\underline{\varphi}}^{mn} \otimes \underline{\underline{\varphi}}^{pq})(\underline{\underline{C}}^{-1} :: \underline{\underline{\varphi}}^{kl} \otimes \underline{\underline{\varphi}}^{rs}) + (\underline{\underline{M}} :: \underline{\underline{\varphi}}^{kl} \otimes \underline{\underline{\varphi}}^{rs})(\underline{\underline{C}}^{-1} :: \underline{\underline{\varphi}}^{mn} \otimes \underline{\underline{\varphi}}^{pq})}{(\underline{\underline{C}}^{-1} :: \underline{\underline{\varphi}}^{kl} \otimes \underline{\underline{\varphi}}^{rs})^2} + \lambda_v$$

$$\text{with } \underline{\underline{M}} = \underline{\underline{C}}^{-1} : D_T \underline{\underline{C}}(\underline{y}) : \underline{\underline{C}}^{-1}.$$

- the third type

$$D_T J(\Omega_\mu^m)(\underline{y}) = D_T \underline{\underline{C}}(\underline{y}) :: \underline{\underline{\varphi}}^{mn} \otimes \underline{\underline{\varphi}}^{pq} + \lambda_v$$

- the fourth type

$$D_T J(\Omega_\mu^m)(\underline{y}) = (D_T \underline{\underline{C}}(\underline{y}) :: \underline{\underline{\varphi}}^{mn} \otimes \underline{\underline{\varphi}}^{pq})(\underline{\underline{C}} :: \underline{\underline{\varphi}}^{kl} \otimes \underline{\underline{\varphi}}^{rs}) + (D_T \underline{\underline{C}}(\underline{y}) :: \underline{\underline{\varphi}}^{kl} \otimes \underline{\underline{\varphi}}^{rs})(\underline{\underline{C}} :: \underline{\underline{\varphi}}^{mn} \otimes \underline{\underline{\varphi}}^{pq}) + \lambda_v$$

The aforementioned topological derivative formulations are used to measure the sensitivity of J to changes in the topology. To minimize the cost function in Equation 5.17, these formulations provide a feasible descent direction and thus allow the algorithm to interchange matrix materials and inclusion materials. This procedure relies on a level-set domain representation described below. The detailed algorithm is devised by S. Amstutz in [1].

With the adoption of a level-set domain representation, the material domain Ω_μ^i and Ω_μ^m is characterised by a function $\psi \in L^2(\Omega_\mu)$ such that:

$$\Omega_\mu^m = \{\underline{y} \in \Omega_\mu, \psi(\underline{y}) < 0\}, \quad (5.19)$$

$$\Omega_\mu^i = \{\underline{y} \in \Omega_\mu, \psi(\underline{y}) > 0\}. \quad (5.20)$$

According to [1], an obvious sufficient condition of local optimality of Equation 5.17 under circular inclusion perturbations is:

$$D_T J(\Omega_\mu)(\underline{y}) > 0 \quad \underline{y} \in \Omega_\mu \quad (5.21)$$

In order to devise a level set-based algorithm that generates a topology satisfying Equation 5.21, it is advantageous to introduce a topological gradient function $g(\underline{y})$:

$$g(\underline{y}) := \begin{cases} -D_T J(\Omega_\mu^m)(\underline{y}) & \underline{y} \in \Omega_\mu^m \\ D_T J(\Omega_\mu^i)(\underline{y}) & \underline{y} \in \Omega_\mu^i \end{cases} \quad (5.22)$$

By definition, at a point $\underline{y} \in \Omega_\mu$, the topological gradient $g(\underline{y})$ is a number that measures the sensitivity of the criterion $J(\Omega_\mu)(\underline{y})$ with respect to the creation of a small hole around \underline{y} . Thus, the condition 5.21 is satisfied if the following equivalent condition is fulfilled:

$$\theta := \arccos \left[\frac{\langle \underline{g}, \underline{\psi} \rangle}{\|\underline{g}\|_{L^2} \|\underline{\psi}\|_{L^2}} \right] = 0 \quad (5.23)$$

with \underline{g} and $\underline{\psi}$ denote the vectors which store all the pointwise values of the function $g(\underline{y})$ and $\psi(\underline{y})$ at point $\underline{y} \in \Omega_\mu$. The inner product $\langle \cdot, \cdot \rangle$ and the norm $\|\cdot\|$ refer to the Hilbert space $L^2(\Omega_\mu)$. θ is the non-oriented angle between the vectors \underline{g} and $\underline{\psi}$. The optimality condition is satisfied when θ is smaller than a pre-specified convergence tolerance ϵ_θ .

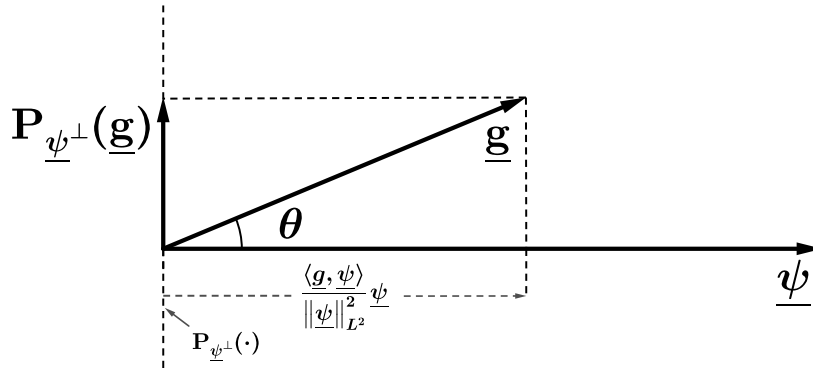


Figure 5.3: Illustration of vectors \underline{g} and $\underline{\psi}$

Let us now discuss the level set function of i -th iteration, denoted by $(\psi_i(\underline{y}))_{i \in \mathbb{N}}$, which describes the corresponding RVE topologies. It provides successive approximations to the sufficient optimality condition 5.23. We define firstly $P_{\psi(\underline{y})^\perp}$ the orthogonal projector onto the orthogonal complement of $\psi(\underline{y})$, i.e.

$$P_{\psi(\underline{y})^\perp}(g(\underline{y})) = g(\underline{y}) - \frac{\langle \underline{g}, \underline{\psi} \rangle}{\|\underline{\psi}\|_{L^2}^2} \psi(\underline{y}) \quad (5.24)$$

The resulting vector of $P_{\psi(\underline{y})^\perp}(g(\underline{y}))$ is denoted by $P_{\underline{\psi}^\perp}(\underline{g})$. The sequence $(\psi_i)_{i \in \mathbb{N}}$ of level set functions:

$$\psi_{i+1}(\underline{y}) = \cos(\kappa_i \theta_i) \psi_i(\underline{y}) + \sin(\kappa_i \theta_i) \frac{P_{\psi_i^\perp}(\underline{g}(\underline{y}))}{\|P_{\psi_i^\perp}(\underline{g})\|} \quad (5.25)$$

with $\kappa_i \in [0, 1]$ the step size (yet to be defined) and θ_i defined in [Equation 5.23](#).

By using trigonometric formulas, and normalizing the level set function in each iteration ($\|\underline{\psi}_i\|_{L^2} = 1$), the following relation is obtained:

$$\psi_{i+1}(\underline{y}) = \frac{1}{\sin \theta_i} \left[(\sin((1 - \kappa_i) \theta_i) \psi_i(\underline{y}) + \sin(\kappa_i \theta_i) \frac{\underline{g}_i(\underline{y})}{\|\underline{g}_i\|_{L^2}}) \right] \quad (5.26)$$

as it indicates, the updated level set function $\psi_{i+1}(\underline{y})$ depends on the step size value, which combines the previous level set function $\psi_i(\underline{y})$ and topological gradient function $\underline{g}_i(\underline{y})$: the larger the step size, the greater the impact of perturbation factor from $\underline{g}_i(\underline{y})$ will be taken into account.

5.4 Finite element implementation

The finite element implementation has been done for FEniCS version 2019.1.0, and the code can be downloaded at “[A level set based optimisation code using FEniCS](#)”.

The present algorithm is of simple implementation, since exact formulas are given for each step, no artificial algorithmic parameters or post-processing strategies are required throughout the iterations. The computation starts from the finite element discretization of the [Equation 5.12](#), the nodal-valued solution of $\tilde{\mathbf{u}}^{(kl)}$ under the periodic boundary condition [5.5](#) is obtained. Then the homogenized elasticity tensor \mathbb{C} and its topological derivative $D_T \mathbb{C}$ are completed respectively with [Equation 5.11](#) and [Equation 5.14](#). These two solutions will be used for the computation of $D_T J$ with [Equation 5.18](#). The updated level set function $\psi_{i+1}(\mathbf{y})$ is generated according to [Equation 5.26](#), which is a linear combination between the known function $\psi_i(\mathbf{y})$ and the corresponding function $g_i(\mathbf{y})$ (it depends on $D_T J$ according to [Equation 5.22](#)). In this step, a finite element approximation by a smoothed nodal version of g_n will be used. The material associated by Ω_μ^m (resp. Ω_μ^i) is assigned to the field with negative (resp. positive) level set function value. From the description above, we propose an overall algorithm:

Algorithm 1 A level set-based optimisation algorithm

Initialization: Choose an initial level set function ψ_0 and an initial step κ_0 .

if The target value of J is not reached **then** ▷ stopping criteria in [Appendix B](#)

Construct the domain Ω_μ by [\(5.19\)](#)

Solve the elasticity problem [\(5.12\)](#)

Compute the topological gradient $g(\mathbf{y})$ by [\(5.22\)](#)

Update the level set function by [\(5.26\)](#)

if $J_{i+1} > J_i$ **then**

Line search by adjusting the step size ▷ line search process in [Appendix B](#)

Update the level set function

else if $J_{i+1} < J_i$ **then**

Continue

end if

else if The target value of J is reached **then**

if Optimality condition is not satisfied **then**

Refinement of RVE

else if Optimality condition is satisfied **then**

Stop

end if

end if

A complete flowchart of this algorithm is given in [Appendix B](#). It can be seen that the implementation process described previously is primarily based on the fundamental mathematical framework. In addition to this, it also includes other crucial implementation processes: subdomain definition, line search as well as stopping criteria. They are all detailed in [Appendix B](#).

Here, we come up with some numerical examples:

5.4.1 Initialization

The RVE domain is taken as a unit square cell $\Omega_\mu = (0, 1) \times (0, 1)$ with $V_\mu = 1$, the mesh is built using the line:

```
1 mesh=RectangleMesh(Point(0.0,0.0),Point(1,1),Nx,Ny,"crossed")
```

The class `RectangleMesh` creates a mesh in a 2D rectangle spanned by two points (opposing corners) of the rectangle. The arguments `Nx`, `Ny` specify the number of divisions in x and y directions, and the optional argument `crossed` means that each square of the grid is divided into four triangles realized by the crossing diagonals of the square. The choice of this mesh type is crucial for achieving symmetric deformation, thereby ensuring consistent symmetry in the design throughout the optimization iterations. We set initially `Nx=Ny=40` and the initial topology is given by the following level set function:

$$\psi(\underline{y}) = \frac{1}{N} (\cos^2(\pi(y_x - 0.5)) \cos^2(\pi(y_y - 0.5)) - 0.5) \quad (5.27)$$

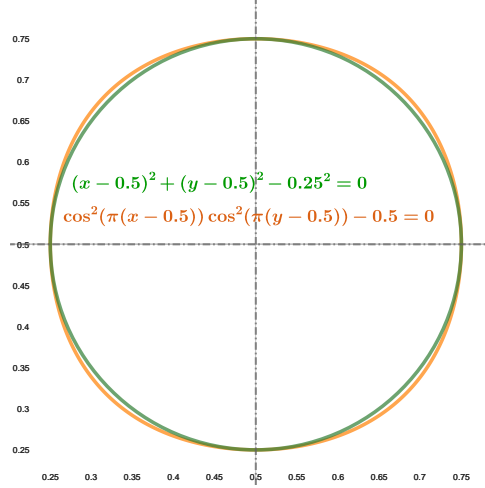


Figure 5.4: Illustration of the initial level set function

with $\underline{y} = (y_x, y_y)$ the coordinate of the point $\underline{y} \in \Omega_\mu$ and N is the normalizing constant that ensures $\|\underline{\psi}\|_{L^2} = 1$. The initial topology of the RVE domain is illustrated as follows:

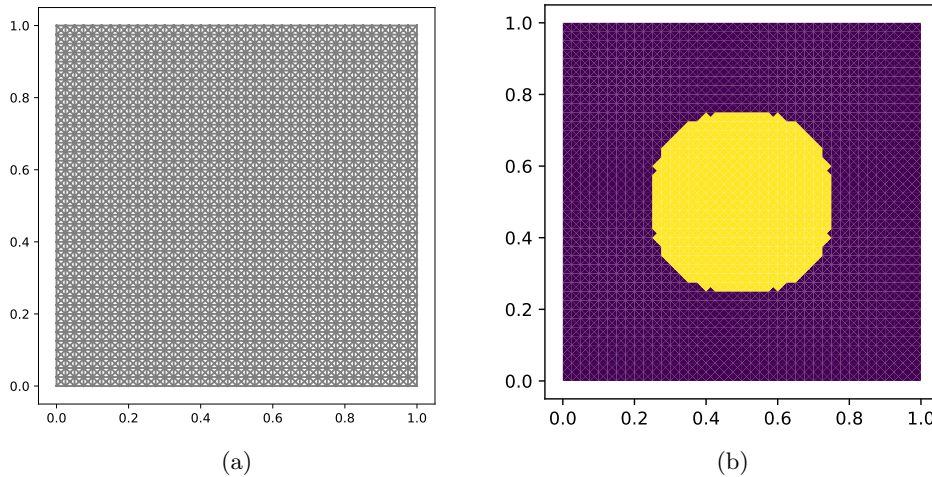


Figure 5.5: Initial microstructure (a) Initial finite element mesh adopted and (b) Initial topology

The mesh consists of 6400 triangular elements and a total of 3281 nodes. Note that the level set based RVE domain topology depends directly on the fineness of the mesh (i.e. the rough contour in [Figure 5.5a](#)), a uniform mesh refinement will be used throughout the iterations to further improve the accuracy of the results and the resolution of the optimized topology.

The elasticity parameters of Young's modulus and Poisson ratio used for each phase are $E^m = 1$, $E^i = \gamma^*$ and $\nu^m = \nu^i = 0.3$. Following the Kelvin convention, we write the homogenized elasticity tensor $\underline{\underline{C}}$ of the initial topology in Figure 5.5a in matrix form:

$$[\underline{\underline{C}}] = \begin{pmatrix} 0.646 & 0.167 & 0 \\ 0.167 & 0.646 & 0 \\ 0 & 0 & 0.344 \end{pmatrix}_{\kappa} \Rightarrow [\underline{\underline{C}}^{-1}] = \begin{pmatrix} 1.659 & -0.429 & 0 \\ -0.429 & 1.659 & 0 \\ 0 & 0 & 11.300 \end{pmatrix}_{\kappa} \quad (5.28)$$

it is of tetragonal symmetry ($I_2 = 0$ and $J_2 \neq 0$ in section 3.7). Since the effective material properties, i.e. the Young's, bulk and shear moduli as well as the Poisson's ratio (numerical result given in subsection 5.4.2), are all related to the component of the compliance tensor $\underline{\underline{S}}$ ($\underline{\underline{S}} = \underline{\underline{C}}^{-1}$), its Kelvin representation is:

$$[\underline{\underline{S}}] = \begin{pmatrix} (\underline{\underline{S}})_{1111} & (\underline{\underline{S}})_{1122} & 0 \\ (\underline{\underline{S}})_{1122} & (\underline{\underline{S}})_{1111} & 0 \\ 0 & 0 & 2(\underline{\underline{S}})_{1212} \end{pmatrix}_{\kappa} = \begin{pmatrix} \frac{1}{E} & -\frac{\nu}{E} & 0 \\ -\frac{\nu}{E} & \frac{1}{E} & 0 \\ 0 & 0 & \frac{2}{G} \end{pmatrix}_{\kappa}$$

with E and ν the effective Young's moduli and Poisson's ratio. G is the effective in-plane shear modulus.

5.4.2 Numerical examples

The application of the above optimisation algorithm to the mesostructure design is illustrated here by several simple numerical examples. These examples are widely discussed in the literature, the object here is to validate our implementation.

For the following examples, the function $h(\underline{\underline{C}})$ is all of the first type. The elasticity parameters of Young's modulus and Poisson's ratio are $E^m = 1$, $E^i = 0.01$ and $\nu^m = \nu^i = 0.3$, meaning that the phase contract parameter γ^* is set to 0.01.

Before introducing the numerical examples, it has to be noted that the maximisation of material parameters such as Young's modulus and shear modulus by reducing the fraction of Ω_{μ}^m is not possible (as can be observed, for the following first two examples, the optimised material parameters are smaller than the initial ones), thus we introduce the volume constraint by λ_v , which prevents the trivial solution of a unit domain without inclusion and allows us to obtain an optimisation design with maximised value of parameters based on a volume fraction considered.

Horizontal rigidity maximization

The function $h(\underline{\underline{C}})$ is defined with $\varphi^{mn} = \varphi^{pq} = \underline{\underline{e}}_1 \otimes \underline{\underline{e}}_1$, we have:

$$h(\underline{\underline{C}}) := (\underline{\underline{C}}^{-1})_{1111} = \frac{1}{E}$$

the penalisation parameter λ_v is chosen as 10 (same value as is chosen in [2]). Thus, the corresponding cost function is:

$$J(\Omega_{\mu}^m) = (\underline{\underline{C}}^{-1})_{1111} + 10f_v$$

the minimisation of $J(\Omega_{\mu}^m)$ corresponds to the optimisation of the longitudinal Young's modulus E with less volume fraction of Ω_{μ}^m .

The initialisation is given in subsection 5.4.1 with the initial Young's modulus as $E = 0.614$. The optimized topology is shown in Figure 5.6 with the volume fraction of Ω_μ^m is $f_v = 0.4$ and the associated optimised Young's modulus is $E = 0.41$.

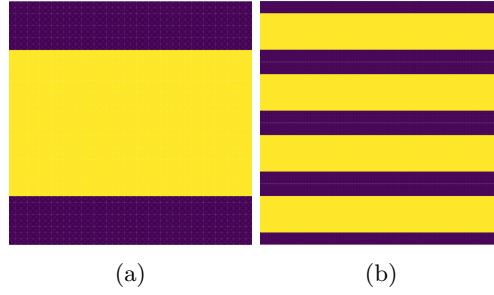


Figure 5.6: Horizontal rigidity maximization: (a) Optimised RVE topology, and (b) Corresponding periodic mesostructure.

The optimized elasticity tensor is:

$$[\underset{\approx}{\mathbb{C}}^{-1}] = \begin{pmatrix} 2.461 & -0.738 & 0 \\ -0.738 & 55.167 & 0 \\ 0 & 0 & 313.972 \end{pmatrix}_{\mathcal{K}}$$

The evolution of the cost function and angle θ throughout the iterations are shown in Figure 5.7. Since the residual angle θ is not sufficiently small at iteration 20, a mesh refinement step has been performed at the subsequent iteration, resulting in a significant decrease of the angle θ and the final convergence is attained.

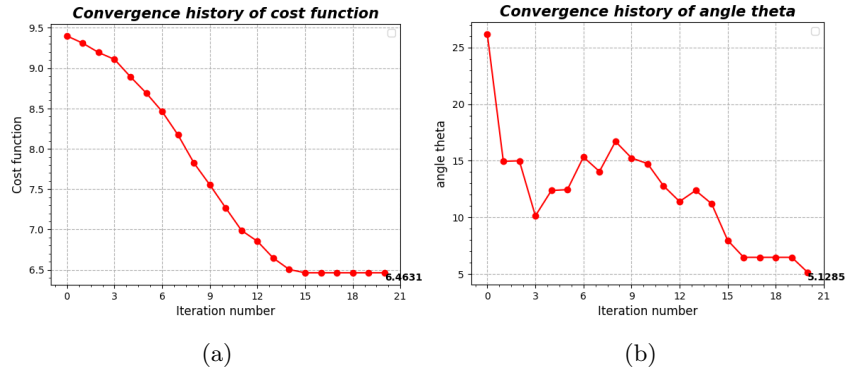


Figure 5.7: Horizontal rigidity maximization. Convergence history: (a) Cost function, and (b) Angle θ

There exists an analytical solution for the elasticity tensor homogenisation of a two-component laminate [146]. The elasticity tensors $\underset{\approx}{\mathbb{C}}^m$, $\underset{\approx}{\mathbb{C}}^i$ are considered to be isotropic. An analytical solution of homogenized elasticity tensor for a finite-rank microstructure is given in [146]:

$$(\underset{\approx}{\mathbb{C}}^{\text{hom}})^{-1} = (\underset{\approx}{\mathbb{C}}^m)^{-1} + c_2((\underset{\approx}{\mathbb{C}}^i)^{-1} - (\underset{\approx}{\mathbb{C}}^m)^{-1}) : [\underset{\approx}{\mathbb{I}} - c_1 \underset{\approx}{\mathbb{f}} : (((\underset{\approx}{\mathbb{C}}^i)^{-1} - (\underset{\approx}{\mathbb{C}}^m)^{-1})^{-1} + c_1 \underset{\approx}{\mathbb{f}})^{-1}]$$

with,

- c_r : The volume fraction of each component, here $c_1 = c_2 = 0.5$;
- $\underset{\approx}{\mathbb{I}}$: Identity tensor of order 4, $(\underset{\approx}{\mathbb{I}})_{ijkl} = \frac{1}{2}(\delta_{ik}\delta_{jl} + \delta_{il}\delta_{jk})$;
- $\underset{\approx}{\mathbb{C}}^r$: Elasticity tensor for each component $r = m$ or i , we have for 2D case

$$(\mathbb{C}^r)_{ijkl} = \lambda^r \delta_{ij} \delta_{kl} + \mu^r (\delta_{ik} \delta_{jl} + \delta_{il} \delta_{jk})$$

with $\lambda^r = \frac{\nu^r E^r}{(1 + \nu^r)(1 - 2\nu^r)}$ for 3D case and $\lambda^r = \frac{\nu^r E^r}{(1 + \nu^r)(1 - \nu^r)}$ for 2D case, and $\mu^r = \frac{E^r}{2(1 + \nu^r)}$. we define here $E^m = 1$, $E^i = 1 \times 10^{-3}$ and $\nu^m = \nu^i = 0.3$.

- \mathbf{f} : $\mathbf{f} = E^m \sum_{n=1}^N p_n (t_n \otimes t_n) \otimes (t_n \otimes t_n)$; E_1 is the Young's modulus of rigid phase, and t_n represents the tangent vector of layer n , while $p_n \geq 0$ describes the relative contribution of the n -th layer.

Thus, the analytical homogenized elasticity tensor is:

$$[\mathbb{C}^{-1}]_{\approx} = \begin{pmatrix} 2.463 & -0.739 & 0 \\ -0.739 & 55.186 & 0 \\ 0 & 0 & 313.426 \end{pmatrix}_{\mathcal{K}}$$

It can be observed that the numerical result closely aligns with this analytical result. Thus, we validate this optimisation code. It is used to do some benchmarks with the following two cases.

Shear modulus maximization

Shear modulus G is defined as the ratio of shear stress σ_{12} and shear strain ε_{12} . Thus, we take here $\varphi^{mn} = \varphi^{pq} = \underline{e}_1 \otimes \underline{e}_2$ so that the function $h(\mathbb{C})$ is defined by:

$$h(\mathbb{C}) := 4(\mathbb{C}^{-1})_{1212} = \frac{4}{G}$$

For the maximisation of the shear modulus with the volume constraint (the penalisation parameter is chosen as $\lambda_v = 50$), we propose the cost function:

$$J(\Omega_{\mu}^m) = 4(\mathbb{C}^{-1})_{1212} + 50f_v$$

the minimisation of $J(\Omega_{\mu}^m)$ corresponds to the maximisation of the shear modulus G with less volume fraction of Ω_{μ}^m . Equation 5.28 indicates that the initial shear modulus is $G = 0.18$.

The optimized topology is shown in Table 5.2 on the left side. The rest two designs are benchmarks in literature, respectively, the middle one is obtained in [2] with the same algorithm and the right one is obtained in [147] by deep learning algorithm.

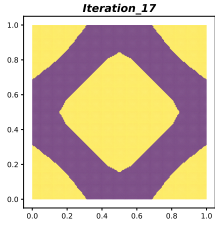
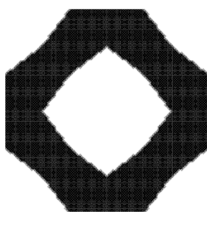

Shear modulus maximization		
My result	Amstutz S. results [Amstutz2010,p12]	Deep learning results [Kollmann2020, p11]
 <p>Iteration 17</p>		
$h(\mathbb{C}) = 28.78$ $f_v = 0.51$	- -	- $f_v = 0.47$

Table 5.1: Comparison between optimised topology for shear modulus maximization

It can be seen that our mesostructure design has achieved a perfect match with other results. It is evident that there are noticeable curves appearing in the contours of the mesostructure, which is crucial for a more refined structural design. The optimized elasticity tensor is:

$$[\underset{\approx}{\mathbb{C}}^{-1}] = \begin{pmatrix} 9.115 & -6.510 & 0 \\ -6.510 & 9.115 & 0 \\ 0 & 0 & 14.388 \end{pmatrix}_{\kappa}$$

The optimised shear modulus is $G = 0.14$ with its corresponding volume fraction $f_v = 0.51$.

Minimization of a modified Poisson's ratio

The modified Poisson's ratio is defined as $\frac{\nu}{E}$, which corresponds to the opposite of the homogenised tensor component $(\underset{\approx}{\mathbb{C}})_{1122}$. We take here $\underset{\approx}{\varphi}^{mn} = \underline{e}_1 \otimes \underline{e}_1$ and $\underset{\approx}{\varphi}^{pq} = -\underline{e}_2 \otimes \underline{e}_2$ so that the function $h(\underset{\approx}{\mathbb{C}})$ is:

$$h(\underset{\approx}{\mathbb{C}}) := -(\underset{\approx}{\mathbb{C}}^{-1})_{1122} = \frac{\nu}{E}$$

The penalisation parameter is chosen as $\lambda = 0.5$, thus the cost function is:

$$J(\Omega_{\mu}^m) = -(\underset{\approx}{\mathbb{C}}^{-1})_{1122} + 0.5f_v$$

Equation 5.28 indicates that the initial value of modified Poisson's ratio is $\frac{\nu}{E} = 0.429$. The optimized topology is shown in Table 5.2 on the left side as well as the two benchmarks.

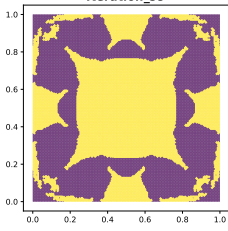
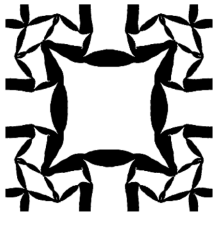

Minimization of modified Poisson's ratio		
My result	Amstutz S. results [Amstutz2010,p12]	Deep learning results [Kollmann2020, p11]
		
$\nu = -0.22 \quad f_v = 0.51$	$\nu = -0.42 \quad -$	$- \quad f_v = 0.66$

Table 5.2: Comparison between optimised topology for minimization of a modified Poisson's ratio

In this example, although our design fits well with the result obtained from the deep learning algorithm, it does not achieve a 'rod joints' lattice structure, as observed in the result obtained in [2] using the same algorithm. This could be primarily attributed to different choices of penalisation parameters, mesh refinement, and step size setting strategies.

The optimized elasticity tensor is:

$$[\underset{\approx}{\mathbb{C}}^{-1}] = \begin{pmatrix} 9.570 & 2.140 & 0 \\ 2.140 & 9.570 & 0 \\ 0 & 0 & 66.667 \end{pmatrix}_{\kappa}$$

The minimised function value is $h(\underset{\approx}{\mathbb{C}}) = \frac{\nu}{E} = -2.140$. The volume fraction of the obtained topology is $f_v = 0.51$.

Several observations can be made from the implementation of previous examples:

- The optimised topology depend on the initial geometry. For the following topology optimisations, the geometry of the initial inclusion is recommended to be of the same symmetry type as its corresponding target symmetry class;
- The optimisation parameters such as step size κ and penalisation parameter λ_ν will influence the processes of how the optimisation carries out. For different optimisation cases, they are supposed to be determined accordingly.

5.5 Numerical result for exotic material: R_0 -Orthotropy

We aim here to provide a geometry of a unit cell that generates an effective R_0 -orthotropic elastic material. We do not claim that it is the only specific design producing such exotic behaviour, nor the best one. For our computation, the rigid matrix phase is constituted of an elastic isotropic material with:

$$E_m = 1, \quad \nu_m = 0.3.$$

while the soft is considered with $E_i = \gamma^*$, with $\gamma^* = 10^{-3}$ and $\nu_i = 0.3$.

The initial unit cell contains an ellipsoidal soft inclusion (cf. [Figure 5.8](#)), and is intended to initiate the algorithm from an effective orthotropic material. The considered level set is

$$\psi(\underline{y}) = \cos^2(0, 55\pi(y_x - 0, 5)) \cos^2(0, 3\pi(y_y - 0, 5)) - 0, 95.$$

A structured mesh is considered in order to preserve, at best, the symmetries of the unit cell, and hence of the effective tensor. The following calculations were performed using a mesh of 57600 standard linear triangular elements.

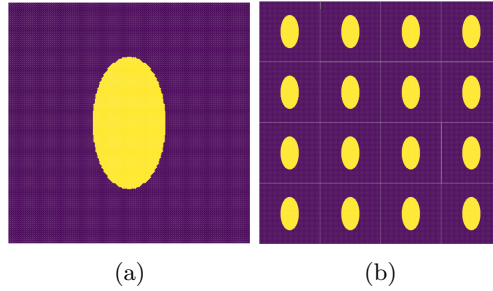


Figure 5.8: Initialisation: (a) Initial unit cell used for computation and (b) Initial lattice assembled of unit cells

The matrix form of the initial effective tensor resulting from these choices is:

$$[\underset{\sim}{\mathbb{C}}] = 10^{-1} \begin{pmatrix} 6.49 & 2.03 & 0 \\ 2.03 & 8.48 & 0 \\ 0 & 0 & 4.60 \end{pmatrix}_{\kappa}.$$

with the following set of invariants

$$(I_1, J_1, I_2, J_2, I_3) = (9.52 \cdot 10^{-1}, 5.03 \cdot 10^{-1}, 1.98 \cdot 10^{-2}, 3.66 \cdot 10^{-3}, 8.46 \cdot 10^{-4}).$$

The ratio $\frac{J_2}{I_2} \sim 20\%$ is not small enough to consider J_2 as being negligible with respect to I_2 . Hence the

initial elastic material should be considered as orthotropic, but not R_0 -orthotropic.

The cost function to be minimised by the algorithm was chosen to be

$$J = h(\underline{\underline{\mathbb{C}}}) = aJ_2(\underline{\underline{\mathbb{C}}}) + \frac{b}{I_2(\underline{\underline{\mathbb{C}}})}.$$

and we specifically consider $(a, b) = (20000, 0.5)$. This condition corresponds to the characterisation of the open set $\Sigma_{[D_2]}^e$ (4.1). Without considering any constraint on the volume fraction of Ω_μ^m , adding the term $\frac{b}{I_2(\underline{\underline{\mathbb{C}}})}$ prevents the trivial solution of a unit domain without inclusion³. Considering this cost function, the optimal mesostructure depicted on Figure 5.9 is obtained.

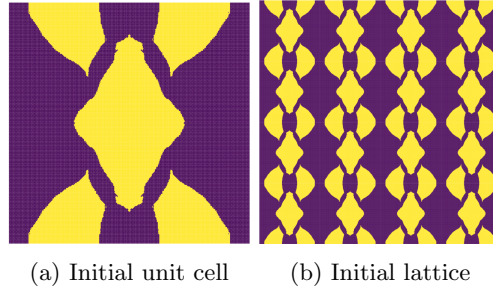


Figure 5.9: Optimised design

The matrix form of the effective tensor obtained at the end of the optimisation process is:

$$[\underline{\underline{\mathbb{C}}}] = 10^{-1} \cdot \begin{pmatrix} 0.367 & 0.490 & 0 \\ 0.490 & 3.920 & 0 \\ 0 & 0 & 1.640 \end{pmatrix}_{\mathcal{K}}.$$

The invariants of the effective stiffness tensor of the optimal geometry are

$$(I_1, J_1, I_2, J_2, I_3) = (2.634 \cdot 10^{-1}, 1.647 \cdot 10^{-1}, 6.312 \cdot 10^{-2}, 9.113 \cdot 10^{-7}, 4.261 \cdot 10^{-5}).$$

The optimized elastic material is obviously R_0 -orthotropic since J_2 is negligible with respect to I_2 , the ratio $\frac{J_2}{I_2} \sim 0.0014\%$. To the contrary, the invariants of the associated compliance tensor are

$$(I_1^-, J_1^-, I_2^-, J_2^-, I_3^-) = (2.318 \cdot 10^1, 1.380 \cdot 10^1, 4.394 \cdot 10^2, 2.922, -5.313 \cdot 10^2).$$

which obviously shows that the resulting material is not r_0 -orthotropic. This numerical result substantiates the statement in section 4.2 that R_0 -orthotropic is not inverse stable.

5.6 Numerical results for semi-exotic material: Cauchy elasticity

We now consider the geometry of a unit cell that generates an effective Cauchy elasticity material. Since the condition for Cauchy elasticity concerns only the isotropic harmonic components, the optimized topology depends strongly on the initial geometry. Thus, two types of level set functions will be applied, one of tetragonal symmetry and the other of orthotropic symmetry:

- Tetragonal

$$\psi(\underline{y}) = \cos^2(\pi(y_x - 0.5)) \cos^2(\pi(y_y - 0.5)) - 0.5.$$

³Such a trivial case is isotropic and hence verify $J_2 = I_2 = 0$.

- Orthotropic

$$\psi(\underline{y}) = \cos^2(0.55\pi(y_x - 0.5)) \cos^2(0.3\pi(y_y - 0.5)) - 0.95.$$

The computations will be performed using a mesh of 14400 standard linear triangular elements (with $N_x = N_y = 60$). The material properties are set the same as for R_0 -orthotropic case, such as $E_m = 1, E_i = 0.01$ and $\nu_m = \nu_i = 0.3$.

The initialization is illustrated as follows:

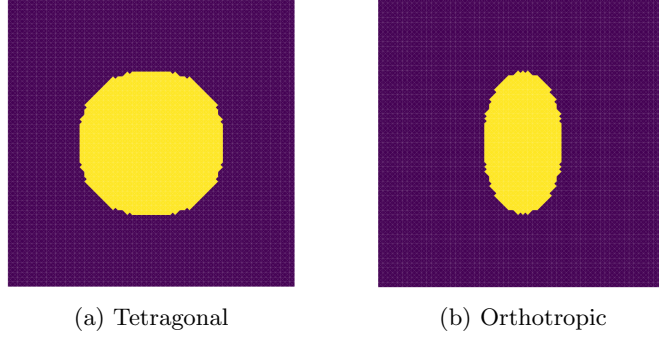


Figure 5.10: Initial unit cell of different symmetry types

The initial effective tensor is :

- Tetragonal

$$[\underset{\approx}{\mathbb{C}}] = 10^{-1} \cdot \begin{pmatrix} 6.43 & 1.66 & 0 \\ 1.66 & 6.43 & 0 \\ 0 & 0 & 3.42 \end{pmatrix}_{\mathcal{K}}$$

$$(I_1, J_1, I_2, J_2, I_3) = (4.10 \cdot 10^{-1}, 8.09 \cdot 10^{-1}, 0, 9.11 \cdot 10^{-3}, 0).$$

- Orthotropic

$$[\underset{\approx}{\mathbb{C}}] = 10^{-1} \cdot \begin{pmatrix} 7.12 & 2.23 & 0 \\ 2.23 & 8.86 & 0 \\ 0 & 0 & 5.10 \end{pmatrix}_{\mathcal{K}}$$

$$(I_1, J_1, I_2, J_2, I_3) = (5.43 \cdot 10^{-1}, 1.022, 1.5 \cdot 10^{-2}, 2 \cdot 10^{-3}, 5 \cdot 10^{-4}).$$

The condition for Cauchy elasticity is $2I_1 - J_1 = 0$, since no constraint should be made on (I_2, J_2, I_3) , we will evaluate the initial value of $2I_1 - J_1$ with respect to I_1 :

- Tetragonal

$$\left| \frac{2I_1 - J_1}{I_1} \right| \sim 2.7\%$$

- Orthotropic

$$\left| \frac{2I_1 - J_1}{I_1} \right| \sim 11.8\%$$

All these ratios are not small enough to consider $|2I_1 - J_1|$ as being negligible with respect to I_1 . Hence, the initial elastic materials in [Figure 5.10](#) are not considered as Cauchy elasticity.

We propose here a cost function $h(\underset{\approx}{\mathbb{C}})$:

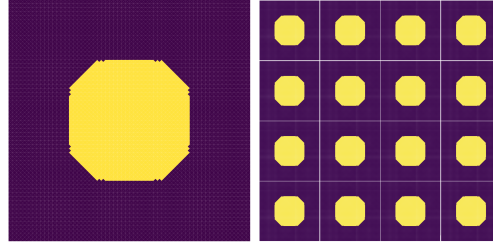
$$J = h(\underset{\approx}{\mathbb{C}}) = a(2I_1 - J_1)^2 + \frac{b}{I_1^2} + \lambda f_v \quad (5.29)$$

As this formula shows, the constraint of the volume fraction of Ω_μ^m is incorporated into the optimization of Cauchy elasticity. Based on our observation, the addition of this component allows to speed up the convergence process. $I_1 = J_1 = 0$ is a special case of Cauchy elasticity, which will not be considered here. Thus, the components $\frac{b}{I_1^2}$ is added to avoid the omitting of (I_1, J_1) . In terms of the components of the elasticity tensor, it reads:

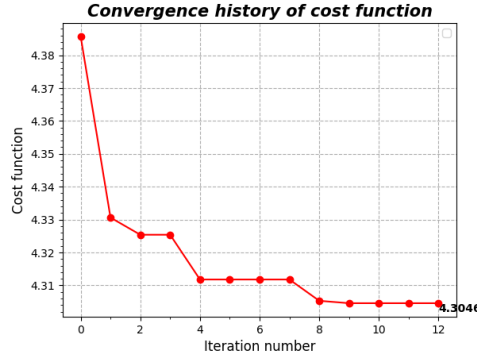
$$J = a(C_{1122} - C_{1212})^2 + \frac{b}{(C_{1111} - 2C_{1122} + 4C_{1212} + C_{2222})^2}$$

We will specifically consider $(a, b) = (3000, 1)$, $\lambda = 5$ for the tetragonal case, and $\lambda = 20$ for the orthotropic one, the optimal mesostructures are obtained as follows.

- Tetragonal



(a) Optimised unit cell (b) Optimised lattice



(c) Convergence history of the cost function

Figure 5.11: Design for Cauchy elasticity materials with tetragonal initialisation

the optimized topology remains as tetragonal symmetry with the volume ratio of rigid material $f_v = 0.778$. As we can see in the convergence history, the algorithm does not converge well initially (the value of J stops decreasing with $\theta = 20^\circ$ at iteration 7). We perform a uniform mesh refinement at iteration 8 and obtain a better convergence with the final topology having $\theta < 5^\circ$. The kelvin representation of the corresponding \mathbb{C} is:

$$[\mathbb{C}] \approx 10^{-1} \cdot \begin{pmatrix} 6.226 & 1.554 & 0 \\ 1.554 & 6.226 & 0 \\ 0 & 0 & 3.109 \end{pmatrix}_{\mathcal{K}}$$

$$(I_1, J_1, I_2, J_2, I_3) = (0.389, 0.778, 0, 1.2212 \cdot 10^{-2}, 0).$$

The ratio $|\frac{2I_1 - J_1}{I_1}| \sim 0.03\%$ is much smaller than the initial value of 2.7%. The obtained topology is thus considered as Cauchy elasticity.

- Orthotropic

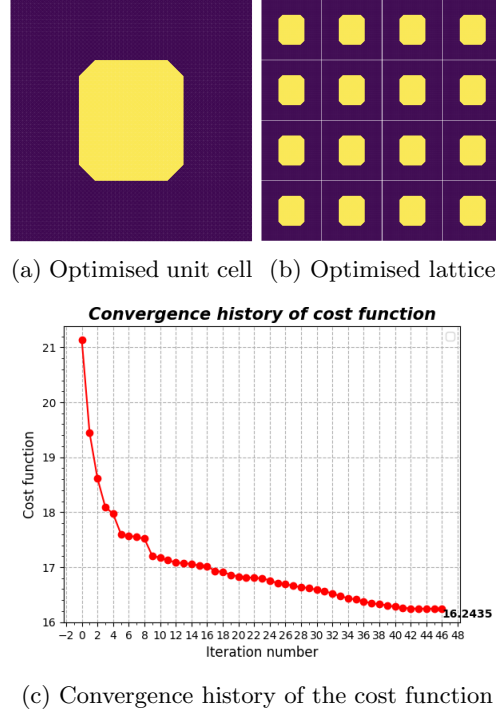


Figure 5.12: Design for Cauchy elasticity materials with orthotropic initialisation

the volume ratio of rigid material is $f_v = 0.8$. No mesh refinement has been applied during optimisation process. The kelvin representation of the corresponding \mathbb{C} is:

$$[\mathbb{C}] = 10^{-1} \cdot \begin{pmatrix} 6.12 & 1.53 & 0 \\ 1.53 & 6.65 & 0 \\ 0 & 0 & 3.06 \end{pmatrix}_{\mathcal{K}}$$

$$(I_1, J_1, I_2, J_2, I_3) = (3.958 \cdot 10^{-1}, 7.921 \cdot 10^{-1}, 1.418 \cdot 10^{-3}, 1.601 \cdot 10^{-2}, 1.271 \cdot 10^{-4}).$$

since $I_2^2 J_2 - 2I_3^2 \sim 0$, the optimised topology remains as orthotropic symmetry. And the ratio $|\frac{2I_1 - J_1}{J_1}| \sim 0.1\%$, the final topology is thus considered as Cauchy elasticity.

Remark. *It can be noted that regardless of whether tetragonal or orthotropic initialization is used, the optimized geometry converges into an octagonal shape with four sides on diagonals being relatively shorter than the others.*

5.7 Synthesis

This chapter introduces an algorithm proposed by S. Amstutz et al. [1] for the optimization of mesostructure. This approach is based on an exact formula for the topological derivative of the macroscopic elasticity tensor and a level set representation. This algorithm is used in [2] to realize the mesostructure design for some classical examples, and in this chapter, some of them are recapped. Furthermore, to realize the design of exotic or semi-exotic materials, the existing proposed function type of $h(\mathbb{C})$ is not sufficient, and we proposed two new types in section 5.3. They are used to construct the cost function for optimizing exotic materials. Based on it, the mesostructure for R_0 -orthotropic material and Cauchy elasticity material is realised. These two materials are already well-discussed in the literature, but their mesostructure design has seldom been reached.

Part III

Extension to 3D linear elasticity

Chapter 6

Geometry of 3D linear elasticity tensors space

6.1	From $O(3)$ to $SO(3)$ subgroups	85
6.1.1	$O(3)$ and its subgroups	85
6.1.2	Symmetry group of an even order tensor	86
6.1.3	$SO(3)$ and its subgroups	87
6.2	Harmonic decompositions of $\mathbb{E}la$	89
6.2.1	3D harmonic tensor space: \mathbb{H}^n	89
6.2.2	Harmonic structure	91
6.2.3	Explicit harmonic decompositions	93
6.3	Symmetry classes of $\mathbb{E}la$	96
6.4	Condition of belonging to a symmetry class	98
6.4.1	Polynomial invariants and their limitation	99
6.4.2	Covariants: a geometric path	101
6.4.3	Covariant-based membership relations	102

The geometric tools proposed in [chapter 2](#) will be applied to 3D linear elasticity in this chapter. To simplify the notation, $\mathbb{E}la(3)$ will be abbreviated to $\mathbb{E}la$. In the particular case of an even order tensor, we will show in [section 6.1](#) that the symmetry classification can be reduced to $SO(3)$ instead of $O(3)$. To fully explore $\mathbb{E}la$, this space will be decomposed into harmonic spaces in [section 6.2](#) along with some classical explicit decompositions. The symmetry classes of $\mathbb{E}la$ can be naturally obtained ([section 6.3](#)) by using clips operations. They will be identified by polynomial covariant conditions in [section 6.4](#).

6.1 From O(3) to SO(3) subgroups

By definition, the symmetry group of a physical property described by a tensor $T \in \mathbb{T}^n$ is defined as the set of operations $\mathbf{g} \in O(3)$ leaving this tensor invariant. The symmetry group of T in \mathbb{R}^3 is :

$$G_T := \{\mathbf{g} \in O(3), | T = \mathbf{g} \star T\} \quad (6.1)$$

meaning that the physical symmetry group of T corresponds to a closed subgroup of $O(3)$. Hence, in [subsection 6.1.1](#), $O(3)$ and its subgroups will be introduced. In the particular case of an even order tensor, the symmetry classification can be reduced to $SO(3)$, this point will be detailed in the following content of this section.

6.1.1 O(3) and its subgroups

For \mathbb{R}^3 , let $O(3)$ be the set of invertible transformations \mathbf{g} of \mathbb{R}^3 defined as:

$$O(3) := \{\mathbf{g} \in GL(3), \mathbf{g}^T = \mathbf{g}^{-1}\}$$

The complete collection of the subgroups of $O(3)$ is provided in [\[102, 107\]](#). These subgroups are classified into three types with regard to the nature of their elements:

Type I (Chiral) A subgroup Γ is of type I if it is a subgroup of $SO(3)$. Type I subgroups are also said to be *chiral* subgroups;

Type II (Centrosymmetric) A subgroup Γ is of type II if $-1 \in \Gamma$. In that case, $\Gamma = K \otimes Z_2^c$ where K is some $SO(3)$ closed subgroup and $Z_2^c := \{\mathbf{e}, -1\}$. Type II subgroups are also said to be *centrosymmetric*;

Type III A subgroup Γ is of type III if $-1 \notin \Gamma$ and Γ is not a subgroup of $SO(3)$.

The three associated generators: rotations, reflections and inversions are detailed in the formula as follows.

- Rotations

It is denoted by $\mathbf{r}(\underline{\mathbf{n}}, \theta)$, the rotation of angle θ around the unit vector $\underline{\mathbf{n}} \in \mathbb{R}^3$ is provided by well-known Rodrigues formula [\[148\]](#), consider ρ as its representation, we have ¹:

$$\mathbf{r}(\underline{\mathbf{n}}, \theta) = \cos(\theta) \underset{\sim}{1} - \sin(\theta) \underset{\sim}{\epsilon} \cdot \underline{\mathbf{n}} + (1 - \cos(\theta)) \underline{\mathbf{n}} \otimes \underline{\mathbf{n}}$$

in which $\underset{\sim}{1} = \mathbf{g}^T \mathbf{g}$ and $\underset{\sim}{\epsilon}$ denotes the Levi-Civita third-order tensor in \mathbb{R}^3 , specifically:

$$\varepsilon_{ijk} = \begin{cases} +1 & \text{if } (i, j, k) \text{ is } (1, 2, 3), (2, 3, 1) \text{ or } (3, 1, 2) \\ -1 & \text{if } (i, j, k) \text{ is } (3, 2, 1), (2, 1, 3) \text{ or } (1, 3, 2) \\ 0 & \text{if } i = j \text{ or } j = k \text{ or } k = i \end{cases} \quad (6.2)$$

Let $\mathcal{B} = \{\underline{\mathbf{e}}_1, \underline{\mathbf{e}}_2, \underline{\mathbf{e}}_3\}$ be the orthonormal basis of \mathbb{R}^3 , in the case of $\underline{\mathbf{n}} = \underline{\mathbf{e}}_3$, its matrix reads:

$$[\mathbf{r}(\underline{\mathbf{e}}_3, \theta)] := \begin{pmatrix} \cos \theta & -\sin \theta & 0 \\ \sin \theta & \cos \theta & 0 \\ 0 & 0 & 1 \end{pmatrix}_{\mathcal{B}} \quad (6.3)$$

¹The representation of an element \mathbf{g} of group $SO(3)$, denoted by $\rho(\mathbf{g})$, will be simplified by \mathbf{g} , and thus its matrix form reads $[\mathbf{g}]$.

which represents the anticlockwise rotation around the axis \underline{e}_3 . The rotation $\mathbf{r}(\underline{e}_3, \theta)$ is a proper transformation.

- Reflections

It is denoted by $\mathbf{m}_{\underline{n}}$, the reflection through a plane of normal \underline{n} :

$$\mathbf{m}_{\underline{n}} = 1 - 2\underline{n} \otimes \underline{n}$$

The matrix representation of $\mathbf{m}_{\underline{e}_3}$ reads:

$$[\mathbf{m}_{\underline{e}_3}] := \begin{pmatrix} 1 & 0 & 0 \\ 0 & 1 & 0 \\ 0 & 0 & -1 \end{pmatrix}_{\mathcal{B}}$$

The reflection $\mathbf{m}_{\underline{n}}$ is an improper transformation.

- Inversion

It is denoted by -1 , the inversion with respect to the origin. Its matrix representation in $\mathcal{B} = \{\underline{e}_1, \underline{e}_2, \underline{e}_3\}$ is :

$$[-1] := \begin{pmatrix} -1 & 0 & 0 \\ 0 & -1 & 0 \\ 0 & 0 & -1 \end{pmatrix}_{\mathcal{B}}$$

The inversion -1 is an improper transformation.

Moreover, we have the following property:

Proposition 6.1. *In \mathbb{R}^3 , any improper transformation $\mathbf{g} \in O(3) \setminus SO(3)$ can be broken down as follows:*

$$\forall \mathbf{g} \in O(3) \setminus SO(3) \quad \mathbf{g} = (-1) \cdot \mathbf{r}, \quad \mathbf{r} \in SO(3) \quad (6.4)$$

We illustrate it through the following example:

Example 3

Let $\mathbf{g} = \mathbf{m}_{\underline{e}_3} \in O(3) \setminus SO(3)$, it can be written as the product of inversion -1 and rotation $\mathbf{r}(\underline{e}_3, \pi)$, that is:

$$\mathbf{m}_{\underline{e}_3} = (-1) \cdot \mathbf{r}(\underline{e}_3, \pi)$$

In terms of matrix, it reads,

$$\begin{pmatrix} 1 & 0 & 0 \\ 0 & 1 & 0 \\ 0 & 0 & -1 \end{pmatrix}_{\mathcal{B}} = \begin{pmatrix} -1 & 0 & 0 \\ 0 & -1 & 0 \\ 0 & 0 & -1 \end{pmatrix}_{\mathcal{B}} \begin{pmatrix} -1 & 0 & 0 \\ 0 & -1 & 0 \\ 0 & 0 & 1 \end{pmatrix}_{\mathcal{B}}$$

6.1.2 Symmetry group of an even order tensor

To get knowledge of possible symmetry groups of an even order tensor, the following observation is preliminary:

$$(-1) \star \mathbb{T}^{2n} = (-1)^{2n} \mathbb{T}^{2n} = \mathbb{T}^{2n} \quad (6.5)$$

which indicates that the inversion $-\mathbf{1}$ always belong to $G_{T^{2n}}$, i.e. $(-\mathbf{1}) \in G_{T^{2n}}$.

Based on the observation of [Equation 6.4](#) and [Equation 6.5](#), it can be observed that any $\mathbf{g} \in O(3) \setminus SO(3)$ acts on an even order tensor T^{2n} reads:

$$\mathbf{g} \star T^{2n} = \mathbf{r} \star T^{2n}$$

As such, any symmetry group of an even-order tensor is defined as follows:

$$G_{T^{2n}} = H \otimes Z_2^c, \quad Z_2^c = \{\mathbf{1}, -\mathbf{1}\} \text{ and } H \in SO(3).$$

$G_{T^{2n}}$ is conjugate to a type II subgroups of $O(3)$ with H a subgroup of $SO(3)$. Since the only relevant part for the classification of Ela is the closed subgroup H , it is customary to classify symmetry properties of even order tensors with respect to $SO(3)$ [5, 149]. In this case, the definition in [Equation 6.1](#) can be "reduced" to $SO(3)$:

$$G_{T^{2n}} := \{\mathbf{r} \in SO(3), | T^{2n} = \mathbf{r} \star T^{2n}\}$$

To simplify the notation, in the following content, even-order tensors will be denoted by T instead of T^{2n} .

Remark.

1. *a physical symmetry problem encoded by an even order tensor can be reduced to $SO(3)$. However, the classification of material symmetry should still be deduced with respect to $O(3)$.*
2. *the reduction of $O(d) \rightarrow SO(d)$ is not true for $d = 2$, it depends on the dimension of the physical space.*
3. *when combining even and odd order tensors (for instance for piezoelectricity [150] or strain-gradient elasticity [151]), this reduction is not allowed and should be classified with respect to $O(3)$.*

As already pointed out in the notion of the symmetry group, the orientation of the elements with respect to a reference is important. The symmetry class² of the even-order tensor T , denoted by $[G_T]$, is thus defined here as the conjugacy class of its symmetry group, i.e.

$$[G_T] := \{\mathbf{r}G_T\mathbf{r}^T, | \mathbf{r} \in SO(3)\}$$

Physically speaking, the symmetry classes of T correspond to its symmetry group modulo its orientation in $SO(3)$. Furthermore, it is known that for orthogonal groups, there is only a finite number of symmetry classes [102], these symmetry classes are conjugate to the subgroups of $SO(3)$.

6.1.3 $SO(3)$ and its subgroups

The special orthogonal group $SO(3)$ is defined as:

$$SO(3) := \{\mathbf{g} \in GL(3) | \mathbf{g}^T = \mathbf{g}^{-1}, \det \mathbf{g} = 1\}$$

The group $SO(3)$ is generated by $\mathbf{r}(\underline{n}, \theta)$, with \underline{n} a unit vector in \mathbb{R}^3 . Every closed subgroup of $SO(3)$ is conjugate to an element of the following collection [152]:

$$\{[1], [Z_n], [D_n], [\mathcal{T}], [\mathcal{O}], [Z], [SO(2)], [O(2)], [SO(3)]\}_{n \geq 2}$$

²The determination of the symmetry classes of odd-order tensors is detailed in [59].

Remark. The generators for subgroup D_n in 2D and 3D are different. In 2D it is generated by rotation \mathbf{r}_θ and reflection $\mathbf{m}_{\underline{e}_2}$. In 3D, since the out-of-plane rotation is possible, it is generated by two rotations $\mathbf{r}(\underline{e}_3, \theta)$ and $\mathbf{r}(\underline{e}_1, \pi)$, and $\mathbf{r}(\underline{e}_1, \pi)$ can be regarded as the extension of $\mathbf{m}_{\underline{e}_2}$ in 2D (denoted by $\mathbf{m}_{\underline{e}_2}^{2D}$) to 3D. In terms of matrix, we have the following observation from 2D \rightarrow 3D:

$$\begin{array}{l}
 \mathbf{m}_{\underline{e}_2}^{2D} = \begin{pmatrix} 1 & 0 \\ 0 & -1 \end{pmatrix}_B \quad \begin{array}{l} \nearrow \\ \searrow \end{array} \\
 \mathbf{m}_{\underline{e}_2}^{3D} = \begin{pmatrix} \mathbf{m}_{\underline{e}_2}^{2D} & : \\ .. & 1 \end{pmatrix}_B \quad \notin \text{SO}(3) \\
 \mathbf{r}(\underline{e}_1, \pi) = \begin{pmatrix} \mathbf{m}_{\underline{e}_2}^{2D} & : \\ .. & -1 \end{pmatrix}_B \quad \in \text{SO}(3)
 \end{array}$$

The closed subgroups of SO(3) can be distinguished into two parts:

Plane groups: $\{[1], [Z_n], [D_n], [\text{SO}(2)], [\text{O}(2)]\}_{n \geq 2}$.

They are the closed subgroups of O(2), with:

- 1 is the trivial subgroup, containing only the unit element;
- Z_n is the cyclic subgroup of SO(2) generated by $\mathbf{r}(\underline{n}, \theta)$, with the convention that $Z_1 = 1$;
- D_n is the dihedral group generated by $\mathbf{r}(\underline{n}, \theta)$ and $\mathbf{r}(\underline{k}, \pi)$ (\underline{n} and \underline{k} are orthogonal vectors), with the convention that $D_1 = 1$;
- SO(2) is the group of rotations $\mathbf{r}(\underline{n}, \theta)$, with $\theta \in [0, 2\pi[$;
- O(2) is the orthogonal group generated by $\mathbf{r}(\underline{n}, \theta)$ and $\mathbf{r}(\underline{k}, \pi)$ (\underline{n} and \underline{k} are orthogonal vectors).

Exceptional groups: $\{[\mathcal{T}], [\mathcal{O}], [\mathcal{I}], [\text{SO}(3)]\}$.

They are the groups leaving invariant the Platonic solids (Table 6.1) and sphere. Specifically:

- \mathcal{T} is the tetrahedral group of order 12 of the rotations fixing the tetrahedron;
- \mathcal{O} is the octahedral group of order 24 of the rotations fixing the cube and the octahedron;
- \mathcal{I} is the icosahedral group of order 60 of the rotations fixing the icosahedron and the dodecahedron;
- SO(3) is the special orthogonal group that leaves the sphere invariant.

Since they will not be used in my thesis, the detailed information on associated generators of these groups will not be detailed here and can be found in many elasticity literature including [5, 115, 153, 154].


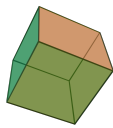
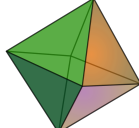
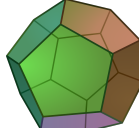
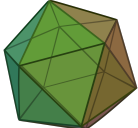
\mathcal{T}	\mathcal{O}		\mathcal{I}	
Tetrahedron	Cube	Octahedron	Dodecahedron	Icosahedron
				

Table 6.1: The Platonic solids

6.2 Harmonic decompositions of $\mathbb{E}la$

The symmetry classes of $\mathbb{E}la$ can be deduced by *group theory*. To be more specific, a group action $\mathbf{g} \in \text{SO}(3)$ will be imposed to $\underset{\approx}{\mathbb{C}} \in \mathbb{E}la$ by:

$$\underset{\approx}{\mathbb{C}} = \mathbf{g} \star \underset{\approx}{\mathbb{C}}$$

and the symmetry group of $\underset{\approx}{\mathbb{C}}$ is described by a set of $\mathbf{g} \in \text{SO}(3)$ which keep $\underset{\approx}{\mathbb{C}}$ unchanged, i.e. $\underset{\approx}{\mathbb{C}} = \mathbf{g} \star \underset{\approx}{\mathbb{C}}$. Since $\underset{\approx}{\mathbb{C}}$ is a fourth-order tensor, the index form of the action $\mathbf{g} \in \text{SO}(3)$ on $\underset{\approx}{\mathbb{C}} \in \mathbb{E}la$ is:

$$(\mathbf{g} \star \underset{\approx}{\mathbb{C}})_{i_1 i_2 i_3 i_4} = g_{i_1 j_1} g_{i_2 j_2} g_{i_3 j_3} g_{i_4 j_4} C_{j_1 j_2 j_3 j_4}, \quad \mathbf{g} \in \text{SO}(3), \underset{\approx}{\mathbb{C}} \in \mathbb{E}la$$

it can be observed that the object $g_{i_1 j_1} g_{i_2 j_2} g_{i_3 j_3} g_{i_4 j_4}$ is of eight-order which complicates the orthogonal transformation of $\underset{\approx}{\mathbb{C}}$.

In what follows, to simplify this problem, we will use the notion of harmonic decomposition to decompose the tensor space $\mathbb{E}la$ into a direct sum of harmonic spaces \mathbb{H}^n with smaller dimensions.

Remark. *The dimension of the space $\mathbb{E}la$ is 21, i.e. an elasticity tensor for a general anisotropic material in \mathbb{R}^3 has 21 independent components as it should.*

6.2.1 3D harmonic tensor space: \mathbb{H}^n

The spaces of n -th order harmonic tensors in \mathbb{R}^3 will be denoted by \mathbb{H}^n , which are $\text{SO}(3)$ -irreducible spaces³. Any tensor $\mathbb{H} \in \mathbb{H}^n$ satisfies the following two properties:

- Totally symmetric with respect to index permutation:

$$H_{i_1 i_2 \dots i_n} = H_{i_{\sigma(1)} i_{\sigma(2)} \dots i_{\sigma(n)}}$$

with σ a permutation of the symbols $\{1, 2, \dots, n\}$;

- Traceless with respect to any two indices :

$$\text{trH} := \left(\sum_{i=1}^3 H_{i_{\sigma(1)} i_{\sigma(2)} \dots i_{\sigma(n-2)} ii} \right) \underline{e}_{i_1} \otimes \underline{e}_{i_2} \otimes \dots \otimes \underline{e}_{i_{n-2}} = 0$$

with $\text{trH} \in \mathbb{H}^{n-2}$ and thus 0 here represents the null of $(n-2)$ -th order tensor.

These properties result in the following lemma [[107], Corollary 1.4.3]:

Lemma 6.1 (Dimension of \mathbb{H}^n). *For $n \geq 0$, we have:*

$$\dim \mathbb{H}^n = 2n + 1$$

Example 4

- \mathbb{H}^0 is the space of scalars, that is isotropic components;
- \mathbb{H}^1 is the space of vectors;
- \mathbb{H}^2 is the space of deviators;
- $\mathbb{H}^n (n \geq 2)$ is the space of n -th order deviators.

³Recall that a space \mathbb{V} is said to be G -irreducible if \mathbb{V} and $\{0\}$ are distinct and are the only two G -stable subspaces.

The harmonic parametrisation of tensors in \mathbb{H}^n are necessary for further use. Consider here the vector $\underline{v} \in \mathbb{H}^1$, the tensor $\underline{h} \in \mathbb{H}^2$ and $\underline{H} \in \mathbb{H}^4$, the former two are rather standard and well known, while the last case is not classical. Their representations are given as follows in terms of matrix representations. With respect to the orthogonal basis $\mathcal{B} = \{\underline{e}_1, \underline{e}_2, \underline{e}_3\}$, a vector $\underline{v} \in \mathbb{H}^1$ can be written as:

$$[\underline{v}] := (v_1, v_2, v_3)_{\mathcal{B}}^T$$

For $\underline{h} \in \mathbb{H}^2$, the following parametrisation can be used:

$$[\underline{h}] := \begin{pmatrix} h_1 + h_5 & h_2 & h_3 \\ * & -h_1 + h_5 & h_4 \\ * & * & -2h_5 \end{pmatrix}_{\mathcal{B}} \quad (6.6)$$

The advantage of this parametrisation is that it well-behaves with respect to a rotation around \underline{e}_3 . We define an orthonormal basis $\mathcal{C} = \{\underline{c}_1, \underline{c}_2, \underline{c}_3, \underline{c}_4, \underline{c}_5\}$ as follows:

$$\begin{cases} \underline{c}_1 = \frac{\sqrt{2}}{2}(\underline{e}_1 \otimes \underline{e}_1 - \underline{e}_2 \otimes \underline{e}_2) \\ \underline{c}_2 = \frac{\sqrt{2}}{2}(\underline{e}_1 \otimes \underline{e}_2 + \underline{e}_2 \otimes \underline{e}_1) \\ \underline{c}_3 = \frac{\sqrt{2}}{2}(\underline{e}_1 \otimes \underline{e}_3 + \underline{e}_3 \otimes \underline{e}_1) \\ \underline{c}_4 = \frac{\sqrt{2}}{2}(\underline{e}_2 \otimes \underline{e}_3 + \underline{e}_3 \otimes \underline{e}_2) \\ \underline{c}_5 = \frac{\sqrt{6}}{6}(\underline{e}_1 \otimes \underline{e}_1 + \underline{e}_2 \otimes \underline{e}_2 - 2\underline{e}_3 \otimes \underline{e}_3) \end{cases}$$

within this basis, \underline{h} can be rewritten as:

$$\{\underline{h}\}_{\mathcal{C}} = \sqrt{2}(h_1, h_2, h_3, h_4, \sqrt{3}h_5)_{\mathcal{C}}^T = (\bar{h}_1, \bar{h}_2, \bar{h}_3, \bar{h}_4, \bar{h}_5)_{\mathcal{C}}^T$$

Using this basis, the transformation of an element of \mathbb{H}^2 , i.e. $\mathbf{r}(\underline{e}_3, \theta)$, can thus be expressed as:

$$\begin{pmatrix} h_1^* \\ h_2^* \\ h_3^* \\ h_4^* \\ h_5^* \end{pmatrix}_{\mathcal{C}} = \begin{pmatrix} \cos(2\theta) & -\sin(2\theta) & 0 & 0 & 0 \\ \sin(2\theta) & \cos(2\theta) & 0 & 0 & 0 \\ 0 & 0 & \cos(\theta) & -\sin(\theta) & 0 \\ 0 & 0 & \sin(\theta) & \cos(\theta) & 0 \\ 0 & 0 & 0 & 0 & 1 \end{pmatrix}_{\mathcal{C}} \begin{pmatrix} \bar{h}_1 \\ \bar{h}_2 \\ \bar{h}_3 \\ \bar{h}_4 \\ \bar{h}_5 \end{pmatrix}_{\mathcal{C}}$$

The parametrization of $\underline{H} \in \mathbb{H}^4$ has received little attention in the mechanical community. We define a Kelvin basis $\mathcal{K} = \{\underline{k}_1^{(4)}, \underline{k}_2^{(4)}, \underline{k}_3^{(4)}, \underline{k}_4^{(4)}, \underline{k}_5^{(4)}, \underline{k}_6^{(4)}\}$ as follows:

$$\begin{cases} \underline{k}_1^{(2)} = \underline{e}_1 \otimes \underline{e}_1 \\ \underline{k}_2^{(2)} = \underline{e}_2 \otimes \underline{e}_2 \\ \underline{k}_3^{(2)} = \underline{e}_3 \otimes \underline{e}_3 \\ \underline{k}_4^{(2)} = \frac{\sqrt{2}}{2}(\underline{e}_2 \otimes \underline{e}_3 + \underline{e}_3 \otimes \underline{e}_2) \\ \underline{k}_5^{(2)} = \frac{\sqrt{2}}{2}(\underline{e}_1 \otimes \underline{e}_3 + \underline{e}_3 \otimes \underline{e}_1) \\ \underline{k}_6^{(2)} = \frac{\sqrt{2}}{2}(\underline{e}_1 \otimes \underline{e}_2 + \underline{e}_2 \otimes \underline{e}_1) \end{cases}$$

Based on it, a parametrization in Kelvin representation is proposed in [155]:

$$\begin{pmatrix} -H_8 - H_9 & H_9 & H_8 & \sqrt{2}(-H_5 - H_6) & \sqrt{2}H_2 & \sqrt{2}H_1 \\ * & -H_7 - H_9 & H_7 & \sqrt{2}H_5 & \sqrt{2}(-H_2 - H_4) & \sqrt{2}H_3 \\ * & * & -H_7 - H_8 & \sqrt{2}H_6 & \sqrt{2}H_4 & \sqrt{2}(-H_1 - H_3) \\ * & * & * & 2H_7 & 2(-H_1 - H_3) & 2(-H_2 - H_4) \\ * & * & * & * & 2H_8 & 2(-H_5 - H_6) \\ * & * & * & * & * & 2H_9 \end{pmatrix} \kappa$$

Remark. If we take the harmonic component H_1 for example, its basis is expressed as $\frac{\sqrt{2}}{2}(k_1^{(2)} \otimes k_6^{(2)} + k_6^{(2)} \otimes k_1^{(2)})$, we have:

$$\begin{aligned} & \frac{\sqrt{2}}{2}(k_1^{(2)} \otimes k_6^{(2)} + k_6^{(2)} \otimes k_1^{(2)}) \\ = & \frac{\sqrt{2}}{2} \left(\frac{\sqrt{2}}{2}(\underline{e}_1 \otimes \underline{e}_2 + \underline{e}_2 \otimes \underline{e}_1) \otimes (\underline{e}_1 \otimes \underline{e}_1) + \frac{\sqrt{2}}{2}(\underline{e}_1 \otimes \underline{e}_1) \otimes (\underline{e}_1 \otimes \underline{e}_2 + \underline{e}_2 \otimes \underline{e}_1) \right) \\ = & \frac{1}{2}(\underline{e}_1 \otimes \underline{e}_2 \otimes \underline{e}_1 \otimes \underline{e}_1 + \underline{e}_2 \otimes \underline{e}_1 \otimes \underline{e}_1 \otimes \underline{e}_1 + \underline{e}_1 \otimes \underline{e}_1 \otimes \underline{e}_1 \otimes \underline{e}_2 + \underline{e}_1 \otimes \underline{e}_1 \otimes \underline{e}_2 \otimes \underline{e}_1) \end{aligned}$$

It can be observed that it's totally symmetric.

6.2.2 Harmonic structure

In general, we can decompose any tensor space \mathbb{T}^n into harmonic spaces, and by grouping the same order harmonic tensor spaces we can obtain its harmonic structure (also called isotypic structure [75] in maths). The detailed information is given by the following proposition [156]:

Proposition 6.2. For any linear $\text{SO}(3)$ -representation of finite dimension (ρ_n, \mathbb{T}^n) , we have:

$$\mathbb{T}^n \simeq \bigoplus_{i=1}^q \mathbb{H}^{k_i}$$

with $k_i < +\infty$ and \simeq represents a $\text{SO}(3)$ -equivariant isomorphism. We can group together harmonic spaces of the same order and obtain its harmonic structure:

$$\mathbb{T}^n \simeq \bigoplus_{i=1}^m \alpha_i \mathbb{H}^{k_i}, \quad \alpha_i \mathbb{H}^{k_i} = \bigoplus_{l=1}^{\alpha_i} \mathbb{H}^{k_i} \quad (6.7)$$

the integer α_i indicates the multiplicity of \mathbb{H}^{k_i} .

To be more specific, for the case of $\mathbb{E}a$, as indicated at the very beginning of this section, the advantage of its harmonic structure lies in the ability to derive the set of symmetry classes of $\mathbb{E}a$. To this end, we are supposed to determine the α_i in Equation 6.7 for $\mathbb{E}a$. As illustrated by [67, 69, 107], it can be done by considering the tensor product of harmonic spaces and using Clebsch-Gordan formulas.

Lemma 6.2 (Clebsch-Gordan formulas). The product of 2 harmonic spaces are reducible and can decompose as:

$$\mathbb{H}^i \otimes \mathbb{H}^j = \bigoplus_{k=|i-j|}^{i+j} \mathbb{H}^k$$

In the case where the spaces are identical, the tensor product can be decomposed into a symmetrized product S^2 and an anti-symmetrized product Λ^2 :

Lemma 6.3 (Clebsch-Gordan formulas). *The product of 2 identical harmonic spaces is reducible and can decompose as:*

$$\forall n \geq 1, \mathbb{H}^n \otimes \mathbb{H}^n = S^2(\mathbb{H}^n) \oplus \Lambda^2(\mathbb{H}^n)$$

The definition of S^2 and Λ^2 is given [section 3.3](#). The previous formula can be completed by:

Lemma 6.4 (Clebsch-Gordan formulas). *For all $n \geq 1$, we have the following harmonic structures:*

$$S^2(\mathbb{H}^n) = \bigoplus_{k=0}^n \mathbb{H}^{2k}, \quad \Lambda^2(\mathbb{H}^n) = \bigoplus_{k=1}^n \mathbb{H}^{2k-1}$$

for $n = 0$, the previous formulas become $S^2(\mathbb{H}^0) = \mathbb{H}^0$ and $\Lambda^2(\mathbb{H}^0) = 0$.

Based on these lemmas, the harmonic structure of $\mathbb{E}la$ is provided:

Proposition 6.3. *The space $\mathbb{E}la$ has the following harmonic structure [[67](#), [69](#), [157](#)]:*

$$\mathbb{E}la \simeq 2\mathbb{H}^0 \oplus 2\mathbb{H}^2 \oplus \mathbb{H}^4$$

in which \simeq indicates $SO(3)$ -equivariant isomorphism.

Proof. $\mathbb{E}la$ can be seen as $S^2(S^2(\mathbb{R}^3))$:

$$\begin{aligned} \mathbb{E}la &\simeq S^2(S^2(\mathbb{R}^3)) \simeq S^2(S^2(\mathbb{H}^1)) \simeq S^2(\mathbb{H}^0 \oplus \mathbb{H}^2) \\ &\simeq S^2(\mathbb{H}^0) \oplus S^2(\mathbb{H}^2) \oplus (\mathbb{H}^0 \otimes \mathbb{H}^2) \\ &\simeq 2\mathbb{H}^0 \oplus 2\mathbb{H}^2 \oplus \mathbb{H}^4 \end{aligned}$$

□

Based on this harmonic structure, we can split any elasticity tensor $\mathbb{C} \underset{\approx}{\simeq}$ into an

- isotropic part defined by two scalars $\alpha, \beta \in \mathbb{H}^0$;
- anisotropic part with $\underset{\sim}{h}^a, \underset{\sim}{h}^b \in \mathbb{H}^2$ and $\underset{\cong}{H} \in \mathbb{H}^4$, for which $(\underset{\sim}{h}^a, \underset{\sim}{h}^b, \underset{\cong}{H})$ is called a harmonic triplet in \mathbb{R}^3 .

As already pointed out, the harmonic structure of a tensor space is sufficient to determine its symmetry classes [[5](#)], the result for $\mathbb{E}la$ is given in [section 6.3](#) by using clips operation [[156](#), [58](#)]. However, it does not provide an explicit construction of the decomposition. In what follows, this problem will be addressed.

It is important to recall that when the harmonic structure contains several spaces of the same order, its explicit decomposition is not uniquely defined (as mentioned in [section 2.3](#)). The knowledge of this non-unicity is important since many different harmonic decompositions are possible, and possess different physical meanings. These different physical content will be exploited for defining different exotic materials. In other words, it gives a mechanical interpretation of *hypersymmetry* mentioned in the definition of exotic materials.

For $\mathbb{E}la(2)$ case, the non-unicity concerns only the isotropic part. However, for $\mathbb{E}la(3)$, it involves both the isotropic and anisotropic parts and therefore is more complicated.

6.2.3 Explicit harmonic decompositions

Let us denote by f an explicit harmonic decomposition, each elasticity tensor $\mathbb{C} \in \mathbb{E}la$ can be written as:

$$\mathbb{C} \underset{\approx}{=} f(\alpha, \beta, \underset{\approx}{\mathbb{h}}^a, \underset{\approx}{\mathbb{h}}^b, \underset{\approx}{\mathbb{H}}) \quad (6.8)$$

The $SO(3)$ -equivariance property means:

$$\forall \mathbf{g} \in SO(3), \quad \mathbf{g} \star \mathbb{C} \underset{\approx}{=} f(\alpha, \beta, \mathbf{g} \star \underset{\approx}{\mathbb{h}}^a, \mathbf{g} \star \underset{\approx}{\mathbb{h}}^b, \mathbf{g} \star \underset{\approx}{\mathbb{H}})$$

Several explicit harmonic decompositions can be found in the literature [67, 69, 77, 5, 158]. We introduce here three of them [159]:

Generalized Lamé

This decomposition is the most classical one to be found in publications [77, 5], which can be considered as an anisotropic generalization of Lamé's isotropic parametrization by (λ, μ) ⁴. However, it has the disadvantages that the corresponding basis is not orthogonal, and it lacks physical content.

Proposition 6.4. *The tensor $\mathbb{C} \in \mathbb{E}la$ admits the uniquely defined Lamé harmonic decomposition*

$$\mathbb{C} \underset{\approx}{=} \alpha \underset{\approx}{1} \otimes \underset{\approx}{1} + \beta \underset{\approx}{1} \otimes \underset{\approx}{1} + 2(\underset{\approx}{\mathbb{h}}^a \otimes \underset{\approx}{1} + \underset{\approx}{1} \otimes \underset{\approx}{\mathbb{h}}^a) + (\underset{\approx}{\mathbb{h}}^b \otimes \underset{\approx}{1} + \underset{\approx}{1} \otimes \underset{\approx}{\mathbb{h}}^b) + \underset{\approx}{\mathbb{H}}$$

with \otimes the tensorial product defined as $(\mathbf{a} \otimes \mathbf{b})_{ijkl} = \frac{1}{2}(a_{ik}b_{jl} + a_{ij}b_{kl})$

It can be expressed in components:

$$C_{ijkl} = \alpha \delta_{ij} \delta_{kl} + \frac{\beta}{2} (\delta_{ik} \delta_{jl} + \delta_{il} \delta_{jk}) + (\delta_{ik} h_{jl}^a + \delta_{jl} h_{ik}^a + \delta_{il} h_{jk}^a + \delta_{jk} h_{il}^a) + (\delta_{ij} h_{kl}^b + \delta_{kl} h_{ij}^b) + H_{ijkl}$$

For isotropy, this generalized Lamé decomposition reduces to:

$$\mathbb{C} \underset{\approx}{=} \alpha \underset{\approx}{1} \otimes \underset{\approx}{1} + \beta \underset{\approx}{1} \otimes \underset{\approx}{1}$$

with $\alpha = \lambda$ and $\beta = 2\mu$.

Clebsch-Gordan

It is based on the spherical-deviatoric decomposition (the case for $\mathbb{E}la(2)$ is introduced in section 3.3). It is a generalisation of the Bulk-Shear modulus parameterization of isotropic tensors. A detailed construction of this decomposition is given below.

We decompose the space $S^2(\mathbb{R}^3)$ into a deviatoric space and a spherical space:

$$S^2(\mathbb{R}^3) \simeq \underbrace{\mathbb{H}^2}_{\text{Deviatoric space}} \oplus \underbrace{\mathbb{H}^0}_{\text{Spheric space}}$$

the projectors $\{\underset{\approx}{J}, \underset{\approx}{K}\}$ from $S^2(\mathbb{R}^3)$ onto \mathbb{H}^2 and \mathbb{H}^0 are defined in \mathbb{R}^3 as follows:

$$\underset{\approx}{K} = \frac{1}{3} \underset{\approx}{1} \otimes \underset{\approx}{1}, \quad \underset{\approx}{J} = \underset{\approx}{I} - \frac{1}{3} \underset{\approx}{1} \otimes \underset{\approx}{1}$$

⁴The shear modulus μ is denoted by G later when paired to the bulk modulus K .

with $(\mathbb{I})_{ijkl} = \frac{1}{2}(\delta_{ik}\delta_{jl} + \delta_{il}\delta_{jk})$. The projectors $\{\mathbb{J}, \mathbb{K}\}$ verify:

$$\underset{\approx}{\mathbb{J}} : \underset{\approx}{\mathbb{J}} = \underset{\approx}{\mathbb{J}} \quad \underset{\approx}{\mathbb{J}} : \underset{\approx}{\mathbb{K}} = \underset{\approx}{\mathbb{K}} : \underset{\approx}{\mathbb{J}} = \underset{\approx}{0} \quad \underset{\approx}{\mathbb{K}} : \underset{\approx}{\mathbb{K}} = \underset{\approx}{\mathbb{K}}$$

The elasticity tensor space $\mathbb{E}la$ is a symmetric linear application on $S^2(\mathbb{R}^3)$:

$$\mathbb{E}la \simeq \mathcal{L}^s(\mathbb{H}^2 \oplus \mathbb{H}^0) \simeq \mathcal{L}^s(\mathbb{H}^2) \oplus \mathcal{L}^s(\mathbb{H}^0, \mathbb{H}^2) \oplus \mathcal{L}^s(\mathbb{H}^0)$$

Hence, from a mechanical point of view, $\underset{\approx}{\mathbb{C}} \in \mathbb{E}la$ can be interpreted in blocks:

$$\begin{pmatrix} \underset{\approx}{\sigma}^d \\ \underset{\approx}{\sigma}^s \end{pmatrix} = \begin{pmatrix} \underset{\approx}{\mathbb{C}}^{dd} & \underset{\approx}{\mathbb{C}}^{ds} \\ \underset{\approx}{\mathbb{C}}^{sd} & \underset{\approx}{\mathbb{C}}^{ss} \end{pmatrix} \begin{pmatrix} \underset{\approx}{\varepsilon}^d \\ \underset{\approx}{\varepsilon}^s \end{pmatrix} \quad (6.9)$$

in which $\underset{\approx}{t}^s, \underset{\approx}{t}^d$ denote respectively the spheric and deviatoric part of $\underset{\approx}{t}$ and each tensor:

$$\underset{\approx}{\mathbb{C}}^{dd} \in \mathcal{L}^s(\mathbb{H}^2); \quad \underset{\approx}{\mathbb{C}}^{ds} \in \mathcal{L}(\mathbb{H}^0, \mathbb{H}^2); \quad \underset{\approx}{\mathbb{C}}^{ss} \in \mathcal{L}^s(\mathbb{H}^0)$$

Proposition 6.5. *The tensor $\underset{\approx}{\mathbb{C}} \in \mathbb{E}la$ admits the uniquely defined Clebsch-Gordan Harmonic Decomposition associated with the family of projectors $\{\mathbb{J}, \mathbb{K}\}$:*

$$\underset{\approx}{\mathbb{C}} = \alpha \underset{\approx}{\mathbb{J}} + \beta \underset{\approx}{\mathbb{K}} + \underset{\approx}{h}^a \boxtimes \underset{\approx}{1} + \frac{1}{3}(\underset{\approx}{h}^b \otimes \underset{\approx}{1} + \underset{\approx}{1} \otimes \underset{\approx}{h}^b) + \underset{\approx}{\mathbb{H}}, \quad (6.10)$$

in which $(\alpha, \beta, \underset{\approx}{h}^a, \underset{\approx}{h}^b, \underset{\approx}{\mathbb{H}}) \in \mathbb{H}^0 \times \mathbb{H}^0 \times \mathbb{H}^2 \times \mathbb{H}^2 \times \mathbb{H}^4$, the tensor $\underset{\approx}{h}^a$ belongs to \mathbb{H}^2 in $\mathcal{L}^s(\mathbb{H}^2)$ and $\underset{\approx}{h}^b$ is from $\mathcal{L}^s(\mathbb{H}^0, \mathbb{H}^2)$. \boxtimes is the special tensorial product defined as follows:

$$\underset{\approx}{a} \boxtimes \underset{\approx}{b} = \frac{1}{7}(-4(\underset{\approx}{a} \otimes \underset{\approx}{b} + \underset{\approx}{b} \otimes \underset{\approx}{a}) + 6(\underset{\approx}{a} \otimes \underset{\approx}{b} + \underset{\approx}{b} \otimes \underset{\approx}{a}))$$

Conversely, the different elements of the decomposition can be computed as a function of $\underset{\approx}{\mathbb{C}}$:

\mathbb{H}^0	\mathbb{H}^2	\mathbb{H}^4
$\beta = \frac{1}{3} \underset{\approx}{1} : \underset{\approx}{\mathbb{C}} : \underset{\approx}{1}$	$\underset{\approx}{h}^b = \underset{\approx}{\mathbb{J}} : \underset{\approx}{\mathbb{C}} : \underset{\approx}{1}$	
$\alpha = \frac{1}{5} \underset{\approx}{\mathbb{D}} :: \underset{\approx}{\mathbb{J}}$	$\underset{\approx}{h}^a = (\text{tr}_{13} \underset{\approx}{\mathbb{D}}) : \underset{\approx}{\mathbb{J}}$	$\underset{\approx}{\mathbb{H}} = \underset{\approx}{\mathbb{D}} - \underset{\approx}{h}^a \boxtimes \underset{\approx}{1} - \alpha \underset{\approx}{\mathbb{J}}$

in which $\underset{\approx}{\mathbb{D}} = \underset{\approx}{\mathbb{J}} : \underset{\approx}{\mathbb{C}} : \underset{\approx}{\mathbb{J}}$ is used to characterise the deviatoric linear elasticity.

The index form for special tensorial product defined as:

$$(\underset{\approx}{a} \boxtimes \underset{\approx}{b})_{ijkl} = \frac{1}{7}(3(a_{ik}b_{jl} + a_{il}b_{jk} + a_{jl}b_{ik} + a_{jk}b_{il}) - 4(a_{ij}b_{kl} + a_{kl}b_{ij}))$$

Thus, Equation 6.10 reads:

$$\begin{aligned} (\underset{\approx}{\mathbb{C}})_{ijkl} = & \frac{\alpha}{2}(\delta_{ik}\delta_{jl} + \delta_{il}\delta_{jk} - \frac{2}{3}\delta_{ij}\delta_{kl}) + \frac{\beta}{3}\delta_{ij}\delta_{kl} + \\ & \frac{3}{7}(h_{ik}^a\delta_{jl} + h_{il}^a\delta_{jk} + h_{jl}^a\delta_{ik} + h_{jk}^a\delta_{il} - \frac{4}{3}h_{ij}^a\delta_{kl} - \frac{4}{3}h_{kl}^a\delta_{ij}) + \\ & \frac{1}{3}(\delta_{ij}h_{kl}^b + \delta_{kl}h_{ij}^b) + \\ & H_{ijkl} \end{aligned}$$

With these definitions, Equation 6.9 can be interpreted by:

$$\begin{pmatrix} \underset{\sim}{\sigma}^d \\ \underset{\sim}{\sigma}^s \end{pmatrix} = \begin{pmatrix} \underset{\approx}{\mathbb{H}} + \underset{\sim}{h}^a \underset{\approx}{\mathbb{1}} + \alpha \underset{\approx}{\mathbb{J}} & \frac{1}{3} \underset{\sim}{h}^b \underset{\approx}{\mathbb{1}} \\ \frac{1}{3} \underset{\approx}{\mathbb{1}} \underset{\sim}{h}^b & \beta \underset{\approx}{\mathbb{K}} \end{pmatrix} \begin{pmatrix} \underset{\sim}{\varepsilon}^d \\ \underset{\sim}{\varepsilon}^s \end{pmatrix} \quad (6.11)$$

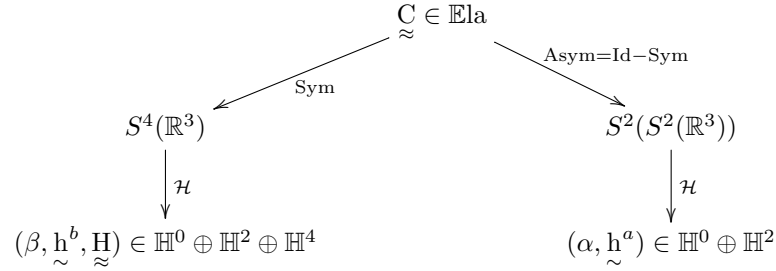
For isotropic elasticity tensor, the Clebsch-Gordan decomposition reduces to:

$$\underset{\approx}{\mathbb{C}} = \alpha \underset{\approx}{\mathbb{J}} + \beta \underset{\approx}{\mathbb{K}}$$

which corresponds to the Shear Modulus (G) and Bulk modulus (K) parameterization with $\alpha = 2G$ and $\beta = 3K$.

Schur-Weyl

This decomposition is based on the decomposition of the elasticity tensor into a complete symmetric (index symmetry) part and an asymmetric one, the corresponding spaces are orthogonal. The related work can be found in [67, 69]. The process is to first consider the decomposition of $\mathbb{E}la$ into $GL(3)$ -irreducible spaces, and then each space is decomposed to $SO(3)$ -irreducible spaces. It is summarized in the diagram as follows:



with Sym, Id and \mathcal{H} represent respectively: complete index symmetrization, identity and trace removal. The first layer of decomposition reads:

Lemma 6.5 ($GL(3)$ -irreducible decomposition of $\mathbb{E}la$). *The decomposition of $\mathbb{E}la$ into irreducible components under the action of $GL(3)$ is given by:*

$$\mathbb{E}la = S^4(\mathbb{R}^3) \oplus S^2(S^2(\mathbb{R}^3))$$

the elements $\underset{\approx}{\mathbb{S}} \in S^4(\mathbb{R}^3)$ and $\underset{\approx}{\mathbb{A}} \in S^2(S^2(\mathbb{R}^3))$ are defined by:

$$S_{ijkl} = \frac{1}{3}(C_{ijkl} + C_{ikjl} + C_{iljk}), \quad A_{ijkl} = \frac{1}{3}(2C_{ijkl} - C_{ikjl} - C_{iljk})$$

The completely symmetrical element $\underset{\approx}{\mathbb{S}}$ corresponds to the so-called *Cauchy elasticity* introduced in subsection 4.4.2. The asymmetrical element $\underset{\approx}{\mathbb{A}}$ verifies the relation:

$$A_{ijkl} + A_{iklj} + A_{iklj} = 0$$

Once this first layer of decomposition has been done, it remains now to decompose the space $S^4(\mathbb{R}^3)$ and $S^2(S^2(\mathbb{R}^3))$ into $SO(3)$ -irreducible spaces. To this end, an explicit harmonic decomposition is proposed as follows:

Proposition 6.6. *The tensor $\mathbb{C} \in \mathbb{E}la$ admits the uniquely defined Schur-Weyl harmonic decomposition:*

$$\mathbb{C} = \alpha \underset{\sim}{1} \otimes_{(2,2)} \underset{\sim}{1} + \beta \underset{\sim}{1} \otimes_{(4)} \underset{\sim}{1} + \mathfrak{h}^a \otimes_{(2,2)} \underset{\sim}{1} + \mathfrak{h}^b \otimes_{(4)} \underset{\sim}{1} + \mathbb{H} \quad (6.12)$$

in which $(\alpha, \beta, \mathfrak{h}^a, \mathfrak{h}^b, \mathbb{H}) \in \mathbb{H}^0 \times \mathbb{H}^0 \times \mathbb{H}^2 \times \mathbb{H}^2 \times \mathbb{H}^4$, the symmetrized tensor products $\otimes_{(4)}$ and $\otimes_{(2,2)}$ between two symmetric second-order tensors $(\underset{\sim}{t}_1, \underset{\sim}{t}_2)$ are defined as:

$$\begin{cases} \underset{\sim}{t}_1 \otimes_{(4)} \underset{\sim}{t}_2 = \frac{1}{6}(\underset{\sim}{t}_1 \otimes \underset{\sim}{t}_2 + \underset{\sim}{t}_2 \otimes \underset{\sim}{t}_1 + 2\underset{\sim}{t}_1 \overline{\otimes} \underset{\sim}{t}_2 + 2\underset{\sim}{t}_2 \overline{\otimes} \underset{\sim}{t}_1) \\ \underset{\sim}{t}_1 \otimes_{(2,2)} \underset{\sim}{t}_2 = \frac{1}{6}(2\underset{\sim}{t}_1 \otimes \underset{\sim}{t}_2 + 2\underset{\sim}{t}_2 \otimes \underset{\sim}{t}_1 - \underset{\sim}{t}_1 \overline{\otimes} \underset{\sim}{t}_2 - \underset{\sim}{t}_2 \overline{\otimes} \underset{\sim}{t}_1) \end{cases}$$

In terms of harmonic tensors, this gives us:

$$\begin{aligned} \mathbb{S} &= \beta \underset{\sim}{1} \otimes_{(4)} \underset{\sim}{1} + \mathfrak{h}^b \otimes_{(4)} \underset{\sim}{1} + \mathbb{H} \\ \mathbb{A} &= \alpha \underset{\sim}{1} \otimes_{(2,2)} \underset{\sim}{1} + \mathfrak{h}^a \otimes_{(2,2)} \underset{\sim}{1} \end{aligned}$$

This decomposition has a physical meaning with regard to the propagation of waves [160, 161], damage mechanics [162, 163, 164] and also used to define an exotic anisotropic material with isotropic Young's modulus as observed by He in [10] (see also the relevant work in [165]).

Note that this list of explicit harmonic decomposition is not exhaustive and other constructions can be proposed. Anyway, in what follows only the Clebsch-Gordan and Schur-Weyl decompositions will be considered (in the next chapter) for investigating 3D elastic exotic materials.

6.3 Symmetry classes of $\mathbb{E}la$

The symmetry classes of $\mathbb{E}la$ have been obtained for the first time by Vianello [5]. In this section, following the work of Olive [156, 58], we will use *clips operations* to retrieve this result. This approach combines the symmetry class of elementary harmonic tensors. These elementary results have been obtained by Irigh and Golubitsky in [166]. We start with the following results:

Theorem 6.1: Symmetry classes of \mathbb{H}^2 and \mathbb{H}^4

The symmetry classes of \mathbb{H}^2 are:

$$[\mathbb{D}_2], [\mathbb{O}(2)], [\mathbb{SO}(3)]$$

The symmetry classes of \mathbb{H}^4 are:

$$[1], [\mathbb{Z}_2], [\mathbb{D}_2], [\mathbb{D}_3], [\mathbb{D}_4], [\mathbb{O}(2)], [\mathcal{O}], [\mathbb{SO}(3)]$$

The above results can be combined using the clips products detailed in the table below.

Theorem 6.2: Clips operations between $SO(3)$ -closed subgroups

\odot	$[Z_n]$	$[D_n]$	$[\mathcal{T}]$	$[\mathcal{O}]$	$[\mathcal{Z}]$	$[SO(2)]$	$[O(2)]$
$[Z_m]$	$[1], [Z_d]$						
$[D_m]$	$[1], [Z_d]$ $[Z_{d_2}]$	$[1]$ $[Z_2], [Z_d]$ $[D_{dz}], [D_d]$					
$[\mathcal{T}]$	$[1]$ $[Z_{d_2}]$ $[Z_{d_3}]$	$[1], [Z_2]$ $[Z_{d_3}], [D_{d_2}]$	$[1], [Z_2]$ $[Z_3], [D_2]$ $[\mathcal{T}]$				
$[\mathcal{O}]$	$[1]$ $[Z_{d_2}]$ $[Z_{d_3}]$ $[Z_{d_4}]$	$[1], [Z_2]$ $[Z_{d_3}], [Z_{d_4}]$ $[D_{d_2}], [D_{d_3}]$ $[D_{d_4}]$	$[1], [Z_2]$ $[Z_3], [D_2]$ $[\mathcal{T}]$	$[1], [Z_2]$ $[Z_3], [Z_4]$ $[D_2], [D_3]$ $[D_4], [\mathcal{O}]$			
$[\mathcal{Z}]$	$[1]$ $[Z_{d_2}]$ $[Z_{d_3}]$ $[Z_{d_5}]$	$[1], [Z_2]$ $[Z_{d_3}], [Z_{d_5}]$ $[D_{d_2}], [D_{d_3}]$ $[D_{d_5}]$	$[1], [Z_2]$ $[Z_3], [\mathcal{T}]$	$[1], [Z_2]$ $[Z_3], [D_3]$ $[\mathcal{T}]$	$[1], [Z_2]$ $[Z_3], [Z_5]$ $[D_3], [D_5]$ $[\mathcal{Z}]$		
$[SO(2)]$	$[1], [Z_n]$	$[1], [Z_2]$ $[Z_n]$	$[1], [Z_2]$ $[Z_3]$	$[1], [Z_2]$ $[Z_3], [Z_4]$	$[1], [Z_2]$ $[Z_3], [Z_5]$	$[1]$ $[SO(2)]$	
$[O(2)]$	$[1], [Z_{d_2}]$ $[Z_n]$	$[1], [Z_2]$ $[D_{k_2}], [D_n]$	$[1], [Z_2]$ $[Z_3], [D_2]$	$[1], [Z_2]$ $[D_2], [D_3]$ $[D_4]$	$[1], [Z_2]$ $[D_2], [D_3]$ $[D_5]$	$[1], [Z_2]$ $[SO(2)]$	$[Z_2], [D_2]$ $[O(2)]$

Table 6.2: Clips operations for $SO(3)$

with the following notations:

$$\begin{aligned}
 d &:= \gcd(m, n), & d_2 &:= \gcd(n, 2), & k_2 &:= 3 - d_2, \\
 d_3 &:= \gcd(n, 3), & d_5 &:= \gcd(n, 5), \\
 dz &:= 2, \text{ if } m \text{ and } n \text{ even,} & dz &:= 1, \text{ otherwise,} \\
 d_4 &:= 4, \text{ if } 4 \text{ divide } n, & d_4 &:= 1, \text{ otherwise,} \\
 Z_1 = D_1 &:= 1
 \end{aligned}$$

The symmetry classes of $\mathbb{E}la$ can now be computed using the above theorems. We have:

Theorem 6.3: Strata of $\mathbb{E}la$

$\mathbb{E}la$ is partitioned into 8 strata [107] :

$$\mathbb{E}la = \Sigma_{[1]} \cup \Sigma_{[Z_2]} \cup \Sigma_{[D_2]} \cup \Sigma_{[D_3]} \cup \Sigma_{[D_4]} \cup \Sigma_{[O(2)]} \cup \Sigma_{[\mathcal{O}]} \cup \Sigma_{[SO(3)]} \quad (6.13)$$

Proof. As established above, the space of elasticity tensor is decomposed into harmonic spaces as follows:

$$\mathbb{E}la \simeq 2\mathbb{H}^0 \oplus 2\mathbb{H}^2 \oplus \mathbb{H}^4$$

The symmetry classes of the harmonic spaces are obtained by Theorem 6.1:

$$\begin{aligned}
 \mathfrak{I}(\mathbb{H}^2) &= \{[D_2], [O(2)], [SO(3)]\} \\
 \mathfrak{I}(\mathbb{H}^4) &= \{[1], [Z_2], [D_2], [D_3], [D_4], [O(2)], [\mathcal{O}], [SO(3)]\}
 \end{aligned}$$

Using the previous results and the clips operation table provided in Theorem 6.2, we compute iteratively:

$$\mathfrak{J}(\mathbb{H}^2 \oplus \mathbb{H}^2) = \mathfrak{J}(\mathbb{H}^2) \odot \mathfrak{J}(\mathbb{H}^2) = \{[1], [Z_2], [D_2], [O(2)], [SO(3)]\},$$

then

$$\mathfrak{J}(\mathbb{E}la) = \mathfrak{J}(\mathbb{H}^4) \odot \mathfrak{J}(\mathbb{H}^2 \oplus \mathbb{H}^2) = \{[1], [Z_2], [D_2], [D_3], [D_4], [O(2)], [O], [SO(3)]\}$$

Thus,

$$\mathbb{E}la = \Sigma_{[1]} \cup \Sigma_{[Z_2]} \cup \Sigma_{[D_2]} \cup \Sigma_{[D_3]} \cup \Sigma_{[D_4]} \cup \Sigma_{[O(2)]} \cup \Sigma_{[O]} \cup \Sigma_{[SO(3)]}$$

□

Remark. In mechanical terms, $\Sigma_{[1]}$ corresponds to the set of triclinic tensors, $\Sigma_{[Z_2]}$ to the set of monoclinic tensors, $\Sigma_{[D_2]}$ to the orthotropic tensors, $\Sigma_{[D_3]}$ to the set of trigonal tensors, $\Sigma_{[D_4]}$ to the set of tetragonal tensors, $\Sigma_{[O(2)]}$ to the set of transverse isotropic tensors, $\Sigma_{[O]}$ to the set of cubic tensors and $\Sigma_{[SO(3)]}$ to the set of isotropic tensors.

The transition between the different symmetry classes is (the number in parentheses indicates the dimensions of the corresponding fixed point spaces [76]):

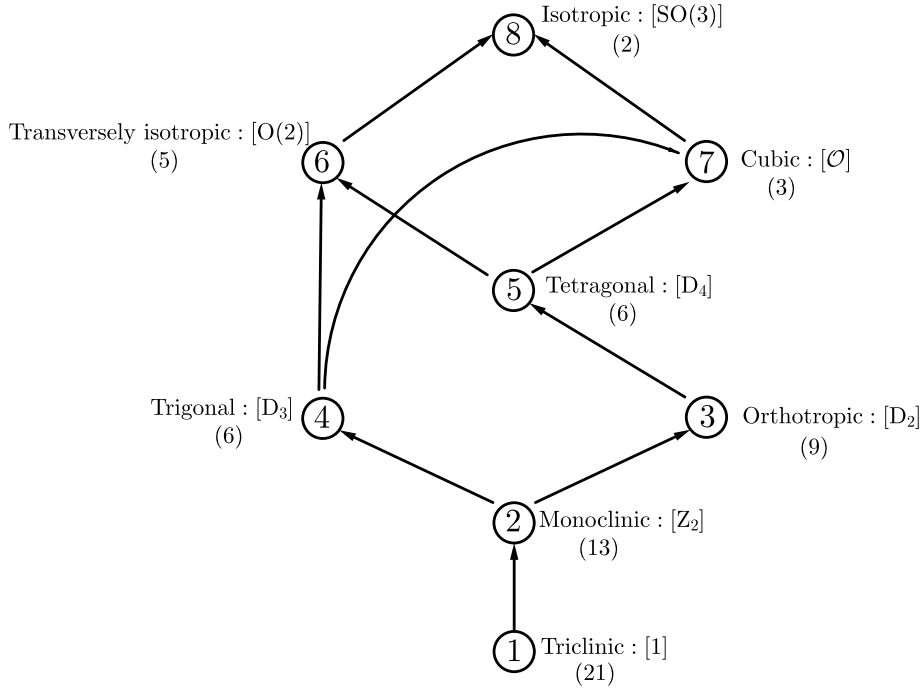


Figure 6.1: A complete structure of different symmetry classes of $\mathbb{E}la$

6.4 Condition of belonging to a symmetry class

Since the 8 symmetry classes have been obtained in Theorem 6.3, a natural question is now, given an elasticity tensor, how to determine its symmetry class? If the matrix of this tensor is expressed with a symmetry-adapted basis, e.g. in its normal form, the question is rather simple. But it turns out to be rather complicated if the matrix is expressed within a random basis.

This issue has been widely discussed in the literature and several approaches are proposed including:

- Spectral approach: it concerns the use of *Kelvin representation* of the elasticity tensor [61], which formulates sufficient conditions involving the multiplicity of the 6 eigenvalues of the Kelvin representation and of the eigenvalues of its eigenvectors;
- Maxwell multipoles: based on the harmonic decomposition of the elasticity tensor $\underset{\approx}{\mathbb{C}} = f(\alpha, \beta, \underset{\approx}{h}^a, \underset{\approx}{h}^b, \underset{\approx}{\mathbb{H}})$, this approach consists in decomposing a harmonic tensor of order n as a n -tuple vectors, and in this way to detect the different symmetries of $\underset{\approx}{\mathbb{C}}$ (see the relevant work in [67, 167]);
- Polynomial invariants relations: based on the harmonic decomposition of the elasticity tensor, this approach has been used to determine the symmetry class of $\underset{\approx}{\mathbb{C}}$ in \mathbb{R}^2 [75]. More recently, in [76], the authors have used polynomial relations between elements of the integrity basis to characterise the symmetry class of a fourth-order harmonic tensor $\underset{\approx}{\mathbb{H}} \in \mathbb{H}^4$.

We aim to extend the polynomial invariants approach for studying $\mathbb{E}la$ in \mathbb{R}^3 . However, it becomes far too complex, and to the best of the author’s knowledge, the determination of its symmetry classes using this approach has not been carried out in the literature. The limitation of this approach is explained as follows.

6.4.1 Polynomial invariants and their limitation

Our study for \mathbb{R}^2 case in section 3.5 and section 3.7 indicates that once the invariants of an elasticity tensor are available, it is possible to establish polynomial relations between them to characterise its symmetry class. However, it should be noted that the number of invariants constituting the integrity basis and their degrees are very large in \mathbb{R}^3 (we have 294 invariants in total). This makes it almost impossible to extend the approach from \mathbb{R}^2 to \mathbb{R}^3 .

To understand the question of the large number of invariants for 3D elasticity, several things need to be clarified.

Functional basis VS. integrity basis: strictly speaking, if we need to separate orbits, i.e. give different names to different elastic materials, what we need is a separating basis. In mechanics, such a basis is called a functional basis. The definition of functional basis can be found in section 2.5. The determination of such a basis is a geometric problem and there is currently no algorithm for simply finding such a basis. Instead, we determine an integrity basis, i.e. a basis of the algebra of G-invariant polynomials, which we know how to formulate and solve. Besides, any minimal integrity basis constitutes a functional basis that is not necessarily minimal. Thus, the cardinal of the system will be higher than the minimal number of invariants ensuring separation.

Singularity problem VS. overall problem: since our objective is to identify the different symmetry classes of $\mathbb{E}la$, to this end, from a geometrical point of view, finding the separators for a given tensor space means finding a set of quantities that allow the elasticity tensor to be reconstructed in all possible symmetry classes. It is this all that leads to the explosion of the problem, a point well detailed in a publication by Smith in the case of a simpler situation [168]. To well understand the underlying mechanism of this complexity, we recall in Figure 6.2 the illustration of the partition of tensor space with respect to their symmetry classes: Since $[\mathbb{H}_2]$ is more symmetric than $[\mathbb{H}_1]$, additional invariants are required to impose more restrictive conditions on $[\mathbb{H}_2]$. Thus, a separating set used to separate the orbits of symmetry class $[\mathbb{H}_1]$ is supposed to be the subset of the separating set for that of symmetry class $[\mathbb{H}_2]$.

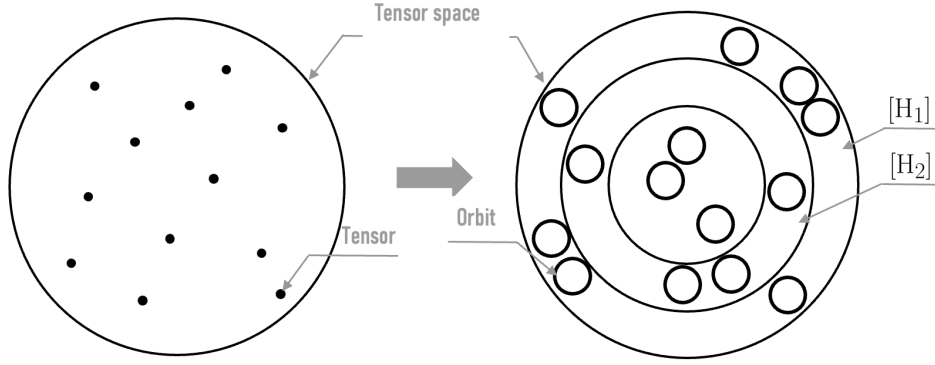


Figure 6.2: Illustration of the partition of tensor space with respect to their symmetry classes

If the elasticity tensor is generic, i.e. absolutely arbitrary with no cancellation or 'alignment' of the elements of its harmonic decomposition, then we need 18 quantities⁵. It should be noted here that generic is even more restrictive than triclinic because special triclinics can be defined (More details of this observation can be found in the beginning of [chapter 7](#)). However, these 18 quantities are not enough, because if a harmonic component is zero, I would need a Plan B to ensure reconstruction. A system of minimal separators is a system that provides for all backup plans. The analysis of inverse clips carried out in [chapter 7](#) shows that we can already count around 170 degenerate configurations of the triplet $(\tilde{h}^a, \tilde{h}^b, \tilde{H})$. The minimal number of separators is necessarily very high.

Recall the harmonic structure of $\mathbb{E}la$:

$$\mathbb{E}la \simeq 2\mathbb{H}^0 \oplus 2\mathbb{H}^2 \oplus \mathbb{H}^4$$

from this collection of harmonic spaces, we can define two types of invariants:

- **Proper invariants:** They characterise each covariant of the harmonic decomposition separately, which can be seen as norms. For $\mathbb{E}la$, we have 15 proper invariants in total: one invariant for each space \mathbb{H}^0 , 2 for each space \mathbb{H}^4 (that would be $\{\text{tr}(\tilde{h}^a)^2, \text{tr}(\tilde{h}^a)^3, \text{tr}(\tilde{h}^b)^2, \text{tr}(\tilde{h}^b)^3\}$) and 9 for space \mathbb{H}^4 (listed in [\[169\]](#), Equation 5.1);
- **Joint invariants:** They include different covariants of the harmonic decomposition. These quantities can be seen as evaluating the relative 'orientation' of the different covariants. For $\mathbb{E}la$, the joint invariants are obtained from the couples of $\mathbb{H}^2 \oplus \mathbb{H}^2$ and two $\mathbb{H}^2 \oplus \mathbb{H}^4$, as well as the triplet $\mathbb{H}^2 \oplus \mathbb{H}^2 \oplus \mathbb{H}^4$. We have 279 joint invariants in total.

The determination of integrity basis involves not only the proper invariants but also the joint ones. The joint invariants of $\mathbb{H}^2 \oplus \mathbb{H}^2$ has been analysed by Boehler [\[77\]](#). The most challenging aspect is to determine the joint invariants implied by \mathbb{H}^4 , i.e. $\mathbb{H}^2 \oplus \mathbb{H}^4$ and $\mathbb{H}^2 \oplus \mathbb{H}^2 \oplus \mathbb{H}^4$. Before my Ph.D. study, this issue was addressed by the collaboration work between N. Auffray and mathematicians B. Kolev and M. Olive and a computer scientist M. Petitot, from which M. Olive has determined a minimal integrity basis for elasticity tensor in [\[78\]](#):

⁵The strata dimension of $\mathbb{E}la$ 21 minus the 3 parameters of $SO(3)$ gives the orbit dimension of $\mathbb{E}la/SO(3)$, which is 18.

Theorem 6.4: Integrity basis for $\mathbb{E}a$

The minimum integrity basis of the $\mathbb{E}a$ for the $SO(3)$ -action consists of 294 elements. The number, type and degree of these elements are summarized in the following table:

degree	\mathbb{H}^0	\mathbb{H}^2	\mathbb{H}^4	$\mathbb{H}^2 \oplus \mathbb{H}^2$	$\mathbb{H}^2 \oplus \mathbb{H}^4$	$\mathbb{H}^2 \oplus \mathbb{H}^2 \oplus \mathbb{H}^4$	Σ
1	1						2
2		1	1	1			4
3		1	1	2	2	1	10
4			1	1	4	6	16
5			1		7	18	33
6			1		10	36	57
7			1		11	53	76
8			1		10	45	66
9			1		5	10	21
10			1		2	2	7
11					1		2
Total	2×1	2×2	9	4	2×52	171	294

Remark. It should be noted that this basis is minimal for the polynomial invariant algebra of $\mathbb{E}a$, the result for functional basis (algebraically independent) can be further reduced.

This result closes the question posed previously, i.e. the integrity basis to separate the orbit space $\mathbb{E}a/SO(3)$. However, the obtained basis is of more academic than practical interest. To be able to build conditions of belonging to a symmetry class, we will refer to another strategy via covariants formulations [78].

6.4.2 Covariants: a geometric path

In this section, following the recent work of M. Olive et al. in [78], a definitive answer to the classification problem for $\mathbb{E}a$ will be given, using covariants instead of invariants.

We give a brief definition of covariant as follows [78]. A more general and abstract definition of this concept can be found in [170].

6.4.1 Definition (Covariant)

Let V and W be finite-dimensional representations of a group G . The covariant algebra of V of type W , noted $Cov(V, W)$, is defined as the invariant algebra

$$Cov(V, W) := \mathbb{R}[V \oplus W^*]^G,$$

where W^* is the linear application of W .

In our case, we will consider $G = SO(3)$ with $V = \mathbb{E}a$ and $W = \mathbb{R}^3$. Based on the harmonic decomposition, the linear application of \mathbb{R}^3 is of type $S^n(\mathbb{R}^3)$. Thus, the covariant algebra of $\mathbb{E}a$ of type \mathbb{R}^3 is defined as:

$$Cov(\mathbb{E}a, \mathbb{R}^3) := \mathbb{R}[\mathbb{E}a \oplus S^n(\mathbb{R}^3)]^{SO(3)}$$

in the following content, since there is no ambiguity on covariant algebra type (always \mathbb{R}^3) and we want

to clarify the order of polynomial covariants, the notion $\text{Cov}(\mathbb{E}la, \mathbb{R}^3)$ will be rewritten as $\text{Cov}_n(\mathbb{E}la)$.

Remark. *The polynomial covariants of $\mathbb{E}la$ of order $n = 0$ can be considered as its invariants.*

Any polynomial covariant $p(\underset{\approx}{\mathbb{C}}) \in \text{Cov}_n(\mathbb{E}la)$ of $\underset{\approx}{\mathbb{C}} \in \mathbb{E}la$ is $\text{SO}(3)$ -equivariant:

$$p(\mathbf{g} \star \underset{\approx}{\mathbb{C}}) = \mathbf{g} \star p(\underset{\approx}{\mathbb{C}}), \quad \forall \underset{\approx}{\mathbb{C}} \in \mathbb{E}la, \mathbf{g} \in \text{SO}(3)$$

It can be seen that the five harmonic components $\alpha, \beta, \underset{\approx}{h}^a, \underset{\approx}{h}^b, \underset{\approx}{H}$ are covariants of $\underset{\approx}{\mathbb{C}}$, with respectively:

- $\alpha, \beta \in \text{Cov}_0(\mathbb{E}la)$, they are invariants of $\underset{\approx}{\mathbb{C}}$
- $\underset{\approx}{h}^a, \underset{\approx}{h}^b \in \text{Cov}_2(\mathbb{E}la)$
- $\underset{\approx}{H} \in \text{Cov}_4(\mathbb{E}la)$

It should be noted that the characterisation of the symmetry classes by covariants is independent of the choice of an explicit harmonic decomposition. Apart from the three covariants $\{\underset{\approx}{h}^a, \underset{\approx}{h}^b, \underset{\approx}{H}\}$ of $\underset{\approx}{\mathbb{C}}$, the following covariants will be used (an explicit list of covariants has been computed in [[78], Table2]) to characterise the symmetry classes of elasticity tensors :

$$\underset{\approx}{d}_2 := \text{tr}_{13}\underset{\approx}{H}^2, \quad \underset{\approx}{d}_3 := \text{tr}_{13}\underset{\approx}{H}^3, \quad \underset{\approx}{c}_k := \underset{\approx}{H}^{k-2} : \underset{\approx}{d}_2, \quad k \geq 3$$

where $\underset{\approx}{H}^n := \underset{\approx}{H} : \underset{\approx}{H}^{n-1}$ for $n \geq 2$ and $\text{tr}_{13}\underset{\approx}{A}$ is defined in orthonormal basis as $(\text{tr}_{13}\underset{\approx}{A})_{ij} := (\underset{\approx}{A})_{kikj}$. We will also use the simplified notation $\underset{\approx}{a} \underset{\approx}{b} := \underset{\approx}{a} \cdot \underset{\approx}{b}$ and let $\underset{\approx}{a}^d$ be the deviatoric part of $\underset{\approx}{a}$. The quadratic covariant $\underset{\approx}{d}_2$ was first introduced in [77] and plays an important role in the classification of the fourth-order harmonic tensor (Appendix C).

The symmetry class of an elasticity tensor is thus characterised by polynomial equations involving its covariants. From the mechanical point of view, these polynomial equations provide necessary and sufficient conditions for membership in each of the eight symmetry classes. Based on the harmonic decomposition, the advantage of using covariants-based criteria is that they are particularly simple. One merely needs to verify the vanishing of certain polynomial functions defined on the harmonic components of the elasticity tensor. It offers a more geometric perspective rather than relying solely on complex algebraic equation systems.

6.4.3 Covariant-based membership relations

Let's start by introducing a few operations on tensors.

6.4.2 Definition (Symmetric tensor product)

The symmetry tensor product between two tensors $\mathbb{T}^{(p)} \in \mathbb{T}^p(\mathbb{R}^3)$ and $\mathbb{T}^{(q)} \in \mathbb{T}^q(\mathbb{R}^3)$ is defined as

$$\mathbb{T}^{(p)} \odot \mathbb{T}^{(q)} := (\mathbb{T}^{(p)} \otimes \mathbb{T}^{(q)})^s \in S^{p+q}(\mathbb{R}^3)$$

The total symmetrisation of a tensor $\mathbb{T} \in \mathbb{T}^n(\mathbb{R}^3)$, noted $\mathbb{T}^s \in S^n(\mathbb{R}^3)$ is defined as:

$$T_{i_1 i_2 \dots i_n}^s := \frac{1}{n!} \sum_{\sigma \in G_n} T_{i_{\sigma(1)} i_{\sigma(2)} \dots i_{\sigma(n)}}$$

with σ the permutation of the letters $\{1, 2, \dots, n\}$ and G_n is the corresponding symmetric group on n letters.

6.4.3 Definition (Generalised cross product)

The generalised cross product between two totally symmetric tensors $\mathbb{T}^{(p)} \in S^p(\mathbb{R}^3)$ and $\mathbb{T}^{(q)} \in S^q(\mathbb{R}^3)$ is defined as

$$\mathbb{T}^{(p)} \times \mathbb{T}^{(q)} := -(\mathbb{T}^{(p)} \cdot \underline{\varepsilon} \cdot \mathbb{T}^{(q)})^s \in S^{p+q-1}(\mathbb{R}^3).$$

where $\underline{\varepsilon}$ is the Levi-Civita tensor. On any orthonormal basis, we get

$$(\mathbb{T}^{(p)} \times \mathbb{T}^{(q)})_{i_1 \dots i_{p+q-1}} := ((\underline{\varepsilon})_{i_1 j k} \mathbb{T}_{j i_2 \dots i_p}^{(p)} \mathbb{T}_{k i_{p+1} \dots i_{p+q-1}}^{(q)})^s$$

Note first that the symmetry class of $\underline{\underline{\mathbb{C}}}$ is the same as the symmetry class of the triplet $(\underline{\underline{\mathbb{h}}^a}, \underline{\underline{\mathbb{h}}^b}, \underline{\underline{\mathbb{H}}})$. The covariants used to characterise the symmetry classes of an elasticity tensor are:

$$\{\underline{\underline{\mathbb{h}}^a}, \underline{\underline{\mathbb{h}}^b}, \underline{\underline{\mathbb{H}}}, \underline{\underline{\mathbb{d}}_2}, \underline{\underline{\mathbb{d}}_3}, \underline{\underline{\mathbb{c}}_3}, \underline{\underline{\mathbb{c}}_4}\}$$

The following theorem has been proved in [78]:

Theorem 6.5: Characterisation of the symmetry class of $\underline{\underline{\mathbb{C}}} \in \mathbb{E}la$

Let $\underline{\underline{\mathbb{C}}} = f(\alpha, \beta, \underline{\underline{\mathbb{h}}^a}, \underline{\underline{\mathbb{h}}^b}, \underline{\underline{\mathbb{H}}}) \in \mathbb{E}la$ be an harmonic decomposition of an elasticity tensor $\underline{\underline{\mathbb{C}}}$, where α, β are scalars, $\underline{\underline{\mathbb{h}}^a}, \underline{\underline{\mathbb{h}}^b} \in \mathbb{H}^2$ and $\underline{\underline{\mathbb{H}}} \in \mathbb{H}^4$. Then,

1. $\underline{\underline{\mathbb{C}}} \in \Sigma_{[SO(3)]}$ if and only if $\underline{\underline{\mathbb{h}}^a} = \underline{\underline{\mathbb{h}}^b} = \underline{\underline{\mathbb{d}}_2} = 0$.
2. $\underline{\underline{\mathbb{C}}} \in \Sigma_{[O]}$ if and only if $\underline{\underline{\mathbb{h}}^a} = \underline{\underline{\mathbb{h}}^b} = \underline{\underline{\mathbb{d}}_2^d} = 0$ and $\underline{\underline{\mathbb{d}}_2} \neq 0$.
3. $\underline{\underline{\mathbb{C}}} \in \Sigma_{[O(2)]}$ if and only if $(\underline{\underline{\mathbb{h}}^a}, \underline{\underline{\mathbb{h}}^b}, \underline{\underline{\mathbb{d}}_2})$ is transversely isotropic and

$$\underline{\underline{\mathbb{H}}} \times \underline{\underline{\mathbb{h}}^a} = \underline{\underline{\mathbb{H}}} \times \underline{\underline{\mathbb{h}}^b} = \underline{\underline{\mathbb{H}}} \times \underline{\underline{\mathbb{d}}_2} = 0.$$

4. $\underline{\underline{\mathbb{C}}} \in \Sigma_{[D_4]}$ if and only if $(\underline{\underline{\mathbb{h}}^a}, \underline{\underline{\mathbb{h}}^b}, \underline{\underline{\mathbb{d}}_2})$ is transversely isotropic and

$$\text{tr}(\underline{\underline{\mathbb{H}}} \times \underline{\underline{\mathbb{h}}^a}) = \text{tr}(\underline{\underline{\mathbb{H}}} \times \underline{\underline{\mathbb{h}}^b}) = \text{tr}(\underline{\underline{\mathbb{H}}} \times \underline{\underline{\mathbb{d}}_2}) = 0,$$

and

$$\underline{\underline{\mathbb{H}}} \times \underline{\underline{\mathbb{h}}^a} \neq 0 \quad \text{or} \quad \underline{\underline{\mathbb{H}}} \times \underline{\underline{\mathbb{h}}^b} \neq 0 \quad \text{or} \quad \underline{\underline{\mathbb{H}}} \times \underline{\underline{\mathbb{d}}_2} \neq 0.$$

5. $\underline{\underline{\mathbb{C}}} \in \Sigma_{[D_3]}$ if and only if $(\underline{\underline{\mathbb{h}}^a}, \underline{\underline{\mathbb{h}}^b}, \underline{\underline{\mathbb{d}}_2})$ is transversely isotropic and

$$\underline{\underline{\mathbb{h}}^a} \times (\underline{\underline{\mathbb{H}}} : \underline{\underline{\mathbb{h}}^a}) = \underline{\underline{\mathbb{h}}^b} \times (\underline{\underline{\mathbb{H}}} : \underline{\underline{\mathbb{h}}^b}) = \underline{\underline{\mathbb{d}}_2} \times (\underline{\underline{\mathbb{H}}} : \underline{\underline{\mathbb{d}}_2}) = 0,$$

and

$$\text{tr}(\underline{\underline{\mathbb{H}}} \times \underline{\underline{\mathbb{h}}^a}) \neq 0 \quad \text{or} \quad \text{tr}(\underline{\underline{\mathbb{H}}} \times \underline{\underline{\mathbb{h}}^b}) \neq 0 \quad \text{or} \quad \text{tr}(\underline{\underline{\mathbb{H}}} \times \underline{\underline{\mathbb{d}}_2}) \neq 0.$$

6. $\underline{\underline{\mathbb{C}}} \in \Sigma_{[D_2]}$ if and only if the family of second-order tensors \mathcal{F}_o is orthotropic.

$$\mathcal{F}_o = \{\underline{\underline{\mathbb{h}}^a}, \underline{\underline{\mathbb{h}}^b}, \underline{\underline{\mathbb{d}}_2}, \underline{\underline{\mathbb{c}}_3}, \underline{\underline{\mathbb{c}}_4}, \underline{\underline{\mathbb{H}}} : \underline{\underline{\mathbb{h}}^a}, \underline{\underline{\mathbb{H}}} : \underline{\underline{\mathbb{h}}^b}, \underline{\underline{\mathbb{H}}} : (\underline{\underline{\mathbb{h}}^a})^2, \underline{\underline{\mathbb{H}}} : (\underline{\underline{\mathbb{h}}^b})^2\}$$

7. $\underline{\underline{\mathbb{C}}} \in \Sigma_{[Z_2]}$ if and only if the family of second-order tensors \mathcal{F}_m is monoclinic.

$$\mathcal{F}_m = \{\underline{\underline{\mathbb{h}}^a}, \underline{\underline{\mathbb{h}}^b}, \underline{\underline{\mathbb{d}}_2}, \underline{\underline{\mathbb{c}}_3}, \underline{\underline{\mathbb{c}}_4}, \underline{\underline{\mathbb{H}}} : \underline{\underline{\mathbb{h}}^a}, \underline{\underline{\mathbb{H}}} : \underline{\underline{\mathbb{h}}^b}, \underline{\underline{\mathbb{H}}} : (\underline{\underline{\mathbb{h}}^a})^2, \underline{\underline{\mathbb{H}}} : (\underline{\underline{\mathbb{h}}^b})^2, \underline{\underline{\mathbb{H}}} : (\underline{\underline{\mathbb{h}}^a} \underline{\underline{\mathbb{h}}^b})^s, \underline{\underline{\mathbb{H}}} : (\underline{\underline{\mathbb{h}}^a} \underline{\underline{\mathbb{d}}_2})^s, \underline{\underline{\mathbb{H}}} : (\underline{\underline{\mathbb{h}}^b} \underline{\underline{\mathbb{d}}_2})^s\}$$

8. $\underline{\underline{\mathbb{C}}} \in \Sigma_{[1]}$ if and only if none of the preceding conditions hold.

This theorem is completed by the following remarks:

Remark.

1. If \mathbb{C}_{\approx} is transversely isotropic, tetragonal or trigonal then the triplet $(\mathfrak{h}^a, \mathfrak{h}^b, \mathfrak{d}_2)$ is transversely isotropic. The explicit covariant conditions for $(\mathfrak{h}^a, \mathfrak{h}^b, \mathfrak{d}_2)$ to be of this symmetry class is provided in Theorem C.1;
2. The explicit covariant conditions on the finite family $\mathcal{F}_o, \mathcal{F}_m$ to characterise the corresponding symmetry classes are given in Theorem C.1;
3. Covariant conditions of transitions from one symmetry class to another (as is done for 2D case in Equation 3.16) are not yet completely obtained.

The corresponding harmonic representation for these 8 situations is shown below:

Table 6.3: Polynomial conditions for membership of an open stratum

stratum	Covariant conditions	Tensor representations
$\Sigma_{[1]}$	Condition 8 (in Theorem 6.5)	$(\alpha, \beta, \mathfrak{h}^a, \mathfrak{h}^b, \mathbb{H})$
$\Sigma_{[Z_2]}$	Condition 7	
$\Sigma_{[D_2]}$	Condition 6	
$\Sigma_{[D_3]}$	Condition 5	
$\Sigma_{[D_4]}$	Condition 4	
$\Sigma_{[O(2)]}$	Condition 3	
$\Sigma_{[O]}$	Condition 2	$(\alpha, \beta, 0, 0, \mathbb{H})$
$\Sigma_{[SO(3)]}$	Condition 1	$(\alpha, \beta, 0, 0, 0)$

From the point of view of the tensor representations, it can be observed that not all types of tensor representations are included, for instance, $(\alpha, \beta, \mathfrak{h}^a, \mathfrak{h}^b, 0)$ and $(\alpha, \beta, 0, \mathfrak{h}^b, \mathbb{H})$ are not listed, which are considered as the exotic sets beyond symmetry classes. Besides these, there exist plenty of other exotic possibilities, which will be detailed in chapter 7.

We will introduce in the next chapter several examples of exotic sets, which are mainly obtained from the explicit decompositions in subsection 6.2.3 and based on it, their characterization by covariants conditions will also be discussed.

Chapter 7

3D exotic sets

7.1	Exotic sets of $\mathbb{E}la(3)$	106
7.1.1	Clips operation for $\mathbb{E}la(3)$	107
7.1.2	Determination of exotic sets	109
7.2	Covariants conditions for exotic sets	112
7.3	Exotic elastic materials	117
7.3.1	R_0 -orthotropy in \mathbb{R}^3	117
7.3.2	Triclinic exotic elastic material	121
7.3.3	Anisotropic materials with isotropic Young's modulus	123

In this chapter, inspired by the determination of exotic sets in \mathbb{R}^2 , we will revisit the same topic in \mathbb{R}^3 . The situation will be more intricate, as what could be simplified in a 2D context now requires careful consideration within a 3D problem. In this way, it provides a more general framework for studying exotic sets of other constitutive laws. We start by clips operations in [section 7.1](#) along with the determination of a complete list of exotic sets for $\mathbb{E}la(3)$. These exotic sets are then identified by polynomial covariant conditions in [section 7.2](#). Among all the exotic possibilities, three of them are discussed in [section 7.3](#) along with some mechanical interpretations.

7.1 Exotic sets of $\mathbb{E}la(3)$

It is known that the symmetry class $[G]$ of $\mathbb{C} \in \mathbb{E}la$ can be seen as the symmetry class of its harmonic bouquet $(\underset{\sim}{h}^a, \underset{\sim}{h}^b, \underset{\approx}{H})$ [[78], Section 6], in which $([G_1]_{\underset{\sim}{h}^a}, [G_2]_{\underset{\sim}{h}^b}, [G_3]_{\underset{\approx}{H}})$ denotes the corresponding symmetry classes of its components. Here, the notation $[G]_X$ indicates the symmetry class of X . A careful analysis reveals that the symmetry class $[G]$ of $\mathbb{E}la$ is not uniquely obtained, such diversity comes from two aspects of consideration:

- **Aspect I:** For a given symmetry class $[G]$, the symmetry classes of individual components, that is $([G_1]_{\underset{\sim}{h}^a}, [G_2]_{\underset{\sim}{h}^b}, [G_3]_{\underset{\approx}{H}})$, is not necessarily unique.
- **Aspect II:** For a given triplet $([G_1]_{\underset{\sim}{h}^a}, [G_2]_{\underset{\sim}{h}^b}, [G_3]_{\underset{\approx}{H}})$, the underlying symmetry classes of coupled components, that is $([G_4]_{(\underset{\sim}{h}^a, \underset{\sim}{h}^b)}, [G_5]_{(\underset{\sim}{h}^a, \underset{\approx}{H})}, [G_6]_{(\underset{\sim}{h}^b, \underset{\approx}{H})})$, is not necessarily unique.

These two aspects of the "not necessarily unique" phenomenon constitute the fundamental basis of what we call *exotic materials*. The definition of exotic materials is recalled here :

7.1.1 Definition (Exotic materials)

An elasticity material will be said to be *exotic*, provided

1. **Specific design:** it satisfies constraints independent of those that may be imposed by symmetry arguments;
2. **Hypersymmetric:** its behavior appears to be more symmetrical than that imposed by the material symmetries.

To summarise, we say that the harmonic bouquet $(\underset{\sim}{h}^a, \underset{\sim}{h}^b, \underset{\approx}{H})$ being of type:

$$([G_1]_{\underset{\sim}{h}^a}, [G_2]_{\underset{\sim}{h}^b}, [G_3]_{\underset{\approx}{H}}, [G_4]_{(\underset{\sim}{h}^a, \underset{\sim}{h}^b)}, [G_5]_{(\underset{\sim}{h}^a, \underset{\approx}{H})}, [G_6]_{(\underset{\sim}{h}^b, \underset{\approx}{H})}) \quad (7.1)$$

Following what introduced previously, this harmonic bouquet type is not necessarily unique to determine the symmetry class $[G]$ of $(\underset{\sim}{h}^a, \underset{\sim}{h}^b, \underset{\approx}{H})$, meaning that the corresponding strata of $[G]$, denoted by $\Sigma_{[G]}$ can be partitioned into different subsets accordingly. Besides, among all the subsets of $\Sigma_{[G]}$, the corresponding subsets for exotic materials will be referred to as *exotic sets*, denoted by $\Sigma_{[G]}^e$, and the others are called *generic sets* denoted by $\Sigma_{[G]}^g$. We have:

$$\Sigma_{[G]} = \Sigma_{[G]}^g \cup \Sigma_{[G]}^e$$

Unlike the 2D case that there is just one exotic set, it should be noted that in 3D case, for a given $[G]$, $\Sigma_{[G]}^e$ is not always unique. We have:

$$\Sigma_{[G]}^e = \bigcup_{i \in N} \Sigma_{[G]}^{e_i}$$

To simplify the upcoming expressions, a symmetry class $[G]$ with its corresponding stratum of type $\Sigma_{[G]}^g$ will be referred to as *generic*, and *exotic* otherwise. The associated notations are clarified as follows:

	generic	exotic
$\Sigma_{[G]}$	generic sets: $\Sigma_{[G]}^g$	exotic sets: $\Sigma_{[G]}^e$
materials	-	exotic materials

The previous initial observations indicate the richness of elasticity tensor space, it is not only dominated by 8 symmetry classes but also by intermediate possibilities (referred to as exotic) beyond symmetry classes. The objectif of this chapter is to determine all these exotic sets of $\mathbb{E}la$ and, through some examples, to investigate the underlying mechanical properties which make them being *hypersymmetric*.

Remark. *We consider a symmetry class $[G]$ as exotic based on the observation that, for some sollicitations, its linear elasticity behaves more symmetric than its ground symmetry class. Be careful that in this process, we do not create any new symmetry classes. There are only 8 symmetry classes of $\mathbb{E}la$ and all $\mathbb{C} \in \mathbb{E}la$ possess one symmetry class among these 8 possibilities.*

Thus, to determine the exotic sets of $\mathbb{E}la$, we will reproduce the clips operation between $\mathcal{J}(\mathbb{H}^4)$, $\mathcal{J}(\mathbb{H}^2)$ and $\mathcal{J}(\mathbb{H}^2)$ with fully taking into account the intermediate results of clips product between coupled harmonic components. A natural successive step is to identify these obtained exotic sets by polynomial covariant conditions. The polynomial conditions stated in Theorem 6.2 serve solely to determine the membership to symmetry class within the 8 distinct symmetry classes of $\mathbb{E}la$. They do not possess the ability to differentiate between generic and exotic. To deal with all these issues, a three-step process is proposed as below :

- Step-1: Harmonic structure of the constitutive tensors space: the result for $\mathbb{E}la$ is given in [section 6.2](#);
- Step-2: A complete iterative clips operation between symmetry classes of different harmonic spaces. It will be introduced in [subsection 7.1.1](#);
- Step-3: Distinguish between the generic sets and exotic sets from the results of Step-2 and then characterise the exotic sets by polynomial covariant conditions, this will be introduced in [section 7.2](#).

Remark. *This three-steps structure is general, meaning that it can be applied to any other constitutive tensors space to determine their exotic sets.*

7.1.1 Clips operation for $\mathbb{E}la(3)$

In response to the two aspects mentioned earlier, here we will correspondingly introduce two clips products: a simple case and a complete case. The results of both operations play a crucial role in enumerating exotic sets.

Clips operation: direct product

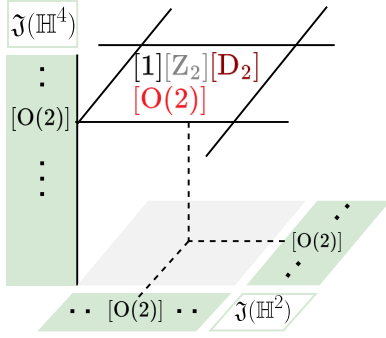
Consider the harmonic structure of the elasticity tensor space $\mathbb{E}la = 2\mathbb{H}^0 \oplus 2\mathbb{H}^2 \oplus \mathbb{H}^4$, the clips operation between individual symmetry classes $([G_1]_{\mathbb{H}^a}, [G_2]_{\mathbb{H}^b}, [G_3]_{\mathbb{H}})$ will result in the symmetry class $[G]$:

$$[G_1]_{\mathbb{H}^a} \odot [G_2]_{\mathbb{H}^b} \odot [G_3]_{\mathbb{H}} = [G] \quad (7.2)$$

To illustrate this clips product, we put in each horizontal stage ([Figure 7.1](#)) the clips product between $[G_1]_{\mathbb{H}^a} \in \mathcal{J}(\mathbb{H}^2)$ and $[G_2]_{\mathbb{H}^b} \in \mathcal{J}(\mathbb{H}^2)$. On the vertical axis are addressed the symmetry classes of $[G_3]_{\mathbb{H}} \in \mathcal{J}(\mathbb{H}^4)$, a successive clips product between the previous result of $[G_1]_{\mathbb{H}^a} \odot [G_2]_{\mathbb{H}^b}$ and $[G_3]_{\mathbb{H}}$ will be computed. As a consequence, we show in the horizontal block the final results of $[G_1]_{\mathbb{H}^a} \odot [G_2]_{\mathbb{H}^b} \odot [G_3]_{\mathbb{H}}$.

Here comes an example:

Example 5



We show here an example of the clips operation of $[O(2)] \odot [O(2)] \odot [O(2)]$ for $\mathbb{E}a$ case. It can be observed that it results in four different symmetry classes, we will define later $[O(2)]$ as generic while the others are exotic.

Figure 7.1: Illustration of clips operations

As shown in this example, the resulting symmetry class $[G]$ is not the only outcome of this operation. This situation is in fact general, and has strong implication when it comes to "inverse" the clips operation:

$$[G] = [G_1]_{\tilde{h}^a} \odot [G_2]_{\tilde{h}^b} \odot [G_3]_{\tilde{H}} \tag{7.3}$$

the symmetry class $[G]$ can be obtained from different collections $([G_1]_{\tilde{h}^a}, [G_2]_{\tilde{h}^b}, [G_3]_{\tilde{H}})$, and the corresponding strata will result in two situations: generic sets or exotic sets. Take the case in Figure 7.1 for instance, the obtained $[O(2)]$ is generic while $[1]$, $[Z_2]$ and $[D_2]$ are exotic.

This allows us to explore the possibilities of exotic sets in a direct manner. The operation is simple and yield very tentative results (listed in Figure 7.3). However, the problem with this direct approach, is that it does not count the diverse combinations producing the same result. From the view of clips product, it lacks one-to-one correspondence between the obtained exotic set and its triplet collection, which make it incapable of insight into the determination of complete exotic sets. Consider for instance the orthotropic class $[D_2]$ obtained from the triple $([O(2)]_{\tilde{h}^a}, [O(2)]_{\tilde{h}^b}, [O(2)]_{\tilde{H}})$. The Figure 7.1 only indicates that this outcome is possible, to count the diverse combination leading to this result, it is important to consider also symmetry classes of pairs, as illustrated in Table 7.1.

$[G]$	$[G_1]$	$[G_2]$	$[G_3]$	$[G_4]$	$[G_5]$	$[G_6]$	Number
$[D_2]$	$[O(2)]$	$[O(2)]$	$[O(2)]$	$[D_2]$ or $[O(2)]$	$[D_2]$ or $[O(2)]$	$[D_2]$ or $[O(2)]$	$2 \times 2 \times 2$

Table 7.1: An example of complete clips operation structure.

From this example, it can be observed that the exotic set $[D_2]$ obtained by simple clips operation $[O(2)]_{\tilde{h}^a} \odot [O(2)]_{\tilde{h}^b} \odot [O(2)]_{\tilde{H}}$ encompasses greater possibilities of exotic sets, provided that the intermediate results of coupled clips product, that is $([G_4]_{(\tilde{h}^a, \tilde{h}^b)}, [G_5]_{(\tilde{h}^a, \tilde{H})}, [G_6]_{(\tilde{h}^b, \tilde{H})})$, are taken into consideration. These coupled results were previously introduced as Aspect II consideration. For this example, we obtain 8 exotic sets instead of 1.

Clips operation: complete product

Based on the preceding discussion, we present here the complete one-to-one correspondence structure of the clips operations $[G_1]_{\tilde{h}^a} \odot [G_2]_{\tilde{h}^b} \odot [G_3]_{\tilde{H}}$:

$$[G] = \{[G_1]_{\tilde{h}^a} \odot [G_2]_{\tilde{h}^b} \odot [G_3]_{\tilde{H}} \mid [G_1]_{\tilde{h}^a} \odot [G_2]_{\tilde{h}^b} = [G_4], [G_1]_{\tilde{h}^a} \odot [G_3]_{\tilde{H}} = [G_5], [G_2]_{\tilde{h}^b} \odot [G_3]_{\tilde{H}} = [G_6]\} \quad (7.4)$$

To illustrate this complete clips product, we present the following structure:

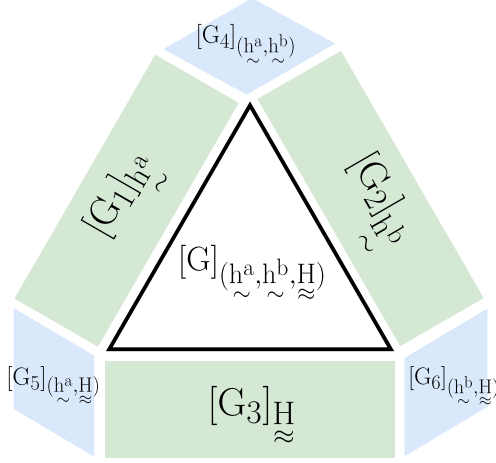


Figure 7.2: Illustration of complete clips operations structure

It shows the structure of complete clips operation of Equation 7.4 for $\mathbb{E}a$ case. The final result is placed within an equilateral triangle, and its derivation takes into account:

1. Aspect I the symmetry classes of the individual components (placed in green rectangles located at the sides of the triangle);
2. Aspect II the symmetry classes of the paired components (placed in blue parallelogram located at vertices of the triangle).

Remark. *The restriction on the symmetry class of the paired components can be seen as the restriction imposed on the "orientation" between these components.*

The results of both these cases of clips operation will be listed in the next subsection, and thus help us to determine the exotic sets.

7.1.2 Determination of exotic sets

We recalled the clips operations, a tool for deducing the symmetry classes of a tensor space from its harmonic decomposition. For $\mathbb{E}a$, we previously discussed two cases of clips operation, and now we will furnish two distinct outcomes in alignment with those cases. At this juncture, a natural question arises: how to select from the many possibilities of $[G]$ that really define exotic materials? To address this, the outcomes will be presented in a manner that is both comprehensible and intuitive.

Intermediate classification of exotic sets

The example in Figure 7.3 is extended here to obtain the intermediate classification of exotic sets for $\mathbb{E}a$. Since there exist 8 symmetry classes for \mathbb{H}^4 and 3 symmetry classes for \mathbb{H}^2 , we have 3×3 horizontal blocks and 8 stages. Obviously, since two \mathbb{H}^2 are involved, the 9 horizontal blocks are symmetric, we will illustrate only a part of the results. To easily distinguish between them, the different symmetry classes are illustrated by different colors, it reads:

$$\{[1], [Z_2], [D_2], [D_3], [D_4], [O(2)], [O], [SO(3)]\}$$

And our result reads:

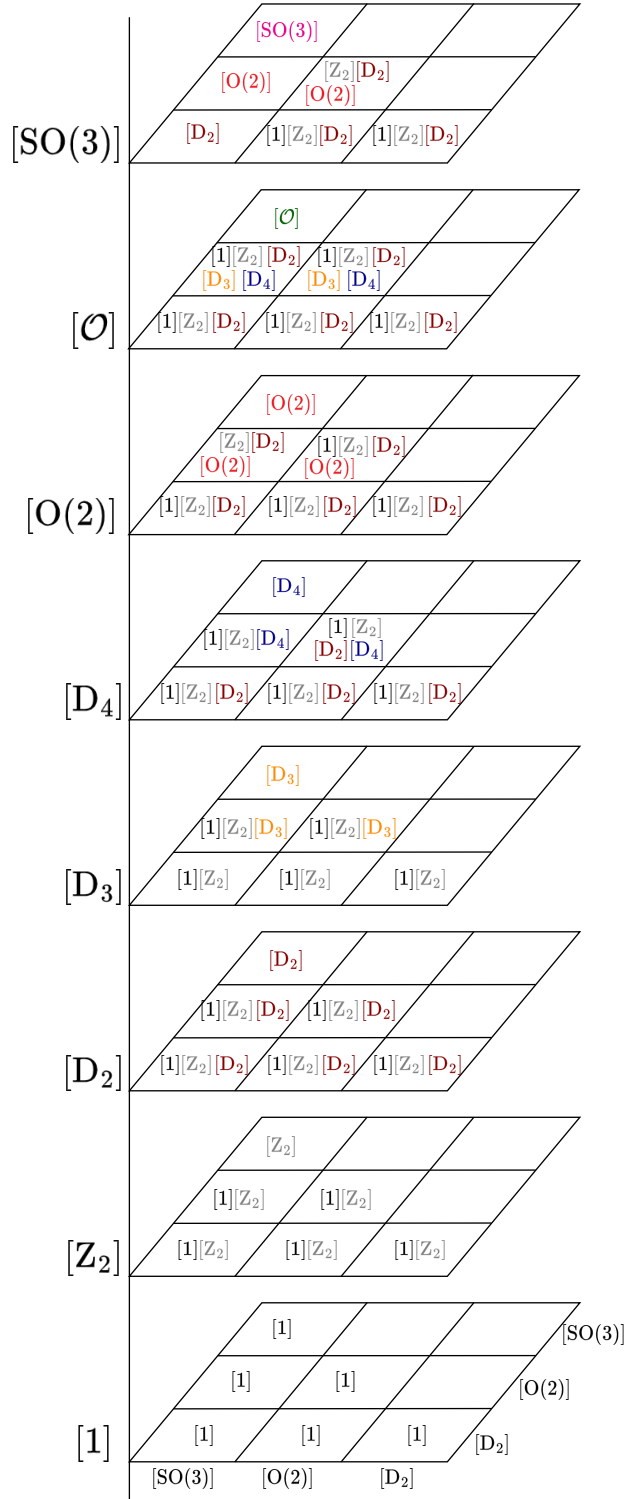


Figure 7.3: Clips operation results for $\mathbb{E}a$

Remark. *Apart from $[SO(3)]$ and $[O]$, the other symmetry classes can be generated differently.*

Indeed, from the result obtained above, we can determine whether a symmetry class $[G]$ is exotic or not: according to the definition of exotic materials in Definition 7.1.1, among all the same type of symmetry class $[G]$, the so-called generic is the one that results from a collection of triplet symmetry classes which are the least symmetric among all.

[G]	$\mathfrak{J}(\mathbb{H}^2)$	$\mathfrak{J}(\mathbb{H}^2)$	$\mathfrak{J}(\mathbb{H}^4)$	Number	Nature
	[G ₁]	[G ₂]	[G ₃]		
[SO(3)]	[SO(3)]	[SO(3)]	[SO(3)]	1	Generic
[O]	[SO(3)]	[SO(3)]	[O]	1	Generic
[O(2)]	[O(2)]	[O(2)]	[O(2)]	1	Generic
	[O(2)]	[SO(3)]	[O(2)]	2	Exotic
	[O(2)]	[O(2)]	[SO(3)]	1	
	[O(2)]	[SO(3)]	[SO(3)]	2	
	[SO(3)]	[SO(3)]	[O(2)]	1	
[D ₄]	[O(2)]	[O(2)]	[D ₄]	1	Generic
	[O(2)]	[SO(3)]	[D ₄]	2	Exotic
	[SO(3)]	[SO(3)]	[D ₄]	1	
	[O(2)]	[O(2)]	[O]	1	
	[SO(3)]	[O(2)]	[O]	2	
[D ₃]	[O(2)]	[O(2)]	[D ₃]	1	Generic
	[SO(3)]	[O(2)]	[D ₃]	2	Exotic
	[SO(3)]	[SO(3)]	[D ₃]	1	
	[O(2)]	[O(2)]	[O]	1	
	[SO(3)]	[O(2)]	[O]	2	

Table 7.2: Intermediate clips operation results for $\mathbb{E}a$ and determination of exotic sets

Remark. *The number here counts the possibilities of exotic set within the intermediate classification. The number equal to 2 is based on the fact that the clips product between symmetry classes of two \mathbb{H}^2 is commutative.*

We’ve just listed in Table 7.2 the possibilities for [SO(3)], [O], [O(2)], [D₄] and [D₃], the ones for [D₂], [Z₂] and [1] are too numerous, we’ll put them in section D.1. The cases marked with a gray background are generic ones. To summarize, there are intermediately 163 exotic sets in total for tensors in $\mathbb{E}a$. Specifically, we have 6 exotic sets of $\Sigma_{[O(2)]}$, 6 exotic sets of $\Sigma_{[D_4]}$, 6 exotic sets of $\Sigma_{[D_3]}$, 36 exotic sets of $\Sigma_{[D_2]}$, 52 exotic sets of $\Sigma_{[Z_2]}$ and 57 exotic sets of $\Sigma_{[1]}$. As the symmetry degree of the considered symmetry class decreases, the number of exotic sets increases sharply.

Certainly, as we’ve learned from the previous discussion about the clips operation that the outcomes obtained through direct clips products do not encompass all exotic sets. A complete list of exotic sets will be provided in the subsequent part of this subsection.

This does not mean, however, that the results obtained lack precision; on the contrary, they have some significance: in what follows we shall find that many of the exotic sets expressed in the complete product manner (Equation 7.4) can be simplified to the intermediate results given here, which allow us to simplify the characterization of these exotic sets. For instance, the three examples of exotic materials presented in section 7.3 can all be reduced to results obtained by a direct clips product without having to consider the symmetry classes of the pairs.

Complete list of exotic sets

The results obtained previously are not exhaustive. As shown in Table 7.1, when considering the symmetry classes of coupled components, a previously obtained exotic set might encompass additional exotic sets. Thus, by applying the Equation 7.4, we enumerate the complete exotic sets. The results for [SO(3)], [O], [O(2)], [D₄] and [D₃] are as follows:

[G]	[G ₁]	[G ₂]	[G ₃]	[G ₄]	[G ₅]	[G ₆]	Number	Generic/Exotic
[SO(3)]	[SO(3)]	[SO(3)]	[SO(3)]	[SO(3)]	[SO(3)]	[SO(3)]	1	Generic
[O]	[SO(3)]	[SO(3)]	[O]	[SO(3)]	[O]	[O]	1	Generic
[O(2)]	[O(2)]	[O(2)]	[O(2)]	[O(2)]	[O(2)]	[O(2)]	1	Generic
	[O(2)]	[SO(3)]	[O(2)]	[O(2)]	[O(2)]	[O(2)]	2	Exotic
	[O(2)]	[O(2)]	[SO(3)]	[O(2)]	[O(2)]	[O(2)]	1	
	[O(2)]	[SO(3)]	[SO(3)]	[O(2)]	[O(2)]	[SO(3)]	2	
	[SO(3)]	[SO(3)]	[O(2)]	[SO(3)]	[O(2)]	[O(2)]	1	
[D ₄]	[O(2)]	[O(2)]	[D ₄]	[O(2)]	[D ₄]	[D ₄]	1	Generic
	[O(2)]	[SO(3)]	[D ₄]	[O(2)]	[D ₄]	[D ₄]	2	Exotic
	[SO(3)]	[SO(3)]	[D ₄]	[SO(3)]	[D ₄]	[D ₄]	1	
	[O(2)]	[O(2)]	[O]	[O(2)]	[D ₄]	[D ₄]	1	
	[SO(3)]	[O(2)]	[O]	[O(2)]	[O]	[D ₄]	2	
[D ₃]	[O(2)]	[O(2)]	[D ₃]	[O(2)]	[D ₃]	[D ₃]	1	Generic
	[SO(3)]	[O(2)]	[D ₃]	[O(2)]	[D ₃]	[D ₃]	2	Exotic
	[SO(3)]	[SO(3)]	[D ₃]	[SO(3)]	[D ₃]	[D ₃]	1	
	[O(2)]	[O(2)]	[O]	[O(2)]	[D ₃]	[D ₃]	1	
	[SO(3)]	[O(2)]	[O]	[O(2)]	[O]	[D ₃]	2	

Table 7.3: clips operation results for Ela and determination of exotic sets

It's worth noting that the final results are consistent with what was obtained in Table 7.2, meaning that for a given set $([G_1], [G_2], [G_3])$, the corresponding set $([G_4], [G_5], [G_6])$ is unique. This phenomenon is easy to be explained: as the obtained degree of symmetry increases, the requirements for symmetry class pertaining to each individual component, as well as the symmetry class of the coupled components, become more stringent. This will not be the case for symmetry classes with lower symmetry, that is $[D_2], [Z_2], [1]$, the results for these three cases can be found in section D.2.

To summarise, we obtain 8 generic sets and 1052 exotic sets in total. The exotic sets are respectively 6 for $\Sigma_{[O(2)]}$, 6 for $\Sigma_{[D_4]}$, 6 for $\Sigma_{[D_3]}$, 58 for $\Sigma_{[D_2]}$, 283 for $\Sigma_{[Z_2]}$ and 693 for $\Sigma_{[1]}$.

It should be noted that the obtained results outlined the theoretical potential of exotic sets, and they remain in the mathematical stage. However, whether their corresponding materials can actually exist, or how the so-called "exotic" are specifically manifested in mechanical behavior, is not yet known at this stage. It is necessary to combine the current results with a specific harmonic decomposition in order to describe the "hypersymmetric" behavior stated in Definition 7.1.1 to really define an exotic material. This will be discussed in section 7.3.

7.2 Covariants conditions for exotic sets

The Theorem 6.5 used to characterise the symmetry class of an elasticity tensor is based on the fact that the symmetry class of \mathbb{C} is the same as the symmetry class of the harmonic bouquet $(\mathbb{h}^a, \mathbb{h}^b, \mathbb{H})$, that is $[G]_{(\mathbb{h}^a, \mathbb{h}^b, \mathbb{H})}$, or simply written as $[G]$. It characterise the generic state by imposing conditions on hamronic components as well as the pairs. These conditions can be used to identify different $\Sigma_{[G]}$, but for a given $[G]$, it can not be used to distinguish different $\Sigma_{[G]}^{e_i}$. In other words, the exotic sets obtained in the previous section cannot be charecterised by using these polynomial conditions. To characterise the exotic sets, it is necessary to add to these conditions new conditions involving either the norms of the harmonic components, the "orientations" or even both (the same as we done for $\mathbb{E}la(2)$).

Thus, in this section, based on the results (Theorem 6.5) in the previous chapter, along with the framework laid by M. Olive et al.'s work in [78], we propose here complete polynomial covariant conditions. These conditions aim to characterise the symmetry class $[G]_{(\tilde{h}^a, \tilde{h}^b, \tilde{H})}$ of \mathbb{C} while taking into account the symmetry class set $([G_1]_{\tilde{h}^a}, [G_2]_{\tilde{h}^b}, [G_3]_{\tilde{H}}, [G_4]_{(\tilde{h}^a, \tilde{h}^b)}, [G_5]_{(\tilde{h}^a, \tilde{H})}, [G_6]_{(\tilde{h}^b, \tilde{H})})$. The construction of these conditions includes the following tripartite elements :

- Polynomial covariant conditions used to characterise the symmetry class of $(\tilde{h}^a, \tilde{h}^b, \tilde{H})$;
- Extra covariant conditions used to impose restrictions on the symmetry class of each element \tilde{h}^a , \tilde{h}^b and \tilde{H} ;
- Extra covariant conditions used to impose restrictions on the symmetry class of the pair $(\tilde{h}^a, \tilde{h}^b)$, (\tilde{h}^a, \tilde{H}) and (\tilde{h}^b, \tilde{H}) .

The conditions of first aspect have been clarified in Theorem 6.5. For the conditions of the second aspect, by combining Lemma C.1 and Theorem C.2 in Appendix C (based on the work of M. Olive et al. in [78]), we have:

Theorem 7.1: Characterisation of the symmetry class for second-order harmonic tensors [78]

For a second-order harmonic tensor $\underset{\sim}{h}$, its symmetry class is characterised as follows:

Symmetry class	Covariants conditions
[D ₂]	$\underset{\sim}{h} \times \underset{\sim}{h}^2 \neq 0$
[O(2)]	$\underset{\sim}{h} \times \underset{\sim}{h}^2 = 0, \quad \underset{\sim}{h} \neq 0$
[SO(3)]	$\underset{\sim}{h} = 0$

Theorem 7.2: Characterisation of the symmetry class for fourth-order harmonic tensors [78]

For a fourth-order harmonic tensor $\underset{\sim}{H}$, its symmetry class is characterised as follows:

Symmetry class	Covariants conditions
[1]	None of the following conditions satisfied
[Z ₂]	$(\text{tr}(\underset{\sim}{d}_2 \times \underset{\sim}{c}_3) \neq 0, \quad (\underset{\sim}{c}_4 \text{tr}(\underset{\sim}{d}_2 \times \underset{\sim}{c}_3)) \times \text{tr}(\underset{\sim}{d}_2 \times \underset{\sim}{c}_3) = 0)$ or $(\text{tr}(\underset{\sim}{d}_2 \times \underset{\sim}{c}_4) \neq 0, \quad (\underset{\sim}{c}_3 \text{tr}(\underset{\sim}{d}_2 \times \underset{\sim}{c}_4)) \times \text{tr}(\underset{\sim}{d}_2 \times \underset{\sim}{c}_4) = 0)$ or $(\text{tr}(\underset{\sim}{c}_3 \times \underset{\sim}{c}_4) \neq 0, \quad (\underset{\sim}{d}_2 \text{tr}(\underset{\sim}{c}_3 \times \underset{\sim}{c}_4)) \times \text{tr}(\underset{\sim}{c}_3 \times \underset{\sim}{c}_4) = 0)$
[D ₂]	$\underset{\sim}{v}_5 = \underset{\sim}{v}_6 = 0; \quad \text{tr}(\underset{\sim}{d}_2 \times \underset{\sim}{c}_3) = 0$ and $(\underset{\sim}{d}_2 \times \underset{\sim}{d}_2^2 \neq 0 \text{ or } \underset{\sim}{c}_3 \times \underset{\sim}{c}_3^2 \neq 0 \text{ or } \underset{\sim}{d}_2 \times \underset{\sim}{c}_3 \neq 0)$
[D ₃]	$\underset{\sim}{d}_2 \times \underset{\sim}{d}_2^2 = 0, \quad \underset{\sim}{d}_2^{\text{d}} \neq 0, \quad (\underset{\sim}{H} : \underset{\sim}{d}_2) \times \underset{\sim}{d}_2 = 0$ and $\text{tr}(\underset{\sim}{H} \times \underset{\sim}{d}_2) \neq 0$
[D ₄]	$\underset{\sim}{d}_2 \times \underset{\sim}{d}_2^2 = 0, \quad \underset{\sim}{d}_2^{\text{d}} \neq 0, \quad \underset{\sim}{H} \times \underset{\sim}{d}_2 \neq 0$ and $\text{tr}(\underset{\sim}{H} \times \underset{\sim}{d}_2) = 0$
[O(2)]	$\underset{\sim}{d}_2 \times \underset{\sim}{d}_2^2 = 0, \quad \underset{\sim}{d}_2^{\text{d}} \neq 0, \quad \underset{\sim}{H} \times \underset{\sim}{d}_2 = 0$
[O]	$\underset{\sim}{d}_2 \neq 0, \quad \underset{\sim}{d}_2^{\text{d}} = 0$
[SO(3)]	$\underset{\sim}{d}_2 = 0$ or $\underset{\sim}{H} = 0$

with

$$\begin{aligned} \underset{\sim}{d}_2 &= \text{tr}_{13}(\underset{\sim}{H}^2) & \underset{\sim}{d}_3 &= \text{tr}_{13}\underset{\sim}{H}^3, & \underset{\sim}{c}_k &= \underset{\sim}{H}^{k-2} : \underset{\sim}{d}_2, \quad k \geq 3 \\ \underset{\sim}{v}_5 &= \underset{\sim}{\varepsilon} : (\underset{\sim}{d}_2 \underset{\sim}{c}_3) & \underset{\sim}{v}_6 &= \underset{\sim}{\varepsilon} : (\underset{\sim}{d}_2 \underset{\sim}{c}_4) \end{aligned}$$

and $\underset{\sim}{\varepsilon}$ denotes the Levi-Civita third-order tensor in \mathbb{R}^3 defined in Equation 6.2.

The construction of polynomial conditions for the third aspect can be seen as the special case of the first aspect (the relative contents are discussed in [78]): $(\underset{\sim}{h}^a, \underset{\sim}{h}^b)$ is the special case of $(\underset{\sim}{h}^a, \underset{\sim}{h}^b, \underset{\sim}{H})$ with $\underset{\sim}{H} = 0$ or $\mathfrak{I}(\mathbb{H}^4) = [\text{SO}(3)]$. $(\underset{\sim}{h}^a, \underset{\sim}{H})$ can be considered as $(\underset{\sim}{h}^a, \underset{\sim}{h}^b, \underset{\sim}{H})$ with $\underset{\sim}{h}^b = 0$ or $\mathfrak{I}(\mathbb{H}^2) = [\text{SO}(3)]$ and likewise for $(\underset{\sim}{h}^b, \underset{\sim}{H})$. Therefore, we apply the Theorem 6.5 to the current context and derive the following theorem, The proofs of the two aforementioned theorems can be done by combining Theorem 6.5 and Theorem C.1.

Theorem 7.3: Characterisation of the symmetry class of pair $(\underset{\sim}{h}^a, \underset{\sim}{h}^b)$ [78]

Let $\underset{\sim}{h}^a, \underset{\sim}{h}^b \in \mathbb{H}^2$, then

1. $(\underset{\sim}{h}^a, \underset{\sim}{h}^b) \in \Sigma_{[\text{SO}(3)]}$ if and only if $\underset{\sim}{h}^a = \underset{\sim}{h}^b = 0$;
2. $(\underset{\sim}{h}^a, \underset{\sim}{h}^b) \in \Sigma_{[\text{O}(2)]}$ if and only if there exists $\underset{\sim}{h}^i$ ($i = a$ or b) such that

$$(\underset{\sim}{h}^i)^d \neq 0, \quad \underset{\sim}{h}^i \times (\underset{\sim}{h}^i)^2 = 0 \text{ and } \underset{\sim}{h}^a \times \underset{\sim}{h}^b = 0$$

3. $(\underset{\sim}{h}^a, \underset{\sim}{h}^b) \in \Sigma_{[\text{D}_2]}$ if and only if

$$\text{tr}(\underset{\sim}{h}^a \times \underset{\sim}{h}^b) = 0,$$

and there exists $\underset{\sim}{h}^i$ ($i = a$ or b) such that $\underset{\sim}{h}^i \times (\underset{\sim}{h}^i)^2 \neq 0$ or $\underset{\sim}{h}^a \times \underset{\sim}{h}^b \neq 0$

4. $(\underset{\sim}{h}^a, \underset{\sim}{h}^b) \in \Sigma_{[\text{Z}_2]}$ if and only if $\underline{w} := \text{tr}(\underset{\sim}{h}^a \times \underset{\sim}{h}^b) \neq 0$ and

$$(\underset{\sim}{h}^i \underline{w}) \times \underline{w} = 0, \quad i = a \text{ or } b.$$

5. $(\underset{\sim}{h}^a, \underset{\sim}{h}^b) \in \Sigma_{[1]}$ if and only if none of the preceding conditions hold.

Next, we will discuss the situation for $(\underset{\sim}{h}^a, \underset{\cong}{H})$ and $(\underset{\sim}{h}^b, \underset{\cong}{H})$, since they hold the same results, we will only discuss $(\underset{\sim}{h}^a, \underset{\cong}{H})$ here.

Theorem 7.4: Characterisation of the symmetry class of $(\underset{\sim}{h}^a, \underset{\cong}{H})$

Let $\underset{\sim}{h}^a \in \mathbb{H}^2$ and $\underset{\cong}{H} \in \mathbb{H}^4$, then

1. $(\underset{\sim}{h}^a, \underset{\cong}{H}) \in \Sigma_{[\text{SO}(3)]}$ if and only if $\underset{\sim}{h}^a = \underset{\sim}{d}_2 = 0$.
2. $(\underset{\sim}{h}^a, \underset{\cong}{H}) \in \Sigma_{[\emptyset]}$ if and only if $\underset{\sim}{h}^a = \underset{\sim}{d}_2^d = 0$ and $\underset{\sim}{d}_2 \neq 0$.
3. $(\underset{\sim}{h}^a, \underset{\cong}{H}) \in \Sigma_{[\text{O}(2)]}$ if and only if $(\underset{\sim}{h}^a, \underset{\sim}{d}_2)$ is transversely isotropic and

$$\underset{\cong}{H} \times \underset{\sim}{h}^a = \underset{\cong}{H} \times \underset{\sim}{d}_2 = 0.$$

4. $(\underset{\sim}{h}^a, \underset{\cong}{H}) \in \Sigma_{[\text{D}_4]}$ if and only if $(\underset{\sim}{h}^a, \underset{\sim}{d}_2)$ is transversely isotropic and

$$\text{tr}(\underset{\cong}{H} \times \underset{\sim}{h}^a) = \text{tr}(\underset{\cong}{H} \times \underset{\sim}{d}_2) = 0,$$

and

$$\underset{\cong}{H} \times \underset{\sim}{h}^a \neq 0 \quad \text{or} \quad \underset{\cong}{H} \times \underset{\sim}{d}_2 \neq 0.$$

5. $(\underset{\sim}{h}^a, \underset{\cong}{H}) \in \Sigma_{[\text{D}_3]}$ if and only if $(\underset{\sim}{h}^a, \underset{\sim}{d}_2)$ is transversely isotropic and

$$\underset{\sim}{h}^a \times (\underset{\cong}{H} : \underset{\sim}{h}^a) = \underset{\sim}{d}_2 \times (\underset{\cong}{H} : \underset{\sim}{d}_2) = 0,$$

and

$$\text{tr}(\underset{\cong}{H} \times \underset{\sim}{h}^a) \neq 0 \quad \text{or} \quad \text{tr}(\underset{\cong}{H} \times \underset{\sim}{d}_2) \neq 0.$$

6. $(\underset{\sim}{h}^a, \underset{\cong}{H}) \in \Sigma_{[\text{D}_2]}$ if and only if the family of second-order tensors \mathcal{F}_o is orthotropic.

$$\mathcal{F}_o = \{\underset{\sim}{h}^a, \underset{\sim}{d}_2, \underset{\sim}{c}_3, \underset{\sim}{c}_4, \underset{\cong}{H} : \underset{\sim}{h}^a, \underset{\cong}{H} : (\underset{\sim}{h}^a)^2\}$$

7. $(\underset{\sim}{h}^a, \underset{\cong}{H}) \in \Sigma_{[\text{Z}_2]}$ if and only if the family of second-order tensors \mathcal{F}_m is monoclinic.

$$\mathcal{F}_m = \{\underset{\sim}{h}^a, \underset{\sim}{d}_2, \underset{\sim}{c}_3, \underset{\sim}{c}_4, \underset{\cong}{H} : \underset{\sim}{h}^a, \underset{\cong}{H} : (\underset{\sim}{h}^a)^2, \underset{\cong}{H} : (\underset{\sim}{h}^a \underset{\sim}{d}_2)^s\}$$

8. $(\underset{\sim}{h}^a, \underset{\cong}{H}) \in \Sigma_{[1]}$ if and only if none of the preceding conditions hold.

Unlike the characterisation of the symmetry class of \mathbb{C} in Theorem 6.5, which omits the essential covariants conditions for symmetry classes of $([\text{G}_1]_{\underset{\sim}{h}^a}, [\text{G}_2]_{\underset{\sim}{h}^b}, [\text{G}_3]_{\underset{\cong}{H}}, [\text{G}_4]_{(\underset{\sim}{h}^a, \underset{\sim}{h}^b)}, [\text{G}_5]_{(\underset{\sim}{h}^a, \underset{\cong}{H})}, [\text{G}_6]_{(\underset{\sim}{h}^b, \underset{\cong}{H})}$), the preceding four theorems make up for this limitation.

For a given exotic set, the final conditions to characterise it are obtained by first imposing independently the tripartite conditions (stated in Theorem 6.5, Theorem 7.1, Theorem 7.2, Theorem 7.3 and Theorem 7.4) and then eliminating the overlapping ones. It's worth noting that this process can be significantly simplified in many cases: as stated in Table 7.3, after determining the symmetry classes of individual harmonic components $([\text{G}_1]_{\underset{\sim}{h}^a}, [\text{G}_2]_{\underset{\sim}{h}^b}, [\text{G}_3]_{\underset{\cong}{H}})$, the symmetry classes $([\text{G}_4]_{(\underset{\sim}{h}^a, \underset{\sim}{h}^b)}, [\text{G}_5]_{(\underset{\sim}{h}^a, \underset{\cong}{H})}, [\text{G}_6]_{(\underset{\sim}{h}^b, \underset{\cong}{H})})$ of paired components formed by these individual ones can be uniquely determined. To characterise these exotic sets, only the conditions for $([\text{G}]_{(\underset{\sim}{h}^a, \underset{\sim}{h}^b, \underset{\cong}{H})}, [\text{G}_1]_{\underset{\sim}{h}^a}, [\text{G}_2]_{\underset{\sim}{h}^b}, [\text{G}_3]_{\underset{\cong}{H}})$ will be considered.

In the next section, we will present three such examples. Since the symmetry classes of paired components are uniquely determined, they will be illustrated in a way like in Figure 7.1 instead of in Figure 7.2. These three cases will be detailed in the next section, once a specific explicit harmonic decomposition

has been chosen, the corresponding exotic materials can be accordingly defined, and they exhibit exotic mechanical properties, which we refer to as *hypersymmetric* in the Definition 7.1.1. Interestingly, these examples have already been mentioned, either directly or indirectly, within the literature under different frameworks [10]. This highlights the robustness and applicability of our approach, and it provides theoretical support for further investigations into a wider array of exotic materials.

7.3 Exotic elastic materials

In this section, three types of exotic materials will be described in detail (through some extensions, a total of 5 exotic materials will be mentioned). Before starting, consider again the two conditions for defining exotic materials:

1. **Special design:** The point is to impose additional requirements that are independent of those that can be imposed by symmetry arguments. This is achieved by first determining exotic sets based on clip operations and then characterizing them by polynomial conditions. These processes have been discussed previously, and the proposed exotic materials are all listed in the previous results, of course, detailed explanations are given for each of these cases;
2. **Hypersymmetric:** This second condition will be the focus of this section. Based on specific explicit harmonic decompositions (Clebsch-Gordan and Schur-Weyl), we will show the *hypersymmetric* properties of each proposed exotic material.

In order to demonstrate that the corresponding elasticity tensors of these exotic materials are positive definite, we will provide examples of matrix representation (under the Kelvin convention) of their corresponding stiffness tensor $\underline{\underline{C}}$. On this matrix will be then performed the Clebsch-Gordan and the Schur-Weyl harmonic decomposition and the different exotic anisotropic properties will be analysed accordingly. All the matrix representations come from the computation by using Wolfram Mathematica software in file “[Examples of exotic materials](#)”.

7.3.1 R_0 -orthotropy in \mathbb{R}^3

A generic set of $[D_2]$ is obtained by clips operation:

$$[D_2] = [D_2]_{\underline{\underline{h}}^a} \odot [D_2]_{\underline{\underline{h}}^b} \odot [D_2]_{\underline{\underline{H}}}$$

and apart from the *Condition 6* in Theorem 6.5, the additional polynomial covariants conditions used to characterise this generic set $\Sigma_{[D_2]}^g$ is :

$$\begin{aligned} \underline{\underline{h}}^a \times (\underline{\underline{h}}^a)^2 \neq 0, \quad \underline{\underline{h}}^b \times (\underline{\underline{h}}^b)^2 \neq 0, \quad \underline{\underline{v}}_5 = \underline{\underline{v}}_6 = 0 \quad \text{and} \\ (\underline{\underline{d}}_2 \times \underline{\underline{d}}_2^2 \neq 0 \text{ or } \underline{\underline{c}}_3 \times \underline{\underline{c}}_3^2 \neq 0 \text{ or } \underline{\underline{d}}_2 \times \underline{\underline{c}}_3 \neq 0) \end{aligned}$$

Based on this, we will be interested in an exotic orthotropic material, which can be considered as the extension of R_0 -orthotropy in \mathbb{R}^2 to \mathbb{R}^3 . To this end, we will reuse the Clebsch-Gordan parameterization:

$$\underline{\underline{C}} = \alpha \underline{\underline{J}} + \beta \underline{\underline{K}} + \underline{\underline{h}}^a \boxtimes \underline{\underline{1}} + \frac{1}{3} (\underline{\underline{h}}^b \otimes \underline{\underline{1}} + \underline{\underline{1}} \otimes \underline{\underline{h}}^b) + \underline{\underline{H}},$$

Remark. *Based on the choice of the basis in this explicit decomposition, the linear combination of $(\underline{\underline{h}}^a, \underline{\underline{h}}^b)$ has been fixed, and their physical significations are different. Thus, the commutativity of $\underline{\underline{h}}^a$ and $\underline{\underline{h}}^b$ will*

be no longer valid.

Namely, the aim of this decomposition is to re-write the elasticity tensor as:

$$\begin{pmatrix} \tilde{\sigma}^d \\ \tilde{\sigma}^s \end{pmatrix} = \begin{pmatrix} \tilde{\mathbb{C}}^{dd} & \tilde{\mathbb{C}}^{ds} \\ \tilde{\mathbb{C}}^{sd} & \tilde{\mathbb{C}}^{ss} \end{pmatrix} \begin{pmatrix} \tilde{\varepsilon}^d \\ \tilde{\varepsilon}^s \end{pmatrix} \quad (7.5)$$

with $\tilde{\mathbb{C}}^{dd} = \mathbb{H} + \tilde{\mathbf{h}}^a \otimes \tilde{\mathbf{1}} + \alpha \tilde{\mathbf{J}}$, $\tilde{\mathbb{C}}^{ds} = \frac{1}{3} \tilde{\mathbf{h}}^b \otimes \tilde{\mathbf{1}}$, $\tilde{\mathbb{C}}^{sd} = \frac{1}{3} \tilde{\mathbf{1}} \otimes \tilde{\mathbf{h}}^b$ and $\tilde{\mathbb{C}}^{ss} = \beta \tilde{\mathbf{K}}$. This expresses elasticity as a coupled behaviour: spherical elasticity (denoted by exponent s) and deviatoric elasticity (denoted by exponent d).

Example 6

To be more specific, a random orthotropic elasticity tensor is given :

$$[\tilde{\mathbb{C}}] = \begin{pmatrix} 58 & 20 & 10 & 0 & 0 & 0 \\ * & 47 & -9 & 0 & 0 & 0 \\ * & * & 52 & 0 & 0 & 0 \\ * & * & * & 46 & 0 & 0 \\ * & * & * & * & 100 & 0 \\ * & * & * & * & * & 144 \end{pmatrix}_{\mathcal{K}} \quad (7.6)$$

It is generated from a 6×6 random diagonal matrix whose elements are only strictly positive:

$$\{73.6, 72, 58.2, 50, 25.2, 23\}$$

Based on it, we obtain the terms of the decomposed elasticity tensor in [Equation 7.5](#):

$$\begin{aligned} [\tilde{\mathbb{C}}^{dd}] &= \begin{pmatrix} \frac{193}{9} & -\frac{59}{9} & -\frac{134}{9} & 0 & 0 & 0 \\ * & -\frac{274}{9} & -\frac{215}{9} & 0 & 0 & 0 \\ * & * & \frac{349}{9} & 0 & 0 & 0 \\ * & * & * & 46 & 0 & 0 \\ * & * & * & * & 100 & 0 \\ * & * & * & * & * & 144 \end{pmatrix}_{\mathcal{K}} & [\tilde{\mathbb{C}}^{ds}] &= \begin{pmatrix} \frac{65}{9} & \frac{65}{9} & \frac{65}{9} & 0 & 0 & 0 \\ * & -\frac{25}{9} & -\frac{25}{9} & 0 & 0 & 0 \\ * & * & -\frac{40}{9} & 0 & 0 & 0 \\ * & * & * & 0 & 0 & 0 \\ * & * & * & * & 0 & 0 \\ * & * & * & * & * & 0 \end{pmatrix}_{\mathcal{K}} \\ [\tilde{\mathbb{C}}^{sd}] &= \begin{pmatrix} \frac{65}{9} & -\frac{25}{9} & -\frac{40}{9} & 0 & 0 & 0 \\ * & -\frac{25}{9} & -\frac{40}{9} & 0 & 0 & 0 \\ * & * & -\frac{40}{9} & 0 & 0 & 0 \\ * & * & * & 0 & 0 & 0 \\ * & * & * & * & 0 & 0 \\ * & * & * & * & * & 0 \end{pmatrix}_{\mathcal{K}} & [\tilde{\mathbb{C}}^{ss}] &= \frac{199}{9} \begin{pmatrix} 1 & 1 & 1 & 0 & 0 & 0 \\ * & 1 & 1 & 0 & 0 & 0 \\ * & * & 1 & 0 & 0 & 0 \\ * & * & * & 0 & 0 & 0 \\ * & * & * & * & 0 & 0 \\ * & * & * & * & * & 0 \end{pmatrix}_{\mathcal{K}} \end{aligned}$$

Characterisation of 3D R_0 -orthotropy

The expression [Equation 7.5](#) allows reproducing the same non-standard mechanical property as R_0 -orthotropy in \mathbb{R}^2 , that is an orthotropic material possesses its deviatoric elasticity isotropic. This situation is defined by the following harmonic structure:

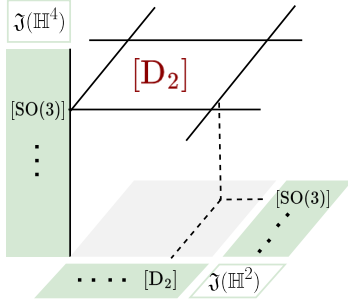
$$\tilde{\mathbb{C}} = f(\alpha, \beta, 0, \tilde{\mathbf{h}}^b, 0) \quad (7.7)$$

with the second order harmonic tensor \tilde{h}^b being of type $[D_2]_{\tilde{h}^b}$. From a mechanical point of view:

$$\begin{pmatrix} \tilde{\sigma}^d \\ \tilde{\sigma}^s \end{pmatrix} = \begin{pmatrix} \alpha \underset{\approx}{J} & \frac{1}{3} \underset{\approx}{h}^b \otimes \underset{\approx}{1} \\ \frac{1}{3} \underset{\approx}{1} \otimes \underset{\approx}{h}^b & \beta \underset{\approx}{K} \end{pmatrix} \begin{pmatrix} \tilde{\varepsilon}^d \\ \tilde{\varepsilon}^s \end{pmatrix} \quad (7.8)$$

It can be observed that it satisfies the first point of the Definition 7.1.1, that is, the restriction does not only come from a symmetry requirement but also should satisfy extra constraints, which are $\tilde{h}^a = 0, \tilde{H} = 0$. Besides, despite the anisotropic coupling between spherical and deviatoric modes, the deviatoric elasticity is isotropic. It produces more symmetrical behaviour than imposed by material symmetries since isotropic deviatoric elasticity only manifests generically for isotropic materials. Thus, it satisfies the second requirement in Definition 7.1.1. We can conclude that it is an exotic elastic material. As stated before, this situation is the 3D generalisation of R_0 -orthotropy and is called *3D R_0 -orthotropy*.

Now we are ready to come back to the discussion of the polynomial covariant condition used to characterise 3D R_0 -orthotropy. It is defined by eliminating a second-order harmonic component and the fourth-order harmonic component in its harmonic structure, which is illustrated as follows :


 Table 7.4: 3D R_0 -orthotropy

\odot	$[D_2] = [SO(3)]_{\tilde{h}^a} \odot [D_2]_{\tilde{h}^b} \odot [SO(3)]_{\tilde{H}}$
Conditions	$\tilde{h}^a = 0, \tilde{H} = 0, \text{ and } \tilde{h}^b \times (\tilde{h}^b)^2 \neq 0$

The polynomial condition for the transition between the strata of generic orthotropy (denoted by $\Sigma_{[D_2]}^g$) and 3D R_0 -orthotropy (denoted here by $\Sigma_{[D_2]}^e$) is:

$$\Sigma_{[D_2]}^g \xrightarrow[\approx]{\tilde{h}^a=0, \tilde{H}=0} \Sigma_{[D_2]}^e$$

Example 7

Based on the random generic orthotropic elasticity tensor represented in Equation 7.6, by applying the conditions in Table 7.4, we provide an example of a matrix that the corresponding material can be called as 3D R_0 -orthotropy:

$$[\underset{\approx}{C}] = \frac{1}{45} \begin{pmatrix} 3929 & 53 & -22 & 0 & 0 & 0 \\ * & 3029 & -472 & 0 & 0 & 0 \\ * & * & 2879 & 0 & 0 & 0 \\ * & * & * & 3426 & 0 & 0 \\ * & * & * & * & 3426 & 0 \\ * & * & * & * & * & 3426 \end{pmatrix}_{\mathcal{K}} \quad (7.9)$$

it is positive definite with its eigenvalues strictly positive $\{87.4, 76.1, 55, 38, 38, 38\}$. Despite the diagonal values of the 3×3 bottom-left submatrix being the same, the matrix $[\underset{\approx}{C}]$ belongs to none of the matrix normal form listed in [[79], Section 2], it remains as totally anisotropic (triclinic).

Among all terms in Equation 7.5, it can be observed that the three same values in the 3×3

bottom-left submatrix come from the term $\underset{\approx}{C}^{dd}$:

$$[\underset{\approx}{C}^{dd}] = \frac{1}{45} \begin{pmatrix} 2284 & -1142 & -1142 & 0 & 0 & 0 \\ * & 2284 & -1142 & 0 & 0 & 0 \\ * & * & 2284 & 0 & 0 & 0 \\ * & * & * & 3426 & 0 & 0 \\ * & * & * & * & 3426 & 0 \\ * & * & * & * & * & 3426 \end{pmatrix}_{\kappa} \quad (7.10)$$

this matrix is characterised by 3 different parameters (one of which is dependent on the two others, that is $3426 = 2 \times (2284 + 1142)$), and presents the same structure of an isotropic matrix. We conclude then that the deviatoric elasticity is isotropic.

Besides, the r_0 -orthotropic materials can be defined by the same process, its harmonic structure reads:

$$\underset{\approx}{C}^{-1} = f(\alpha^-, \beta^-, 0, \underset{\approx}{h}^{b-}, 0) \quad (7.11)$$

with $\{\alpha^-, \beta^-, \underset{\approx}{h}^{a-}, \underset{\approx}{h}^{b-}, \underset{\approx}{H}^-\}$ the harmonic components of $\underset{\approx}{C}^{-1}$. The covariant conditions used to define r_0 -orthotropy are also changed accordingly. With the aforementioned example, it is possible to show that R_0 -orthotropy is not stable by inversion, since:

$$[\underset{\approx}{S}^{dd}] = \frac{1}{45} \begin{pmatrix} 0.0092 & -0.0045 & -0.0046 & 0 & 0 & 0 \\ * & 0.0088 & -0.0043 & 0 & 0 & 0 \\ * & * & 0.0089 & 0 & 0 & 0 \\ * & * & * & 0.026 & 0 & 0 \\ * & * & * & * & 0.026 & 0 \\ * & * & * & * & * & 0.026 \end{pmatrix}_{\kappa} \quad (7.12)$$

the matrix normal form of isotropic symmetry class is no longer kept in $[\underset{\approx}{S}^{dd}]$.

Extension to another exotic material

It should be noted that an anisotropic material with its deviatoric elasticity isotropic is not uniquely defined in \mathbb{R}^3 , a new situation appears for which $\underset{\approx}{h}^b$ is transversely isotropic. Its clips operation is illustrated as follows, compared to the 3D R_0 -orthotropy, this situation changes the symmetry class of $\underset{\approx}{h}^b$ from $[D_2]$ to $[O(2)]$:

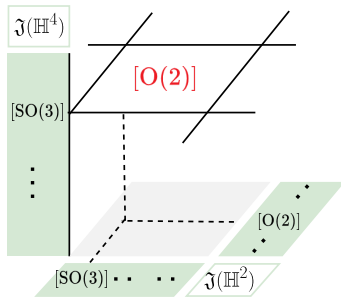


Table 7.5: Transversely isotropic materials with its deviatoric elasticity isotropic

\odot	$[O(2)] = [SO(3)]_{\underset{\approx}{h}^a} \odot [O(2)]_{\underset{\approx}{h}^b} \odot [SO(3)]_{\underset{\approx}{H}}$
Conditions	$\underset{\approx}{h}^a = 0, \quad \underset{\approx}{H} = 0$ and $\underset{\approx}{h}^b \times (\underset{\approx}{h}^b)^2 = 0, \quad \underset{\approx}{h}^b \neq 0$

It is an exotic transversely isotropic elastic material, the deviatoric elasticity of which is isotropic. The complete transition from generic orthotropic to 3D R_0 -orthotropy (denoted by $\Sigma_{[D_2]}^e$) and then to this exotic transversely isotropy (denoted by $\Sigma_{[O(2)]}^e$) are given as follows:

$$\Sigma_{[D_2]}^g \xrightarrow{\tilde{h}^a=0, \tilde{H}=0} \Sigma_{[D_2]}^e \xrightarrow{\tilde{h}^b \times (\tilde{h}^b)^2=0, \tilde{h}^b \neq 0} \Sigma_{[O(2)]}^e$$

7.3.2 Triclinic exotic elastic material

We continue using the Clebsch-Gordan decomposition here to introduce another type of exotic material: a decoupled triclinic exotic material. This kind of material can be obtained starting from a general triclinic material. A generic set of [1] is obtained by clips operation:

$$[1] = [D_2]_{\tilde{h}^a} \odot [D_2]_{\tilde{h}^b} \odot [1]_{\tilde{H}}$$

and the polynomial covariant conditions used to characterise this generic set is the *Condition 8* in Theorem 6.5 and *Condition for [1]* in Theorem 7.2 as well as :

$$\tilde{h}^a \times (\tilde{h}^a)^2 \neq 0, \tilde{h}^b \times (\tilde{h}^b)^2 \neq 0$$

Based on it, the decoupled triclinic exotic material is defined as follows:

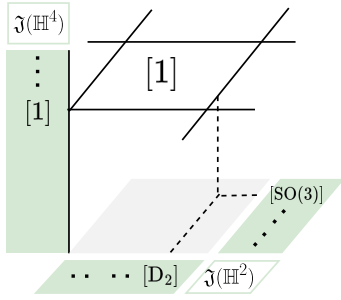


Table 7.6: Triclinic exotic elastic materials

\odot	$[1] = [D_2]_{\tilde{h}^a} \odot [SO(3)]_{\tilde{h}^b} \odot [1]_{\tilde{H}}$
Conditions	$\tilde{h}^b = 0, \tilde{h}^a \times (\tilde{h}^a)^2 \neq 0$

The polynomial condition of the transition between the corresponding strata of these two different symmetry classes is:

$$\Sigma_{[1]}^g \xrightarrow{\tilde{h}^b=0} \Sigma_{[1]}^e$$

The cancellation of \tilde{h}^b cannot be done by imposing symmetry restrictions alone, it must be imposed by a specific design of the mesostructure, this aspect satisfies the first requirement of the properties defining exotic materials, as stated in Definition 7.1.1.

From a mechanical standpoint, this situation can be interpreted by Clebsch-Gordan parametrisation. We have:

$$\begin{pmatrix} \tilde{\sigma}^d \\ \tilde{\sigma}^s \end{pmatrix} = \begin{pmatrix} \tilde{H} + \tilde{h}^a \boxtimes \tilde{1} + \alpha \tilde{J} & 0 \\ 0 & \beta \tilde{K} \end{pmatrix} \begin{pmatrix} \tilde{\varepsilon}^d \\ \tilde{\varepsilon}^s \end{pmatrix} \quad (7.13)$$

It corresponds to the triclinic situation in which the coupling tensor has been canceled. This decoupling occurs for symmetry reasons from the cubic classes, thus from the much higher symmetry classes. In consequence, it results in an exotic elastic behaviour. And it is not difficult to find that this exotic behaviour occurs specifically in 3D cases and it is stable by inversion.

Example 8

We provide an example of a matrix that can be used to characterise a decoupled exotic triclinic material:

$$[\underline{\underline{C}}] = \frac{1}{3} \begin{pmatrix} 154 & 71 & 51 & -15 & -29 & 1 \\ * & 198 & 7 & 30 & 55 & -2 \\ * & * & 218 & -15 & -26 & 1 \\ * & * & * & 198 & 33 & 30 \\ * & * & * & * & 225 & 51 \\ * & * & * & * & * & 63 \end{pmatrix}_{\mathcal{K}} \quad (7.14)$$

it is triclinic and positive definite with its eigenvalues $\{101.9, 92, 59.7, 58.1, 27.9, 12.2\}$. Given $\underline{\underline{1}}$ an eigentensor of $\underline{\underline{C}}$, we have:

$$[\underline{\underline{C}} : \underline{\underline{1}}] = \begin{pmatrix} 92 & 0 & 0 \\ * & 92 & 0 \\ * & * & 92 \end{pmatrix}$$

Hence the spheric and deviatoric modes are uncoupled.

This situation leads to the fact that a sphere of material under hydrostatic loading deforms isotropically. However, in the standard triclinic case, the deformation would be an ellipse whose parameters would be related to the spectral properties of $\underline{\underline{h}}^b$. In order to illustrate it, a numerical test will be implemented on FEniCS: a spherical-shaped triclinic material under hydrostatic loading. To this end, the initial state of this material can be observed in [Figure 7.4a](#), along with its mesh. The hydrostatic loading is imposed upon the external surface of the sphere and is normal to the boundary facets. For the first test, a randomly generated triclinic elasticity tensor is used to characterise the linear elasticity of this material. And then, by solving the linear problem based on Hooke's law, we can obtain the deformed state of this material. In [Figure 7.4b](#), it is possible to notice that a triclinic material does not react with the same behaviour in all directions, but becomes more elliptical with respect to the traction/compression force applied.

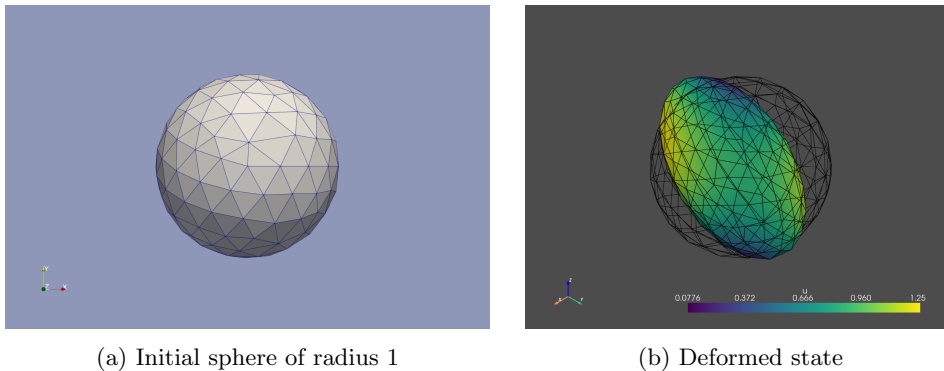


Figure 7.4: Result of a numerical test on a coupled triclinic material under hydrostatic loading (compression)

We then perform the same test on a decoupled triclinic material characterised by [Equation 7.13](#). The former randomly generated triclinic elasticity tensor will be replaced by a decoupled triclinic tensor to define a new linear problem. After solving the problem, we are able to plot the new result in [Figure 7.5](#). It is easy to see that the deformed sphere maintains a spherical shape.

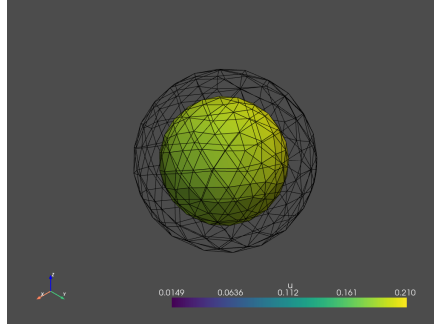


Figure 7.5: Result of a numerical test on a decoupled triclinic material under hydrostatic loading (compression)

7.3.3 Anisotropic materials with isotropic Young's modulus

Young's modulus of a linear elastic isotropic material is isotropic or orientation-independent. Is it possible for an anisotropic material to exhibit an isotropic Young's modulus? This section is inspired by the work of He [10], in which he concluded that an anisotropic material exhibiting an isotropic Young's modulus can be only either transversely isotropic or orthotropic. This definitive answer will be deduced as follows. Moreover, we aim at giving complete polynomial covariant conditions to characterise these kinds of exotic materials.

Given \underline{n} as a unit direction vector, Young's modulus of a material can be expressed in function of \underline{n} , that is $E(\underline{n})$. The parameter $\frac{1}{E(\underline{n})}$ depends on the compliance tensor $\underset{\approx}{\mathbb{S}} = \underset{\approx}{\mathbb{C}}^{-1}$ only through the associated totally symmetric tensor $\underset{\approx}{\mathbb{S}}^s$ (Cauchy elastic tensor) [10, 165], that is:

$$\frac{1}{E(\underline{n})} = \underset{\approx}{\mathbb{S}}^s :: \underline{n}^{\otimes 4} \quad (7.15)$$

To get knowledge on what the totally symmetric tensor $\underset{\approx}{\mathbb{S}}^s$ specifically represents for, in the other words, its relationship with harmonic components $\{\alpha^-, \beta^-, \underset{\sim}{h}^{a-}, \underset{\sim}{h}^{b-}, \underset{\approx}{\mathbb{H}}^-\}$ of $\underset{\approx}{\mathbb{S}}$, we will apply the explicit harmonic decomposition of Schur-Weyl:

$$\underset{\approx}{\mathbb{S}} = \alpha^- \underset{\sim}{1} \otimes_{(2,2)} \underset{\sim}{1} + \beta^- \underset{\sim}{1} \otimes_{(4)} \underset{\sim}{1} + \underset{\sim}{h}^{a-} \otimes_{(2,2)} \underset{\sim}{1} + \underset{\sim}{h}^{b-} \otimes_{(4)} \underset{\sim}{1} + \underset{\approx}{\mathbb{H}}^- \quad (7.16)$$

This formulation is well adapted to our problem, effectively decomposing $\underset{\approx}{\mathbb{S}}$ into a totally symmetric part and an asymmetric part. Among these five harmonic components $\{\alpha^-, \beta^-, \underset{\sim}{h}^{a-}, \underset{\sim}{h}^{b-}, \underset{\approx}{\mathbb{H}}^-\}$, the totally symmetric part concerns only three of them, that is $\{\beta^-, \underset{\sim}{h}^{b-}, \underset{\approx}{\mathbb{H}}^-\}$. Thus, the orientation distribution of $\frac{1}{E(\underline{n})}$ in Equation 7.15 take the forms:

$$\frac{1}{E(\underline{n})} = \underset{\approx}{\mathbb{S}}^s :: \underline{n}^{\otimes 4} = \beta^- + \underset{\sim}{h}^{b-} : \underset{\sim}{n}^{\otimes 2} + \underset{\approx}{\mathbb{H}}^- :: \underset{\approx}{n}^{\otimes 4} \quad (7.17)$$

It is now immediately from Equation 7.16 that an isotropic Young's modulus requires the condition $\underset{\sim}{h}^{b-} = 0$ and $\underset{\approx}{\mathbb{H}}^- = 0$. Observe that in this case the corresponding elastic compliance tensor $\underset{\approx}{\mathbb{S}}$ can be anisotropic since $\underset{\sim}{h}^{a-} \neq 0$. Thus, this situation can be defined by the following harmonic structure:

$$\underset{\approx}{\mathbb{C}}^{-1} = f(\alpha^-, \beta^-, \underset{\sim}{h}^{a-}, 0, 0)$$

Since only one anisotropic component $\underset{\sim}{h}^{a-} \in \mathbb{H}^2$ has been concerned in this harmonic structure, the

resulting symmetry classes of \mathbb{S} is either orthotropic $[D_2]$ or transversely isotropic $[O(2)]$. We obtain the following two exotic materials:

- Orthotropic materials with isotropic Young’s modulus:

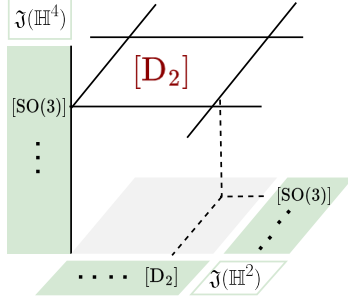


Table 7.7: Orthotropic materials with isotropic Young’s modulus

\odot	$[D_2] = [D_2]_{\mathbb{H}^{a-}} \odot [SO(3)]_{\mathbb{H}^{b-}} \odot [SO(3)]_{\mathbb{H}}$
Conditions	$\mathbb{h}^{a-} \times (\mathbb{h}^{a-})^2 \neq 0, \mathbb{h}^{b-} = 0$ and $\mathbb{H}^- = 0$

The identification of this kind of material requires additional conditions independent of those imposed by the symmetry argument:

$$\Sigma_{[D_2]}^g \xrightarrow{\mathbb{h}^{b-}=0, \mathbb{H}^-=0} \Sigma_{[D_2]}^e \tag{7.18}$$

It fulfils the first requirement stated in Definition 7.1.1 while displaying the characteristic of so-called *hypersymmetric*, as evidenced by its isotropic Young’s modulus. Consequently, we can ascertain that it’s an exotic material.

Example 9

We provide an example of a matrix that can be used to characterise this orthotropic material with isotropic Young’s modulus:

$$[\mathbb{C}]_{\approx} = \begin{pmatrix} 1377 & -1071 & -306 & 0 & 0 & 0 \\ * & 1113 & 42 & 0 & 0 & 0 \\ * & * & 348 & 0 & 0 & 0 \\ * & * & * & 476 & 0 & 0 \\ * & * & * & * & 612 & 0 \\ * & * & * & * & * & 2142 \end{pmatrix}_{\kappa} \tag{7.19}$$

it is positive definite with its eigenvalues $\{2357.2, 2142, 612, 476, 425.9, 254.8\}$. The associated compliance tensor is:

$$[\mathbb{S}]_{\approx} = \frac{1}{4284} \begin{pmatrix} 30 & 28 & 23 & 0 & 0 & 0 \\ * & 30 & 21 & 0 & 0 & 0 \\ * & * & 30 & 0 & 0 & 0 \\ * & * & * & 9 & 0 & 0 \\ * & * & * & * & 7 & 0 \\ * & * & * & * & * & 2 \end{pmatrix}_{\kappa} \tag{7.20}$$

Thus, we obtain isotropic directional Young modulus: $\frac{1}{E(\underline{n})} = \mathbb{S}(\underline{n}) = \frac{5}{714}$.

- Transversely isotropic materials with isotropic Young’s modulus:

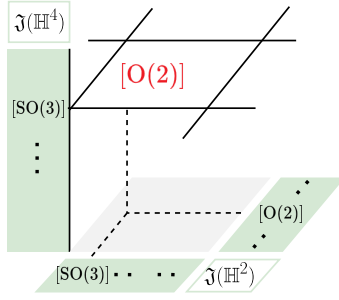


Table 7.8: Transversely isotropic materials with isotropic Young's modulus

\odot	$[O(2)] = [O(2)]_{\tilde{h}^{a-}} \odot [SO(3)]_{\tilde{h}^{b-}} \odot [SO(3)]_{\tilde{H}}$
Conditions	$\tilde{h}^{a-} \times (\tilde{h}^{a-})^2 = 0, \tilde{h}^{a-} \neq 0, \tilde{h}^{b-} = 0$ and $\tilde{H} = 0$

Thus, this exotic case can be obtained based on a generic $[O(2)]$ case, the transition between these two cases is:

$$\Sigma_{[O(2)]}^g \xrightarrow{\tilde{h}^{b-}=0, \tilde{H}^-=0} \Sigma_{[O(2)]}^e \quad (7.21)$$

it can also be obtained based on the previous case in Equation 7.18, the transition between each other shows as follows:

$$\Sigma_{[D_2]}^g \xrightarrow{\tilde{h}^{b-}=0, \tilde{H}^-=0} \Sigma_{[D_2]}^e \xrightarrow{\tilde{h}^a \times (\tilde{h}^a)^2=0, \tilde{h}^a \neq 0} \Sigma_{[O(2)]}^e \quad (7.22)$$

These two different manners to get $\Sigma_{[O(2)]}^e$ indicate two possibilities to realise the corresponding material design, either by an initialisation of a generic transversely isotropic material and setting the cost function by covariant condition in Equation 7.21, or by initialisation of a generic orthotropic material and setting the cost function by covariant condition in Equation 7.22.

Synthesis

In this section, we've listed 5 different exotic materials (Table 7.4-7.8). Among these five exotic materials, we found that some of them possess the same construction of $([G_1]_{\tilde{h}^a}, [G_2]_{\tilde{h}^b}, [G_3]_{\tilde{H}})$. For instance, both the 3D R_0 -orthotropic materials and orthotropic materials with isotropic Young's modulus fall in the case of Table 7.4, indicating that their respective strata $\Sigma_{[D_2]}^e$ are identical. However, they refer to two totally different materials, since the underlying mechanical meanings of harmonic components are differently defined.

This observation highlights the heightened complexity exhibited by the exotic sets within $\mathbb{E}la(3)$. Firstly, within a specific symmetry class, there exist multiple distinct exotic sets. Secondly, for each of these exotic sets, varying interpretations arising from explicit decomposition lead to the emergence of diverse exotic materials.

Part IV

Conclusions and perspectives

Conclusions

This Ph.D. thesis opens a great perspective on the theoretical investigation of anisotropy of a physical property encoded by constitutive tensors. The basic mathematical framework can be dated to 1970 [67], the researchers use symmetry classes (based on the group theory) to identify the anisotropy properties of a given material. Based on this, and thanks to the upcoming work of N. Auffray and its collaboration with mathematicians [107], they have developed an axe of research focused on the geometry of tensor spaces, including clips operation between symmetry classes and the construction of polynomial invariant/covariant conditions to identify each symmetry class. Thanks to this geometrical description of tensor space in a very fine way, my Ph.D. work is aimed at exploring the complete intermediate anisotropy possibilities beyond symmetry classes for a given constitutive law. Some examples have been already documented a priori in the literature [9, 10]. The advantage of these materials is that they process exotic mechanical behaviour. These findings indicate the great potential in this research field.

This thesis focuses on the linear elasticity for 2D and 3D, the important results are as follows:

1. **Determination of a whole range of exotic sets beyond symmetry classes.** The geometrical tools have been applied to linear elasticity, and based on our proposed definition of *exotic materials*, it can be concluded that there is only one exotic set for 2D linear elasticity and there are 1052 exotic sets in 3D. Moreover, the corresponding mechanical interests of some cases have been discussed, which is mainly through the use of harmonic decomposition.
2. **Identification of exotic sets by polynomial conditions.** The polynomial condition for an exotic set in 2D case (that is R_0 -orthotropy) has already been well-developed in literature. This thesis provides a comprehensive overview of various conditions, encompassing polynomial invariant conditions, polynomial covariant conditions, and polar component conditions. Furthermore, it elucidates the interconnections among these conditions and undertakes an extended investigation into the inverse stability of this exotic set. It allows revealing that the compliance behaviour of a R_0 -orthotropic material does not exhibit this particular property. However, we have shown that the situation for 3D is rather complex and the characterisation of exotic sets is possible only by using polynomial covariant conditions. Instead of giving polynomial covariant conditions for all these 1052 exotic sets, we came up with a strategy on how to construct these conditions based on several practical tables. And it was applied to three interesting cases: 3D R_0 -orthotropy, triclinic exotic elastic materials and anisotropic materials with isotropic Young's modulus.
3. **Mesostructure design of exotic materials.** The aforementioned polynomial conditions serve as cost functions in topology optimisation problems. Based on it, we realized the numerical design of R_0 -orthotropic material and a Cauchy elasticity material by using the level set-based topological derivative algorithm.

Despite focusing mainly on linear elasticity, this methodology can be extended to other constitutive laws. For the 2D case, an exact formula is given to compute the total number of exotic sets for a given constitutive law, e.g. Cosserat elasticity and piezoelectricity. The design of 3D exotic materials is still ongoing.

Perspectives

The advantage of our theory is that we provide a unified perspective on the design of architected materials with anisotropic exotic behaviors and, above all, the cases scattered here and there in the

literature can be shown to be the special ones of what is obtained through applying our theoretical tools which indicates a great perspective of the upcoming possibilities. Certainly, as is shown within this document, our study predominantly focused on the theoretical phase and constitutes an attempt at linear elasticity. Based on it, future research can unfold in the following directions.

Design of exotic materials in $\mathbb{E}la(3)$

We believe that the outcome of architected material design will be encouraging since it avoids remaining just on the theoretical aspect and by additive manufacturing of these architected materials, the underlying exotic mechanical properties can be identified by experimental tests.

In the case of 2D materials, we have presented a complete research strategy, ranging from theoretical determination of exotic materials to practical material design in terms of periodic mesostructure (R_0 orthotropy). However, in the case of 3D materials, this thesis is primarily concerned with the theoretical investigation, with the completion of the material design still pending. Nevertheless, this design is within reach, since the polynomial covariant conditions (they are used to define the cost functions for optimisation problems) for the three exotic cases are already given in [section 7.3](#). Thus, we will simply extend the optimization algorithm from 2D to 3D to directly implement the optimization design. This work is still ongoing and will be published in a forthcoming paper.

Identification and validation by experimental tests

Despite major experimental work that has been carried out in the past on the anisotropy of standard materials [171], the study of architected materials has remained very limited. This is largely due to the complexity of their behaviour, which requires a wide range of loadings and measurements (standard biaxial tests can be used to perform tension in 2 perpendicular directions and shear, but always in the same main frame of reference).

The execution of the work in this aspect is independent of the research on exotic materials. A testing machine for periodic architected materials ([Figure 7.6](#)) has already been developed by our partnership with M. Poncelet and T. Dassonville [172] under the MAX-OASIS project. The designed exotic materials during my Ph.D. study require further experimental validation to study the feasibility of theoretical architectures and the sensitivity of their behaviour to manufacturing defects.

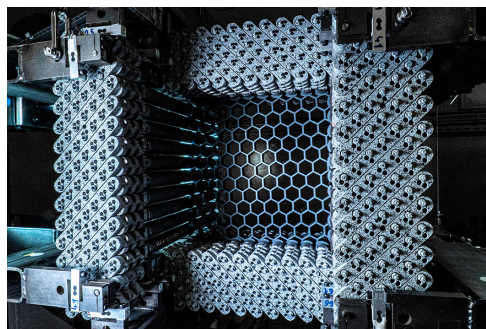


Figure 7.6: Testing device for architected materials

Instability-induced exotic anisotropy

When composed of slender elements, architected materials can undergo large deformations, exhibiting geometric non-linearities through buckling or snapping behaviours of the cell walls [46]. This can

create a new pattern in the material with different properties than the original structure. This can be observed from the hexagonal honeycomb example in [Figure 7.7](#).

The research in this field constitutes one of the threefold axes in MAX-OASIS project and will be accomplished within the Ph.D. study of Rachel Azulay entitled *Conception numérique de matériaux architecturés à instabilités contrôlées*. They proposed a method based on group theory to predict the possible patterns of an architected material following a bifurcation. Such a method aligns closely with the theoretical foundations of the approaches used in my work. Thus, I hold the prospect of combining our works to potentially extend the investigation of exotic materials within the instability-induced context. That is, to design a peculiar architected material, which presents a normal anisotropic property in its initial state but will emerge exotic anisotropy when a specific instability-induced pattern generation occurs. This represents an extension of my current research both in terms of theory and applications (especially with regard to dynamic control of wave propagation).

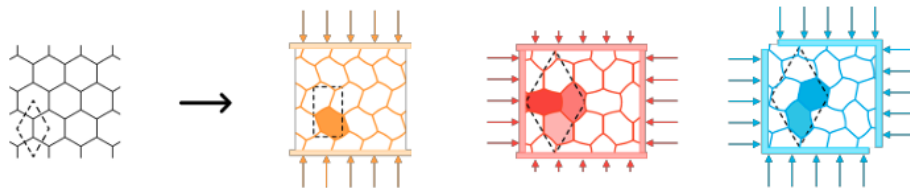


Figure 7.7: In compression, the hexagonal honeycomb generates different patterns depending on its boundary conditions [4] (from right to left: initial geometry, under uniaxial compression, under biaxial compression, and under equibiaxial compression)

Appendix A

Mathematical notations

Index symmetries:

- $T_{(ij)kl}$: minor index symmetry, $T_{(ij)kl} \Leftrightarrow T_{ijkl} = T_{jikl}$;
- $T_{\underline{ij}\underline{kl}}$: major index symmetry, $T_{\underline{ij}\underline{kl}} \Leftrightarrow T_{ijkl} = T_{klij}$;
- $T_{(ijkl)}$: totally index symmetry of a tensor (with respect to any permutation of their indices);

Spaces:

- \mathbb{V} : vector space, noted by \mathbb{V}^d if there is ambiguity about the dimension ;
- \mathbb{R}^d : $\mathbb{R}^d = \{(x_1, x_2, \dots, x_d) : x_1 \in \mathbb{R}, x_2 \in \mathbb{R}, \dots, x_d \in \mathbb{R}\}$, represents the real vector space of dimension d ;
- $\mathbb{T}^n(\mathbb{R}^d) := \otimes^n \mathbb{R}^d$, vector space of tensors of order n on \mathbb{R}^d , $T \in \mathbb{T}^n(\mathbb{R}^d)$. Noted by \mathbb{T}^n when there's no ambiguity about the dimension.;
- $S^n(\mathbb{R}^d)$: the space of totally index symmetric tensors, it is the subspace of $\mathbb{T}^n(\mathbb{R}^d)$;
- $\mathbb{Ela}(\mathbb{R}^d)$: vector space of elasticity tensors on \mathbb{R}^d . $\mathbb{Ela}(\mathbb{R}^d) := \left\{ \underset{\approx}{\mathbb{C}} \in \otimes^4 \mathbb{R}^d \mid C_{(\underline{ij})(\underline{kl})} \right\}$ and $\mathbb{Ela}(\mathbb{R}^d) \in \mathbb{T}^4$;
- $\mathbb{H}^n(\mathbb{R}^d)$: vector space of harmonic tensors of order n in dimension d . For $d = 2$, $\mathbb{H}^n(\mathbb{R}^2)$ denotes \mathbb{K}^n ; For $d = 3$, $\mathbb{H}^n(\mathbb{R}^3)$ denotes \mathbb{H}^n ;
- \mathbb{K}^{-1} : pseudo-scalar space, a physical quantity represented by a number that changes sign when the physical system undergoes polar symmetry or inversion.
- $\mathcal{M}_d(\mathbb{R})$: vector space of real matrices of dimension $d \times d$.

Operations:

- $\text{tr}T$: trace of tensor T . It is obtained by the contraction of any two indices i, j of T .
- \otimes : standard tensor product and \otimes^n indicates its power of n .;
- \oplus : represents the direct sum of vector spaces;
- \odot : clips operation between symmetry classes;

- $*$: harmonic product between two harmonic tensors, in \mathbb{R}^2 it is defined as $X * Y := X \otimes Y - \frac{1}{2} \text{tr}(X \cdot Y) \underset{\sim}{\mathbb{J}}$, with $X, Y \in \mathbb{K}^n$;
- \cdot^n : contraction of order n between two tensors, $T \cdot^n K := T_{i_1 i_2 i_3 \dots i_k p_1 p_2 \dots p_n} K_{p_1 p_2 \dots p_n j_1 j_2 \dots j_i}$;
- $(\cdot)^s$: complete symmetrisation of a tensor;
- \odot : symmetric tensor product between two tensors, in \mathbb{R}^2 we have $S_1 \odot S_2 := (S_1 \otimes S_2)^s \in \mathbb{S}^{n_1+n_2}(\mathbb{R}^2)$, with $S_1 \in \mathbb{S}^{n_1}(\mathbb{R}^2)$, $S_2 \in \mathbb{S}^{n_2}(\mathbb{R}^2)$;
- $*$: the harmonic product between two harmonic tensors, in \mathbb{R}^2 it is defined as $K_1 * K_2$ the projection of the classical tensor product on $\mathbb{K}^{n_1+n_2}$. This product is computed as follows

$$(K_1 * K_2) = K_1 \odot K_2 - \frac{1}{2} (\underset{\sim}{1} \otimes (K_1 \cdot K_2))^s$$

with $K_1 \in \mathbb{K}^{n_1}$ and $K_2 \in \mathbb{K}^{n_2}$;

- \times : the skew-symmetric contraction between two totally symmetric tensors, in \mathbb{R}^2 it is defined as:

$$(S_1 \times S_2) := -(S_1 \cdot \underset{\sim}{\epsilon} \cdot S_2)^s \in \mathbb{S}^{n_1+n_2-2}(\mathbb{R}^2),$$

with $S_1 \in \mathbb{S}^{n_1}(\mathbb{R}^2)$, $S_2 \in \mathbb{S}^{n_2}(\mathbb{R}^2)$ and $\underset{\sim}{\epsilon}$ is the Levi-Civita tensor.

- S : Symmetrized product
- Λ : Anti-symmetrized product

Tensors:

- Tensors of order 0,1,2,4 are respectively represented by $\alpha, \underline{v}, \underset{\sim}{a}, \underset{\sim}{\Lambda}$;
- $\underset{\sim}{1}$: identity tensor of order 2, $1_{ij} = \delta_{ij}$;
- $\underset{\sim}{\mathbb{I}}$: identity tensor of order 4 for $S^2(\mathbb{R}^2)$, $I_{ijkl} = \frac{1}{2}(\delta_{ik}\delta_{jl} + \delta_{il}\delta_{jk})$;
- $\underset{\sim}{K}$: spherical projector of \mathbb{R}^2 , $K_{ijkl} = (\frac{1}{2}\underset{\sim}{1} \otimes \underset{\sim}{1})_{ijkl} = \frac{1}{2}\delta_{ij}\delta_{kl}$;
- $\underset{\sim}{J}$: deviatoric projector of \mathbb{R}^2 , $J_{ijkl} = I_{ijkl} - K_{ijkl} = \frac{1}{2}(\delta_{ik}\delta_{jl} + \delta_{il}\delta_{jk} - \delta_{ij}\delta_{kl})$.
- $\mathbb{T}_{ijkl}^{(1)} = (\underset{\sim}{1} \otimes \underset{\sim}{1})_{ijkl} = \delta_{ij}\delta_{kl}$
- $\mathbb{T}_{ijkl}^{(2)} = (\underset{\sim}{1} \otimes \underset{\sim}{1})_{ijkl} = \delta_{ik}\delta_{jl}$
- $\mathbb{T}_{ijkl}^{(3)} = (\underset{\sim}{1} \otimes \underset{\sim}{1})_{ijkl} = \delta_{il}\delta_{jk}$

Groups:

- $\text{GL}(\mathbb{V}^d)$: group of invertible linear transformations of a vector space \mathbb{V}^d , if $\mathbb{V}^d = \mathbb{R}^d$, $\text{GL}(\mathbb{V}^d)$ is denoted by $\text{GL}(d)$;
- $\text{O}(d)$: group of orthogonal transformations. As a matrix group:

$$\text{O}(d) := \{M \in \mathcal{M}_d(\mathbb{R}) \mid M^T M = I_d\}$$

where M^T is the transpose of M .

Divers:

-
- I_d : identity matrix of dimension $d \times d$;
 - $\mathcal{L}(\mathbb{E}, \mathbb{F})$: space of linear applications from \mathbb{E} to \mathbb{F} ;
 - \simeq : isomorphism relationship;
 - \sim : equivalence relation between two tensors;
 - \mathcal{IB} : integrity basis;
 - $\langle \underline{a}, \underline{b} \rangle$: scalar product between two vectors ;
 - $[T]$: matrix representation of tensor $T \in \mathbb{T}^n$;
 - $\Sigma_{[H]}$: stratum of tensors whose symmetry class is exactly $[H]$;
 - $u_{i,j}$: partial derivative of u : $\frac{\partial u_i}{\partial x_j}$

Appendix B

Level set based topological derivative algorithm

B.1 Flowchart of the algorithm

We summarize in [Figure B.1](#) the algorithm for the optimization of microstructures based on an exact formula for the topological derivative of the macroscopic elasticity tensor (estimated by a multi-scale theory) and a level-set representation [2].

B.2 Defining subdomains for different materials

Different material phases are defined as subdomains in FEniCS by class `SubDomain`, and the material parameters can be defined accordingly. To this end, we first use the level set function to define the boundary, it acts as a shortcut to the subdomain definition. As showed in lines:

```
1 class Omega_0(SubDomain):
2     def inside(self, x, on_boundary):
3         return lsf_project(x[0], x[1]) <= 0 + tol
```

with `lsf_project` is the output of the level set function projects onto a `MeshFunction`¹ space, which allows evaluating the level set value on each vertex. FEniCS will call the `inside` function for each vertex in a cell to determine whether or not the cell belongs to a particular subdomain. Saying that a triangular cell belongs to a subdomain if at least two of its vertices belong to it.

Remark. *For this reason, it is important that the test holds in cells aligned with the boundary. We use a tolerance $tol = 1 \times 10^{-14}$ to make the cells both above and below the internal boundary belong to either Ω_μ^m or Ω_μ^m . That explains the existence of the rough interface contour.*

In our implementation, the subdomain of Ω_μ^m is tagged with the number 0, and the complementary part Ω_μ^i is tagged with number 1. The material property parameters can be assigned to the corresponding subdomains by the values of these tags.

¹The discrete function that can be evaluated at a set of so-called mesh entities.

B.3 Line search

The line search process is dominated by step size $\kappa \in [0, 1]$ (cf. Equation 5.26) in order to decrease the value of the cost function J . In this context, the line search algorithm is separated into two situations based on the different cost function variations (decrease or increase).

- $J_{n+1} < J_n$:

In this case, the main iteration will go on. In order to speed up the algorithm, we divide the current value κ by 0.8 to take larger steps.

- $J_{n+1} > J_n$:

In this case, we jump out of the current loop and return to the previous level set function. The step size κ will be reduced by multiplying it by 0.8, then the level set function will be updated with this new step size. This processes will be stopped and go back to the main loop until the cost function is reduced.

B.4 Stopping criterion

The iterative process is stopped when the maximum difference between the value of the cost function at the current iteration and the values of the four previous iterations is below a certain tolerance. In order to take a smaller tolerance when the mesh gets finer, it will be defined in terms of the mesh size, read $\frac{2J}{N^2}$.

However, if at this stage, the optimality condition 5.23 is not satisfied, which means that the value θ is larger than the desired degree of accuracy $\epsilon_\theta = 5^\circ$, a uniform mesh refinement of the RVE will be carried out, and the iteration will continue.

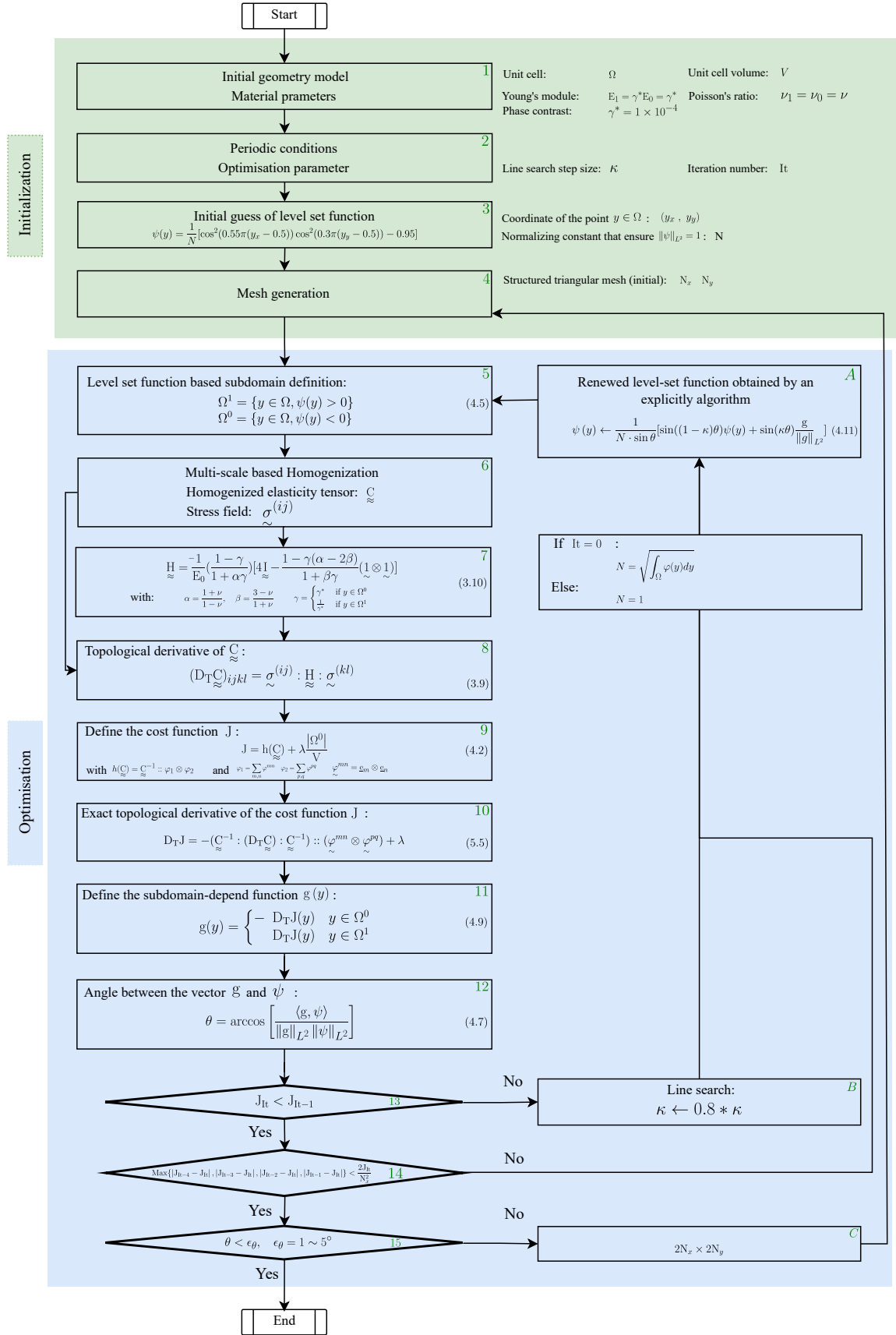


Figure B.1: Flowchart of the level set based topological derivative algorithm

Appendix C

Covariant criteria for tensor's symmetry

The main results of this annex are mainly used to characterise the symmetry classes for a given tensor or an n-tuple tensors, which is used to complete the Theorem 6.5. The proofs are provided in [78].

Lemma C.1 (Second order tensors' symmetry). *Let $\underset{\sim}{\mathbf{a}}$ be a symmetric second-order tensor. Then, $\underset{\sim}{\mathbf{a}}$ is at least transversely isotropic if and only if $\underset{\sim}{\mathbf{a}} \times \underset{\sim}{\mathbf{a}}^2 = 0$.*

Theorem C.1: Characterisation of the symmetry class for n-tuple second-order tensors

Let $(\underset{\sim}{\mathbf{a}}_1, \dots, \underset{\sim}{\mathbf{a}}_n)$ be an n-tuple of second-order symmetric tensors. Then:

1. $(\underset{\sim}{\mathbf{a}}_1, \dots, \underset{\sim}{\mathbf{a}}_n)$ is isotropic if and only if

$$\underset{\sim}{\mathbf{a}}_k^d = 0, \quad 1 \leq k \leq n,$$

where $\underset{\sim}{\mathbf{a}}_k^d$ is the deviatoric part of $\underset{\sim}{\mathbf{a}}_k$.

2. $(\underset{\sim}{\mathbf{a}}_1, \dots, \underset{\sim}{\mathbf{a}}_n)$ is transversely isotropic if and only if there exists $\underset{\sim}{\mathbf{a}}_j$ such that

$$\underset{\sim}{\mathbf{a}}_j^d \neq 0, \quad \underset{\sim}{\mathbf{a}}_j \times \underset{\sim}{\mathbf{a}}_j^2 = 0,$$

and

$$\underset{\sim}{\mathbf{a}}_j \times \underset{\sim}{\mathbf{a}}_k = 0, \quad 1 \leq k \leq n \text{ and } j \neq k$$

3. $(\underset{\sim}{\mathbf{a}}_1, \dots, \underset{\sim}{\mathbf{a}}_n)$ is orthotropic if and only if

$$\text{tr}(\underset{\sim}{\mathbf{a}}_k \times \underset{\sim}{\mathbf{a}}_l) = 0, \quad 1 \leq k, l \leq n$$

and there exists $\underset{\sim}{\mathbf{a}}_j$ such that $\underset{\sim}{\mathbf{a}}_j \times \underset{\sim}{\mathbf{a}}_j^2 \neq 0$ or there exists a pair $(\underset{\sim}{\mathbf{a}}_i, \underset{\sim}{\mathbf{a}}_j)$ such that $\underset{\sim}{\mathbf{a}}_i \times \underset{\sim}{\mathbf{a}}_j \neq 0$

4. $(\underset{\sim}{\mathbf{a}}_1, \dots, \underset{\sim}{\mathbf{a}}_n)$ is monoclinic if and only if there exists a pair $(\underset{\sim}{\mathbf{a}}_i, \underset{\sim}{\mathbf{a}}_j)$ such that $\underline{\mathbf{w}} := \text{tr}(\underset{\sim}{\mathbf{a}}_i \times \underset{\sim}{\mathbf{a}}_j) \neq 0$ and

$$(\underset{\sim}{\mathbf{a}}_k \underline{\mathbf{w}}) \times \underline{\mathbf{w}} = 0, \quad 1 \leq k \leq n.$$

In what follows, we will be interested in the characterisation of symmetry classes of a given fourth-order harmonic tensor $\underset{\sim}{\mathbb{H}} \in \mathbb{H}^4$. Any homogeneous polynomial covariant of $\underset{\sim}{\mathbb{C}} \in \mathbb{E}la$ of type $S^n(\mathbb{R}^3)$ can thus be identified with a polynomial in $\text{Cov}_n(\mathbb{E}la)$.

Lemma C.2 (Relations between $\text{Cov}_1(\underline{\mathbb{H}})$ and $\text{Cov}_2(\underline{\mathbb{H}})$). *Let $\underline{\mathbb{H}} \in \mathbb{H}^4$ be a fourth-order harmonic tensor. Then*

1. $\text{Cov}_1(\underline{\mathbb{H}}) = \{0\}$ *if and only if $\text{Cov}_2(\underline{\mathbb{H}})$ is at least orthotropic;*
2. $\dim\text{Cov}_1(\underline{\mathbb{H}}) = 1$ *if and only if $\text{Cov}_2(\underline{\mathbb{H}})$ is monoclinic;*
3. $\dim\text{Cov}_1(\underline{\mathbb{H}}) = 3$ *if and only if $\text{Cov}_2(\underline{\mathbb{H}})$ is triclinic;*

Theorem C.2: Symmetry classes of \mathbb{H}

Let $\mathbb{H} \in \mathbb{H}^4$ be a fourth order harmonic tensor. The following propositions are equivalent.

Case 1

1. $\text{Cov}_2(\mathbb{H})$ is isotropic;
2. \mathbb{H} is either cubic ($d_2 \neq 0$) or isotropic ($d_2 = 0$);
3. d_2 is isotropic.

Case 2

1. $\text{Cov}_2(\mathbb{H})$ is transversely isotropic;
2. \mathbb{H} is trigonal, tetragonal or transversely isotropic;
3. the pair (d_2, c_3) is transversely isotropic.

Case 3

1. $\text{Cov}_2(\mathbb{H})$ is orthotropic;
2. \mathbb{H} is orthotropic;
3. $v_5 = v_6 = 0$ and the pair (d_2, c_3) is orthotropic.

where $v_5 := \varepsilon : (d_2 c_3)$ and $v_6 := \varepsilon : (d_2 c_4)$.

Case 4

1. $\text{Cov}_2(\mathbb{H})$ is monoclinic;
2. \mathbb{H} is monoclinic;
3. the triplet (d_2, c_3, c_4) is monoclinic.

Case 5

1. $\text{Cov}_2(\mathbb{H})$ is triclinic;
2. \mathbb{H} is triclinic;
3. the triplet (d_2, c_3, c_4) is triclinic.

This theorem is completed by the following lemma which allows to distinguish between the symmetry classes in case 2: trigonal, tetragonal and transversely isotropic.

Lemma C.3 (Distinguish between the symmetry classes in case 2). *Let $\mathbb{H} \in \mathbb{H}^4$ be a fourth-order harmonic tensor. Then*

1. $\underline{\underline{\mathbb{H}}}$ is transversely isotropic if and only if $\underline{\underline{d_2}}$ is transversely isotropic and

$$\underline{\underline{\mathbb{H}}} \times \underline{\underline{d_2}} = 0;$$

2. $\underline{\underline{\mathbb{H}}}$ is tetragonal if and only if $\underline{\underline{d_2}}$ is transversely isotropic and

$$\underline{\underline{\mathbb{H}}} \times \underline{\underline{d_2}} \neq 0, \quad \text{and} \quad \text{tr}(\underline{\underline{\mathbb{H}}} \times \underline{\underline{d_2}}) = 0;$$

3. $\underline{\underline{\mathbb{H}}}$ is trigonal if and only if $\underline{\underline{d_2}}$ is transversely isotropic,

$$\text{tr}(\underline{\underline{\mathbb{H}}} \times \underline{\underline{d_2}}) \neq 0, \quad \text{and} \quad (\underline{\underline{\mathbb{H}}} : \underline{\underline{d_2}}) \times \underline{\underline{d_2}} = 0$$

Lemma C.4 (Symmetry class of a pair $(\underline{\underline{\mathbb{H}}}, \underline{\underline{h}})$). *Let $\underline{\underline{\mathbb{H}}}$ be a cubic fourth-order harmonic tensor ($\underline{\underline{\mathbb{H}}} \in \Sigma_{[\mathcal{O}]}$) and $\underline{\underline{h}} \in S^2(\mathbb{R}^2)$ be transversely isotropic ($\underline{\underline{h}} \in \Sigma_{[\mathcal{O}(2)]}$). Then*

1. $(\underline{\underline{\mathbb{H}}}, \underline{\underline{h}})$ is tetragonal if and only if

$$\text{tr}(\underline{\underline{\mathbb{H}}} \times \underline{\underline{h}}) = 0;$$

2. $(\underline{\underline{\mathbb{H}}}, \underline{\underline{h}})$ is trigonal if and only if

$$\text{tr}(\underline{\underline{\mathbb{H}}} \times \underline{\underline{h}}) \neq 0, \quad \text{and} \quad \underline{\underline{h}} \times (\underline{\underline{\mathbb{H}}} : \underline{\underline{h}}) = 0;$$

3. $(\underline{\underline{\mathbb{H}}}, \underline{\underline{h}})$ is orthotropic if and only if

$$\underline{\underline{h}} \times (\underline{\underline{\mathbb{H}}} : \underline{\underline{h}}) \neq 0, \quad \text{and} \quad \text{tr}(\underline{\underline{h}} \times (\underline{\underline{\mathbb{H}}} : \underline{\underline{h}})) = 0$$

4. $(\underline{\underline{\mathbb{H}}}, \underline{\underline{h}})$ is monoclinic if and only if

$$\text{tr}(\underline{\underline{h}} \times (\underline{\underline{\mathbb{H}}} : \underline{\underline{h}})) \neq 0, \quad \text{and} \quad \text{tr}(\underline{\underline{h}} \times (\underline{\underline{\mathbb{H}}} : \underline{\underline{h}})) \times \text{tr}(\underline{\underline{h}} \times (\underline{\underline{\mathbb{H}}} : \underline{\underline{h}})^2) = 0$$

Appendix D

Generic and exotic sets of $\mathbb{E}la(3)$

We will consider $\Sigma_{[G]}^g$ or $\Sigma_{[G]}^{e_i}$ as the minimal unit of strata of $\mathbb{E}la$. The resulting symmetry class $[G]_{(\tilde{h}^a, \tilde{h}^b, \tilde{H})}$ is thus determined by the elementary symmetry classes of the following

- Proper harmonic tensors: \tilde{h}^a , \tilde{h}^b and \tilde{H} ;
- Joint harmonic tensors: $(\tilde{h}^a, \tilde{h}^b)$, (\tilde{h}^a, \tilde{H}) and (\tilde{h}^b, \tilde{H}) .

which means that $[G]_{(\tilde{h}^a, \tilde{h}^b, \tilde{H})}$ is determined by the knowledge of:

$$([G_1]_{\tilde{h}^a}, [G_2]_{\tilde{h}^b}, [G_3]_{\tilde{H}}, [G_4]_{(\tilde{h}^a, \tilde{h}^b)}, [G_5]_{(\tilde{h}^a, \tilde{H})}, [G_6]_{(\tilde{h}^b, \tilde{H})})$$

In what follows, the representation of these symmetry classes will be simplified by:

$$([G_1], [G_2], [G_3], [G_4], [G_5], [G_6])$$

The computation of the results of generic and exotic sets of $\mathbb{E}la(3)$ requires the following frequently used clips products.

\odot	$[Z_2]$	$[D_2]$	$[D_3]$	$[D_4]$	$[O(2)]$	$[O]$
$[Z_2]$	$[1], [Z_2]$					
$[D_2]$	$[1], [Z_2]$	$[1]$ $[Z_2], [D_2]$				
$[D_3]$	$[1]$	$[1], [Z_2]$	$[1], [Z_2]$ $[Z_3], [D_3]$			
$[D_4]$	$[1], [Z_2]$	$[1], [Z_2]$ $[D_2]$	$[1], [Z_2]$	$[1], [Z_2]$ $[Z_4], [D_2]$ $[D_4]$		
$[O(2)]$	$[1], [Z_2]$	$[1], [Z_2]$ $[D_2]$	$[1], [Z_2]$ $[D_2], [D_3]$	$[1], [Z_2]$ $[D_4]$	$[Z_2]$ $[D_2], [O(2)]$	
$[O]$	$[1], [Z_2]$	$[1], [Z_2]$ $[D_2]$	$[1], [Z_2]$ $[D_2], [Z_3]$ $[D_3]$	$[1], [Z_2]$ $[Z_4], [D_2]$ $[D_4]$	$[1], [Z_2]$ $[D_2], [D_3]$ $[D_4]$	$[1], [Z_2]$ $[Z_3], [Z_4]$ $[D_2], [D_3]$ $[D_4], [O(2)]$

D.1 Preliminary results of exotic sets for $\mathbb{E}a(3)$

[G]	$\mathfrak{J}(\mathbb{H}^2)$	$\mathfrak{J}(\mathbb{H}^2)$	$\mathfrak{J}(\mathbb{H}^4)$	Number	Generic/Exotic
	[G ₁]	[G ₂]	[G ₃]		
[SO(3)]	[SO(3)]	[SO(3)]	[SO(3)]	1	Generic
[\mathcal{O}]	[SO(3)]	[SO(3)]	[\mathcal{O}]	1	Generic
[O(2)]	[O(2)]	[O(2)]	[O(2)]	1	Generic
	[O(2)]	[SO(3)]	[O(2)]	2	Exotic
	[O(2)]	[O(2)]	[SO(3)]	1	
	[O(2)]	[SO(3)]	[SO(3)]	2	
	[SO(3)]	[SO(3)]	[O(2)]	1	
[D ₄]	[O(2)]	[O(2)]	[D ₄]	1	Generic
	[O(2)]	[SO(3)]	[D ₄]	2	Exotic
	[SO(3)]	[SO(3)]	[D ₄]	1	
	[O(2)]	[O(2)]	[\mathcal{O}]	1	
	[SO(3)]	[O(2)]	[\mathcal{O}]	2	
[D ₃]	[O(2)]	[O(2)]	[D ₃]	1	Generic
	[SO(3)]	[O(2)]	[D ₃]	2	Exotic
	[SO(3)]	[SO(3)]	[D ₃]	1	
	[O(2)]	[O(2)]	[\mathcal{O}]	1	
	[SO(3)]	[O(2)]	[\mathcal{O}]	2	
[D ₂]	[D ₂]	[D ₂]	[D ₂]	1	Generic
	[D ₂]	[O(2)]	[D ₂]	2	Exotic
	[D ₂]	[SO(3)]	[D ₂]	2	
	[O(2)]	[O(2)]	[D ₂]	1	
	[O(2)]	[SO(3)]	[D ₂]	2	
	[SO(3)]	[SO(3)]	[D ₂]	1	
	[D ₂]	[D ₂]	[D ₄]	1	
	[D ₂]	[O(2)]	[D ₄]	2	
	[D ₂]	[SO(3)]	[D ₄]	2	
	[O(2)]	[O(2)]	[D ₄]	1	
	[D ₂]	[D ₂]	[O(2)]	1	
	[D ₂]	[O(2)]	[O(2)]	2	
	[D ₂]	[SO(3)]	[O(2)]	2	
	[O(2)]	[O(2)]	[O(2)]	1	
	[O(2)]	[SO(3)]	[O(2)]	2	
	[D ₂]	[D ₂]	[\mathcal{O}]	1	
	[D ₂]	[O(2)]	[\mathcal{O}]	2	
	[D ₂]	[SO(3)]	[\mathcal{O}]	2	
	[O(2)]	[O(2)]	[\mathcal{O}]	1	
	[O(2)]	[SO(3)]	[\mathcal{O}]	2	
[D ₂]	[D ₂]	[SO(3)]	1		

	[D ₂]	[O(2)]	[SO(3)]	2	
	[D ₂]	[SO(3)]	[SO(3)]	2	
	[O(2)]	[O(2)]	[SO(3)]	1	
	[D ₂]	[D ₂]	[Z ₂]	1	Generic
	[D ₂]	[O(2)]	[Z ₂]	2	
	[D ₂]	[SO(3)]	[Z ₂]	2	
	[O(2)]	[O(2)]	[Z ₂]	1	
	[O(2)]	[SO(3)]	[Z ₂]	2	
	[SO(3)]	[SO(3)]	[Z ₂]	1	
	[D ₂]	[D ₂]	[D ₂]	1	
	[D ₂]	[O(2)]	[D ₂]	2	
	[D ₂]	[SO(3)]	[D ₂]	2	
	[O(2)]	[O(2)]	[D ₂]	1	
	[O(2)]	[SO(3)]	[D ₂]	2	
	[D ₂]	[D ₂]	[D ₃]	1	
	[D ₂]	[O(2)]	[D ₃]	2	
	[D ₂]	[SO(3)]	[D ₃]	2	
	[O(2)]	[O(2)]	[D ₃]	1	
	[O(2)]	[SO(3)]	[D ₃]	2	
[Z ₂]	[D ₂]	[D ₂]	[D ₄]	1	
	[D ₂]	[O(2)]	[D ₄]	2	
	[D ₂]	[SO(3)]	[D ₄]	2	
	[O(2)]	[O(2)]	[D ₄]	1	
	[O(2)]	[SO(3)]	[D ₄]	2	
	[D ₂]	[D ₂]	[O(2)]	1	
	[D ₂]	[O(2)]	[O(2)]	2	
	[D ₂]	[SO(3)]	[O(2)]	2	
	[O(2)]	[O(2)]	[O(2)]	1	
	[O(2)]	[SO(3)]	[O(2)]	2	
	[D ₂]	[D ₂]	[O]	1	
	[D ₂]	[O(2)]	[O]	2	
	[D ₂]	[SO(3)]	[O]	2	
	[O(2)]	[O(2)]	[O]	1	
	[O(2)]	[SO(3)]	[O]	2	
	[D ₂]	[D ₂]	[SO(3)]	1	
	[D ₂]	[O(2)]	[SO(3)]	2	
	[O(2)]	[O(2)]	[SO(3)]	1	
[1]	[D ₂]	[D ₂]	[1]	1	Generic
	[D ₂]	[O(2)]	[1]	2	
	[D ₂]	[SO(3)]	[1]	2	
	[O(2)]	[O(2)]	[1]	1	
	[O(2)]	[SO(3)]	[1]	2	
					Exotic

	[SO(3)]	[SO(3)]	[1]	1	
	[D ₂]	[D ₂]	[Z ₂]	1	
	[D ₂]	[O(2)]	[Z ₂]	2	
	[D ₂]	[SO(3)]	[Z ₂]	2	
	[O(2)]	[O(2)]	[Z ₂]	1	
	[O(2)]	[SO(3)]	[Z ₂]	2	
	[D ₂]	[D ₂]	[D ₂]	1	
	[D ₂]	[O(2)]	[D ₂]	2	
	[D ₂]	[SO(3)]	[D ₂]	2	
	[O(2)]	[O(2)]	[D ₂]	1	
	[O(2)]	[SO(3)]	[D ₂]	2	
	[D ₂]	[D ₂]	[D ₃]	1	
	[D ₂]	[O(2)]	[D ₃]	2	
	[D ₂]	[SO(3)]	[D ₃]	2	
	[O(2)]	[O(2)]	[D ₃]	1	
	[O(2)]	[SO(3)]	[D ₃]	2	
[1]	[D ₂]	[D ₂]	[D ₄]	1	Exotic
	[D ₂]	[O(2)]	[D ₄]	2	
	[D ₂]	[SO(3)]	[D ₄]	2	
	[O(2)]	[O(2)]	[D ₄]	1	
	[O(2)]	[SO(3)]	[D ₄]	2	
	[D ₂]	[D ₂]	[O(2)]	1	
	[D ₂]	[O(2)]	[O(2)]	2	
	[O(2)]	[SO(3)]	[O(2)]	2	
	[O(2)]	[O(2)]	[O(2)]	1	
	[D ₂]	[D ₂]	[O]	1	
	[D ₂]	[O(2)]	[O]	2	
	[D ₂]	[SO(3)]	[O]	2	
	[O(2)]	[O(2)]	[O]	1	
	[O(2)]	[SO(3)]	[O]	2	
	[D ₂]	[D ₂]	[SO(3)]	1	
	[D ₂]	[O(2)]	[SO(3)]	2	

D.2 Complete list of exotic sets for $\mathbb{E}la(3)$

What follows are the final results. As we can see, for a given set $([G_1], [G_2], [G_3])$ of these resulting symmetry classes, the corresponding set $([G_4], [G_5], [G_6])$ is unique. This will not be the case for lower symmetry classes, that is $[D_2], [Z_2], [1]$.

[G]	[G ₁]	[G ₂]	[G ₃]	[G ₄]	[G ₅]	[G ₆]	Number
[SO(3)]	[SO(3)]	[SO(3)]	[SO(3)]	[SO(3)]	[SO(3)]	[SO(3)]	1
[O]	[SO(3)]	[SO(3)]	[O]	[SO(3)]	[O]	[O]	1
[O(2)]	[O(2)]	[O(2)]	[O(2)]	[O(2)]	[O(2)]	[O(2)]	1
	[O(2)]	[SO(3)]	[O(2)]	[O(2)]	[O(2)]	[O(2)]	1×2
	[O(2)]	[O(2)]	[SO(3)]	[O(2)]	[O(2)]	[O(2)]	1
	[O(2)]	[SO(3)]	[SO(3)]	[O(2)]	[O(2)]	[SO(3)]	1×2
	[SO(3)]	[SO(3)]	[O(2)]	[SO(3)]	[O(2)]	[O(2)]	1
[D ₄]	[O(2)]	[O(2)]	[D ₄]	[O(2)]	[D ₄]	[D ₄]	1
	[O(2)]	[SO(3)]	[D ₄]	[O(2)]	[D ₄]	[D ₄]	1×2
	[SO(3)]	[SO(3)]	[D ₄]	[SO(3)]	[D ₄]	[D ₄]	1
	[O(2)]	[O(2)]	[O]	[O(2)]	[D ₄]	[D ₄]	1
	[SO(3)]	[O(2)]	[O]	[O(2)]	[O]	[D ₄]	1×2
[D ₃]	[O(2)]	[O(2)]	[D ₃]	[O(2)]	[D ₃]	[D ₃]	1
	[SO(3)]	[O(2)]	[D ₃]	[O(2)]	[D ₃]	[D ₃]	1×2
	[SO(3)]	[SO(3)]	[D ₃]	[SO(3)]	[D ₃]	[D ₃]	1
	[O(2)]	[O(2)]	[O]	[O(2)]	[D ₃]	[D ₃]	1
	[SO(3)]	[O(2)]	[O]	[O(2)]	[O]	[D ₃]	1×2
[D ₂]	[D ₂]	[D ₂]	[D ₂]	[D ₂]	[D ₂]	[D ₂]	1
	[D ₂]	[O(2)]	[D ₂]	[D ₂]	[D ₂]	[D ₂]	1×2
	[D ₂]	[SO(3)]	[D ₂]	[D ₂]	[D ₂]	[D ₂]	1×2
	[O(2)]	[O(2)]	[D ₂]	$\begin{pmatrix} [D_2] \\ [O(2)] \end{pmatrix}$	[D ₂]	[D ₂]	2
	[O(2)]	[SO(3)]	[D ₂]	[O(2)]	[D ₂]	[D ₂]	1×2
	[SO(3)]	[SO(3)]	[D ₂]	[SO(3)]	[D ₂]	[D ₂]	1
	[D ₂]	[D ₂]	[D ₄]	[D ₂]	[D ₂]	[D ₂]	1
	[D ₂]	[O(2)]	[D ₄]	[D ₂]	[D ₂]	[D ₄]	1×2
	[D ₂]	[SO(3)]	[D ₄]	[D ₂]	[D ₂]	[D ₄]	1×2
	[O(2)]	[O(2)]	[D ₄]	$\begin{pmatrix} [D_2] \\ [O(2)] \end{pmatrix}$	[D ₄]	[D ₄]	2
	[D ₂]	[D ₂]	[O(2)]	[D ₂]	[D ₂]	[D ₂]	1
	[D ₂]	[O(2)]	[O(2)]	[D ₂]	[D ₂]	$\begin{pmatrix} [D_2] \\ [O(2)] \end{pmatrix}$	2×2
	[D ₂]	[SO(3)]	[O(2)]	[D ₂]	[D ₂]	[O(2)]	1×2
	[O(2)]	[O(2)]	[O(2)]	$\begin{pmatrix} [D_2] \\ [O(2)] \end{pmatrix}$	$\begin{pmatrix} [D_2] \\ [O(2)] \end{pmatrix}$	$\begin{pmatrix} [D_2] \\ [O(2)] \end{pmatrix}$	$2 \times 2 \times 2$

	$[\text{O}(2)]$	$[\text{SO}(3)]$	$[\text{O}(2)]$	$[\text{O}(2)]$	$\begin{pmatrix} [\text{D}_2] \\ [\text{O}(2)] \end{pmatrix}$	$[\text{O}(2)]$	2×2
	$[\text{D}_2]$	$[\text{D}_2]$	$[\mathcal{O}]$	$[\text{D}_2]$	$[\text{D}_2]$	$[\text{D}_2]$	1
	$[\text{D}_2]$	$[\text{O}(2)]$	$[\mathcal{O}]$	$[\text{D}_2]$	$[\text{D}_2]$	$\begin{pmatrix} [\text{D}_2] \\ [\text{D}_4] \end{pmatrix}$	2×2
	$[\text{D}_2]$	$[\text{SO}(3)]$	$[\mathcal{O}]$	$[\text{D}_2]$	$[\text{D}_2]$	$[\mathcal{O}]$	1×2
	$[\text{O}(2)]$	$[\text{O}(2)]$	$[\mathcal{O}]$	$\begin{pmatrix} [\text{D}_2] \\ [\text{O}(2)] \end{pmatrix}$	$\begin{pmatrix} [\text{D}_2] \\ [\text{D}_3] \end{pmatrix}$	$\begin{pmatrix} [\text{D}_2] \\ [\text{D}_3] \end{pmatrix}$	$2 \times 2 \times 2$
	$[\text{O}(2)]$	$[\text{SO}(3)]$	$[\mathcal{O}]$	$[\text{O}(2)]$	$[\text{D}_2]$	$[\mathcal{O}]$	1×2
	$[\text{D}_2]$	$[\text{D}_2]$	$[\text{SO}(3)]$	$[\text{D}_2]$	$[\text{D}_2]$	$[\text{D}_2]$	1
	$[\text{D}_2]$	$[\text{O}(2)]$	$[\text{SO}(3)]$	$[\text{D}_2]$	$[\text{D}_2]$	$[\text{O}(2)]$	1×2
	$[\text{D}_2]$	$[\text{SO}(3)]$	$[\text{SO}(3)]$	$[\text{D}_2]$	$[\text{D}_2]$	$[\text{SO}(3)]$	1×2
	$[\text{O}(2)]$	$[\text{O}(2)]$	$[\text{SO}(3)]$	$[\text{D}_2]$	$[\text{O}(2)]$	$[\text{O}(2)]$	1
$[\text{Z}_2]$	$[\text{D}_2]$	$[\text{D}_2]$	$[\text{Z}_2]$	$\begin{pmatrix} [\text{Z}_2] \\ [\text{D}_2] \end{pmatrix}$	$[\text{Z}_2]$	$[\text{Z}_2]$	2
	$[\text{D}_2]$	$[\text{O}(2)]$	$[\text{Z}_2]$	$\begin{pmatrix} [\text{Z}_2] \\ [\text{D}_2] \end{pmatrix}$	$[\text{Z}_2]$	$[\text{Z}_2]$	2×2
	$[\text{D}_2]$	$[\text{SO}(3)]$	$[\text{Z}_2]$	$[\text{D}_2]$	$[\text{Z}_2]$	$[\text{Z}_2]$	1×2
	$[\text{O}(2)]$	$[\text{O}(2)]$	$[\text{Z}_2]$	$\begin{pmatrix} [\text{Z}_2] \\ [\text{D}_2] \\ [\text{O}(2)] \end{pmatrix}$	$[\text{Z}_2]$	$[\text{Z}_2]$	3
	$[\text{O}(2)]$	$[\text{SO}(3)]$	$[\text{Z}_2]$	$[\text{O}(2)]$	$[\text{Z}_2]$	$[\text{Z}_2]$	1×2
	$[\text{SO}(3)]$	$[\text{SO}(3)]$	$[\text{Z}_2]$	$[\text{SO}(3)]$	$[\text{Z}_2]$	$[\text{Z}_2]$	1
	$[\text{D}_2]$	$[\text{D}_2]$	$[\text{D}_2]$	$\begin{pmatrix} [\text{Z}_2] \\ [\text{D}_2] \end{pmatrix}$	$\begin{pmatrix} [\text{Z}_2] \\ [\text{D}_2] \end{pmatrix}$	$\begin{pmatrix} [\text{Z}_2] \\ [\text{D}_2] \end{pmatrix}$	$2 \times 2 \times 2$
	$[\text{D}_2]$	$[\text{O}(2)]$	$[\text{D}_2]$	$\begin{pmatrix} [\text{Z}_2] \\ [\text{D}_2] \end{pmatrix}$	$\begin{pmatrix} [\text{Z}_2] \\ [\text{D}_2] \end{pmatrix}$	$\begin{pmatrix} [\text{Z}_2] \\ [\text{D}_2] \end{pmatrix}$	$2 \times 2 \times 2$
	$[\text{D}_2]$	$[\text{SO}(3)]$	$[\text{D}_2]$	$[\text{D}_2]$	$[\text{Z}_2]$	$[\text{D}_2]$	1×2
	$[\text{O}(2)]$	$[\text{O}(2)]$	$[\text{D}_2]$	$\begin{pmatrix} [\text{Z}_2] \\ [\text{D}_2] \\ [\text{O}(2)] \end{pmatrix}$	$\begin{pmatrix} [\text{Z}_2] \\ [\text{D}_2] \end{pmatrix}$	$\begin{pmatrix} [\text{Z}_2] \\ [\text{D}_2] \end{pmatrix}$	$3 \times 2 \times 2$
	$[\text{O}(2)]$	$[\text{SO}(3)]$	$[\text{D}_2]$	$[\text{O}(2)]$	$[\text{Z}_2]$	$[\text{D}_2]$	1×2
	$[\text{D}_2]$	$[\text{D}_2]$	$[\text{D}_3]$	$[\text{D}_2]$	$[\text{Z}_2]$	$[\text{Z}_2]$	1
	$[\text{D}_2]$	$[\text{O}(2)]$	$[\text{D}_3]$	$[\text{D}_2]$	$[\text{Z}_2]$	$\begin{pmatrix} [\text{Z}_2] \\ [\text{D}_2] \\ [\text{D}_3] \end{pmatrix}$	3×2
	$[\text{D}_2]$	$[\text{SO}(3)]$	$[\text{D}_3]$	$[\text{D}_2]$	$[\text{Z}_2]$	$[\text{D}_3]$	1×2
	$[\text{O}(2)]$	$[\text{O}(2)]$	$[\text{D}_3]$	$\begin{pmatrix} [\text{D}_2] \\ [\text{O}(2)] \end{pmatrix}$	$\begin{pmatrix} [\text{Z}_2] \\ [\text{D}_2] \\ [\text{D}_3] \end{pmatrix}$	$\begin{pmatrix} [\text{Z}_2] \\ [\text{D}_2] \\ [\text{D}_3] \end{pmatrix}$	$2 \times 3 \times 3$
$[\text{O}(2)]$	$[\text{SO}(3)]$	$[\text{D}_3]$	$[\text{O}(2)]$	$[\text{Z}_2]$	$[\text{D}_3]$	1×2	

	$[D_2]$	$[D_2]$	$[D_4]$	$\begin{pmatrix} [Z_2] \\ [D_2] \end{pmatrix}$	$\begin{pmatrix} [Z_2] \\ [D_2] \end{pmatrix}$	$\begin{pmatrix} [Z_2] \\ [D_2] \end{pmatrix}$	$2 \times 2 \times 2$
	$[D_2]$	$[O(2)]$	$[D_4]$	$\begin{pmatrix} [Z_2] \\ [D_2] \end{pmatrix}$	$\begin{pmatrix} [Z_2] \\ [D_2] \end{pmatrix}$	$\begin{pmatrix} [Z_2] \\ [D_2] \end{pmatrix}$	$2 \times 2 \times 2 \times 2$
	$[D_2]$	$[SO(3)]$	$[D_4]$	$[D_2]$	$[Z_2]$	$[D_4]$	1×2
	$[O(2)]$	$[O(2)]$	$[D_4]$	$\begin{pmatrix} [Z_2] \\ [D_2] \\ [O(2)] \end{pmatrix}$	$\begin{pmatrix} [Z_2] \\ [D_4] \end{pmatrix}$	$\begin{pmatrix} [Z_2] \\ [D_4] \end{pmatrix}$	$2 \times 2 \times 3$
	$[O(2)]$	$[SO(3)]$	$[D_4]$	$[O(2)]$	$\begin{pmatrix} [Z_2] \\ [D_4] \end{pmatrix}$	$[D_4]$	2×2
	$[D_2]$	$[D_2]$	$[O(2)]$	$\begin{pmatrix} [Z_2] \\ [D_2] \end{pmatrix}$	$\begin{pmatrix} [Z_2] \\ [D_2] \end{pmatrix}$	$\begin{pmatrix} [Z_2] \\ [D_2] \end{pmatrix}$	$2 \times 2 \times 2$
	$[D_2]$	$[O(2)]$	$[O(2)]$	$\begin{pmatrix} [Z_2] \\ [D_2] \end{pmatrix}$	$\begin{pmatrix} [Z_2] \\ [D_2] \end{pmatrix}$	$\begin{pmatrix} [Z_2] \\ [D_2] \\ [O(2)] \end{pmatrix}$	$2 \times 2 \times 3 \times 2$
	$[D_2]$	$[SO(3)]$	$[O(2)]$	$[D_2]$	$[Z_2]$	$[O(2)]$	1×2
	$[O(2)]$	$[O(2)]$	$[O(2)]$	$\begin{pmatrix} [Z_2] \\ [D_2] \\ [O(2)] \end{pmatrix}$	$\begin{pmatrix} [Z_2] \\ [D_2] \\ [O(2)] \end{pmatrix}$	$\begin{pmatrix} [Z_2] \\ [D_2] \\ [O(2)] \end{pmatrix}$	$3 \times 3 \times 3$
	$[O(2)]$	$[SO(3)]$	$[O(2)]$	$[O(2)]$	$[Z_2]$	$[O(2)]$	1×2
	$[D_2]$	$[D_2]$	$[O]$	$\begin{pmatrix} [Z_2] \\ [D_2] \end{pmatrix}$	$\begin{pmatrix} [Z_2] \\ [D_2] \end{pmatrix}$	$\begin{pmatrix} [Z_2] \\ [D_2] \end{pmatrix}$	$2 \times 2 \times 2$
	$[D_2]$	$[O(2)]$	$[O]$	$\begin{pmatrix} [Z_2] \\ [D_2] \end{pmatrix}$	$\begin{pmatrix} [Z_2] \\ [D_2] \end{pmatrix}$	$\begin{pmatrix} [Z_2] \\ [D_2] \\ [D_3] \\ [D_4] \end{pmatrix}$	$2 \times 2 \times 4 \times 2$
	$[D_2]$	$[SO(3)]$	$[O]$	$[D_2]$	$[Z_2]$	$[O]$	1×2
	$[O(2)]$	$[O(2)]$	$[O]$	$\begin{pmatrix} [Z_2] \\ [D_2] \\ [O(2)] \end{pmatrix}$	$\begin{pmatrix} [Z_2] \\ [D_2] \\ [D_3] \\ [D_4] \end{pmatrix}$	$\begin{pmatrix} [Z_2] \\ [D_2] \\ [D_3] \\ [D_4] \end{pmatrix}$	$3 \times 4 \times 4$
	$[O(2)]$	$[SO(3)]$	$[O]$	$[O(2)]$	$[Z_2]$	$[O]$	1×2
	$[D_2]$	$[D_2]$	$[SO(3)]$	$[Z_2]$	$[D_2]$	$[D_2]$	1
	$[D_2]$	$[O(2)]$	$[SO(3)]$	$[Z_2]$	$[D_2]$	$[O(2)]$	1×2
	$[O(2)]$	$[O(2)]$	$[SO(3)]$	$[Z_2]$	$[O(2)]$	$[O(2)]$	1
[1]	$[D_2]$	$[D_2]$	$[1]$	$\begin{pmatrix} [1] \\ [Z_2] \\ [D_2] \end{pmatrix}$	$[1]$	$[1]$	3
	$[D_2]$	$[O(2)]$	$[1]$	$\begin{pmatrix} [1] \\ [Z_2] \\ [D_2] \end{pmatrix}$	$[1]$	$[1]$	3×2
	$[D_2]$	$[SO(3)]$	$[1]$	$[D_2]$	$[1]$	$[1]$	1×2

[O(2)]	[O(2)]	[1]	$\begin{pmatrix} [Z_2] \\ [D_2] \\ [O(2)] \end{pmatrix}$	[1]	[1]	3
[O(2)]	[SO(3)]	[1]	[O(2)]	[1]	[1]	1×2
[SO(3)]	[SO(3)]	[1]	[SO(3)]	[1]	[1]	1
[D ₂]	[D ₂]	[Z ₂]	$\begin{pmatrix} [1] \\ [Z_2] \\ [D_2] \end{pmatrix}$	$\begin{pmatrix} [1] \\ [Z_2] \end{pmatrix}$	$\begin{pmatrix} [1] \\ [Z_2] \end{pmatrix}$	$3 \times 2 \times 2$
[D ₂]	[O(2)]	[Z ₂]	$\begin{pmatrix} [1] \\ [Z_2] \\ [D_2] \end{pmatrix}$	$\begin{pmatrix} [1] \\ [Z_2] \end{pmatrix}$	$\begin{pmatrix} [1] \\ [Z_2] \end{pmatrix}$	$2 \times 2 \times 3 \times 2$
[D ₂]	[SO(3)]	[Z ₂]	[D ₂]	[1]	[Z ₂]	1×2
[O(2)]	[O(2)]	[Z ₂]	$\begin{pmatrix} [Z_2] \\ [D_2] \\ [O(2)] \end{pmatrix}$	$\begin{pmatrix} [1] \\ [Z_2] \end{pmatrix}$	$\begin{pmatrix} [1] \\ [Z_2] \end{pmatrix}$	$2 \times 2 \times 3$
[O(2)]	[SO(3)]	[Z ₂]	[O(2)]	[1]	[Z ₂]	1×2
[D ₂]	[D ₂]	[D ₂]	$\begin{pmatrix} [1] \\ [Z_2] \\ [D_2] \end{pmatrix}$	$\begin{pmatrix} [1] \\ [Z_2] \\ [D_2] \end{pmatrix}$	$\begin{pmatrix} [1] \\ [Z_2] \\ [D_2] \end{pmatrix}$	$3 \times 3 \times 3$
[D ₂]	[O(2)]	[D ₂]	$\begin{pmatrix} [1] \\ [Z_2] \\ [D_2] \end{pmatrix}$	$\begin{pmatrix} [1] \\ [Z_2] \\ [D_2] \end{pmatrix}$	$\begin{pmatrix} [1] \\ [Z_2] \\ [D_2] \end{pmatrix}$	$3 \times 3 \times 3 \times 2$
[D ₂]	[SO(3)]	[D ₂]	[D ₂]	[1]	[D ₂]	1×2
[O(2)]	[O(2)]	[D ₂]	$\begin{pmatrix} [Z_2] \\ [D_2] \\ [O(2)] \end{pmatrix}$	$\begin{pmatrix} [1] \\ [Z_2] \\ [D_2] \end{pmatrix}$	$\begin{pmatrix} [1] \\ [Z_2] \\ [D_2] \end{pmatrix}$	$3 \times 3 \times 3$
[O(2)]	[SO(3)]	[D ₂]	[D ₂]	[1]	[D ₂]	1×2
[D ₂]	[D ₂]	[D ₃]	$\begin{pmatrix} [1] \\ [Z_2] \\ [D_2] \end{pmatrix}$	$\begin{pmatrix} [1] \\ [Z_2] \end{pmatrix}$	$\begin{pmatrix} [1] \\ [Z_2] \end{pmatrix}$	$2 \times 2 \times 3$
[D ₂]	[O(2)]	[D ₃]	$\begin{pmatrix} [1] \\ [Z_2] \\ [D_2] \end{pmatrix}$	$\begin{pmatrix} [1] \\ [Z_2] \end{pmatrix}$	$\begin{pmatrix} [1] \\ [Z_2] \\ [D_2] \\ [D_3] \end{pmatrix}$	$3 \times 2 \times 4 \times 2$
[D ₂]	[SO(3)]	[D ₃]	[D ₂]	[1]	[D ₃]	1×2
[O(2)]	[O(2)]	[D ₃]	$\begin{pmatrix} [Z_2] \\ [D_2] \\ [O(2)] \end{pmatrix}$	$\begin{pmatrix} [1] \\ [Z_2] \\ [D_2] \\ [D_3] \end{pmatrix}$	$\begin{pmatrix} [1] \\ [Z_2] \\ [D_2] \\ [D_3] \end{pmatrix}$	$3 \times 4 \times 4$
[O(2)]	[SO(3)]	[D ₃]	[O(2)]	[1]	[D ₃]	1×2

	$[D_2]$	$[D_2]$	$[D_4]$	$\begin{pmatrix} [1] \\ [Z_2] \\ [D_2] \end{pmatrix}$	$\begin{pmatrix} [1] \\ [Z_2] \\ [D_2] \end{pmatrix}$	$\begin{pmatrix} [1] \\ [Z_2] \\ [D_2] \end{pmatrix}$	$3 \times 3 \times 3$
	$[D_2]$	$[O(2)]$	$[D_4]$	$\begin{pmatrix} [1] \\ [Z_2] \\ [D_2] \end{pmatrix}$	$\begin{pmatrix} [1] \\ [Z_2] \\ [D_2] \end{pmatrix}$	$\begin{pmatrix} [1] \\ [Z_2] \\ [D_4] \end{pmatrix}$	$3 \times 3 \times 3 \times 2$
	$[D_2]$	$[SO(3)]$	$[D_4]$	$[D_2]$	$[1]$	$[D_4]$	1×2
	$[O(2)]$	$[O(2)]$	$[D_4]$	$\begin{pmatrix} [Z_2] \\ [D_2] \\ [O(2)] \end{pmatrix}$	$\begin{pmatrix} [1] \\ [Z_2] \\ [D_4] \end{pmatrix}$	$\begin{pmatrix} [1] \\ [Z_2] \\ [D_4] \end{pmatrix}$	$3 \times 3 \times 3$
	$[O(2)]$	$[SO(3)]$	$[D_4]$	$[O(2)]$	$[1]$	$[D_4]$	1×2
	$[D_2]$	$[D_2]$	$[O(2)]$	$\begin{pmatrix} [1] \\ [Z_2] \\ [D_2] \end{pmatrix}$	$\begin{pmatrix} [1] \\ [Z_2] \\ [D_2] \end{pmatrix}$	$\begin{pmatrix} [1] \\ [Z_2] \\ [D_2] \end{pmatrix}$	$3 \times 3 \times 3$
	$[D_2]$	$[O(2)]$	$[O(2)]$	$\begin{pmatrix} [1] \\ [Z_2] \\ [D_2] \end{pmatrix}$	$\begin{pmatrix} [1] \\ [Z_2] \\ [D_2] \end{pmatrix}$	$\begin{pmatrix} [Z_2] \\ [D_2] \\ [O(2)] \end{pmatrix}$	$3 \times 3 \times 3 \times 2$
	$[D_2]$	$[SO(3)]$	$[O(2)]$	$[D_2]$	$[1]$	$[O(2)]$	1×2
	$[O(2)]$	$[O(2)]$	$[O(2)]$	$\begin{pmatrix} [Z_2] \\ [D_2] \\ [O(2)] \end{pmatrix}$	$\begin{pmatrix} [Z_2] \\ [D_2] \\ [O(2)] \end{pmatrix}$	$\begin{pmatrix} [Z_2] \\ [D_2] \\ [O(2)] \end{pmatrix}$	$3 \times 3 \times 3$
	$[D_2]$	$[D_2]$	$[\mathcal{O}]$	$\begin{pmatrix} [1] \\ [Z_2] \\ [D_2] \end{pmatrix}$	$\begin{pmatrix} [1] \\ [Z_2] \\ [D_2] \end{pmatrix}$	$\begin{pmatrix} [1] \\ [Z_2] \\ [D_2] \end{pmatrix}$	$3 \times 3 \times 3$
	$[D_2]$	$[O(2)]$	$[\mathcal{O}]$	$\begin{pmatrix} [1] \\ [Z_2] \\ [D_2] \end{pmatrix}$	$\begin{pmatrix} [1] \\ [Z_2] \\ [D_2] \end{pmatrix}$	$\begin{pmatrix} [1] \\ [Z_2] \\ [D_2] \\ [D_3] \\ [D_4] \end{pmatrix}$	$3 \times 3 \times 5 \times 2$
	$[D_2]$	$[SO(3)]$	$[\mathcal{O}]$	$[D_2]$	$[1]$	$[\mathcal{O}]$	1×2
	$[O(2)]$	$[O(2)]$	$[\mathcal{O}]$	$\begin{pmatrix} [Z_2] \\ [D_2] \\ [O(2)] \end{pmatrix}$	$\begin{pmatrix} [1] \\ [Z_2] \\ [D_2] \\ [D_3] \\ [D_4] \end{pmatrix}$	$\begin{pmatrix} [1] \\ [Z_2] \\ [D_2] \\ [D_3] \\ [D_4] \end{pmatrix}$	$3 \times 5 \times 5$
	$[O(2)]$	$[SO(3)]$	$[\mathcal{O}]$	$[O(2)]$	$[1]$	$[\mathcal{O}]$	1×2
	$[D_2]$	$[D_2]$	$[SO(3)]$	$[1]$	$[D_2]$	$[D_2]$	1
	$[D_2]$	$[O(2)]$	$[SO(3)]$	$[1]$	$[D_2]$	$[O(2)]$	1×2

Thus, we obtain 8 generic sets and 1052 exotic sets. The exotic sets are respectively 6 for $\Sigma_{[O(2)]}$, 6 for $\Sigma_{[D_4]}$, 6 for $\Sigma_{[D_3]}$, 58 for $\Sigma_{[D_2]}$, 283 for $\Sigma_{[Z_2]}$ and 693 for $\Sigma_{[1]}$.

Bibliography

- [1] S. Amstutz and H. Andrä, “A new algorithm for topology optimization using a level-set method,” *Journal of computational physics*, vol. 216, no. 2, pp. 573–588, 2006.
- [2] S. Amstutz, S. M. Giusti, A. A. Novotny, and E. A. De Souza Neto, “Topological derivative for multi-scale linear elasticity models applied to the synthesis of microstructures,” *International Journal for Numerical Methods in Engineering*, vol. 84, no. 6, pp. 733–756, 2010.
- [3] M. P. Bendsoe and O. Sigmund, *Topology optimization: theory, methods, and applications*. Springer Science & Business Media, 2003.
- [4] C. Combescure, P. Henry, and R. S. Elliott, “Post-bifurcation and stability of a finitely strained hexagonal honeycomb subjected to equi-biaxial in-plane loading,” *International Journal of Solids and Structures*, vol. 88, pp. 296–318, 2016.
- [5] S. Forte and M. Vianello, “Symmetry classes for elasticity tensors,” *Journal of Elasticity*, vol. 43, no. 2, pp. 81–108, 1996.
- [6] G. Geymonat and T. Weller, “Classes de symétrie des solides piézoélectriques,” *Comptes Rendus Mathématique*, vol. 335, no. 10, pp. 847–852, 2002.
- [7] H. Le Quang and Q.-C. He, “The number and types of all possible rotational symmetries for flexoelectric tensors,” *Proceedings of the Royal Society A: Mathematical, Physical and Engineering Sciences*, vol. 467, no. 2132, pp. 2369–2386, 2011.
- [8] J. Rychlewski, “Elastic waves under unusual anisotropy,” *Journal of the Mechanics and Physics of Solids*, vol. 49, no. 11, pp. 2651–2666, 2001.
- [9] P. Vannucci, “A special planar orthotropic material,” *Journal of Elasticity*, vol. 67, pp. 81–96, 2002.
- [10] Q. C. He, “Characterization of the anisotropic materials capable of exhibiting an isotropic Young or shear or area modulus,” *International Journal of Engineering Science*, vol. 42, no. 19-20, pp. 2107–2118, 2004.
- [11] A. Ferrer, J. C. Cante, J. A. Hernández, and J. Oliver, “Two-scale topology optimization in computational material design: An integrated approach,” *International Journal for Numerical Methods in Engineering*, vol. 114, no. 3, pp. 232–254, 2018.
- [12] J. Wu, O. Sigmund, and J. p. Groen, “Topology optimization of multi-scale structures: a review,” *Structural and Multidisciplinary Optimization*, vol. 63, no. 3, pp. 1455–1480, 2021.
- [13] S. Amstutz, “An introduction to the topological derivative,” *Engineering Computations*, 2021.
- [14] A. Laurain, “A level set-based structural optimization code using FEniCS,” *Structural and Multidisciplinary Optimization*, vol. 58, no. 3, pp. 1311–1334, 2018.

- [15] B. Durand, A. Lebée, P. Seppecher, and K. Sab, “Predictive strain-gradient homogenization of a pantographic material with compliant junctions,” *Journal of the Mechanics and Physics of Solids*, vol. 160, no. November 2021, p. 104773, 2022.
- [16] M. Camar-Eddine and P. Seppecher, “Determination of the Closure of the Set of Elasticity Functionals,” *Archive for Rational Mechanics and Analysis*, vol. 170, no. 3, pp. 211–245, 2003.
- [17] T. Bückmann, R. Schittny, M. Thiel, M. Kadic, G. W. Milton, and M. Wegener, “On three-dimensional dilational elastic metamaterials,” *New Journal of Physics*, vol. 16, 2014.
- [18] M. Ashby, “Designing architected materials,” *Scripta Materialia*, vol. 68, no. 1, pp. 4–7, 2013.
- [19] Y. Brechet and J. D. Embury, “Architected materials: Expanding materials space,” *Scripta Materialia*, vol. 68, no. 1, pp. 1–3, 2013.
- [20] P. Gong, C.-Z. Hu, X. Zhou, L. Miao, and X. Wang, “Isotropic and anisotropic physical properties of quasicrystals,” *The European Physical Journal B-Condensed Matter and Complex Systems*, vol. 52, pp. 477–481, 2006.
- [21] Y. Wang and O. Sigmund, “Quasiperiodic mechanical metamaterials with extreme isotropic stiffness,” *Extreme Mechanics Letters*, vol. 34, p. 100596, 2020.
- [22] J. Novák, A. Kučerová, and J. Zeman, “Microstructural enrichment functions based on stochastic wang tilings,” *Modelling and Simulation in Materials Science and Engineering*, vol. 21, no. 2, p. 025014, 2013.
- [23] M. Tyburec and J. Zeman, “Optimization-based approach to tiling of finite areas with arbitrary sets of wang tiles,” *Acta Polytechnica CTU Proceedings*, vol. 13, pp. 135–141, 2017.
- [24] T. Maconachie, M. Leary, B. Lozanovski, X. Zhang, M. Qian, O. Faruque, and M. Brandt, “SLM lattice structures: Properties, performance, applications and challenges,” *Materials & Design*, vol. 183, p. 108137, 2019.
- [25] J. J. Andrew, P. Verma, and S. Kumar, “Impact behavior of nanoengineered, 3d printed plate-lattices,” *Materials & Design*, vol. 202, p. 109516, 2021.
- [26] K. Yeranee and Y. Rao, “A review of recent investigations on flow and heat transfer enhancement in cooling channels embedded with Triply Periodic Minimal Surfaces (TPMS),” *Energies*, vol. 15, no. 23, p. 8994, 2022.
- [27] S. Zhao, S. Li, W. Hou, Y. Hao, R. Yang, and R. Misra, “The influence of cell morphology on the compressive fatigue behavior of Ti-6Al-4V meshes fabricated by electron beam melting,” *Journal of the mechanical behavior of biomedical materials*, vol. 59, pp. 251–264, 2016.
- [28] X. Li, X. Yu, and W. Zhai, “Additively manufactured deformation-recoverable and broadband sound-absorbing microlattice inspired by the concept of traditional perforated panels,” *Advanced Materials*, vol. 33, no. 44, p. 2104552, 2021.
- [29] S. C. Kapfer, S. T. Hyde, K. Mecke, C. H. Arns, and G. E. Schröder-Turk, “Minimal surface scaffold designs for tissue engineering,” *Biomaterials*, vol. 32, no. 29, pp. 6875–6882, 2011.
- [30] F. Bobbert, K. Lietaert, A. A. Eftekhari, B. Pouran, S. Ahmadi, H. Weinans, and A. Zadpoor, “Additively manufactured metallic porous biomaterials based on minimal surfaces: a unique combination of topological, mechanical, and mass transport properties,” *Acta biomaterialia*, vol. 53, pp. 572–584, 2017.

- [31] J. Berger, H. Wadley, and R. McMeeking, “Mechanical metamaterials at the theoretical limit of isotropic elastic stiffness,” *Nature*, vol. 543, no. 7646, pp. 533–537, 2017.
- [32] N. Guo and M. C. Leu, “Additive manufacturing: technology, applications and research needs,” *Frontiers of mechanical engineering*, vol. 8, pp. 215–243, 2013.
- [33] P. F. Jacobs, “Fundamentals of stereolithography,” in *1992 international solid freeform fabrication symposium*, 1992.
- [34] J. Comb, W. Priedeman, and P. W. Turley, “FDM® Technology process improvements,” in *1994 international solid freeform fabrication symposium*, 1994.
- [35] J. J. Beaman, J. W. Barlow, D. L. Bourell, R. H. Crawford, H. L. Marcus, and K. P. McAlea, *Solid freeform fabrication: a new direction in manufacturing*, vol. 2061. Springer, 1997.
- [36] C. Y. Yap, C. K. Chua, Z. L. Dong, Z. H. Liu, D. Q. Zhang, L. E. Loh, and S. L. Sing, “Review of selective laser melting: materials and applications,” *Applied physics reviews*, vol. 2, no. 4, p. 041101, 2015.
- [37] M. Feygin and B. Hsieh, “Laminated object manufacturing (LOM): a simpler process,” in *1991 International Solid Freeform Fabrication Symposium*, 1991.
- [38] E. Sachs, C. M. HJ, and P. Williams, “Three-dimensional printing techniques, US Patent 5204055,” 1989.
- [39] J. Mazumder, A. Schifferer, and J. Choi, “Direct materials deposition: designed macro and microstructure,” *Materials Research Innovations*, vol. 3, no. 3, pp. 118–131, 1999.
- [40] K. V. Wong and A. Hernandez, “A review of additive manufacturing,” *International scholarly research notices*, vol. 2012, 2012.
- [41] T. A. Schaedler and W. B. Carter, “Architected cellular materials,” *Annual Review of Materials Research*, vol. 46, pp. 187–210, 2016.
- [42] X. Zheng, H. Lee, T. H. Weisgraber, M. Shusteff, J. DeOtte, E. B. Duoss, J. D. Kuntz, M. M. Biener, Q. Ge, J. A. Jackson, *et al.*, “Ultralight, ultrastiff mechanical metamaterials,” *Science*, vol. 344, no. 6190, pp. 1373–1377, 2014.
- [43] L. R. Meza, S. Das, and J. R. Greer, “Strong, lightweight, and recoverable three-dimensional ceramic nanolattices,” *Science*, vol. 345, no. 6202, pp. 1322–1326, 2014.
- [44] T. A. Schaedler, A. J. Jacobsen, A. Torrents, A. E. Sorensen, J. Lian, J. R. Greer, L. Valdevit, and W. B. Carter, “Ultralight metallic microlattices,” *Science*, vol. 334, no. 6058, pp. 962–965, 2011.
- [45] X. W. Gu and J. R. Greer, “Ultra-strong architected cu meso-lattices,” *Extreme Mechanics Letters*, vol. 2, pp. 7–14, 2015.
- [46] R. Azulay, C. Combescure, and J. Dirrenberger, “Instability-induced pattern generation in architected materials—a review of methods,” *International Journal of Solids and Structures*, p. 112240, 2023.
- [47] S. Shan, S. H. Kang, J. R. Raney, P. Wang, L. Fang, F. Candido, J. A. Lewis, and K. Bertoldi, “Multistable architected materials for trapping elastic strain energy,” *Advanced Materials*, vol. 27, no. 29, pp. 4296–4301, 2015.

- [48] T. Frenzel, C. Findeisen, M. Kadic, P. Gumbsch, and M. Wegener, “Tailored buckling microlattices as reusable light-weight shock absorbers,” *Advanced Materials*, vol. 28, no. 28, pp. 5865–5870, 2016.
- [49] S. Shan, S. H. Kang, P. Wang, C. Qu, S. Shian, E. R. Chen, and K. Bertoldi, “Harnessing multiple folding mechanisms in soft periodic structures for tunable control of elastic waves,” *Advanced Functional Materials*, vol. 24, no. 31, pp. 4935–4942, 2014.
- [50] K. H. Matlack, A. Bauhofer, S. Krödel, A. Palermo, and C. Daraio, “Composite 3D-printed metastructures for low-frequency and broadband vibration absorption,” *Proceedings of the National Academy of Sciences*, vol. 113, no. 30, pp. 8386–8390, 2016.
- [51] J. R. Raney, N. Nadkarni, C. Daraio, D. M. Kochmann, J. A. Lewis, and K. Bertoldi, “Stable propagation of mechanical signals in soft media using stored elastic energy,” *Proceedings of the National Academy of Sciences*, vol. 113, no. 35, pp. 9722–9727, 2016.
- [52] R. Lakes, “Advances in negative Poisson’s ratio materials,” *Advanced materials*, vol. 5, pp. 242–317, 1993.
- [53] Y. Ding, Z. Liu, C. Qiu, and J. Shi, “Metamaterial with simultaneously negative bulk modulus and mass density,” *Physical review letters*, vol. 99, no. 9, p. 093904, 2007.
- [54] T. Bückmann, M. Kadic, N. Stenger, M. Thiel, and M. Wegener, “On the feasibility of pentamode mechanical metamaterials,” in *The Sixth International Congress on Advanced Electromagnetic Materials in Microwaves and Optics*, 2012.
- [55] G. Verchery, “Les Invariants des Tenseurs d’Ordre 4 du Type de l’Elasticite,” tech. rep., 1982.
- [56] H. Yong-Zhong and G. Del Piero, “On the completeness of the crystallographic symmetries in the description of the symmetries of the elastic tensor,” *Journal of Elasticity*, vol. 25, pp. 203–246, 1991.
- [57] P. Chadwick, M. Vianello, and S. C. Cowin, “A new proof that the number of linear elastic symmetries is eight,” *Journal of the Mechanics and Physics of Solids*, vol. 49, no. 11, pp. 2471–2492, 2001.
- [58] M. Olive and N. Auffray, “Symmetry classes for even-order tensors,” *Mathematics and Mechanics of Complex Systems*, vol. 1, no. 2, pp. 177–210, 2013.
- [59] M. Olive and N. Auffray, “Symmetry classes for odd-order tensors,” *ZAMM-Journal of Applied Mathematics and Mechanics*, vol. 94, no. 5, pp. 421–447, 2014.
- [60] J. Rychlewski, “On Hooke’s law,” *Journal of Applied Mathematics and Mechanics*, no. 3, pp. 303–314, 1984.
- [61] A. Bóna, I. Bucataru, and M. A. Slawinski, “Coordinate-free characterization of the symmetry classes of elasticity tensors,” *Journal of Elasticity*, vol. 87, pp. 109–132, 2007.
- [62] M. M. Mehrabadi and S. C. Cowin, “Eigentensors of linear anisotropic elastic materials,” *The Quarterly Journal of Mechanics and Applied Mathematics*, vol. 43, no. 1, pp. 15–41, 1990.
- [63] P. Vannucci, “Plane anisotropy by the polar method,” *Meccanica*, vol. 40, no. 4, pp. 437–454, 2005.
- [64] B. Desmorat and R. Desmorat, “Tensorial polar decomposition of 2D fourth order tensors,” *comptes rendus mecanique*, vol. 343, 2015.

- [65] M. Francois, G. Geymonat, and Y. Berthaud, “Determination of the symmetries of an experimentally determined stiffness tensor: application to acoustic measurements,” *International journal of solids and structures*, vol. 35, no. 31-32, pp. 4091–4106, 1998.
- [66] H. Le Quang, Q.-C. He, and N. Auffray, “Classification of first strain-gradient elasticity tensors by symmetry planes,” *Proceedings of the Royal Society A*, vol. 477, no. 2251, p. 20210165, 2021.
- [67] G. Backus, “A geometrical picture of anisotropic elastic tensors,” *Reviews of geophysics*, vol. 8, no. 3, pp. 633–671, 1970.
- [68] J. C. Maxwell, *A treatise on electricity and magnetism*, vol. 1. Oxford: Clarendon Press, 1873.
- [69] R. Baerheim, “Harmonic decomposition of the anisotropic elasticity tensor,” *Quarterly Journal of Mechanics and Applied Mathematics*, vol. 46, no. 3, pp. 391–418, 1993.
- [70] W.-N. Zou, C.-X. Tang, and E. Pan, “Symmetry types of the piezoelectric tensor and their identification,” *Proceedings of the Royal Society A: Mathematical, Physical and Engineering Sciences*, vol. 469, no. 2155, p. 20120755, 2013.
- [71] W.-N. Zou, C.-X. Tang, and W.-H. Lee, “Identification of symmetry type of linear elastic stiffness tensor in an arbitrarily orientated coordinate system,” *International Journal of Solids and Structures*, vol. 50, no. 14-15, pp. 2457–2467, 2013.
- [72] P. Azzi, R. Desmorat, B. Kolev, and F. Priziac, “The distance to cubic symmetry class as a polynomial optimization problem,” *arXiv preprint arXiv:2203.14562*, 2022.
- [73] P. Azzi, *Géométrie des classes d’isotropie des représentations de groupes avec applications à la Mécanique des Matériaux*. PhD thesis, Sorbonne université, 2023.
- [74] M. Vianello, “An integrity basis for plane elasticity tensors,” *Archives of Mechanics*, vol. 49, no. 1, pp. 197–208, 1997.
- [75] B. Desmorat and N. Auffray, “Space of 2D elastic materials: a geometric journey,” *Continuum Mechanics and Thermodynamics*, vol. 31, pp. 1205–1229, 2019.
- [76] N. Auffray, B. Kolev, and M. Petitot, “On anisotropic polynomial relations for the elasticity tensor,” *Journal of Elasticity*, vol. 115, no. 1, pp. 77–103, 2014.
- [77] J.-P. Boehler, A. Kirillov, and E. T. Onat, “On the polynomial invariants of the elasticity tensor,” *Journal of elasticity*, vol. 34, no. 2, pp. 97–110, 1994.
- [78] M. Olive, B. Kolev, R. Desmorat, and B. Desmorat, “Characterization of the symmetry class of an elasticity tensor using polynomial covariants,” *Mathematics and Mechanics of Solids*, vol. 27, no. 1, pp. 144–190, 2022.
- [79] S. Abramian, B. Desmorat, R. Desmorat, B. Kolev, and M. Olive, “Recovering the normal form of an elasticity tensor,” *Journal of Elasticity*, vol. 142, pp. 1–33, Nov. 2020.
- [80] G. Milton, M. Briane, and D. Harutyunyan, “On the possible effective elasticity tensors of 2-dimensional and 3-dimensional printed materials,” *Mathematics and Mechanics of Complex Systems*, vol. 5, no. 1, pp. 41–94, 2017.
- [81] H. Yang, B. E. Abali, D. Timofeev, and W. H. Müller, “Determination of metamaterial parameters by means of a homogenization approach based on asymptotic analysis,” *Continuum mechanics and thermodynamics*, vol. 32, pp. 1251–1270, 2020.

- [82] M. P. Bendsøe and N. Kikuchi, “Generating optimal topologies in structural design using a homogenization method,” *Computer methods in applied mechanics and engineering*, vol. 71, no. 2, pp. 197–224, 1988.
- [83] M. P. Bendsøe, “Optimal shape design as a material distribution problem,” *Structural optimization*, vol. 1, pp. 193–202, 1989.
- [84] M. Zhou and G. Rozvany, “The COC algorithm, Part II: Topological, geometrical and generalized shape optimization,” *Computer methods in applied mechanics and engineering*, vol. 89, no. 1-3, pp. 309–336, 1991.
- [85] H. Mlejnek, “Some aspects of the genesis of structures,” *Structural optimization*, vol. 5, pp. 64–69, 1992.
- [86] G. Allaire, F. Jouve, and A.-M. Toader, “A level-set method for shape optimization,” *Comptes Rendus Mathématique*, vol. 334, no. 12, pp. 1125–1130, 2002.
- [87] M. Y. Wang, X. Wang, and D. Guo, “A level set method for structural topology optimization,” *Computer methods in applied mechanics and engineering*, vol. 192, no. 1-2, pp. 227–246, 2003.
- [88] J. Sokolowski and A. Zochowski, “On the topological derivative in shape optimization,” *SIAM journal on control and optimization*, vol. 37, no. 4, pp. 1251–1272, 1999.
- [89] M. P. Bendsøe and O. Sigmund, “Material interpolation schemes in topology optimization,” *Archive of applied mechanics*, vol. 69, pp. 635–654, 1999.
- [90] O. Sigmund, “Design of multiphysics actuators using topology optimization—Part II: Two-material structures,” *Computer methods in applied mechanics and engineering*, vol. 190, no. 49-50, pp. 6605–6627, 2001.
- [91] F. Ferrari and O. Sigmund, “A new generation 99 line Matlab code for compliance topology optimization and its extension to 3D,” *Structural and Multidisciplinary Optimization*, vol. 62, pp. 2211–2228, 2020.
- [92] E. Andreassen, A. Clausen, M. Schevenels, B. S. Lazarov, and O. Sigmund, “Efficient topology optimization in matlab using 88 lines of code,” *Structural and Multidisciplinary Optimization*, vol. 43, pp. 1–16, 2011.
- [93] S. Osher and J. A. Sethian, “Fronts propagating with curvature-dependent speed: Algorithms based on hamilton-jacobi formulations,” *Journal of computational physics*, vol. 79, no. 1, pp. 12–49, 1988.
- [94] M. Burger and S. J. Osher, “A survey on level set methods for inverse problems and optimal design,” *European journal of applied mathematics*, vol. 16, no. 2, pp. 263–301, 2005.
- [95] J. A. Sethian and A. Wiegmann, “Structural boundary design via level set and immersed interface methods,” *Journal of computational physics*, vol. 163, no. 2, pp. 489–528, 2000.
- [96] G. Allaire, F. Jouve, and A.-M. Toader, “Structural optimization using sensitivity analysis and a level-set method,” *Journal of computational physics*, vol. 194, no. 1, pp. 363–393, 2004.
- [97] M. Y. Wang and X. Wang, “PDE-driven level sets, shape sensitivity and curvature flow for structural topology optimization,” *CMES-Computer Modeling in Engineering and Sciences*, vol. 6, no. 4, p. 373, 2004.

- [98] H. A. Eschenauer, V. V. Koblelev, and A. Schumacher, “Bubble method for topology and shape optimization of structures,” *Structural optimization*, vol. 8, pp. 42–51, 1994.
- [99] S. Garreau, P. Guillaume, and M. Masmoudi, “The topological asymptotic for pde systems: the elasticity case,” *SIAM journal on control and optimization*, vol. 39, no. 6, pp. 1756–1778, 2001.
- [100] E. A. De Souza Neto, S. Amstutz, S. M. Giusti, and A. A. Novotny, “Topological derivative-based optimization of micro-structures considering different multi-scale models,” 2010.
- [101] S. Giusti, A. Novotny, E. de Souza Neto, and R. Feijóo, “Topological derivative in multi-scale linear elasticity models,” in *8th World Congress on Computational Mechanics and 5th European Congress on Computational Methods in Applied Sciences and Engineering, WCCM-ECCOMAS Proceedings, Venice, Italy*, 2008.
- [102] M. Olive, “Effective computation of $SO(3)$ and $O(3)$ linear representation symmetry classes,” *Mathematics and Mechanics of Complex Systems*, vol. 7, no. 3, pp. 203–237, 2019.
- [103] M. Olive, B. Kolev, and N. Auffray, “A minimal integrity basis for the elasticity tensor,” *Archive for Rational Mechanics and Analysis*, vol. 226, no. 1, pp. 1–31, 2017.
- [104] N. Auffray and P. Ropars, “Invariant-based reconstruction of bidimensionnal elasticity tensors,” *International Journal of Solids and Structures*, vol. 87, pp. 183–193, 2016.
- [105] N. Auffray, *Comportement des matériaux cellulaires : élaboration, caractérisation et modélisation prédictive des propriétés*. Thesis, Institut National Polytechnique de Grenoble - INPG, 2008.
- [106] N. Auffray, B. Kolev, and M. Olive, “Handbook of bi-dimensional tensors: Part I: Harmonic decomposition and symmetry classes,” *Mathematics and Mechanics of Solids*, vol. 22, no. 9, pp. 1847–1865, 2017.
- [107] N. Auffray, “Géométrie des espaces de tenseurs, application à l’élasticité anisotrope classique et généralisée,” *Mécanique des solides [physics.class-ph]*. Université Paris-Est, 2017.
- [108] Samuel, Forest and Michel Amestoy, “Mecaniques des milieux continus.” Lecture notes of scholar year 2017-2018. Ecole des mines paris.
- [109] M. A. Armstrong, *Groups and symmetry*. 1967.
- [110] F. Peter and H. Weyl, “Die vollständigkeit der primitiven darstellungen einer geschlossenen kontinuierlichen gruppe,” *Mathematische Annalen*, vol. 97, no. 1, pp. 737–755, 1927.
- [111] G. Mou, B. Desmorat, R. Turlin, and N. Auffray, “On exotic linear materials: 2D elasticity and beyond,” *International Journal of Solids and Structures*, vol. 264, p. 112103, 2023.
- [112] B. Sturmfels, *Algorithms in Invariant Theory*. 2008.
- [113] M. Abud and G. Sartori, “The geometry of spontaneous symmetry breaking,” *Annals of Physics*, vol. 150, no. 2, pp. 307–372, 1983.
- [114] N. Auffray, J. Dirrenberger, and G. Rosi, “A complete description of bi-dimensional anisotropic strain-gradient elasticity,” *International Journal of Solids and Structures*, vol. 69, pp. 195–206, 2015.
- [115] Q. Zheng and J. P. Boehler, “The description, classification, and reality of material and physical symmetries,” *Acta Mechanica*, vol. 102, pp. 73–89, 1994.

- [116] M. A. Armstrong, *Basic topology*. Springer Science & Business Media, 2013.
- [117] B. Desmorat, M. Olive, N. Auffray, R. Desmorat, and B. Kolev, “Computation of minimal covariants bases for 2d coupled constitutive laws,” *arXiv preprint arXiv:2007.01576*, 2020.
- [118] B. Desmorat, M. Olive, N. Auffray, R. Desmorat, and B. Kolev, “Computation of minimal covariants bases for 2d coupled constitutive laws,” *arXiv preprint arXiv:2007.01576*, 2020.
- [119] S. Forte and M. Vianello, “A unified approach to invariants of plane elasticity tensors,” *Meccanica*, vol. 49, no. 9, pp. 2001–2012, 2014.
- [120] N. Auffray, H. Abdoul-Anziz, and B. Desmorat, “Explicit harmonic structure of bidimensional linear strain-gradient elasticity,” *European Journal of Mechanics-A/Solids*, vol. 87, p. 104202, 2021.
- [121] A. BLINOWSKI, J. MACIEJEWSKA, and J. RYCHLEWSKI, “Two-dimensional Hooke’s tensors - isotropic decomposition, effective symmetry criteria,” *Archives of Mechanics*, vol. 48, no. 2, pp. 325–345, 1996.
- [122] Q.-C. He and Q.-S. Zheng, “On the symmetries of 2d elastic and hyperelastic tensors,” *Journal of elasticity*, vol. 43, no. 3, pp. 203–225, 1996.
- [123] A. Antonelli, B. Desmorat, B. Kolev, and R. Desmorat, “Distance to plane elasticity orthotropy by Euler–Lagrange method,” *Comptes Rendus. Mécanique*, vol. 350, pp. 413–430, 2022.
- [124] R. Lakes, “Foam Structures with a Negative Poisson ’ s Ratio,” *American Association for the Advancement of Science*, vol. 235, no. 4792, pp. 1038–1040, 1987.
- [125] G. W. Milton, “Composite materials with poisson’s ratios close to - 1,” *Journal of the Mechanics and Physics of Solids*, vol. 40, no. 5, pp. 1105–1137, 1992.
- [126] B. D. Caddock and K. E. Evans, “Microporous materials with negative Poisson’s ratios. I. Microstructure and mechanical properties,” *Journal of Physics D: Applied Physics*, vol. 22, no. 12, pp. 1877–1882, 1989.
- [127] “Negative-Poisson’s-Ratio Materials: Auxetic Solids,” *Annual Review of Materials Research*, vol. 47, pp. 63–81, 2017.
- [128] H. Poincaré, *Leçons sur la théorie de l’élasticité*. G. Carré, 1892.
- [129] F. W. Hehl and Y. Itin, “The cauchy relations in linear elasticity theory,” *Journal of Elasticity*, vol. 66, no. 2, pp. 185–192, 2002.
- [130] P. Vannucci and B. Desmorat, “Plane anisotropic rari-constant materials,” *Mathematical Methods in the Applied Sciences*, vol. 39, no. 12, pp. 3271–3281, 2016.
- [131] H. Abdoul-Anziz, N. Auffray, and B. Desmorat, “Symmetry classes and matrix representations of the 2d flexoelectric law,” *Symmetry*, vol. 12, no. 4, p. 674, 2020.
- [132] N. Auffray, S. El Ouafa, G. Rosi, and B. Desmorat, “Anisotropic structure of two-dimensional linear cosserat elasticity,” *Mathematics and Mechanics of Complex Systems*, 2021.
- [133] L. D. Landau, J. S. Bell, M. Kearsley, L. Pitaevskii, E. Lifshitz, and J. Sykes, *Electrodynamics of continuous media*, vol. 8. elsevier, 2013.
- [134] A. Meitzler, H. Tiersten, A. Warner, D. Berlincourt, G. Couqin, and F. Welsh III, “Jeee standard on piezoelectricity,” 1988.

- [135] V. A. Eremeyev, L. P. Lebedev, and H. Altenbach, *Foundations of micropolar mechanics*. Springer Science & Business Media, 2012.
- [136] S. Forest, “Mechanics of cosserat media—an introduction,” *Ecole des Mines de Paris, Paris*, pp. 1–20, 2005.
- [137] F. Murat and J. Simon, *Sur le contrôle par un domaine géométrique par François Murat et Jacques Simon*. Université Paris VI, Laboratoire d’Analyse Numérique, 1976.
- [138] J. Sokolowski, J.-P. Zolésio, J. Sokolowski, and J.-P. Zolesio, *Introduction to shape optimization*. Springer, 1992.
- [139] E. de Souza Neto and R. Feijóo, “Variational foundations of multi-scale constitutive models of solid: Small and large strain kinematical formulation,” *LNCC Research & Development Report*, vol. 16, 2006.
- [140] J. Wu, O. Sigmund, and J. P. Groen, “Topology optimization of multi-scale structures: a review,” *Structural and Multidisciplinary Optimization*, vol. 63, pp. 1455–1480, 2021.
- [141] G. I. Rozvany, M. Zhou, and T. Birker, “Generalized shape optimization without homogenization,” *Structural optimization*, vol. 4, pp. 250–252, 1992.
- [142] R. Hill, “A self-consistent mechanics of composite materials,” *Journal of the Mechanics and Physics of Solids*, vol. 13, no. 4, pp. 213–222, 1965.
- [143] J. Mandel, “Plasticité classique et viscoplasticité (CISM Lecture notes, Udine, Italy),” 1971.
- [144] J. Qu and M. Cherkaoui, *Fundamentals of micromechanics of solids*, vol. 735. Wiley Online Library, 2006.
- [145] J.-C. Michel, H. Moulinec, and P. Suquet, “Effective properties of composite materials with periodic microstructure: a computational approach,” *Computer methods in applied mechanics and engineering*, vol. 172, no. 1-4, pp. 109–143, 1999.
- [146] C. M. Leech, “Mechanics of Composites,” *International Journal of Mechanical Engineering Education*, vol. 15, no. 3, pp. 161–179, 1987.
- [147] H. T. Kollmann, D. W. Abueidda, S. Koric, E. Guleryuz, and N. A. Sobh, “Deep learning for topology optimization of 2d metamaterials,” *Materials & Design*, vol. 196, p. 109098, 2020.
- [148] H. Cheng and K. Gupta, “An historical note on finite rotations,” 1989.
- [149] N. Auffray, H. Le Quang, and Q.-C. He, “Matrix representations for 3d strain-gradient elasticity,” *Journal of the Mechanics and Physics of Solids*, vol. 61, no. 5, pp. 1202–1223, 2013.
- [150] M. Olive and N. Auffray, “Symmetry classes in piezoelectricity from second-order symmetries,” *Mathematics and Mechanics of Complex Systems*, vol. 9, no. 1, pp. 77–105, 2021.
- [151] N. Auffray, Q.-C. He, and H. Le Quang, “Complete symmetry classification and compact matrix representations for 3d strain gradient elasticity,” *International Journal of Solids and Structures*, vol. 159, pp. 197–210, 2019.
- [152] M. Golubitsky, I. Stewart, and D. G. Schaeffer, *Singularities and Groups in Bifurcation Theory: Volume II*, vol. 69. Springer Science & Business Media, 2012.

- [153] M. Golubitsky, I. Stewart, and D. G. Schaeffer, *Singularities and Groups in Bifurcation Theory: Volume II*. Springer-Verlag & New York-Berlin, 2012.
- [154] M. E. Gurtin, “The linear theory of elasticity,” in *Linear Theories of Elasticity and Thermoelasticity: Linear and Nonlinear Theories of Rods, Plates, and Shells*, pp. 1–295, Springer, 1973.
- [155] N. Auffray, B. Kolev, and M. Petitot, “Invariant-based approach to symmetry class detection,” *arXiv preprint arXiv:1111.0861*, 2011.
- [156] M. Olive, “Géométrie des espaces de tenseurs : une approche effective appliquée à la mécanique des milieux continus,” *PhD thesis, Aix Marseille université*, 2014.
- [157] S. C. Cowin, “Properties of the anisotropic elasticity tensor,” *The Quarterly Journal of Mechanics and Applied Mathematics*, vol. 42, no. 2, pp. 249–266, 1989.
- [158] S. Forte and M. Vianello, “Restricted invariants on the space of elasticity tensors,” *Mathematics and mechanics of solids*, vol. 11, no. 1, pp. 48–82, 2006.
- [159] Nicolas, Auffray, “Chapter 3: On Harmonic decomposition of even order tensors in \mathbb{R}^3 .” Lecture notes of scholar year 2022-2023. Sorbonne university.
- [160] Y. Itin and F. W. Hehl, “The constitutive tensor of linear elasticity: its decompositions, cauchy relations, null lagrangians, and wave propagation,” *Journal of Mathematical Physics*, vol. 54, no. 4, p. 042903, 2013.
- [161] Y. Itin and F. W. Hehl, “Irreducible decompositions of the elasticity tensor under the linear and orthogonal groups and their physical consequences,” in *Journal of Physics: Conference Series*, vol. 597, p. 012046, IOP Publishing, 2015.
- [162] B. Desmorat and R. Desmorat, “Second order tensorial framework for 2D medium with open and closed cracks,” *European Journal of Mechanics-A/Solids*, vol. 58, pp. 262–277, 2016.
- [163] K. Ken-Ichi, “Distribution of directional data and fabric tensors,” *International journal of engineering science*, vol. 22, no. 2, pp. 149–164, 1984.
- [164] E. Onat, “Effective properties of elastic materials that contain penny shaped voids,” *International Journal of Engineering Science*, vol. 22, no. 8-10, pp. 1013–1021, 1984.
- [165] Y. Itin, “Cauchy relations in linear elasticity: Algebraic and physics aspects,” *arXiv preprint arXiv:2304.09579*, 2023.
- [166] E. Ihrig and M. Golubitsky, “Pattern selection with $O(3)$ symmetry,” *Physica D: Nonlinear Phenomena*, vol. 13, no. 1-2, pp. 1–33, 1984.
- [167] R. Baerheim, “Classification of symmetry by means of maxwell multipoles,” *Quarterly Journal of Mechanics and Applied Mathematics*, vol. 51, no. 1, pp. 73–104, 1998.
- [168] G. F. Smith, “On isotropic functions of symmetric tensors, skew-symmetric tensors and vectors,” *International journal of engineering science*, vol. 9, no. 10, pp. 899–916, 1971.
- [169] R. Desmorat, N. Auffray, B. Desmorat, M. Olive, and B. Kolev, “Minimal functional bases for elasticity tensor symmetry classes,” *Journal of Elasticity*, vol. 147, no. 1-2, pp. 201–228, 2021.
- [170] V. Popov, T. Springer, and E. Vinberg, *Algebraic Geometry IV: Linear Algebraic Groups Invariant Theory*, vol. 55. Springer Science & Business Media, 2012.

- [171] J. Boehler, S. Demmerle, and S. Koss, "A new direct biaxial testing machine for anisotropic materials," *Experimental mechanics*, vol. 34, pp. 1–9, 1994.
- [172] T. Dassonville, M. Poncelet, and N. Auffray, "Toward a homogenizing machine," *International Journal of Solids and Structures*, vol. 191, pp. 534–549, 2020.